The Dissertation Committee for Shuting Liu Certifies that this is the approved version of the following dissertation:

Hydrolysis and Decomposition of Small Peptides in Marine Environments

Committee:

Zhanfei Liu, Supervisor

Jim W. McClelland

Deana Erdner

Wayne S. Gardner

David L. Kirchman

Hydrolysis and Decomposition of Small Peptides in Marine Environments

by

Shuting Liu, B.S.

Dissertation

Presented to the Faculty of the Graduate School of

The University of Texas at Austin

in Partial Fulfillment

of the Requirements

for the Degree of

Doctor of Philosophy

The University of Texas at Austin

May 2016

Dedication

This work is dedicated to my parents. Thank you for supporting me to follow my dreams abroad spiritually and mentally. Without your constant encouragement and confidence on me, I wouldn't be the person I am today. Love my family from my deep heart.

Acknowledgements

I want to take this opportunity to give my big thank to my advisor, Zhanfei Liu. He is such an awesome advisor who gave me invaluable support and guidance on my Ph.D. work and overall science career. His patience in helping me develop my scientific skills and enthusiasm on science inspired me so much and laid my foundation to approaching my future science career. I appreciate the help from every member in the Liu lab (Jing Liu, Kaijun Lu, Hernando Bacosa, Nick Reyna, Jason Jenkins, Meredith Evans) during my lab work, especially thank Hernando Bacosa, Kaijun Lu, Jiqing Liu, Nick Reyna, and Jason Jenkins for helping with water sampling and peptide incubation experiments during the cruise or protists counting in the lab. I thank Drs. Xiaozhen Mou and Leila Hamdan for helping with the cruise. I thank the crew of R/V *Pelican* and R/V *Savannah* for their help with sampling. I am grateful for the analytical and data analysis help from Chunyan Ren, Kaijun Lu, Dr. Wayne Gardner, Dr. Chris Shank, Ellen Knapke, Dr. Tracy Villareal, Cammie Hyatt, Dr. Ed Buskey, Dr. Yefei Pang, Dr. Peter Thomas, Dr. Jianhong Xue, Dr. Tara Connelly, Dr. Linsay Scheef. I am grateful for the bacterial DNA sequencing and community structure analysis by the Research and Testing Laboratory, Lubbock, TX and Oklahoma Medical Research Foundation. I appreciate the guidance from Dr. Boris Wawrik on the DNA-SIP work and his comments on the manuscript. I am grateful for the comments and suggestions provided by my committee members (Drs. Jim McClelland, Deana Erdner, Wayne Gardner, David Kirchman)

throughout my Ph.D. study. I also thank Dr. Wayne Gardner for helping to edit several of my manuscripts. I thank the experimental help from the REU undergraduate students (Alyssa Riesen, Kerollos Halim) in the summer. I am also grateful for the ship time provided by NOAA, NRL and BOEM. This dissertation work is funded by National Science Foundation the Chemical Oceanography Program (OCE-1129659). I am grateful for the fellowship endowed by Lund-Page and Lund-Stuckey, Continuing Bruton fellowship, and Graduate School Dissertation Writing fellowship. I appreciate the travel awards for attending scientific meetings provided by UT Graduate School and UTMSI. I thank Dr. Bob Dickey and Dr. Ken Dunton for nominating me for awards and fellowships. I thank my cohort (Qiyuan Liu, Claire Griffin, Catalina Cuellar Gempeler, John Mohan, Ellen Knapke, Aubrey Lashaway, Kellie Hoppe, Eva Salas) in accompanying me get through difficulties in classes and research, and thank all faculties, staffs and students from UTMSI in creating the friendly and nice research and learning environments.

Hydrolysis and Decomposition of Small Peptides in Marine Environments

Shuting Liu, Ph.D.

The University of Texas at Austin, 2016

Supervisor: Zhanfei Liu

Proteins and peptides are important labile organic matter supporting growth of microorganisms in seawater. Small peptides (<600 Da) are key intermediates linking protein degradation, nutrient regeneration and DON preservation. In this dissertation, hydrolysis and/or decomposition of small peptides in seawater are investigated from both chemistry and biology perspectives. From the chemistry perspective, a new HPLC-MS method was first developed to measure small peptides amended in seawater at nanomolar levels. This method offers an easy and quick protocol to measure peptide concentrations in seawater without desalting pretreatments and lowers the detection limit by two orders of magnitude over the traditional UV method. It provides an analytical foundation for the peptide detection. With this method, hydrolysis of plain peptide without fluorogenic tags and peptide analogs in seawater was compared to assess the reliability of using small plain peptides as proxies. While Lucifer Yellow Anhydride (LYA) tag did not influence peptide hydrolysis rates significantly in many cases, it did affect the peptide hydrolysis pathways and susceptibility of dipeptide bonds to enzymes. This result validates the advantages of using plain peptides to study peptide hydrolysis rates and pathways. Peptide hydrolysis pathways were evaluated further to quantify the relative roles of

different peptidases in seawater. Incubations of peptides with different chemical structures demonstrated that aminopeptidases prefer to cleave N-terminal hydrophobic or basic amino acids rather than polar uncharged or acidic ones in peptides. From the biology perspective, as bacteria are major consumer of labile organic matter such as peptides, linking bacteria communities and peptide decomposition using DNA-stable isotope probing is considered to explore peptide decomposition mechanisms. Different bacterial taxa were involved in peptide utilization between the normoxic and hypoxic seawater in northern Gulf of Mexico, offering insights into the biological roles of bacteria in organic matter decomposition and hypoxia formation. The potential role of microbes other than bacteria, such as protists, in peptide decomposition was also evaluated using size-fractioned seawater incubations, highlighting the need to include relatively large-size microorganisms in microbial loop to understand C and N cycles in ocean. This study examined peptide hydrolysis and decomposition in terms of overall rates, difference of pathways between environments, and interactions with different microorganisms, extending from bulk analysis of peptide degradation rates to detailed mechanisms including enzyme functions and microbial linkages. The results offer insights into labile organic matter cycling, microbial ecology, and nutrient regeneration in seawater, and also open more questions about the factors controlling the hydrolysis and decomposition patterns of labile organic matter, microbial behavior and functions in biogeochemical processes, and DON preservation mechanisms.

Table of Contents

List of Tables

List of Figures

Chapter 1. Introduction

Proteins and peptides play an important role in carbon and nitrogen cycles in marine environments, as they account for 25-70% of phytoplankton and zooplankton biomass (Lewis, 1973; Emerson and Hedges, 2008; Lopez et al., 2010). They can be released from marine biota through extracellular release by phytoplankton, "sloppy feeding" by grazers, leaching from fecal pellets, viral lysis, or bacterial transformation and release during degradation of organic matter (Carlson, 2002). Being labile dissolved organic matter (LDOM), proteins and peptides do not accumulate in natural waters, as only trace amounts are detected (Tanoue, 1996). For example, concentration ranges of dissolved combined amino acids (DCAA), including all hydrolysable proteins and peptides, are only about 0.2-4 μM in the coastal ocean (Bronk, 2002), which indicates that proteins and peptides are metabolized efficiently by microbes, and a balance is usually achieved between the production and removal of proteins and peptides. Although present in low concentrations in ambient seawater, proteins and peptides support a major portion of bacterial growth (Kirchman, 2008). With both carbon and nitrogen in the molecules, proteins and peptides serve as links of dissolved organic carbon (DOC) and dissolved organic nitrogen (DON) in the microbial loop that is crucial for nutrient regeneration.

Proteins and peptides are primarily metabolized by heterotrophic bacteria (Sussman and Gilvarg, 1971; Hoppe, 1983; Pantoja et al., 1997; Foreman et al., 1998). The passive transport of substrates across bacterial cell wall and cell membrane is restricted to small compounds (Weiss et al., 1991; Cunha, 2010). For Gram-negative bacteria, proteins imbedded in outer membrane are known as porins (Payne and Smith, 1994), and the channels formed by porins between the outer membrane and periplasmic

space serve as “molecular sieves” to allow substrates with molecular weight less than ca. 600 Da to pass through them. To diffuse through porin proteins, proteins and large peptides must be first hydrolyzed to small peptides (<600 Da) outside the bacterial cell membrane. Hydrolysis is often considered to be a rate-limiting step for peptide remineralization (Meyerreil and Koster, 1992), although it can sometimes outcompete other processes during organic matter degradation (Arnosti, 2004).

As important intermediates connecting protein degradation, nutrient regeneration and DON preservation (Fig. 1.1), small peptides can be incorporated into bacteria biomass, metabolized to carbon dioxide and ammonium, or released as DOM. To date, two mechanisms have been proposed to explain the utilization of small peptide by bacteria (Sussman and Gilvarg, 1971). A small peptide can be hydrolyzed first to amino acids outside the cytoplasmic membrane either by extracellular peptidases that are dissolved freely in the water or by ectoenzymes attached to the cell wall or in the periplasmic space of bacteria (Chróst, 1991; Sinsabaugh, 1994; Cunha, 2010). Then the free amino acids are actively transported across the cytoplasmic membrane and metabolized within the cell. Alternatively, small peptides are directly transported by permeases (peptide transporters) located in the cytoplasmic membrane. After being taken up by the bacterial cells, the peptides undergo intracellular hydrolysis for further metabolism. At present, no method can differentiate these two mechanisms. Thus, in the following chapters, the decomposition of small peptides includes both extracellular hydrolysis with subsequent uptake for further metabolism and direct uptake for intracellular hydrolysis by microbes.

In marine environments, peptide hydrolysis studies rely mainly on peptide analogs with fluorogenic tags such as leucine-methyl-coumarinylamide (Leu-MCA) (Hoppe, 1983; Talbot and Bianchi, 1997) and Lucifer Yellow anhydride (LYA)-peptide

(Pantoja et al., 1997; Pantoja and Lee, 1999), because these fluorescent analogs can be detected easily with fluorometers. However, several studies suggested that the size and chemical structure of peptides or peptide analogs may affect the hydrolysis rate (Pantoja and Lee, 1999; Obayashi and Suzuki, 2005; Liu et al., 2010). For example, Leu-MCA is hydrolyzed at the same rate as LYA-dipeptide, but much slower than LYA-bonded large peptides, which was interpreted as the lack of dipeptidases (Pantoja and Lee, 1999), but this observation may be due to either the size difference between peptide dimers and longer peptides or the steric effect of the fluorescence tags. Thus, using the fluorogenic dimer to represent all peptides may underestimate the "true" hydrolysis rate. A model presented by Billen (1991) suggested the dominant role of aminopeptidases that cleave peptides from the N-terminus, whereas the important role of carboxypeptidases that cleave peptides from the C-terminus is demonstrated in another study (Hashimoto et al., 1985). The LYA-peptide excludes hydrolysis by aminopeptidases, while Leu-MCA exclude hydrolysis by carboxypeptidase, so both analogs may bias the true peptide hydrolysis rate in seawater. Little work has been done on the plain peptide without fluorogenic tags except for some dipeptides and tetrapeptides (Kirchman and Hodson, 1984; Mulholland and Lee, 2009; Liu et al., 2010), due to the difficulty in detecting plain peptides in low concentration and the limit of commercially available plain peptide standards. Therefore, more work is needed to investigate the hydrolysis rates and pathways of plain peptides that occur in natural forms in seawater.

Since bacteria are major consumers of DOM, understanding how bacteria community responds to organic matter input, such as DOM released during primary production, is important to decipher their role in carbon and nitrogen cycles. As a byproduct of primary production in the ocean, DOM consists of different components such as proteins, carbohydrates and lipids. The interaction between bacteria and proteins

becomes especially conspicuous when an algal bloom occurs, which is frequent in coastal waters (Sellner et al., 2003). Previous studies have tested the role of different bacteria in processing organic matter through enrichment experiments in the laboratory. Bacterial community composition shifts in aquatic environments after amendment with different substrates (Eilers et al., 2000; Harvey et al., 2006; Murray et al., 2007; Teske et al., 2011). For example, a large shift of bacterial community with time was observed in mesocosm tanks amended with diatom and *Phaeocystis* DOM (Murray et al., 2007), and *Gammaproteobacteria* became the dominant bacteria class in the Chesapeake Bay water, while *Bacteroides* became dominant in the lower Delaware Bay water after bovine serum albumin (BSA) amendment (Harvey et al., 2006). However, these studies only provide indirect evidence on the role of different bacteria types in peptide or protein decomposition based on changes of bacterial community structure after peptides or proteins were added. A few studies have linked specific bacterial groups directly with organic matter substrate decomposition in the seawater (Tabor and Neihof, 1982; Ouverney and Fuhrman, 1999; Cottrell and Kirchman, 2000; Gihring et al., 2009; Mayali et al., 2012). However, few studies have revealed which bacteria process small peptides directly. Resolving the question about "who is eating what" is necessary to understand the mechanisms of peptide decomposition and to trace the role of individual bacteria in the DOC and DON remineralization.

A widely accepted idea about the dispersal of bacteria among microbiologists is "everything is everywhere, but environment selects", since bacteria are small organisms and have large population size. Only two bacterial species, an uncultured *Alphaproteobacterium* and a member closely related to *Pelagibacter ubique*, are ubiquitously distributed globally (Fuhrman and Hagstrom, 2008). Species richness of bacteria was higher at low latitude (Pommier et al., 2007). Specific bacterial phylotypes

varying among different water masses in deep Arctic Ocean supports the emerging consensus for the existence of microbial biogeography (Galand et al., 2010). These results suggest that different aquatic environments select bacterial polygenetic groups living in the habitat. To adapt to seawater environment variations, bacteria have two lifestyles (Polz et al., 2006). One is the "opportuni-troph" lifestyle that usually exists in high-concentration substrate environment. Typical examples of organisms with this lifestyle consist of some fast-growing bacteria like *Vibrio* and *Roseobacter*. They sense food source chemically, move towards it actively and grow in bursts (Mouriño-Pérez et al., 2003; Voget et al., 2015). The other lifestyle is the passive oligotroph strategy commonly used by clades of *Pelagibacter* and *Prochlorococcus*. They efficiently use metabolic substrate because they are usually in environments with low substrate concentrations (Rappé et al., 2002; Polz et al., 2006). These two different lifestyles are also reflected in bacterial genomes. "Opportuni-trophs" are often associated with large and flexible genomes, while oligotrophs possess small and optimized genomes to increase metabolic efficiency. Labile small peptides can serve as a "feast" food source, and opportuni-trophic bacteria can probably grow in bursts when peptide input is large, such as during algal blooms. However, we still do not know if this group-specific use of DOM occurs generally in different seawater environments.

Overall, our understanding of peptide hydrolysis and decomposition mechanisms and pathways in marine environments is limited. It is unclear how peptides are transported and cleaved by bacteria, how structural differences affect peptide hydrolysis, and what kinds of bacteria preferentially utilize peptides. In this dissertation with seven chapters, hydrolysis and/or decomposition of small peptides in seawater are addressed from both chemistry and biology perspectives, with Chapters 2-4 focusing on the chemistry aspect and Chapters 5-6 focusing more on the biology aspect. Chapter 1

provides general background information. In Chapter 2, a new-developed HPLC-MS method is introduced to measure small peptides added to seawater at nanomolar levels, which provides an analytical foundation for the peptide detection in the following chapters. In Chapter 3, hydrolysis of plain peptide and peptide analogs in seawater are compared to assess the reliability of using small plain peptides as proxies in this project. With the analytical method and peptide substrate established, peptide hydrolysis pathways are evaluated in Chapter 4 to understand the relative roles of different peptidases in seawater. As bacteria are major consumer of labile organic matter such as peptides, linking bacteria communities and peptide decomposition using DNA-stable isotope probing at different depths is discussed in Chapter 5 to explore peptide decomposition mechanisms from the biological angle. In Chapter 6, the potential role of microbes other than bacteria, such as protists, in peptide decomposition is evaluated using size-fractioned seawater incubations. In Chapter 7 the previous chapters are summarized and broad implications and future work are discussed.

Figure 1.1. A conceptual model of peptide metabolizing pathways in marine environments.

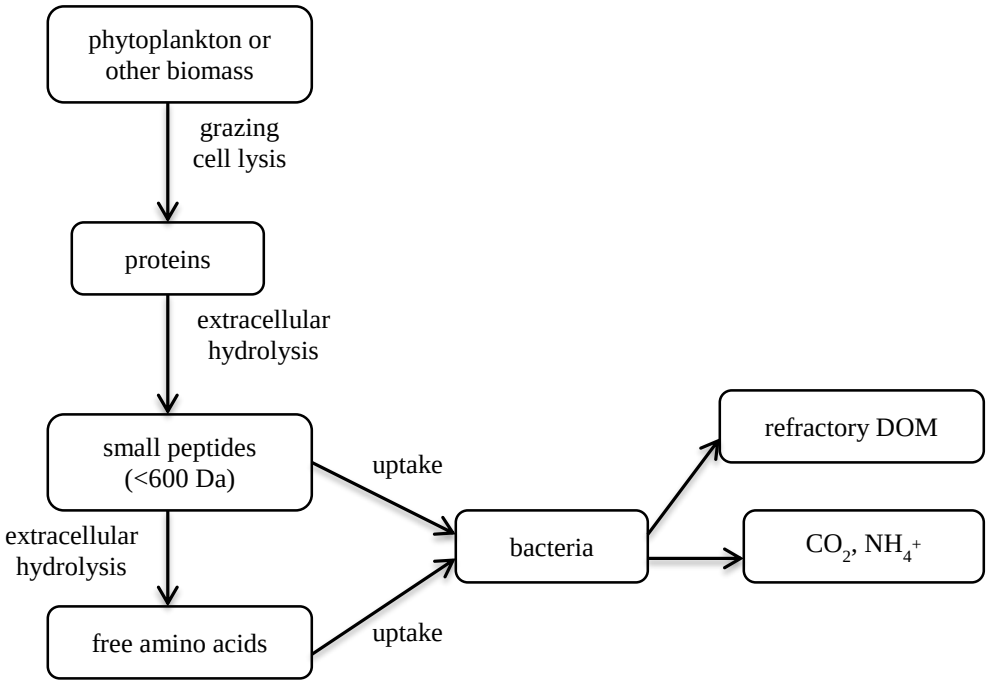

Chapter 2. A new method to measure small peptides amended in seawater using high performance liquid chromatography coupled with mass spectrometry

(Published in Marine Chemistry 164 (2014): 16-24)

ABSTRACT

Quantifying peptide decomposition rate is crucial in understanding marine carbon and nitrogen cycling, because proteins and peptides constitute a major fraction of labile organic matter. However, analytical techniques of detecting small peptides in nanomolar levels in seawater are limited. A new method was developed to measure low concentrations of small peptides amended in seawater, using high performance liquid chromatography coupled with mass spectrometry (HPLC-MS). This technique reduces the detection limit of small peptides by two orders of magnitude relative to the common ultraviolet (UV) detection. A 6-way valve was added before the MS and the valve was programmed to guide the salt peak to waste before the peptide peak was introduced to the MS. Therefore, peptides amended in seawater were injected directly to the HPLC-MS without desalting pretreatment. This new method can detect as low as 0.23 pmol of tetrapeptide alanine-valine-phenylalanine-alanine (AVFA), a peptide fragment of Ribulose-1,5-bisphosphate carboxylase oxygenase (RuBisCO), with less than 5% precision (relative standard deviation). This method was applied successfully to determine decomposition rates of two small peptides, AVFA and serine-tryptophan-glycine-alanine (SWGA), in coastal oceans, and first data of peptide hydrolysis rates using small plain peptides at lower than micromolar concentrations were obtained. Hydrolysis of AVFA and its fluorescent analog was also compared at such low concentration levels. This analytical method broadens our capability to examine the

biogeochemical behavior of small peptides, including their hydrolysis, decomposition, and other possible transformation processes in aquatic environments.

INTRODUCTION

Decomposition of proteins is an important link in marine carbon and nitrogen cycles, as proteins are major biochemical components in biomass of marine organism. For instance, proteins account for 25-70% of plankton biomass (Lewis, 1973; Emerson and Hedges, 2008; Lopez et al., 2010). Proteins can be released into seawater through "sloppy feeding" of zooplankton, leaching from fecal pellets, or viral lysis of bacteria (Lampert, 1978; Alldredge and Silver, 1988). To be metabolized by bacteria, proteins and large peptides must be hydrolyzed to small peptides (M.W. <600 Da) or free amino acids by extracellular enzymes (Benz, 1988; Weiss et al., 1991). Production of peptides has been detected during protein degradation in seawater (Hollibaugh and Azam, 1983; Nunn et al., 2003; Roth and Harvey, 2006). Through further bacterial decomposition, carbon and nitrogen in small peptides can be incorporated into bacteria biomass, released as dissolved organic matter (DOM), or respired into inorganic matter such as ammonium and carbon dioxide. Overall, small peptides are a key link in the conversion of labile proteins to DOM, ammonium, and carbon dioxide, and in the more general carbon and nitrogen cycles in marine ecosystems.

To our knowledge, no individual small peptide has been detected in seawater due to their low concentrations and rapid turnover rate. Instead, studies on small peptides in marine environments have focused on incubations with amended peptide. However, only a few studies have used small plain peptides (i.e. native and unmodified peptide in contrast to peptide analogs with fluorogenic tags) to examine uptake or hydrolysis rates

due to the difficulty in detecting peptides in low concentrations (Kirchman and Hodson, 1984; Mulholland and Lee, 2009; Liu et al., 2010, 2013). In these studies, either high concentrations of peptides (5-10 $\mu mol \cdot L^{-1}$) or isotope-labeled peptides were used. The typical approach to measure small peptide concentrations in seawater involves the use of high performance liquid chromatography (HPLC) with ultraviolet (UV) detection, yet this technique can only quantify relatively high concentration of small peptides due to low analytical sensitivity. For example, the detection limit of UV for analyzing peptide containing a chromophore amino acid, such as phenylalanine (F), is ca. 50 pmol with injection volumes of several hundred μL, corresponding to a concentration of 0.1-0.5 $\mu mol \cdot L^{-1}$ (Liu et al., 2010). This range of values is much higher than ambient concentrations ($nmol \cdot L^{-1}$ or less) of individual proteins or peptides dissolved in seawater (Tanoue, 1995; Powell et al., 2005; Pantoja et al., 2009). Radioisotope-labeled peptides are difficult to synthesize and not available commercially. Measuring *in-situ* peptide hydrolysis in seawater has relied mostly on peptide analogs, such as leucine methylcoumarinylamide (Leu-MCA) or Lucifer yellow anhydride (LYA)-peptide, because their fluorogenic tags can be detected easily by fluorometry with low detection limits (Hoppe, 1983; Hoppe et al., 1988a; Pantoja et al., 1997; Talbot and Bianchi, 1997; Pantoja and Lee, 1999). However, it remains unclear whether the hydrolysis rates from these peptide analogs represent those of the plain peptides because of possible steric effects of the fluorogenic tags on the hydrolysis rates (Stevenson, 1994; Mulholland et al., 2003; Liu et al., 2010). Thus, methods are needed to measure low concentrations of small plain peptides in aquatic environments.

Mass spectrometry (MS) has emerged as a compelling tool for identifying and quantifying proteins and peptides in natural samples due to its high sensitivity (Gharahdaghi et al., 1999; He et al., 2004; Marshall and Hendrickson, 2008; Ahn et al.,

2012). HPLC and MS are often coupled for protein and peptide determination, as HPLC can separate the different proteins and peptides in mixtures before individual compounds are introduced to MS (Andren et al., 1994; Dai et al., 1999; Petritis et al., 2002; Delinsky et al., 2004; Damen et al., 2008; Liu et al., 2011b; Inoue et al., 2012). HPLC-MS has been used widely in protein and peptide identification in biomedical science, but this technique has not been applied in samples of seawater matrix, partially due to the trace background levels of peptides and proteins and partially due to the interference of sea salts (Curtis-Jackson et al., 2009). For example, proteins in seawater have to be concentrated and desalted using tangential flow ultrafiltration before the HPLC-MS analysis (Powell et al., 2005).

Desalting is crucial for MS application, given the limited tolerance of MS to non-volatile substances like sea salts. Sea salts can interfere with the mass spectrometry electrospray ionization source through either clogging the skimmer or suppressing ionization (Roboz et al., 1994; Niessen, 2006). But the desalting pretreatment for seawater samples is usually tedious and time-consuming, and involves issues of recovery efficiency (Gilar et al., 2001). To avoid non-volatile salt interference and the pretreatment procedure, Roboz et al. (1994) designed an on-line buffer removal and fraction selection method for typical peptides and proteins in the biomedical field through gradient capillary HPLC prior to electrospray MS, but this protocol was designed to desalt the buffer salt (potassium phosphate and tris-mix), which should be much easier than sea salts in a complicated seawater matrix.

Here we present a new approach to measure small plain peptides amended in seawater in low concentrations using HPLC-MS with electrospray ionization. A programmable 6-way valve was added in the flow path right before the mass spectrometer, so the salt peak could be directed to waste before the peptide peak being

introduced to the mass spectrometer. Thus, seawater samples can be directly injected to the system without desalting pretreatment. As one application, decomposition of two small peptides was tested using seawater incubation, and the first data were obtained on decomposition rates of small plain peptides in less than micromolar concentrations. Hydrolysis between peptide analog and plain peptide at less than micromolar levels was also compared to evaluate the potential effect of fluorescent tags on peptide hydrolysis.

MATERIALS AND METHODS

Materials

Peptides alanine-valine-phenylalanine-alanine (AVFA) and serine-tryptophan-glycine-alanine (SWGA) were synthesized and purified based on the protocol of Liu et al. (2010). AVFA is a fragment of Ribulose-1,5-bisphosphate carboxylase oxygenase (RuBisCO) that is ubiquitous in the photosynthesis, and SWGA was previously designed due to its strong fluorescence signal for detection purpose (Liu et al., 2010). The hydropathy indices of AVFA and SWGA are 10.6 and -0.3, respectively, so these two peptides represent a large range of peptides with different polarities. Peptide analog LYA-AVFA was synthesized through reflux of LYA dipotassium salt (4-amino-3,6-disulfo-1,8-naphthalic anhydride dipotassium salt, Sigma) and AVFA in lithium acetate (reagent grade, Sigma) based on the protocol of Pantoja et al. (1993). Chemicals for mobile phase solvents include methanol (LC-MS grade, Fisher), acetonitrile (LC-MS grade, Fisher), ammonium acetate (AR grade, Mallinckrodt Baker), ammonium bicarbonate (AR grade, Mallinckrodt Baker), acetic acid (Glacial, AR grade, Mallinckrodt Baker), potassium hydroxide (AR grade, Mallinckrodt Baker), and sodium phosphate (monobasic anhydrous, NaH_2PO_4, ACS grade, VWR). Water was obtained

from an Ultrapure Water System (Barnstead, 18.2 Ω). Materials for peptide incubation and chemistry analysis included *o*-phthaldialdehyde (Sigma), HCl (Certified ACS plus, Fisher), $HgCl_2$ (AR grade, Mallinckrodt Baker), formaldehyde (AR grade, Mallinckrodt Baker), SYBR Green II (Molcular probes), 0.2 μm pore size Nylon syringe filters (Whatman, diam. 25mm), 0.2 μm pore size polyvinylidene fluoride (PVDF) syringe filters (Whatman GD/X, diam. 13 mm), 0.2 μm pore size cellulose acetate (CA) syringe filters (Whatman GD/X, diam. 13 mm), 3 mL plastic disposable syringes (Thermo Fisher), 250 mL and 30 mL amber glass bottles (Fisher), and 2 mL amber HPLC vials (Fisher). All glassware was combusted in a furnace at 450 ºC before use.

HPLC-MS system and sample analysis procedure

The HPLC-MS system (Shimadzu) included photodiode array (PDA, 190-800 nm) and MS detectors (Fig. 2.1). Between the PDA and MS, a 6-way valve was programmed to direct the flow to either waste or MS. When the valve was in the "0" position, the solution was directed to the waste after passing the HPLC column and PDA detector; when in the "1" position, the solution was directed to the MS following the PDA detector.

The HPLC system included a C_{18} column (Alltima C_{18} 5 μm, 150 mm × 4.6 mm), and two mobile phases, solvent A as 10 $mmol \cdot L^{-1}$ ammonium acetate and solvent B as methanol. Other possible mobile phase options were discussed in the Results and Discussion section. In the analysis, solvent B (methanol) was ramped from 20% to 100% during the first 10 min, and then remained at 100% for 5 min. Flow rate was set at 0.3 $mL \cdot min^{-1}$. Controlled by the program, the 6-way valve was switched to "1" position at 8-9.5 min and back to "0" at 11-14 min, changing the solvent pathway to the MS detector

instead of the waste container during 8-14 min. Column temperature was set at 40 ℃ in a column oven and samples were kept at 4 ℃ in the autosampler. The HPLC chromatogram was monitored at 209 nm (above both acetonitrile and methanol cut-off UV wavelengths). The MS consisted of an electrospray ionization (ESI) source and a quadrupole mass analyzer. The MS detector voltage was set at 1.20 kV. Nitrogen gas served as the drying gas at a flow rate of 6 $L \cdot min^{-1}$ and also the nebulizing gas at a flow rate of 1.5 $mL \cdot min^{-1}$. Interface source temperature was set at 350 ℃ and desolvation line (DL) temperature at 250 ℃. Peptide samples were analyzed through positive ion mode with single ion monitoring (SIM) at $[M+H]^+$ ion state, i.e. AVFA at m/z=407 and SWGA at m/z=420.

Peptide incubation and analysis

Decomposition rates of AVFA and SWGA were evaluated by incubating the peptides in seawater. AVFA and SWGA, at an initial concentration of 0.35-0.41 $\mu mol \cdot L^{-1}$, were incubated respectively using unfiltered Gulf of Mexico surface seawater collected from the ship channel (27.84ºN, 97.05ºW) in Port Aransas, Texas, in March 2013. Seawater was collected in a 2-L acid-cleaned polyethylene bottle and processed in the laboratory within 2 h after the collection. Dissolved oxygen (DO) was measured with an oxygen microsensor (Unisense) calibrated by 100% point of air-purged seawater and 0% point of N_2-purged seawater (Table 2.1). Temperature was measured with a thermometer and salinity with a refractometer. The seawater pH was analyzed using a bench-top pH meter (Thermo Fisher Orion 4-star). Seawater was filtered through a 0.2 μm pore size Nylon filter for dissolved free amino acids (DFAA) and total dissolved amino acids (TDAA) analyses. DFAA were measured by an HPLC equipped with a fluorescence

detector (Shimadzu Prominence) after pre-column *o*-phthaldialdehyde derivatization (Lee et al., 2000). TDAA were measured in the same way after the samples were hydrolyzed into individual amino acids with 6 $mol \cdot L^{-1}$ HCl under nitrogen at 110 ºC for 20 h (Kuznetsova and Lee, 2002). DCAA were calculated as the difference between TDAA and DFAA (Table 2.1). Measurements of DFAA and DCAA in replicate samples had relative standard deviations of 10–20%.

The peptide incubation procedure followed the protocol of Liu et al. (2010). Briefly, peptides were incubated in 250 mL amber glass bottles at room temperature (24°C) under dark. At each time point (0, 2, 6, 9, 21, 30, 45, 54 h), duplicate samples (1.5 mL) were taken out and filtered through 0.2 μm syringe filters (PVDF) for peptide and DFAA analyses. Samples were stored frozen at -20 ºC until HPLC-MS and HPLC analysis.

Another peptide incubation experiment comparing the hydrolysis of LYA-AVFA and AVFA was conducted using the surface (2 m) seawater from Sta. T2 (28.85ºN, 89.80ºW) in the Mississippi River plume in the northern Gulf of Mexico. Seawater was collected using Niskin bottles mounted on a CTD rosette while onboard R/V *Pelican* in May 2013. *In-situ* temperature, salinity, DO and chlorophyll *a* (Chl *a*) were obtained from the CTD (Table 2.1). Dissolved organic carbon (DOC) was measured using a Shimadzu total organic carbon analyzer (TOC 5000), and duplicate analyses agreed within 6%. Inorganic nutrient concentrations (NO_3^-, NO_2^-, PO_4^{3-}, NH_4^+) were analyzed using a UV-Vis spectrophotometer (Evolution 160, Thermo Scientific) following established procedures (Bolleter et al., 1961; Murphy and Riley, 1962; Strickland and Parsons, 1968; Jones, 1984). Surface Sta. T2 seawater was highly eutrophic with high DOC and dissolved inorganic nitrogen (DIN) concentrations due to the Mississippi River input (Table 2.1).

LYA-AVFA (0.46 μmol·L^{-1}) and AVFA (0.42 μmol·L^{-1}) were each amended in a 30 mL amber glass bottle filled with seawater. Triplicates were incubated for each peptide under dark at room temperature (24ºC). At 0, 4, 14, 17, 19, 24 h, aliquot samples (1.5 mL) were filtered through 0.2 μm syringe filters (CA) and preserved in 2 mL amber vials at -20 ºC. Another 1mL samples at each time interval were fixed with 3% (final concentration) formaldehyde and preserved at 4 ºC for bacterial abundance analysis. Killed control of AVFA (0.59 μmol·L^{-1}) was also conducted in 180 μmol·L^{-1} $HgCl_2$, a concentration that stops bacterial activity (Lee, 1992). AVFA was analyzed using the HPLC-MS method as described above, and LYA-AVFA was analyzed through HPLC (Shimadzu Prominence) equipped with a C_{18} column (Alltima 5 μm, 250 mm × 4.6 mm) and a fluorescence detector, according to the protocol of Pantoja et al. (1997) with 0.05 mol·L^{-1} NaH_2PO_4 (pH 4.5) and methanol as the mobile phases. For the gradient elution program, methanol increased from 10% to 50% in 25 min, then further to 100% at 26 min, and kept as 100% for 6 min until it went back to 10% at 34 min. Detection was at excitation and emission wavelength of 424 nm and 550 nm, respectively. Bacterial abundance was counted in a flow cytometer (BD Accuri C6) under blue light laser excitation at 488 nm after SYBR Green II staining. Detailed procedure for bacteria counting followed the same protocol in Liu et al. (2013).

RESULTS AND DISCUSSION

Method optimization

Assessing different mobile phases for HPLC

Acetonitrile and methanol (mobile phase B) were compared to find an optimal choice for the AVFA detection due to their wide application in peptide measurement.

With 10 mmol·L^{-1} ammonium acetate as the mobile phase A, AVFA (20 μmol·L^{-1}) in nanopure water with an injection volume of 100 μL was tested with different B mobile phases. The HPLC gradient program for assessments was as described in the HPLC-MS protocol above, except that the flow rate was 1 mL·min^{-1}. The AVFA peak occurred 2.3 min later in the methanol elution than in the acetonitrile elution (Fig. 2.2a, b). Since sea salt usually occurs at the beginning of HPLC chromatograms, the further away the sea salt peak is from the AVFA peak, the less likely is sea salt to be introduced to the MS. Therefore, methanol is a better organic solvent than acetonitrile for our application.

In addition to ammonium acetate, ammonium bicarbonate was tested with methanol as the organic solvent. Again, 20 μmol·L^{-1} AVFA in water (100 μL injection) was used for the assessment. The HPLC chromatograms resulting from using 10 mmol·L^{-1} ammonium acetate and ammonium bicarbonate respectively yielded similar AVFA peak shapes and baseline stabilities (not shown). Thus, either ammonium acetate or ammonium bicarbonate can be used as mobile phase A. Ammonium acetate was used for the assessments below.

Assessing concentrations of buffers for HPLC

Concentrations of buffer (mobile phase A) can affect the MS sensitivity (Garcia, 2005). For reversed-phase HPLC separation, a buffer concentration ranging from 10 mmol·L^{-1} to 50 mmol·L^{-1} is usually adequate (Snyder et al., 1997). Too high of a buffer concentration may lead to precipitation in organic mobile phase, whereas too low of concentration may decrease the quality of the peak shape and precision. Different concentrations of ammonium acetate (50, 20, 10, and 5 mmol·L^{-1}) in mobile phase A were examined, with methanol as mobile phase B, to optimize sensitivity. The sensitivity

factor, also known as response factor, was calculated as the peak area/standard amount (Snyder et al., 1997). Based on the peak area comparison, the sensitivity factor was the largest at the concentration of 10 mmol·L^{-1} (6.26e+8/µmol), followed by 5 mmol·L^{-1} (6.10e+8/µmol), 20 mmol·L^{-1} (5.84e+8/µmol), and 50 mmol·L^{-1} (3.90e+8/µmol). Thus, 10 mmol·L^{-1} was chosen as the concentration of ammonium acetate buffer for the HPLC-MS protocol.

Assessing mobile phase pH effects on HPLC chromatograms

The pH of the mobile phase is important for maintaining peak shape and reproducibility for ionic compounds. The ionization of peptides, with both amine and carboxyl groups, depends on the pH of the mobile phase. The buffer pH was adjusted before organic solvent was added, as the pH measurement is imprecise in the presence of organic solvent (Snyder et al., 1997). The buffer controls pH effectively in the range of buffer $pK_a \pm 1$. The pK_a of ammonium acetate is 4.76 for acetate and 9.2 for ammonium. To assess the effects of pH on chromatogram quality, the pH of mobile phase aqueous solvent A (10 mmol·L^{-1} ammonium acetate) was adjusted from 4.5 to 9.2 with acetic acid or potassium hydroxide (Fig. 2.3). All AVFA peaks showed appropriate shapes in the HPLC chromatograms with different buffer pHs. But the sensitivity factor of AVFA was highest at the original pH 6.7 of the buffer. Thus, pH 6.7 was chosen for the ammonium acetate buffer without adjustment. In addition, the baseline at pH 6.7 was the smoothest among the chromatograms, further consolidating our conclusion of choosing ammonium acetate with its original pH for the HPLC-MS protocol.

Assessing the flow rate effects on the HPLC chromatograms

The effect of flow rate on the shape of HPLC chromatograms was evaluated using AVFA standard (20 μmol·L^{-1} in water). When the flow rate decreased from 1 to 0.3 to 0.2 mL·min^{-1}, the sensitivity of HPLC PDA detector increased accordingly. The sensitivity factor of AVFA at a flow rate of 0.2 mL·min^{-1} was three times larger than that at a flow rate of 0.3 mL·min^{-1}, and 4.5 times larger than that at a flow rate of 1 mL·min^{-1}. Meanwhile, retention time of the AVFA peak was extended from 5 to 15 min when flow rate decreased from 1 to 0.2 mL·min^{-1}. Flow rate affects not only the PDA sensitivity, but also the MS sensitivity. Operating electrospray in a micro-electrospray mode with flow rates ranging from 300 to 900 nL·min^{-1} or in a nano-electrospray mode with flow rates between 10 and 100 nL·min^{-1} could increase the MS sensitivity significantly as compared with higher flow rates, due to the improvement of droplet charging efficiency and reduction of charge competition (Andren et al., 1994; Emmett and Caprioli, 1994; Schmidt et al., 2003; Tang et al., 2004). Considering all factors including analytical time, sensitivity, and MS acceptable ion unsaturation flow rate (if flow rate is too high, an ion excess problem may occur in MS), we chose 0.3 mL·min^{-1} as the optimum flow rate in our HPLC-MS protocol.

Assessing MS detector voltage effects on MS chromatograms

MS detector voltage was evaluated to achieve optimal MS sensitivity. All HPLC-MS instrument and method parameters were set according to those optimized above. Three different detector voltages ascending from 1.12, 1.20 to 1.35 kV were tested. The instrument sensitivity was enhanced twice from 1.12 to 1.20 kV, based on the integrated peak area of 5 nM AVFA in water. Similarly, the 1.35 kV further improved the sensitivity 6 times than that under 1.20 kV. However, higher detector voltage can

decrease the amount of ions that can be tolerated in the ionization source, i.e., higher detector voltages increase chances of ion saturation. Ion saturation, or excessive ions, would cause sample analysis to fail. Thus, the moderate 1.20 kV was chosen as the detector voltage in our HPLC-MS protocol.

Standard calibration curves of AVFA and SWGA

With all the optimized method and instrument parameters of the HPLC-MS protocol, we tested the linearity of small peptide quantification using AVFA standards dissolved in seawater, ranging from 5 nmol·L^{-1} to 1 μmol·L^{-1}. Quantification was based on the peak area obtained from the single ion monitoring (SIM) chromatogram at m/z=407 in a positive ion mode. The standard calibration curves showed excellent linearity in the range of 5 nmol·L^{-1}-1 μmol·L^{-1}, with an injection volume of 100 μL (R^2=1, Fig. 2.4a). The maximum level of quantitation of this method, defined as the highest amount that can be determined reliably, was approximately 1 nmol for AVFA, because the calibration curve bent between 10-20 μmol·L^{-1} of AVFA when tested in distilled water (data not shown). Thus, this new method was suitable for measurement of a wide concentration range for small peptides less than 10 μmol·L^{-1} with a 100 μL-injection volume for AVFA.

Present MS detection commonly offers a dynamic range across 3 to 5 orders of magnitude depending on the compounds and instrument conditions, although the upper limit of the linear dynamic range of ESI-MS is still under debate (Kostiainen and Bruins, 1996; Tang et al., 2004; Liu et al., 2011a). As discussed above, the linear dynamic range of our method was from 0.5 pmol to approximate 1.0 nmol for AVFA, or about 4 orders of magnitude. The nonlinearity in the high-concentration range may result from the

deviation caused by the source injection and ionization process, the adsorption loss in the transition from the ion source to the detector, or the ion saturation occurred in the mass spectrometer (Ong and Mann, 2005; Damen et al., 2008). However, the wide dynamic range in our method is enough to meet the need to measure decomposition or hydrolysis of peptide substrates at different concentrations in seawater, as their concentrations in seawater are much lower than the upper dynamic range.

The limit of quantification (LOQ) and limit of detection (LOD, detection limit) are two important parameters used to evaluate an analytical method. LOQ is the concentration that can be quantified reliably with a specific accuracy or precision, while the LOD is the lowest concentration that can be detected reliably by the instrument (Snyder et al., 1997). From a linear regression curve, LOQ can be calculated as $10 * \sigma/S$ and LOD as $3.3 * \sigma/S$, where σ is the residual standard deviation and S is the slope of the calibration curve (ICH Q2 (R1)). For this HPLC-MS method, the LOQ achieved was as low as 0.70 pmol for AVFA with a less than 5% precision (relative standard deviation, n=5) and the LOD of this method was 0.23 pmol for AVFA at the precision of less than 5%. This low detection limit, which is comparable to the detection limit of fluorescent peptide analogs like LYA-peptides (Pantoja et al., 1997; Pantoja and Lee, 1999), demonstrates a main advantage of this new HPLC-MS method. The sensitivity of the MS for small peptide quantification is two orders of magnitude higher than that of the PDA detector. For example, 1 $\mu mol \cdot L^{-1}$ AVFA was shown as a large and sharp peak in the MS chromatogram while only as a tiny peak in the PDA chromatogram (Fig. 2.5a); the PDA detector cannot detect the AVFA standard peak with a concentration of 5 $nmol \cdot L^{-1}$ and 100 μL injection volume, but MS detector can clearly 'see' the AVFA peak (Fig. 2.5b). This HPLC-MS method can detect a low level of peptide (<5 $nmol \cdot L^{-1}$ in AVFA) amended in seawater, which is much lower than the ambient bulk concentration of

DCAA, often in the range of 0.2-4 μM (Bronk 2002). Moreover, the precision of concentration measurement was less than 5% for the MS, indicating high reproducibility.

The reproducibility of the AVFA calibration curve was tested for more than five times at weekly to monthly intervals over one year, and excellent linearity was obtained (0.98-1 for the R^2, data not shown), demonstrating the quality assurance of this HPLC-MS method. Among a long time interval, there was a certain degree of variation (25-50%) for the absolute MS peak area depending on the MS daily conditions and maintenance such as desolvation line cleaning to prevent clogging, but this would not affect sample quantification, because calibration curves were obtained daily before sample analysis and the daily repeatability of a calibration curve was within 5% variation, as described above.

Similar to AVFA, the standard calibration curve of another small peptide SWGA showed excellent linearity in the range of 0.05-0.5 $\mu mol \cdot L^{-1}$ with 100 μL injection volume (R^2=0.9992, Fig. 2.4b), suggesting the transformative feature of this method to applications with other small peptide substrates. In the following section, decomposition of AVFA and SWGA in seawater was studied using this method.

APPLICATION

Decomposition of small peptides in seawater

We applied this new HPLC-MS method to examine decomposition rates of AVFA and SWGA amended in seawater with low initial concentrations (ca. 350-410 $nmol \cdot L^{-1}$). These concentrations were much lower than the DCAA concentration in the ship channel water (3100 $nmol \cdot L^{-1}$, Table 2.1), accounted for 11-13% of DCAA and comparable to concentrations of amended peptide analogs (50-2500 $nmol \cdot L^{-1}$) in

incubation studies of Pantoja and coworkers (Pantoja et al., 1997; Pantoja and Lee, 1999). The decomposition rates include both ectoenzymatic hydrolysis and uptake, because the molecular weights of these two peptides are less than 600 Da (Weiss et al., 1991). In the incubation, both AVFA and SWGA showed linear decomposition patterns within the initial 21 h ($R^2 > 0.98$), at decomposition rates of 7.2 $nmol \cdot L^{-1} \cdot h^{-1}$ for AVFA and 6.6 $nmol \cdot L^{-1} \cdot h^{-1}$ for SWGA (Fig. 2.6a). In the second stage from 21 h to 54 h, the decomposition rate of AVFA (20.9 $nmol \cdot L^{-1} \cdot h^{-1}$) was three times higher, and SWGA (11.8 $nmol \cdot L^{-1} \cdot h^{-1}$) approximately two times higher, than during the initial 21 h. SWGA decomposition rate was also measured in the ship channel surface seawater collected in October 2011, and lower decomposition rate (3.6 $nmol \cdot L^{-1} \cdot h^{-1}$) was found (data not shown). Decomposition rates derived from the first stage may be closer to the natural rate than those from the second stage, as both bacterial abundance and community may have changed considerably in the later incubation period (McCarren et al., 2010; Liu et al., 2013).

Free amino acids, produced by peptide hydrolysis, were monitored throughout the incubation (Table 2.2). As expected, alanine (A), phenylalanine (F) and valine (V) were produced substantially from AVFA, while S, W, G and A from SWGA. The lability, or bacterial uptake rate, differs among each amino acid (Liu et al., 2013), so the amino acids released may not follow the stoichiometry of their parent peptide. More F and V were released than A from AVFA, even though AVFA contains twice amount of A than V and F, suggesting that the uptake rate of A was much faster than V and F. Similarly, more G was released than S, W and A. Using F and G for their respective mass balance calculation, ~21% of AVFA and ~37% of SWGA were hydrolyzed, while the rest may have been taken up directly by bacteria (Liu et al., 2013). Note that these hydrolyzed percentages were conservative because the uptake of amino acids by bacteria was not

taken into consideration. Other DFAA, except A, V and F in the AVFA incubation and S, W, G and A in the SWGA incubation, generally remained within background levels during the incubation time (Table 2.2).

The decomposition rates (7-20 $nmol \cdot L^{-1} \cdot h^{-1}$) are the first data for small plain peptides amended in less than 13% of the background DCAA concentration. These rates using HPLC-MS were much lower than those of using HPLC (5 to 103 $nmol \cdot L^{-1} \cdot h^{-1}$) with higher initial peptide concentrations amended (10 $\mu mol \cdot L^{-1}$) (Liu et al., 2010), even though the decomposition patterns were similar. In addition, the linearity of the decomposition curves showed that the peptide decomposition followed kinetics of zero order rather than first order, suggesting that the decomposition is limited by enzymes (or bacteria) rather than by substrates.

Comparison of hydrolysis between AVFA and LYA-AVFA

To directly compare the hydrolysis of peptide analog and small peptide, LYA-AVFA and AVFA hydrolysis rates were obtained from on-deck incubation using water from Sta. T2 in the Mississippi River plume (Fig. 2.6b). The linear curves of both LYA-AVFA and AVFA suggest that their hydrolysis followed zero-order kinetics, consistent with those of ship channel water. AVFA was hydrolyzed at a rate of 29 $nmol \cdot L^{-1} \cdot h^{-1}$ and completely hydrolyzed at 14 h. In comparison, LYA-AVFA was hydrolyzed at 21 $nmol \cdot L^{-1} \cdot h^{-1}$ in the same seawater during 24 h. In contrast, AVFA concentrations in the killed control remained constant during the 24-h incubation (Fig. 2.6b), indicating that sorption of peptide on glass wall or particles was minimal. AVFA hydrolysis rate was 1.4 times as high as LYA-AVFA hydrolysis rate and this difference was significant (t test, $p < 0.05$), suggesting that the fluorescent tag (LYA) might affect the AVFA hydrolysis rate.

In addition, peptide hydrolysis rates in the Sta. T2 water were almost twice as high as those in the ship channel seawater, which can be attributed to the potentially high bacterial abundance and activity associated with the eutrophic Mississippi River plume. In the Mississippi River plume water, bacterial abundance in the AVFA incubation decreased 6% within the initial 17 h (Fig. 2.7), during which the AVFA has been completely hydrolyzed (Fig. 2.6). Even though bacterial abundance in the LYA-AVFA incubation increased 13% within the 14 h followed by 3% decrease, the hydrolysis rate of LYA-AVFA was relatively constant throughout the 24 h of incubation (Figs. 1.6 and 1.7). These patterns suggest that the low-concentration addition of the peptide did not significantly disturb the bacterial community within the 15-24 h of incubation (Liu et al., 2013).

CONCLUSIONS AND IMPLICATIONS

Our HPLC-MS method offers a new way to directly detect low concentrations of small peptides amended in seawater without desalting pretreatment. Mobile phase composition, buffer concentration, buffer pH, flow rate and MS detector voltage were consecutively optimized to achieve separation of sea salt and peptide, excellent peak shape, and high sensitivity. This new HPLC-MS method lays an analytical foundation for small peptide analysis in ambient seawater conditions with easy and quick procedures. Its accuracy, precision, and low detection limit enable the detection of peptides amended in seawater at micromolar to nanomolar concentrations, which is close to or lower than ambient DCAA concentrations. This technique makes it possible for further studies of peptide hydrolysis and other transformation processes. If tandem MS system is coupled

with our method, more information about structures of peptides and their metabolites during hydrolysis can be obtained.

Low-concentration small peptide incubation alleviates the possibility of bacteria community or behavior change caused by adding substrates in high concentrations (Liu et al., 2013). This method makes it possible to incubate small plain peptides in less than micromolar concentrations, by which hydrolysis or decomposition patterns (based on hydrolyzed products and cleavage position) can be deciphered. For example, the hydrolysis pathway of AVFA (AVFA → AVF + A → AV + F + A, AVFA → A + VFA → A + V + FA or AVFA → AV + FA) can potentially be assessed by measuring hydrolysis products of VFA, FA, AVF and AV. This new HPLC-MS method with low detection limit also provides a basis for detecting peptides, if existing at relatively high levels (above detection limit of our method), in natural seawater. For example, AVFA, a fragment of RuBisCO that are ubiquitous proteins in phytoplankton, may exist at detectable levels in natural seawater, especially in locations associated with high levels of phytoplankton or marine aggregates (Alldredge and Silver, 1988; Fenchel, 2002). This method is particularly promising, if peptides can be pre-concentrated using solid phase extraction or other techniques (Curtis-Jackson et al., 2009).

Several precautions should be considered before similar peptide seawater sample analysis is undertaken. First, volatile mobile phase composed of organic solution and aqueous solutions should be chosen to separate the salt from the analyte of interest in seawater, and to provide optimal conditions for the MS operation. For hydrophobic peptides, the elution gradient may only need a shorter time to reach a high organic mobile phase percentage needed to prevent analyte from co-eluting with the sea salts. But for hydrophilic peptides, more time with a low organic solvent percentage should be maintained to extend the retention time of the peptide peak to distinguish it from the salt

peak. For very hydrophilic peptides, other HPLC columns such as hydrophilic interaction liquid chromatography (HILIC) column should be considered. Second, the linear dynamic range of MS for specific peptides must be determined for the calibration, because the upper limit of the dynamic range may vary for different compounds due to their different saturation conditions in the MS. Third, the flow rate and injection volume should be adjusted together with the sample concentration to prevent saturation of ion in the ionization source of the MS.

Table 2.1. Water chemistry parameters of coastal surface seawater from the ship channel in Port Aransas, Texas during March 2013 and Sta. T2 from the northern Gulf of Mexico during May 2013. DO-dissolved oxygen; Temp-temperature; Chl *a*-chlorophyll *a*; DOC-dissolved organic carbon; DFAA-dissolved free amino acids; DCAA-dissolved combined amino acids.

Station	DO (mg·L^{-1})	Temp (℃)	Salinity (ppt)	pH	Chl *a* (µg·L^{-1})	DOC (µmol·L^{-1})	DFAA (µmol·L^{-1})	DCAA (µmol·L^{-1})	NO_3^- (µmol·L^{-1})	NO_2^- (µmol·L^{-1})	PO_4^{3-} (µmol·L^{-1})	NH_4^+ (µmol·L^{-1})
Ship channel	8.7	18	32	8.08	NM	NM	0.15	3.10	NM	NM	NM	NM
T2	6.6	25.2	19	NM	0.82	258.3	NM	NM	15.99	BD	0.11	1.97

NM: not measured.
BD: below detection limit (0.03 µmole·L^{-1}).

Table 2.2. Concentrations (nM) of dissolved free amino acids in the AVFA and SWGA incubation in the ship channel seawater in March 2013. Data are presented as average ± error of duplicate samples. Releasing amino acids from peptides are marked in bold.

Sample	ASP[a]	GLU	HIS	SER	ARG	GLY	THR	ALA	TYR	MET	VAL	PHE	TRP	ILE	LEU
AVFA-0h	114±13	10±0	ND	55±5	ND	ND	ND	**35±3**	ND	ND	**10±1**	**3±1**	NM	ND	ND
AVFA-2h	84±3	12±1	ND	62±9	18±2	77±27	ND	**55±4**	ND	13±2	**14±1**	**12±0**	NM	ND	ND
AVFA-6h	84±7	6±1	ND	47±4	12±4	24±24	ND	**54±8**	ND	12±1	**19±3**	**16±1**	NM	ND	ND
AVFA-9h	96±12	7±3	ND	52±15	7±2	ND	ND	**55±5**	ND	9±6	**36±0**	**26±1**	NM	ND	ND
AVFA-21h	75±13	6±1	ND	37±10	2±2	ND	ND	**30±0**	ND	3±0	**57±0**	**72±2**	NM	ND	ND
AVFA-30h	117±1	6±1	ND	60±25	4±1	ND	ND	**17±5**	ND	1±1	**24±6**	**20±2**	NM	ND	ND
AVFA-45h	95±0	5±2	ND	49±13	8±2	ND	ND	**15±1**	ND	3±1	**5±0**	**0±0**	NM	ND	ND
AVFA-54h	105±27	6±3	ND	61±27	7±2	ND	ND	**14±1**	ND	4±0	**2±2**	**0±0**	NM	ND	ND
SWGA-0h	128±32	9±1	ND	**84±9**	3±3	**ND**	ND	**17±2**	ND	ND	3±3	ND	**ND**	ND	ND
SWGA-2h	87±7	7±1	ND	**75±1**	ND	**91±51**	ND	**23±3**	ND	ND	5±0	ND	**ND**	ND	ND
SWGA-6h	97±8	7±0	12±1	**105±13**	1±1	**105±6**	ND	**29±4**	2±2	ND	8±3	ND	**ND**	ND	ND
SWGA-9h	107±2	11±2	ND	**99±15**	ND	**122±15**	4±0	**28±5**	ND	ND	6±4	ND	**ND**	ND	ND
SWGA-21h	105±10	12±5	ND	**44±13**	ND	**154±77**	14±0	**16±1**	7±7	ND	2±2	ND	**5±3**	ND	ND
SWGA-30h	96±5.	10±2	8±1	**82±23**	7±7	**66±4**	5±0	**26±9**	2±2	ND	1±1	ND	**52±5**	ND	ND
SWGA-45h	96±2	8±2	5±5	**62±12**	ND	**73±10**	2±0	**16±6**	1±1	ND	2±2	ND	**ND**	ND	ND
SWGA-54h	110±8	6±4	2±2	**47±7**	ND	**153±58**	ND	**16±5**	ND	ND	3±3	ND	**ND**	3±3	6±6

NM: not measured.
ND: not detectable (<1.5 nM).
[a] ASP: aspartic acid; GLU: glutamic acid; HIS: histidine; SER: serine; ARG: arginine; GLY: glycine; THR: threonine; ALA, alanine; TYR: tyrosine; MET: methionine; VAL, valine; PHE, phenylalanine; TRP, tryptophan; ILE: isoleucine; LEU: leucine.

Figure 2.1. Schematic flow chart of the HPLC-MS instrumnt design.

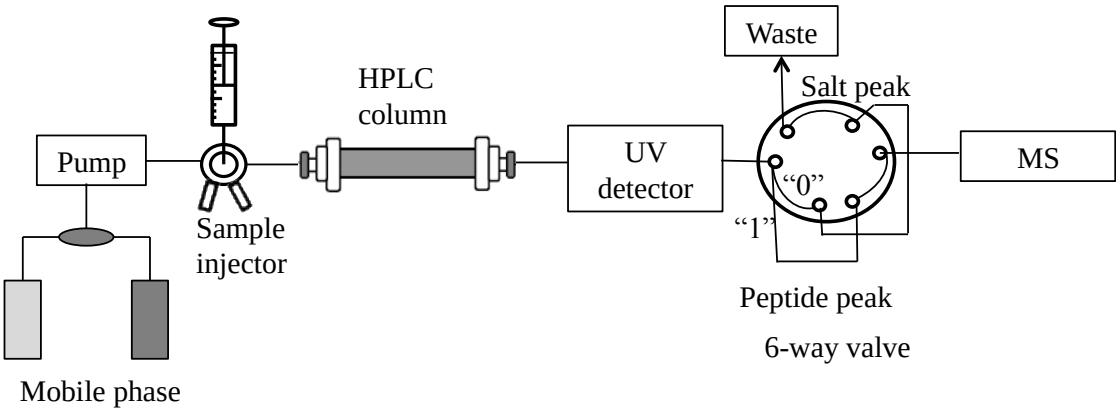

Figure 2.2. HPLC-PDA chromatograms of AVFA standard (20 μmole·L^{-1} in distilled water) using mobile phases consisting of (a) 10 mmol·L^{-1} ammonium acetate and acetonitrile, (b) 10 mmol·L^{-1} ammonium acetate and methanol (target peak labeled as name and retention time).

(a) Acetonitrile

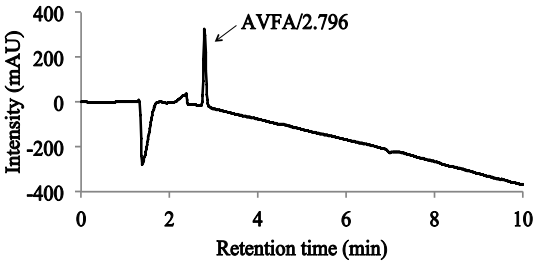

(b) Methanol

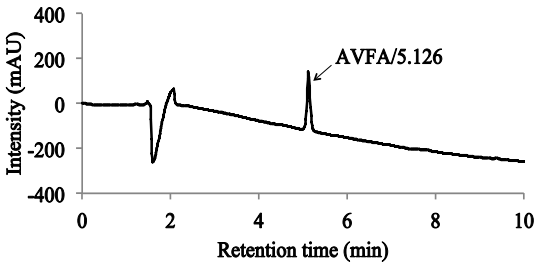

Figure 2.3. HPLC-PDA chromatograms of standard (20 μmole·L^{-1} AVFA in distilled water) using mobile phase composed of methanol and 10 mmol·L^{-1} ammonium acetate of (a) original pH 6.7 and adjusted to (b) pH 5.2, (c) pH 4.5, (d) pH 9.2 (target peak labeled as name and peak area).

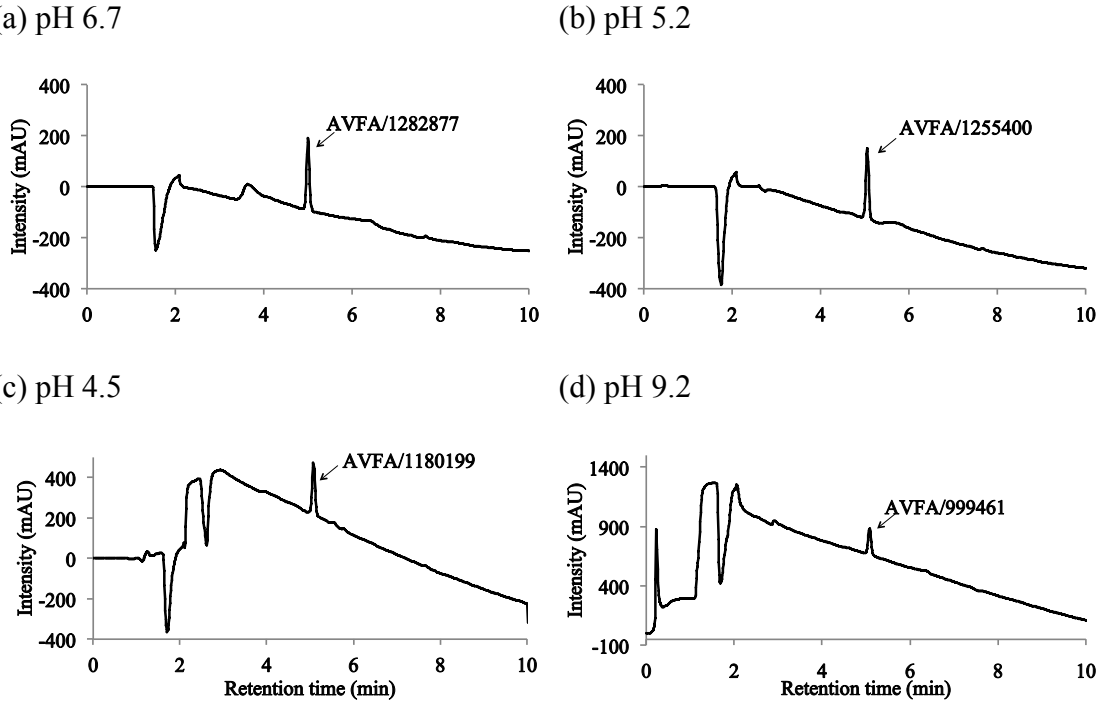

Figure 2.4. (a) Calibration curve of AVFA standard in 0.2-μm filtered seawater ranging from 5 nmol·L^{-1} to 1 μmol·L^{-1} using HPLC-MS. Data points are presented as the average ± SD (n=5); (b) Calibration curve of SWGA standard in distilled water ranging from 0.05 to 0.5 μmol·L^{-1} using HPLC-MS.

(a) AVFA

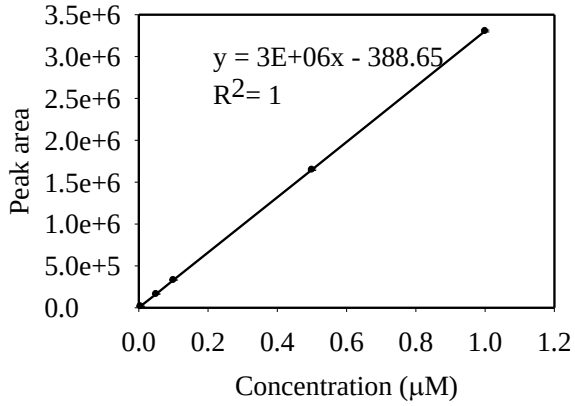

(b) SWGA

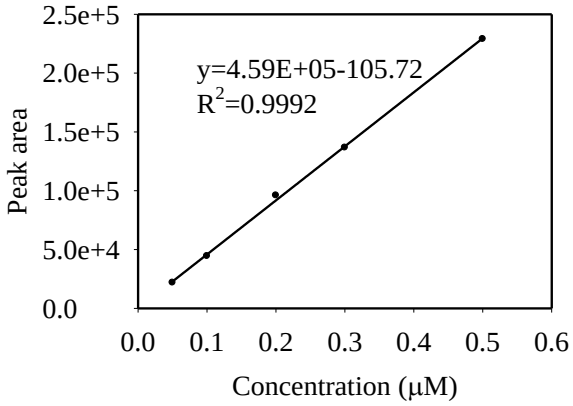

Figure 2.5. Comparison between AVFA (a) 1 μmol·L^{-1} in seawater and 100 μL injection volume; (b) 5 nmol·L^{-1} in seawater and 100 μL injection volume standard peak in HPLC chromatogram with PDA detector and AVFA peak in MS SIM chromatogram at m/z=407 with MS detector. Note that MS detector was off from 0-8 min.

(a) 1 μM

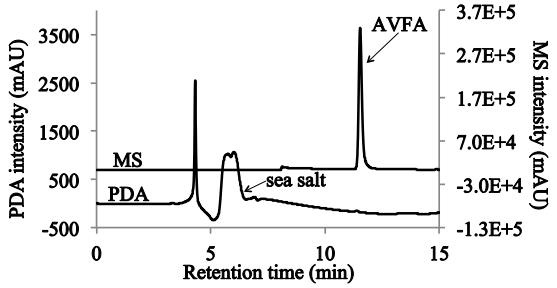

(b) 5 nM

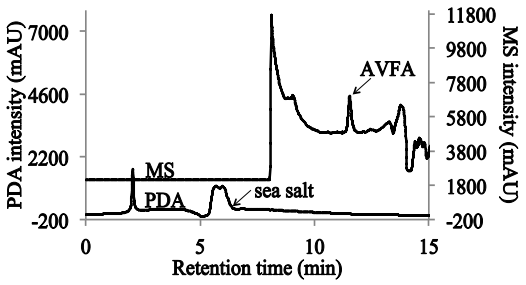

Figure 2.6. (a) AVFA (amendment concentration 0.35 μmol·L^{-1}) and SWGA (amendment concentration 0.41 μmol·L^{-1}) decomposition curves in unfiltered surface seawater collected in the ship channel in Port Aransas, Texas, during 54-h incubations under dark; (b) AVFA (amendment concentration 0.42 μmol·L^{-1}), LYA-AVFA (amendment concentration 0.46 μmole·L^{-1}) hydrolysis curves and AVFA (amendment concentration 0.59 μmol·L^{-1}) concentrations in the killed control in unfiltered surface seawater collected at Sta. T2 in the northern Gulf of Mexico during 24-h incubations under dark.

(a) Ship channel

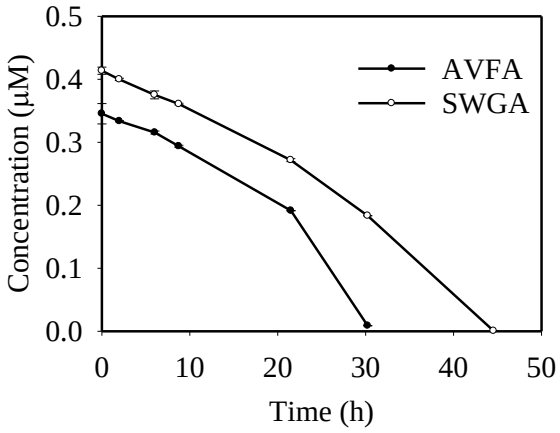

(b) Mississippi River plume

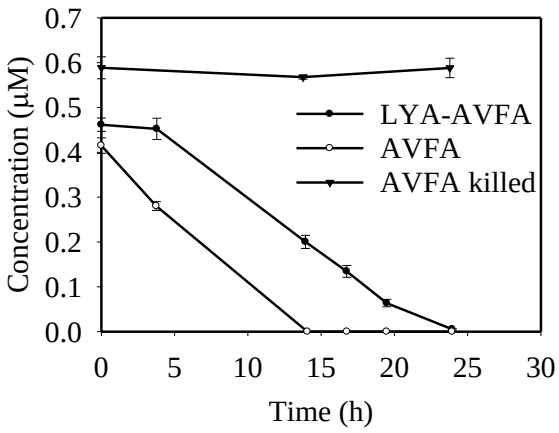

Figure 2.7. Bacterial abundance changes throughout the AVFA and LYA-AVFA incubation in the northern Gulf of Mexico seawater. Data points are presented as the average ± SD (n=3).

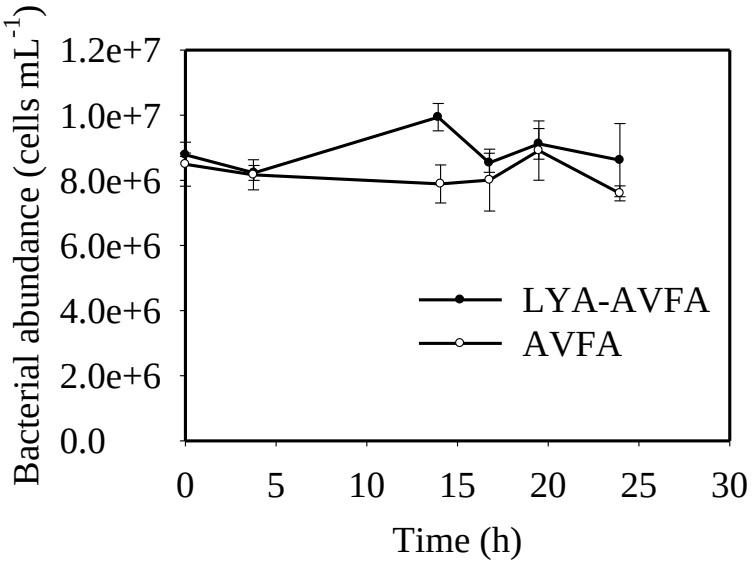

Chapter 3. Comparing extracellular enzymatic hydrolysis between plain peptides and their corresponding analogs in the northern Gulf of Mexico Mississippi River plume

(Published in Marine Chemistry 177 (2015): 398-407)

ABSTRACT

Peptide analogs, such as leucine-methylcoumarinylamide (Leu-MCA) and Lucifer yellow anhydride-tetraalanine (LYA-Ala4), are often used as proxies to quantify extracellular peptidase activities, but how accurately these analogs represent natural peptides remains unclear. Here we compared hydrolysis rates of tetrapeptides alanine-valine-phenylalanine-alanine (AVFA) and tetraalanine (Ala4) with their corresponding LYA analogs along a salinity gradient in the northern Gulf of Mexico Mississippi River plume. Hydrolysis rates were generally similar, but not always, between natural peptides and their analogs in the plume water. For example, hydrolysis rates were similar between LYA-AVFA and AVFA at all stations except one. In contrast, hydrolysis rates of LYA-Ala4 were significantly higher than those of Ala4 at low-salinity (18-19) stations, but significantly lower at one high-salinity (36) station. These results suggest that relative activities of different types of peptidases, measured by the analogs or peptides, depended on biological and chemical properties at each station, such as abundance of certain "opportuni-trophic" bacteria, including *Flavobacterium*, *Ruegeria* and *Roseobacter*. The produced fragments and amino acids from peptide hydrolysis implied further that the hydrolysis pathway depended on specific peptide substrate, and that the LYA tag affected the hydrolysis pathway. Taken together, this study validates the technique of using LYA analogs to study extracellular enzymatic activities, particularly the overall hydrolysis rate,

and provides insights into the patterns of extracellular enzymatic activities in estuarine environments.

INTRODUCTION

As a key step in the cycling of labile organic matter, extracellular enzymatic hydrolysis breaks down proteins or large peptides into small fragments less than approximately 600 Da to allow bacterial uptake in marine environments (Chróst, 1991; Weiss et al., 1991). Extracellular hydrolysis involves enzymes that exist either freely dissolved in seawater or as ectoenzymes that are cell-surface bound or in the periplasmic space (Chróst, 1990). This process, defined here as peptide hydrolysis, not only regulates the turnover rate of carbon and nutrients (Arnosti, 2011), but may also control the types of proteinaceous matter preserved in oceanic dissolved organic matter (Hedges et al., 2000, Aluwihare et al., 2005).

Peptide hydrolysis rates are often estimated using peptide analogs containing fluorogenic tags, such as leucine-methylcoumarinylamide (Leu-MCA) and Lucifer yellow anhydride (LYA)-peptide (Hoppe, 1983; Pantoja et al., 1997; Mulholland et al., 2003; Obayashi and Suzuki, 2005). Hydrolyzed fluorogenic fragments from the analogs, such as MCA from Leu-MCA, can be determined easily by fluorometry. Targeting certain peptidases, these peptide analogs make it possible to compare peptide hydrolysis rates across different aquatic environments, such as lakes, brackish water, fjords, seawater, marine sediments, and coral reefs (Hoppe, 1983; Mow-Robinson and Rheinheimer, 1985; Hoppe et al., 1988a,b; Münster et al., 1989; Rheinheimer et al., 1989). These studies demonstrate the diversity of peptidases and large ranges of enzymatic activities in natural environments.

Despite their extensive application, it remains unclear how representative the peptide analogs are relative to plain peptides without tags, as large fluorogenic tags may affect the enzymatic attack due to the steric effect (Stevenson, 1994; Pantoja et al., 1997; Liu et al., 2010). For example, a large tag containing aromatic rings, such as LYA, can increase the rigidity of a molecule (Wade, 1995), thus possibly affecting how the substrate fits into active sites of enzymes. In addition, fluorogenic tags may block either the N or C terminus of peptides from the peptidase attack, while plain peptides can be attacked from either side or the middle (Arnosti, 2003). Even though plain peptides are presumably more representative, only a few studies have used plain peptides to study peptide hydrolysis or uptake due to the analytical difficulty in detecting plain peptides in close-to-ambient concentrations (Kirchman and Hodson, 1984; Mulholland and Lee, 2009; Liu et al., 2010, 2013). Although it has been demonstrated that protein or plain peptide addition can inhibit the hydrolysis of peptide analogs (Payne, 1980; Hoppe, 1983; Somville and Billen, 1983; Pantoja et al., 1997), no studies have directly compared peptide hydrolysis rates between peptide analogs and plain peptides. Our newly-developed liquid chromatography-mass spectrometry (LC-MS) technique makes this comparison possible by measuring peptides in close-to-ambient concentrations (Liu and Liu, 2014).

In this study we compared peptide hydrolysis rates between two pairs of plain peptides and their corresponding analogs, Ala4 vs. LYA-Ala4 and AVFA vs. LYA-AVFA, along a salinity gradient in the Mississippi River plume of northern Gulf of Mexico (nGOM). AVFA, a fragment of ribulose-1,5-bisphosphate carboxylase/oxygenase (RuBisCO), and Ala4 are two small peptides with molecular weights of 406 and 302 Da, respectively. The AVFA hydrolysis has been examined in several cases (Liu et al., 2010, 2013; Liu and Liu, 2014), but not Ala4. LYA-Ala4 has

been applied to measuring hydrolysis rates in marine environments (Pantoja et al., 1997; Pantoja and Lee, 1999; Mulholland et al., 2002, 2003), but not LYA-AVFA. Owing to the newly developed HPLC-MS technique (Liu and Liu, 2014), peptides were amended in close-to-ambient concentrations of total dissolved amino acids (TDAA), which are comparable to those of peptide analogs used previously (Pantoja et al., 1997, 2009; Mulholland et al., 2003; Powell et al., 2005). The low concentration of amended peptides may simulate *in-situ* environments better without changing much of ambient organic matter concentrations and the bacterial community structure during short-time incubation (Pantoja and Lee, 1999; Kuznetsova and Lee, 2002; Liu et al., 2010, 2013; McCarren et al., 2010).

MATERIALS AND METHODS

Sampling sites

Seawater for peptide incubations was collected from six stations with depths ranging from 17 to 1568 m in the nGOM during a May-2013 cruise on R/V *Pelican*: T1, T2, C6, T3, T6, and DWH (Fig. 3.1 and Table 3.1). Five stations (T1, T2, C6, T3, T6) were located in the Mississippi River plume along the salinity gradient (Breed et al., 2004), and another station was at the site where Deepwater Horizon (DWH) oil spill occurred in 2010. The oil contamination to the surface water at Sta. DWH was not detectable during the sampling (Liu et al., 2014), so results from this station were likely not affected by the oil spill. Based on the salinity (next section and Table 1), these six stations were grouped as low-salinity (18-27) stations (Stas. T1, T2, and C6) and high-salinity (35-36) stations (Stas. T3, T6, and DWH).

Chemical and biological analysis of initial seawater

Surface (2 m) seawater was collected using Niskin bottles mounted on a conductivity-temperature-depth (CTD) rosette (Seabird 911). Simultaneously, *in-situ* temperature, salinity, dissolved oxygen (DO) and chlorophyll *a* were measured by probes in the CTD device (Table 3.1). Seawater was filtered through 0.2 μm Nylon filters (25 mm dia., Whatman) for analyses of dissolved organic carbon (DOC), total dissolved nitrogen (TDN), TDAA, dissolved free amino acids (DFAA) and nutrients. DOC and TDN were analyzed using a total organic carbon analyzer/TDN analyzer (TOC-V/TNM-1, Shimadzu), and errors between duplicate samples were within 6%. DFAA were analyzed by HPLC (Shimadzu Prominence) with fluorescence detection after pre-column *o*-phthaldialdehyde (OPA) derivatization (Lindroth and Mopper, 1979; Lee et al., 2000). TDAA were analyzed in the same way as DFAA but after hydrolysis by 6 N HCl under nitrogen at 110 ºC for 20 h (Kuznetsova and Lee, 2002). Dissolved combined amino acids (DCAA) were calculated as the difference between TDAA and DFAA. Measurements of replicate samples of DFAA and DCAA had standard deviations of 10-20%. Nitrate and nitrite were measured using the cadmium reduction method, phosphate using ascorbic acid method and ammonium using indophenol method through a UV-Vis spectrophotometer (Evolution 160, Thermo Scientific) (Strickland and Parsons, 1968; Jones, 1984). Dissolved organic nitrogen (DON) was calculated after TDN subtracting nitrate, nitrite and ammonium.

For bacterial enumeration, surface water (1 mL) from each station was fixed in 3% (final concentration) formaldehyde and preserved at 4 ºC. Bacteria cells were stained with diluted (1:100 v/v) nucleic acid dye SYBR Green II (Molecular probes) and then enumerated under laser excitation at 488 nm with a flow cytometer (BD Accuri C6)

following procedures described in Liu et al. (2013). The counting error for duplicate samples was about 12%.

Seawater (0.5-1 L) from each station was filtered through 0.2 μm pore-size Nylon filters for bacterial community structure analysis. The filters were sent to the Research and Testing lab (Lubbock, TX) for pyrosequencing following the procedures described in Liu et al. (2013). The community structure analysis was performed based on bacterial tag-encoded FLX amplicon pyrosequencing (bTEFAP) method with 16S universal Eubacterial primers Gray28F 5'TTTGATCNTGGCTCAG and Gray519r 5'GTNTTACNGCGGCKGCTG for PCR (Dowd et al., 2008; Smith et al., 2010). Tag-encoded FLX amplicon pyrosequencing using a Roche 454 FLX instrument with Titanium reagents in a half plate mode followed the RTL protocols (www.researchandtesting.com). Sequences were classified at the genus level with identity scores between 90% and 95%. Community structures (% genera) of heterotrophic bacteria at all stations were compared by principal component analysis (PCA) using MATLAB® (Xue et al., 2011).

Peptide incubation

Ala4 and AVFA were custom-synthesized using a solid phase peptide synthesizer by CS Bio. LYA-Ala4 and LYA-AVFA were synthesized through reflux of LYA dipotassium salt (4-amino-3,6-disulfo-1,8-naphthalic anhydride dipotassium salt, Sigma) and Ala4/AVFA in lithium acetate (reagent grade, Sigma), and purified through HPLC according to the protocol of Pantoja et al. (1993). Ala4, AVFA, LYA-Ala4, and LYA-AVFA were incubated on board immediately after surface seawater was collected from two low-salinity stations (T1, T2) and two high-salinity stations (T3, DWH) (Table 3.1).

Each substrate, with a final concentration in the range of 0.23-0.69 μM that accounted for 4-40% of DCAA (Table 3.1), was respectively amended in 30 mL amber glass bottles (in duplicate for Sta. DWH or triplicate for Stas. T1, T2 and T3) with 2 mL headspace. The incubation lasted for 24 h in the dark at room temperature (24 ºC), which was similar to the *in-situ* temperature (Table 3.1). At time intervals of ca. 0, 4, 8, 10, 12, 16, 20, and 24 h, duplicate or triplicate aliquots (1.5 mL) were sampled from the incubation bottles, filtered through 0.2 μm cellulose acetate (CA) syringe filters (13 mm dia., Whatman GD/X) and preserved at -20 ºC until analysis. One aliquot (1 mL) from each bottle was fixed with 3% (final concentration) formaldehyde for bacterial abundance analysis.

In addition to the incubations at the 4 stations described above, AVFA, with final concentrations of 0.47-0.50 μM, was incubated at two other stations, C6 and T6 (Fig. 3.1). AVFA was incubated in duplicate series of 125 mL amber glass bottles with 25 mL headspace, and duplicate bottles were sacrificed for sampling at 0, 8, 14, and 24 h, respectively. Incubation waters were amended with 180 μM $HgCl_2$ to provide killed controls (Lee et al., 1992). Aliquots were taken for peptide analysis at 0, 8, 16, and 24 h following the same sampling protocols.

Peptide and amino acid analyses

LYA-Ala4 and LYA-AVFA were measured by HPLC with a fluorescence detector (Pantoja et al., 1997). AVFA was measured by HPLC-MS (Liu and Liu, 2014). Ala4 was derivatized with OPA and then quantified with HPLC (Pantoja and Lee, 1999). Detailed analyses of each peptide and their hydrolyzed peptide fragments or amino acids are described below.

LYA-Ala4 and LYA-AVFA, together with the hydrolysis products including LYA-Ala (or A), LYA-Ala2, LYA-Ala3, LYA-AV and LYA-AVF, were analyzed by HPLC (Shimadzu Prominence) with a fluorescence detector (Pantoja et al., 1997). Mobile phase A (aqueous phase) was 0.05 M sodium phosphate (monobasic anhydrous, ACS grade, VWR) with pH of 4.5, and mobile phase B (organic phase) was methanol (HPLC grade, Fisher). Samples were eluted through a C_{18} column (Alltima 5 μm, 250 mm × 4.6 mm) maintaining at 40 ºC at a flow rate of 1 $mL \cdot min^{-1}$. For LYA-Ala4, mobile phase B was increased from 10% to 30% during the first 12 min, then to 50% at 13 min, and further to 100% at 14 min, and held at 100% for 1 min. For LYA-AVFA, mobile phase B was increased from 10% to 50% at 25 min, then from 50% to 100% at 26 min, and held at 100% until 32 min. Target peaks of the peptide analogs were detected with a fluorescence detector (Ex: 424 nm; Em: 550 nm), and quantification was based on external standards. Limited by availability, LYA-AV and LYA-AVF were estimated using the response factor (injection amount/peak area) of LYA-AVFA. This assumption is reasonable as the fluorescence was mainly due to the large LYA tag. For example, similar response factors were observed between LYA-AVFA and LYA-A in our analysis. Authentic standards of LYA-Ala3 and LYA-Ala2 were not synthesized, but LYA-Ala2 and LYA-Ala3 were quantified according to Pantoja and Lee (1999), where similar analytical conditions were used.

Ala4 and its hydrolysis products (Ala3, Ala2 and Ala) were quantified with HPLC after pre-column OPA derivatization (Lindroth and Mopper, 1979; Lee et al., 2000). Briefly, the mobile phase A was 0.05 M sodium acetate (HPLC grade, Fisher) with 5% tetrahydrofuran (HPLC grade, Mallinckrodt Baker) and pH 5.7 and mobile phase B was methanol. For the gradient program, mobile phase B was increased from 20% to 60% during the first 40 min, further to 100% in the next 8 min and then held at 100% for 10

min. Concentrations were quantified by a fluorescence detector (Ex: 330 nm; Em: 418 nm) based on external standards. Since Ala3 overlapped with Ala2 in the HPLC chromatograms, their concentrations were summed using the response factor of Ala3. Note that the summed concentrations might be overestimated because the response factor of Ala3 was higher than that of Ala2, but this problem was not a concern here since their concentrations were close to zero in our samples (see Results).

AVFA and its hydrolyzed fragments were analyzed using HPLC-MS (Shimadzu Prominence) following the protocol of Liu and Liu (2014). In brief, samples were eluted through a C_{18} column (Alltima 5μm, 150 mm × 4.6 mm) with mobile phase A as 10 mM ammonium acetate and mobile phase B as methanol in a gradient program at a flow rate of 0.3 $mL \cdot min^{-1}$. A 6-way valve was programmed to direct the sea salt peak to waste before introducing the targeted peaks to the MS detector, which consists of an electrospray ionization (ESI) source and a quadrupole mass analyzer. The MS detector voltage was set at 1.20 kV, interface source temperature at 350 ºC and desolvation line (DL) temperature at 250 ºC. AVFA and fragments VFA, AVF, VF, FA, AV were analyzed through positive ion mode with selective ion monitoring (SIM) at $[M + H]^+$ ion state of m/z = 407, 336, 265, 237, and 189, respectively. Amino acids released from AVFA hydrolysis were analyzed by HPLC after pre-column OPA derivatization.

Peptide hydrolysis rates were determined as the slope of the linear regression of hydrolysis curves plotted using concentrations vs. incubation time. Note that the regressions were done only for early time intervals before peptide concentrations became undetectable, typically within 8-24 h. Hydrolysis rates between plain peptides and peptide analogs at each station, or AVFA hydrolysis rates among different stations, were compared through one-way ANOVA ($\alpha = 0.05$) and Bonferroni *t* test ($\alpha = 0.05$). Pairwise Spearman rank correlation analysis was applied to the seawater chemical and

biological parameters, and AVFA hydrolysis rates at all stations to avoid issues of non-normal data (Kendall, 1990). Significant correlation between environmental parameters and AVFA hydrolysis rates or among environmental parameters was determined using the rcorr function in the "Hmisc" package in R.

RESULTS

Chemical and biological properties of the initial seawater

Low-salinity Stas. T1, T2, and C6 were located close to the Mississippi River mouth, whereas high-salinity Stas. T3, T6, and DWH were further offshore (Fig. 3.1 and Table 3.1). This salinity gradient corresponds to the unidirectional west/southwest flow of Mississippi River water diluted by oceanic water (Hitchcock et al., 1997; Breed et al., 2004). As expected, chemical and biological properties differed greatly between the low-salinity and high-salinity stations (Table 3.1). Concentrations of chlorophyll *a* and nitrate at the low salinity stations were more than one order of magnitude higher than at the high-salinity stations. Ammonium, DOC and DON concentrations at the low-salinity stations were about twice as high as those at the high-salinity stations except for Sta. DWH. DCAA and DFAA were highest at Sta. T1, and slightly higher at Sta. T2 than at other high-salinity stations except for Sta. DWH. Bacterial abundances in the low-salinity waters were 2-10 times as high as those in the high-salinity waters.

Community structures of heterotrophic bacteria differed greatly between low-salinity and high-salinity waters (Fig. 3.2 and Table 3.2). While the low-salinity waters (T1, T2, C6) were enriched in *Flavobacterium* (13-31%), *Ruegeria* (6-10%) and *Roseobacter* (3-11%), the high-salinity waters (T3, T6, DWH) contained mainly *Candidatus Pelagibacteri* (30-42%) and *Sphigobacterium* (9-11%). This difference was

examined further in the PCA biplot of major heterotrophic bacterial genus at all stations (Fig. 3.3). Bacterial communities at the low-salinity sites were clustered clearly as one group and high-salinity ones as the other along PC1, which explained 91% of the data variance.

Comparison of hydrolysis rates and pathways between plain peptides and LYA analogs

Hydrolysis rates of plain peptides and analogs ranged from near zero in the high-salinity waters to 48 $nM \cdot h^{-1}$ in the low-salinity waters (Figs. 3.4, 3.5, 3.6, 3.7 and 3.8). These rates are consistent with previous incubation studies when similar concentrations of substrates were amended (Pantoja et al., 1997; Pantoja and Lee, 1999; Mulholland et al., 2003; Liu and Liu, 2014). Hydrolysis rates between plain peptides and the corresponding analogs were similar in 4 out of 8 cases (Fig. 3.5). LYA-AVFA and AVFA had similar hydrolysis rates at all stations except at Sta. T2. In contrast, hydrolysis rate of LYA-Ala4 was significantly lower than that of Ala4 at Sta. T3 and similar to that at Sta. DWH, but was higher than those of Ala4 at Stas. T1 and T2. This result was surprising, as we expected that LYA on the N-terminus of Ala4 may block the hydrolysis by aminopeptidases and thus reduce the hydrolysis rate.

LYA-AV and LYA-AVF were the major fragments released during the LYA-AVFA hydrolysis at Stas. T1, T3 and DWH, while LYA-AV was the major hydrolysis products at Sta. T2 (Fig. 3.9). LYA-AV accounted for 70%, 53% and 49%, and LYA-AVF accounted for 25%, 42% and 49% of all peptide fragments at the end of LYA-AVFA incubations at Stas. T1, T3, and DWH, respectively. At Sta. T2, concentration of LYA-AV was 8 times higher than that of LYA-AVF and 3 times higher than that of LYA-A at the end of incubation. In comparison, dipeptide AV or FA fragments were

undetectable during the AVFA hydrolysis at these four stations, and the main hydrolyzed products at all stations were amino acids A, V and F (Fig. 3.10). A, V and F increased with time during peptide hydrolysis at all stations and then decreased after AVFA was completely hydrolyzed at Stas. T1 and T2. Among the three amino acids, concentrations of F were highest, followed by V and A. Accounting for <10% of hydrolyzed AVFA, VFA and AVF were the only peptide fragments observed (Fig. 3.10). Produced VFA concentrations were 2-22 times higher than AVF concentrations at Sta. T1, T2 and DWH, while 6 times more AVF than VFA was released at Sta. T3.

Similar to LYA-AVFA, LYA-Ala2 was the dominant fragment throughout the incubation of LYA-Ala4, and accounted for 93-99% of all fragments at the four stations (Fig. 3.11). During the Ala4 hydrolysis, peptide fragments Ala2 and Ala3 were nearly undetectable, whereas Ala was the only major hydrolysis product (Fig. 3.12). For AVFA and Ala4, concentrations of total hydrolysis products (use the sum of AVF, VFA and F concentrations for AVFA hydrolysis, and use Ala concentrations for Ala4 hydrolysis) accounted for 52-100% of total hydrolyzed peptides, except <40% for Ala4 at Stas. T1 and T3, and the hydrolysis percentages (concentrations of hydrolysis products divided by initial amended peptide concentrations) were generally higher than the uptake percentages (Figs. 3.13 and 3.14).

Concentrations of LYA-Ala4, LYA-AVFA and AVFA in killed controls remained relatively constant during the incubation (Figs. 3.4, 3.6, and 3.7). However, Ala4 concentrations decreased 26-65%, especially at Sta. T2 (Fig. 3.8). This decrease was probably due to some free extracellular enzymes that may specifically hydrolyze Ala4, since $HgCl_2$ does not suppress those extracellular enzymes without sulfhydryl groups (Lee et al., 1992; Liu et al., 2006). This pattern also indicates that the extracellular

enzymes that hydrolyzed Ala4 were different than those hydrolyzing other peptides or analogs.

Changes of bacterial abundances during peptide hydrolysis

At Sta. T1, bacterial abundances during the peptide incubations increased 9-22% from 0 h to 10-12 h, and then increased more rapidly from 12 to 25 h when the peptide hydrolysis was nearly complete (Fig. 3.15a). The rapid bacterial growth after 10-12 h indicates that bacteria began utilizing the hydrolysis products to build their biomass, and this time frame is consistent with bacterial generation time of 9-12 h (Eilers et al., 2000). At Sta. T2, bacterial abundances in the LYA-Ala4, LYA-AVFA and AVFA incubations increased <11% throughout the incubation, but increased 67% at 20 h in the Ala4 treatment (Fig. 3.15b). At Sta. T3, bacterial abundance gradually increased by 3-16% from the initial time to the end of incubation (Fig. 3.15c). Bacterial abundances in the peptide analogs treatments at Sta. DWH increased 18-28% at 24 h, whereas those in the peptide treatments increased 17-25% during 0-8 h and decreased 14-16% afterwards (Fig. 2.15d).

Comparison of AVFA hydrolysis along the salinity gradient

In addition to the hydrolysis comparison between plain peptides and LYA analogs at four stations, we further compared AVFA hydrolysis rates at all 6 stations (Fig. 3.16). AVFA hydrolysis rates differed significantly among all stations except those between Stas. T3 and T6 (Fig. 3.17, $p<0.05$). Hydrolysis rates decreased from 13-23 $nM \cdot h^{-1}$ in the low-salinity waters (T1, T2, C6) to 1-5 $nM \cdot h^{-1}$ in the high-salinity waters (T3, T6, DWH). In contrast, AVFA concentrations remained nearly constant in the killed controls

at these 6 stations (Fig. 3.18), indicating that the decrease of peptide concentrations in the seawater treatments was caused by biological processes instead of physical absorption to glass bottles or particles. Bacterial abundance was highest in the T2 seawater throughout the incubation, followed by T1 and C6 seawater, and then the other high-salinity waters (Fig. 3.19). Bacterial abundance increased 5-56% during 10-20h in the low-salinity waters, and increased 15-30% during 16-24 h in the high-salinity waters.

AVFA hydrolysis rates along the salinity gradient correlated significantly with salinity (Fig. 3.20), chlorophyll *a*, DON, nitrate, bacterial abundance and bacterial community structure (use PC1 as the index) in the initial seawater, especially with salinity at a correlation coefficient of -1.00 (Table 3.3). These environmental factors also co-varied with each other. For instance, significant correlations were found between salinity and chlorophyll *a*, DON, nitrate, bacterial abundance, or bacterial community.

DISCUSSION

Concentrations of peptides and peptide analogs generally decreased linearly during short incubation times (Figs. 3.4, 3.6, 3.7 and 3.8), consistent with previous studies in this region and coastal waters off Port Aransas, TX (Liu et al., 2013; Liu and Liu, 2014). This linearity was consistent with a zero-order reaction model, indicating that the hydrolysis was limited by peptidases rather than substrates. If the hydrolysis is limited by substrate, an exponential decrease (first order reaction) would be expected (Pantoja et al., 1997; Stein, 2011). This linear pattern also indicates that peptide hydrolysis was not significantly affected by biological and chemical changes during incubation, such as the changes of bacterial abundance over time (Figs. 3.15 and 3.19).

Comparing hydrolysis rates and pathways between plain peptides and analogs

We expected that plain peptides would be hydrolyzed faster than their corresponding peptide analogs because the tag may block the attack of peptidases due to steric hindrance, which in turn affects how active sites of the enzyme fit into the peptide bonds. For instance, while plain peptides, such as AVFA and Ala4, can be hydrolyzed from both N and C termini by aminopeptidases and carboxypeptidases and from middle by endopeptidases, their LYA analogs are only hydrolyzed by carboxypeptidases and endopeptidases (Stevenson, 1994; Pantoja et al., 1997; Liu et al., 2010). However, hydrolysis rates derived from LYA-peptide analogs were generally similar to, or higher than, plain peptide in many cases. For example at Stas. T1 and T2, hydrolysis rates of LYA-Ala4 were higher than Ala4 while LYA-AVFA and AVFA were hydrolyzed at similar rates (Fig. 3.5). Apparently, the hydrolysis rate was not affected much by the tag or the types of peptidases that cleave the substrate.

Plain peptides and their analogs were clearly hydrolyzed through different pathways judged from the hydrolyzed products, assuming that their uptake was minimal during the short incubation. This assumption seems reasonable, as the sum of hydrolysis products typically accounted for ca. 52%-100% of the peptide except for <40% for Ala4 at Stas. T1 and T3, and hydrolysis percentages were generally much higher than uptake percentages (Figs. 3.13 and 3.14). The dominance of LYA-AV (Fig. 3.9), with the simultaneous FA produced during the LYA-AVFA incubation (data not shown), indicates that endopeptidases played a major role in the hydrolysis. Similarly, the major production of LYA-Ala2 suggested that LYA-Ala4 was mainly hydrolyzed by endopeptidases at all the four stations (Fig. 3.11). Likewise, carboxypeptidases were important in cleaving LYA-AVFA from C terminus at Stas. T1, T3 and DWH, because concentrations of LYA-AVF were the second highest among all fragments (Fig. 3.9). In contrast, AVFA and

Ala4 hydrolysis produced mainly free amino acids instead of peptide fragments, suggesting a different hydrolysis pathway from that of peptide analogs (Figs. 3.10 and 3.12).

The different hydrolysis pathways between plain peptides and LYA analogs may be caused by the LYA tag. On one hand, the LYA tag may have blocked the attack of aminopeptidases, which could be important for plain peptide as revealed by the high production of VFA fragments during AVFA hydrolysis. On the other hand, the LYA tag may have affected the susceptibility of peptide bonds to peptidases. For example, the dominance of amino acids as hydrolysis products of plain peptides indicated that their sequential hydrolysis was fast and complete, or that all peptide bonds in plain peptides were hydrolyzed by different enzymes in a simultaneous manner. In contrast, the accumulation of LYA-dipeptide products suggests that the peptide bond in LYA-dipeptide was resistant to peptidases, rather than the lack of dipeptidases, as argued by Pantoja and Lee (1999). Otherwise, accumulation of dipeptide would be expected from the hydrolysis of plain peptides. Alternatively, the lack of dipeptide during the hydrolysis may result from direct uptake by bacteria. However, given that the uptake of dipeptides, such as FA and Ala2, is typically slower than that of amino acid A (unpublished preliminary data), the rapid accumulation of amino acids than dipeptides in all incubations indicated that dipeptides were hydrolyzed further into amino acids rather than being taken up directly. Perhaps the steric hindrance of the LYA tag on peptide hydrolysis occurred mostly at the dipeptide bond, because LYA-tetrapeptides were hydrolyzed efficiently to LYA-tripeptides and further to LYA-dipeptides. Therefore, the effect of LYA on hydrolysis may depend on the distance between the LYA and peptide bonds, i.e., steric effects may be higher for closer bonds, as exemplified for LYA-dipeptide. This explanation is consistent with the observation that amino acids directly

attached to aromatic rings are less available to microorganisms than those further away along a peptide chain (Stevenson, 1994). Overall, these comparative results provide evidence that hydrolysis of dipeptide is hindered by the steric effects of analog tags.

The relative activities of peptidases differed at each station, which was likely related to biological parameters at each station. For example, while endopeptidases hydrolyzed LYA-Ala4 faster than aminopeptidases and/or carboxypeptidases hydrolyzed Ala4 in the T1 and T2 seawater, they were less efficient in the T3 and DWH seawater (Fig. 3.5). Ectoenzymes often account for a major fraction of hydrolytic activities in marine environments (Rego et al., 1985; Martinez and Azam, 1993; Davey et al., 2001), and these enzymes are mainly synthesized by bacteria, so variations in enzymatic activities among these stations may be caused by different bacterial community compositions (Nagata, 2008), as the types and activity levels of hydrolytic enzymes differ among bacterial species (Martinez et al., 1996; Arrieta and Herndl, 2002; Arnosti et al., 2005). For example, the cell-specific aminopeptidase activities from 44 marine isolates varied across three orders of magnitude (Martinez et al., 1996). Also, changes of aminopeptidase activity were correlated to bacterial community structure in a mesocosm experiment (Murray et al., 2007). The distinct heterotrophic bacterial community structures observed between low-salinity Stas. T1 and T2 and high-salinity Stas. T3 and DWH may have caused the variation of relative peptidases activities (Fig. 3.2). Perhaps the *Flavobacterium*, *Ruegeria* or *Roseobacter* enriched in the low-salinity waters had higher endopeptidase activities than other bacteria (Cottrell and Kirchman, 2000), leading to significantly higher hydrolysis rates of LYA-Ala4 than Ala4 at Stas. T1 and T2. In addition to bacteria, extracellular peptidases can be produced by protists (Karner et al., 1994; Mohapatra and Fukami, 2004; Salerno and Stoecker, 2009; Thao et al., 2014), which may contribute to the variation of peptidase activities among different stations.

However, our preliminary data showed that the role of protists in peptide hydrolysis at Sta. C6 is limited by comparing peptide hydrolysis between different size-fractioned seawater containing protists vs. without protists in a May-2012 cruise (Liu et al., 2015). Whether this holds true for other stations in this area needs more investigation.

Effects of salinity on peptide hydrolysis

Peptide hydrolysis rates vary in different marine environments, and salinity is often a key environmental parameter that can affect hydrolysis (Mulholland et al., 2003; Roth and Harvey, 2006). In our study, chemical and biological parameters differed greatly between the low-salinity and high-salinity waters, including concentrations of organic matter and nutrients, phytoplankton and bacterial biomass, and bacterial community structures (Table 3.1 and Fig. 3.2). In these different seawater environments, both peptide analogs and plain peptides were hydrolyzed faster in the low-salinity waters than in the high-salinity waters (Figs. 3.5 and 3.20), and hydrolysis rates of AVFA showed an excellent correlation with salinity (Table 3.3 and Fig. 3.20). This pattern may be attributed to the different environmental parameters among the sampling sites, as peptide hydrolysis rate was significantly correlated with chlorophyll *a*, DON, nitrate, bacterial abundance and community structure (using the PC1 index). For instance, higher proportions of *Flavobacterium* were found in low-salinity waters than high-salinity waters (Fig. 3.2), which is consistent with previous studies (Kirchman et al., 2005; Herlemann et al., 2011; Fortunato et al., 2012; Campbell and Kirchman, 2013). *Cytophaga-Flavobacteria* are well known for their capability to degrade biopolymers including proteins (Delong et al., 1993; Cottrell and Kirchman, 2000; Kirchman, 2002). These *Flavobacterium*, some belonging to opportuni-trophs, which are highly motile and

can move towards high-nutrient conditions (Polz et al., 2006; McBride et al., 2009), could have contributed to the observed higher hydrolytic activity in the low-salinity region.

Effects of amino acid compositions on peptide hydrolysis

The hydrolysis fragments of LYA-Ala4 and LYA-AVFA suggest that carboxypeptidases preferred to hydrolyze LYA-AVFA than LYA-Ala4, as much less LYA-Ala3 was produced than LYA-AVF (Figs. 3.9 and 2.11). This preference of carboxypeptidases to LYA-AVFA was perhaps due to stronger van der Waals interactions between carboxypeptidases and the bulkier amino acids F, V than A (Pantoja and Lee, 1999). For example, carboxypeptidase A showed a higher degree of stereospecificity toward the penultimate amino acid from the C-terminus, and the interaction between carboxypeptidase and substrate can be extended to five amino acids beyond the C terminus (Schechter, 1970). Carboxypeptidase A also displayed a preference towards penultimate amino acids with aromatic side chains (Smith, 1948; Christianson and Lipscomb, 1989), so F in LYA-AVFA could fit carboxypeptidases better and thus enhance carboxypeptidase activities relative to LYA-Ala4. Besides carboxypeptidases, substrate composition can affect endopeptidase activities (Obayashi and Suzuki, 2005), thus different amino acid compositions between LYA-AVFA and LYA-Ala4 may have caused endopeptidase activities to vary. More peptide substrates with different sizes and compositions are needed to further examine the peptidase specificity on substrates.

CONCLUSION

This study provides the first dataset on the comparison of peptide hydrolysis rates between plain peptides and their corresponding analogs at low concentrations (less than micromolar) in seawater. Several conclusions were drawn from the results:

1. The overall similar hydrolysis rates between plain peptides their corresponding LYA-tetrapeptides suggest that LYA-tetrapeptides are good proxies to study peptide hydrolysis rates. However, their hydrolysis pathways differed due to the steric effects of the LYA tag.
2. Different hydrolysis patterns occur between peptide analogs and plain peptides, which may relate to different relative peptidase activities in seawater environments with different bacterial community structures. Thus, caution is needed when extrapolating comparison results between plain peptides and analogs from one environment to another.
3. The hydrolysis pathway of a peptide can be affected by its amino acid composition, as carboxypeptidases preferably hydrolyzed peptides with bulkier amino acids, such as F and V.

Overall, this study offers insights into hydrolysis rates and patterns of extracellular enzymes in estuarine environments using both plain peptides and their analogs. Different biological and chemical factors among waters with different salinities, together with amino acid compositions in peptides, contribute to different hydrolysis patterns and pathways in estuarine environments.

Table 3.1. Environmental parameters of initial surface (2 m) seawater at sampling sites.

Site	Coordinates	Temp (℃)	Salinity (ppt)	DO (mg·L^{-1})	Chl *a* (μg·L^{-1})	DOC (μM)	DON (μM)	DCAA (μM)	DFAA (μM)	NO_3^- (μM)	NO_2^- (μM)	PO_4^{3-} (μM)	NH_4^+ (μM)	Bacterial abundance (cells·ml^{-1})
T1	28.97ºN, 89.47ºW	25.2	18	7.4	1.65	216.7	27.9	5.42	0.30	18.43	0.76	0.31	3.65	$1.85*10^6$
T2	28.85ºN, 89.80ºW	25.2	19	6.6	0.82	258.3	35.6	2.95	0.28	15.99	ud	0.11	1.97	$8.49*10^6$
C6	28.87ºN, 90.50ºW	25.5	27	7.9	1.51	233.3	12.9	1.79	0.18	0.54	ud	0.11	0.85	$1.47*10^6$
T3	28.58ºN, 90.05ºW	24.4	36	6.7	0.08	108.3	8.4	2.88	0.11	0.02	ud	0.11	0.90	$8.32*10^5$
T6	27.72ºN, 90.94ºW	25.4	36	6.5	0.04	83.3	6.9	2.34	0.07	0.05	ud	0.11	0.12	$3.66*10^5$
DWH	28.74ºN, 88.36ºW	25.1	35	6.6	0.10	325.0	14.8	5.08	0.13	0.03	ud	0.14	0.89	$9.19*10^5$

ud: under detection limit (ca. 0.03 μM)

Table 3.2. Major heterotrophic bacterial community structure (normalized as genus%) of initial seawater at each station.

Genus	T1	T2	C6	T3	T6	DWH
Flavobacterium	13.4	20.0	31.4	5.8	7.6	10.4
Ruegeria	9.4	10.0	5.7	3.0	0.2	2.4
Candidatus Pelagibacter	4.0	4.3	3.3	41.4	42.3	30.1
Roseobacter	10.7	8.1	3.3	2.9	0.4	2.3
Glaciecola	1.3	2.3	2.1	2.8	0.6	5.1
Sphingobacterium	2.3	2.1	0.0	9.8	8.9	10.7
Microbulbifer	0.3	0.6	0.0	3.9	0.8	5.3
Alteromonas	5.6	0.0	0.0	0.3	2.4	0.0
Others	53.0	52.6	54.0	30.0	36.7	33.7

Table 3.3. Correlation coefficients among environmental parameters or between environmental parameters and AVFA hydrolysis rates. Significant correlation was marked with asterisk (*p<0.05; **p<0.001).

	Temp	Salinity	DO	Chl *a*	DOC	DON	NO_3^-	NO_2^-	PO_4^{3-}	NH_4^+	Bacterial abundance	Bacterial community PC1	AVFA hydrolysis rate
Temp	1												
Salinity	0.33	1											
DO	0.37	-0.47	1										
Chl *a*	-0.12	-0.93*	0.75	1									
DOC	-0.59	-0.46	0.12	0.43	1								
DON	-0.62	-0.87*	0.20	0.71	0.71	1							
NO_3^-	-0.12	-0.90*	0.29	0.77	0.14	0.66	1						
NO_2^-	-0.27	-0.66	0.40	0.65	-0.13	0.39	0.65	1					
PO_4^{3-}	-0.68	-0.51	0.19	0.51	0.30	0.44	0.34	0.77	1				
NH_4^+	-0.50	-0.70	0.32	0.60	0.26	0.77	0.49	0.65	0.51	1			
Bacterial abundance	-0.32	-0.93*	0.41	0.83*	0.60	0.94*	0.77	0.39	0.27	0.71	1		
Bacterial community PC1	0.32	0.93*	-0.23	-0.77	-0.54	-0.89*	-0.89*	-0.39	-0.27	-0.54	-0.94*	1	
AVFA hydrolysis rate	-0.33	-1.00**	0.47	0.93*	0.46	0.87*	0.90*	0.66	0.51	0.70	0.93*	-0.93*	1

Figure 3.1. Sampling sites in the northern Gulf of Mexico. Colored isobath contours show depths of the water column. Solid dots, low-salinity stations (C6, T1, T2); open dots, high-salinity stations (T3, T6, DWH).

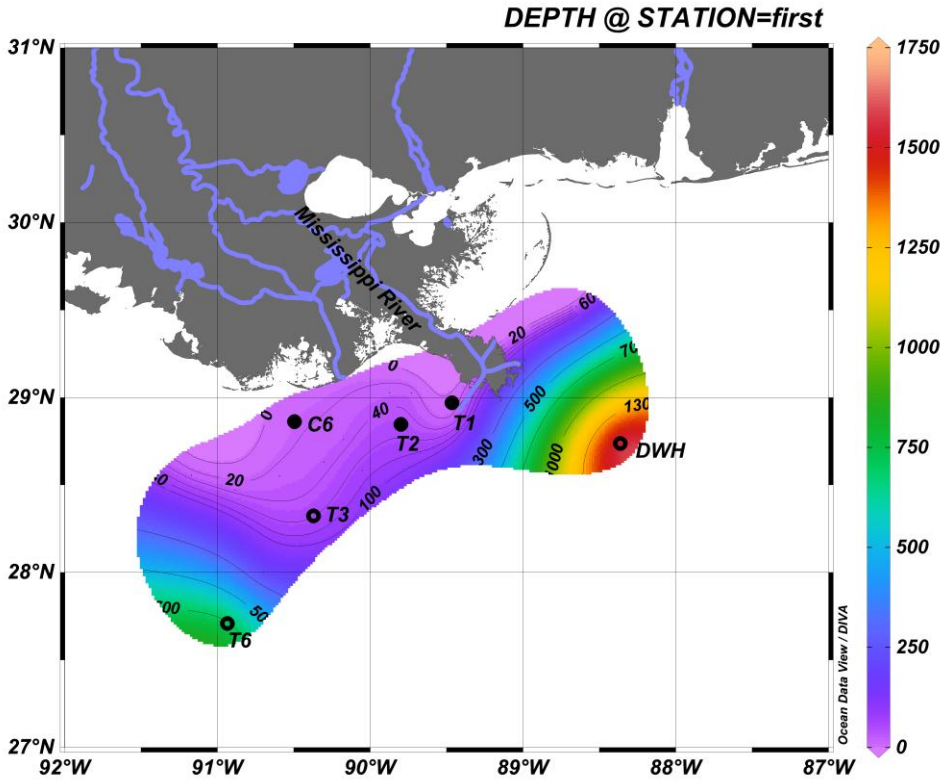

Figure 3.2. Major heterotrophic bacterial genus composition (normalized as percentage) of initial seawater at each station.

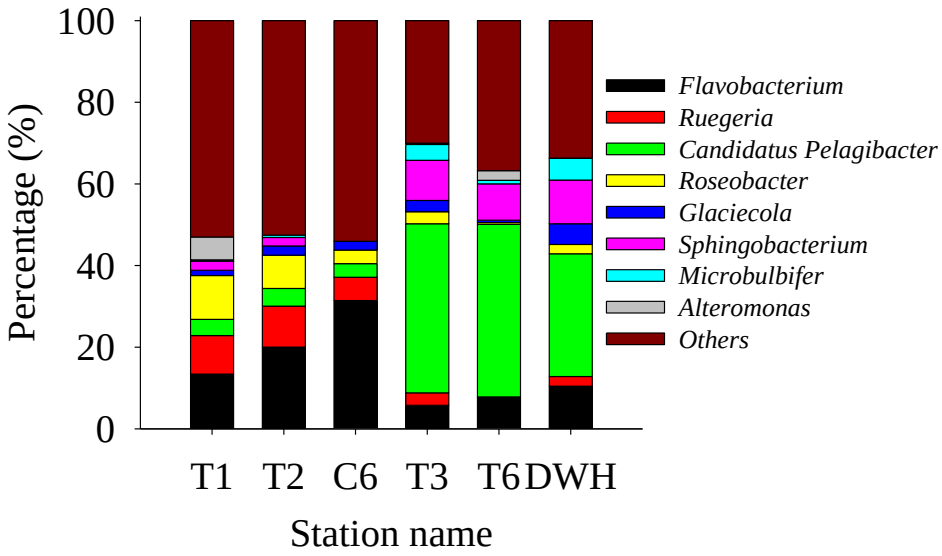

Figure 3.3. PCA analysis of major heterotrophic bacterial genus of initial seawater at sampling stations. Distinct groups were clustered in circles.

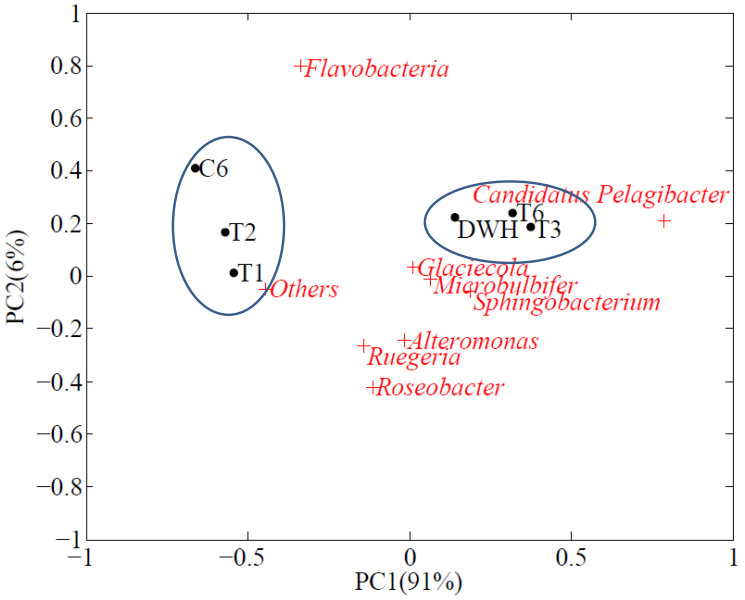

Figure 3.4. LYA-AVFA hydrolysis curves with killed control curves (concentration vs. incubation time) at Stas. (a) T1, (b) T2, (c) T3, and (d) DWH. Data points were presented as average ± standard deviation of replicate samples. Note LYA-AVFA killed control was not conducted at Sta. DWH. Part of the Sta. T2 hydrolysis data was published in Liu and Liu (2014).

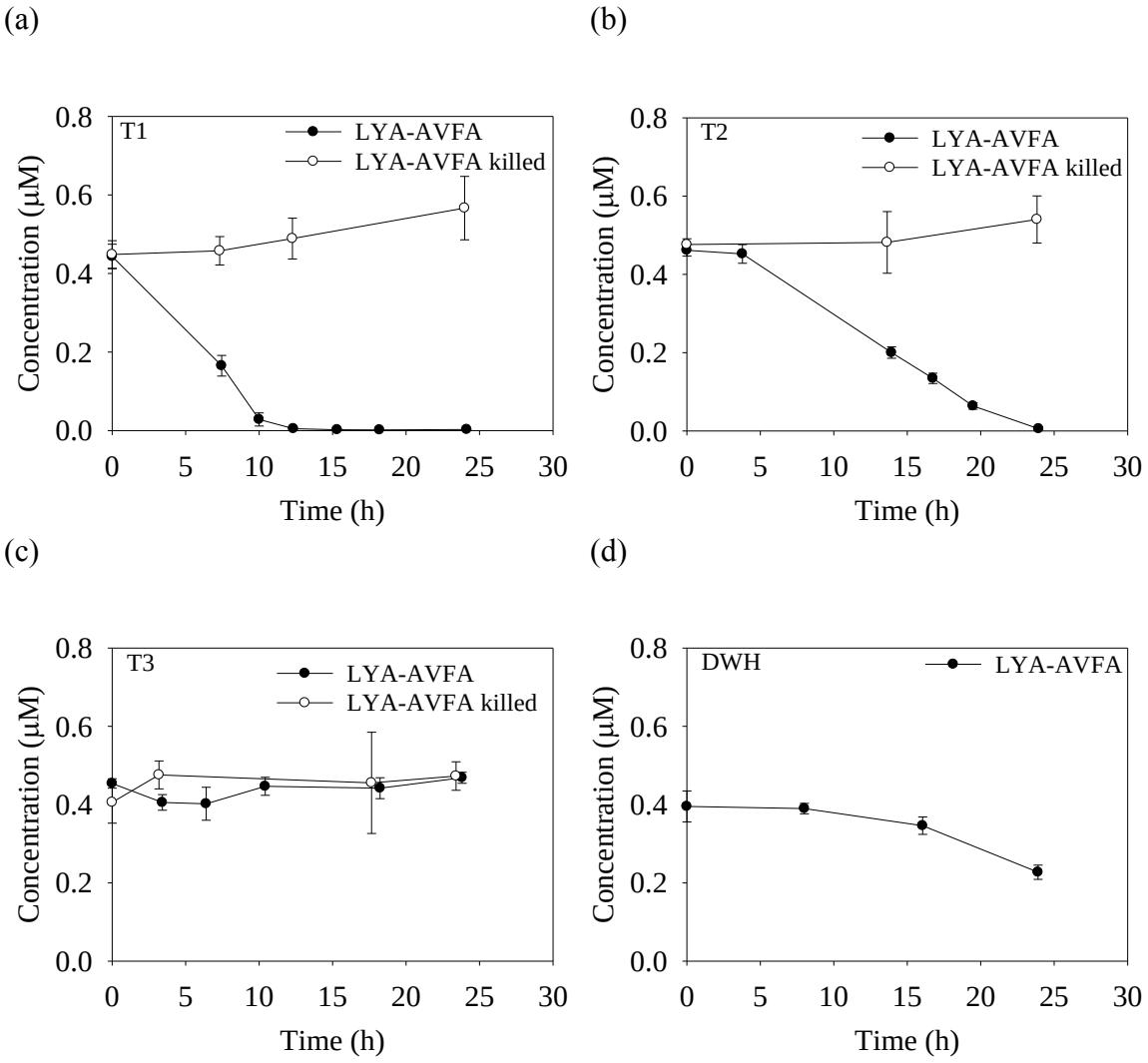

Figure 3.5. Comparison of hydrolysis rates between peptide analogs (LYA-Ala4, LYA-AVFA) and plain peptides (Ala4, AVFA) at Stas. (a) T1, (b) T2, (c) T3, and (d) DWH. Hydrolysis rates were obtained from the slope of linear regression on peptide hydrolysis curves. Error bars represent standard errors of the slope from linear regression. Letters above the bars indicate significant differences (ANOVA and Bonferroni *t* test, $p<0.05$) of the hydrolysis rates.

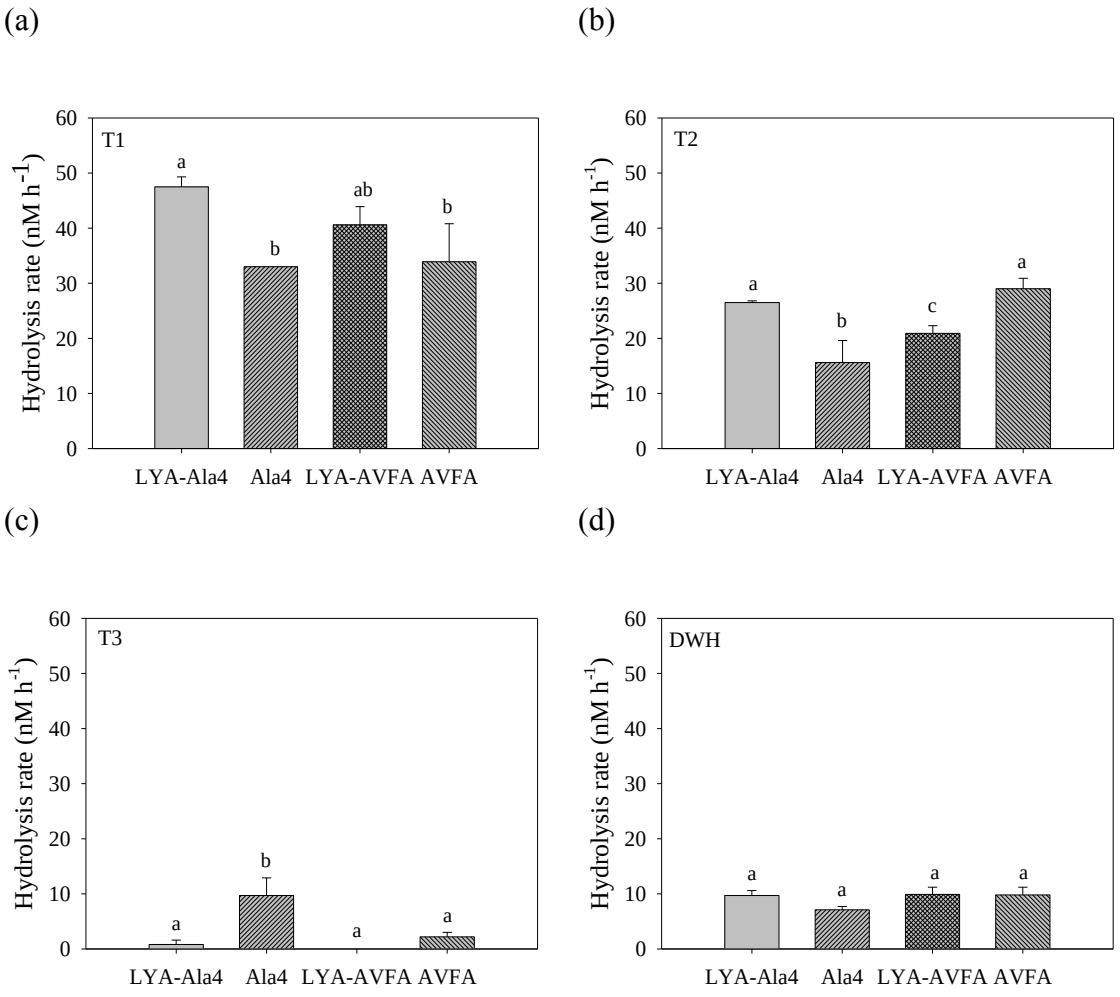

Figure 3.6. AVFA hydrolysis curves together with killed control curves (concentration vs. incubation time) at Stas. (a) T1, (b) T2, (c) T3, and (d) DWH. Data points were presented as average ± standard deviation of replicate samples. Part of the Sta. T2 hydrolysis data was published in Liu and Liu (2014).

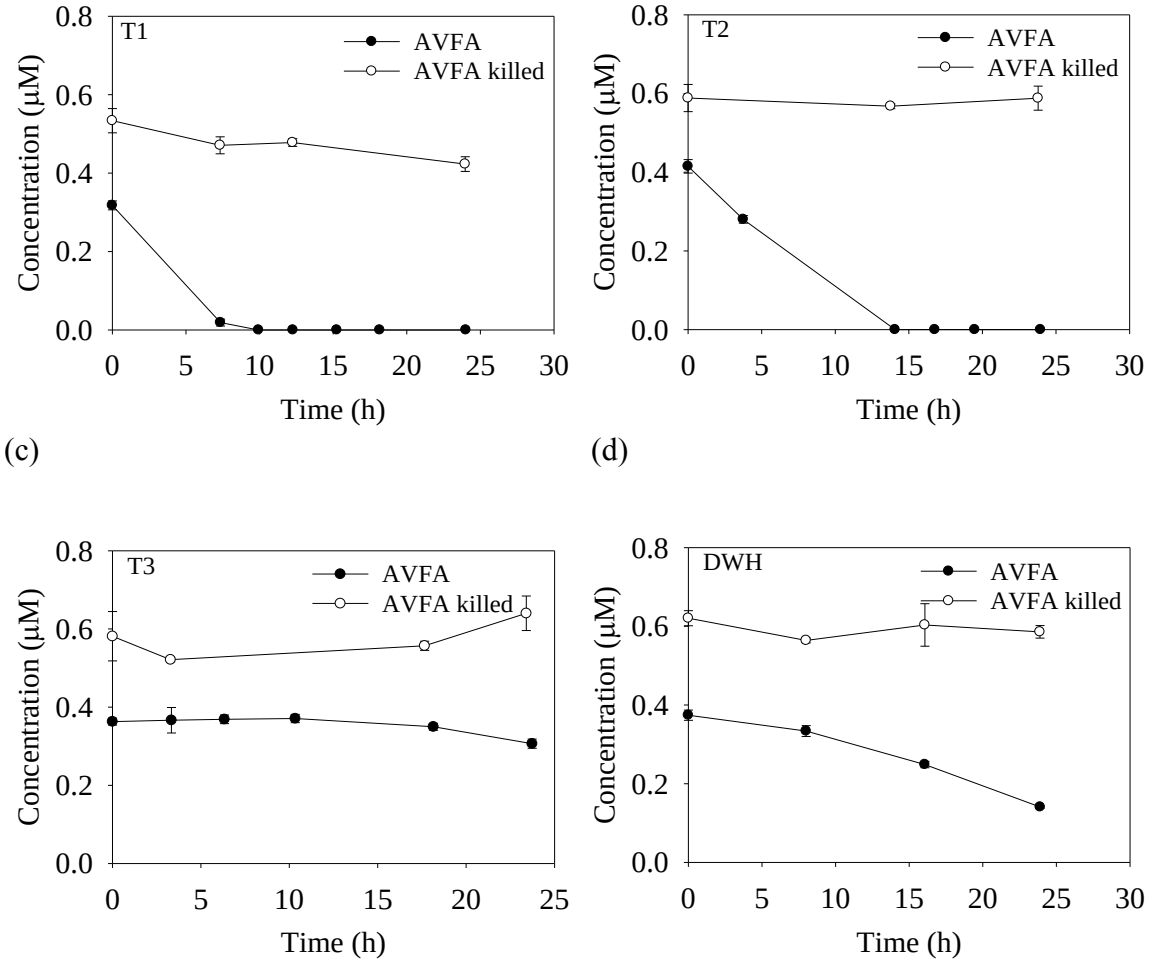

Figure 3.7. LYA-Ala4 hydrolysis curves together with killed control curves (concentration vs. incubation time) at Stas. (a) T1, (b) T2, (c) T3, and (d) DWH. Data points were presented as average ± standard deviation of replicate samples. Note LYA-Ala4 killed control was not conducted at Sta. DWH.

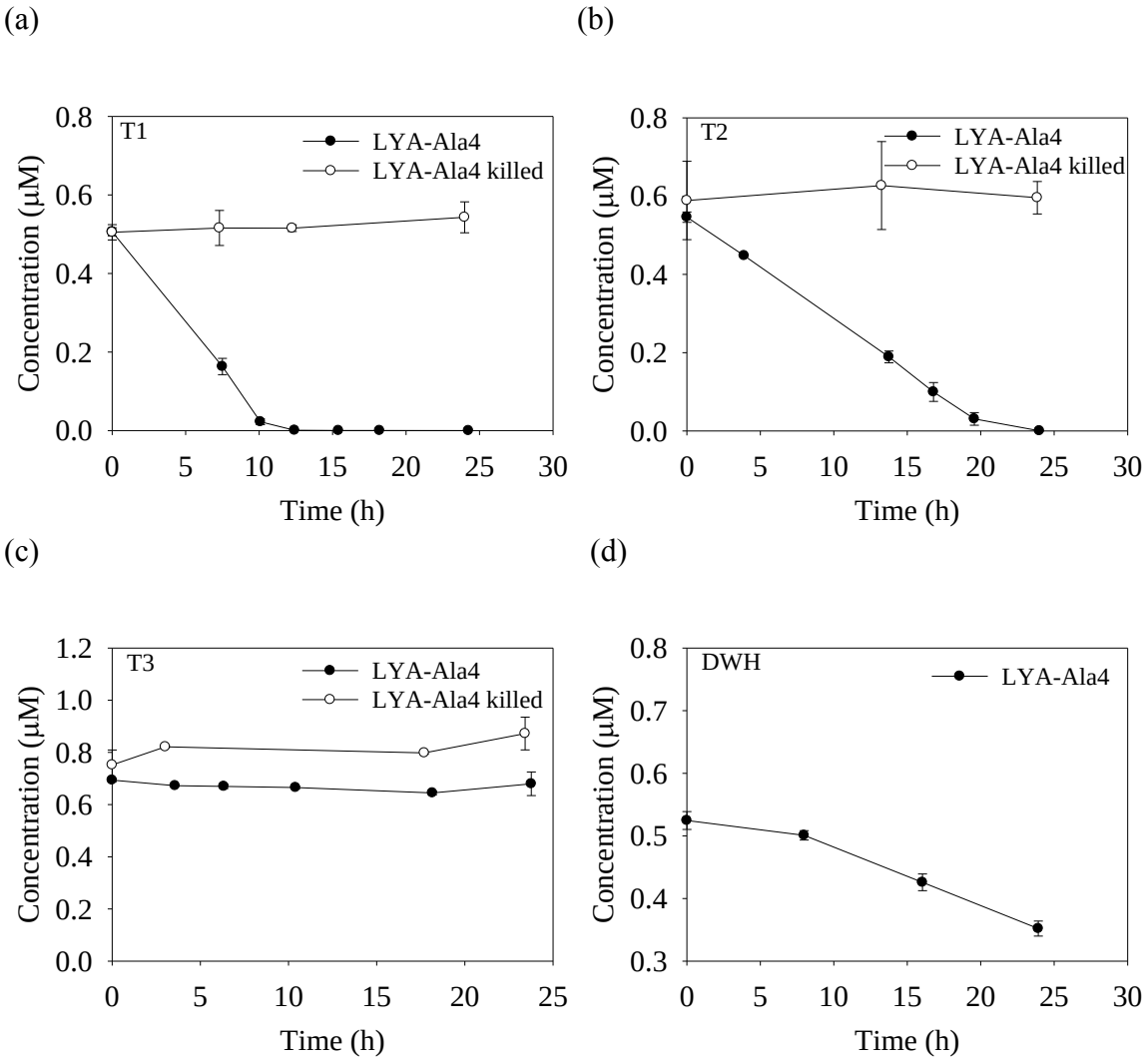

Figure 3.8. Ala4 hydrolysis curves together with killed control curves (concentration vs. incubation time) at Stas. (a) T1, (b) T2, (c) T3, and (d) DWH. Data points were presented as average ± standard deviation of replicate samples. Note Ala4 killed control was not conducted at Sta. DWH.

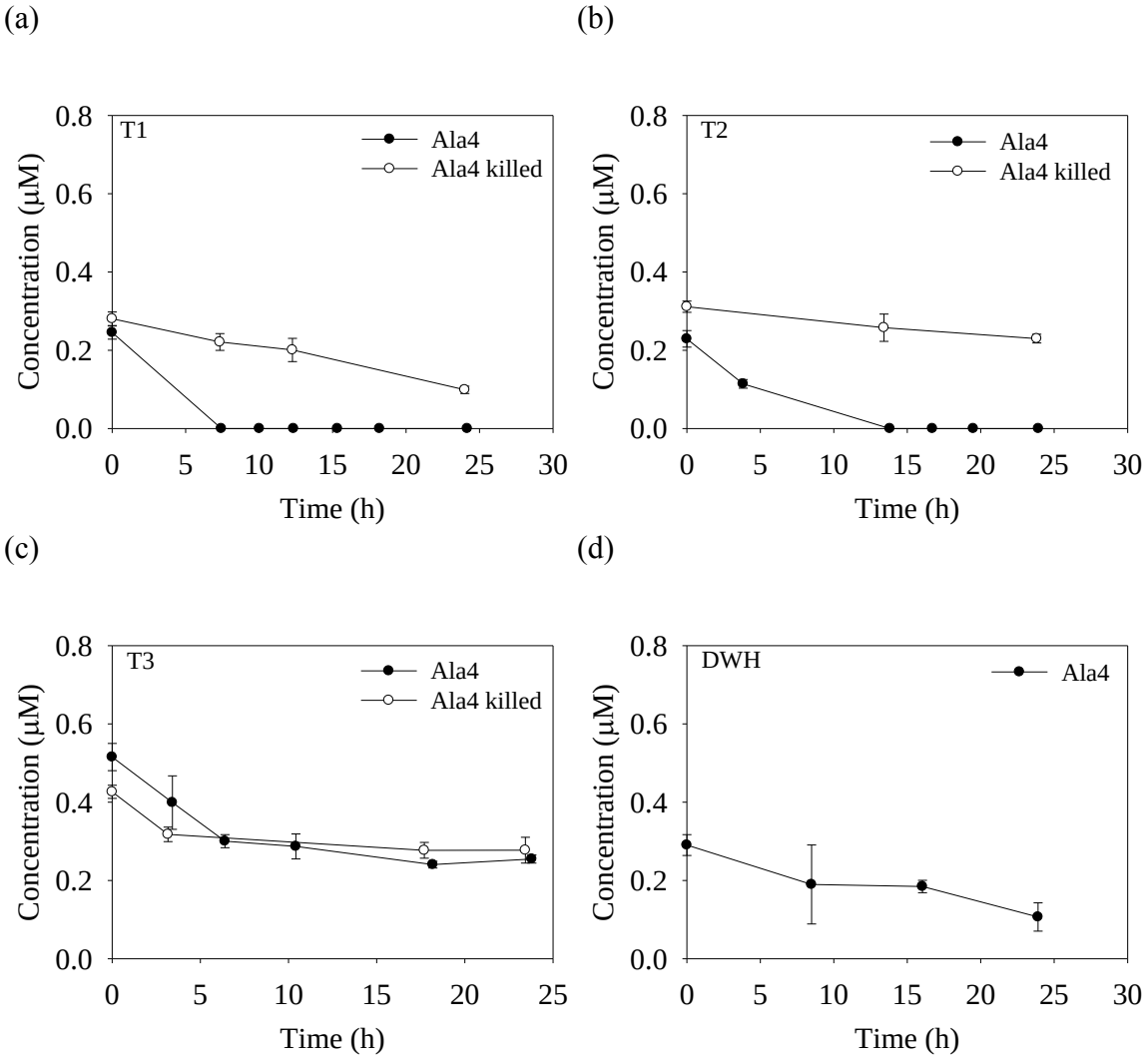

Figure 3.9. Produced peptide fragments (LYA-AVF, LYA-AV, and LYA-A) from LYA-AVFA hydrolysis at Stas. (a) T1, (b) T2, (c) T3, and (d) DWH. Concentrations of LYA-AVF and LYA-AV were calculated by assuming a same response factor between LYA-AVFA and LYA-AVF or LYA-AV from the fluorescence detection. Data points are presented as averages ± standard deviations of replicate samples.

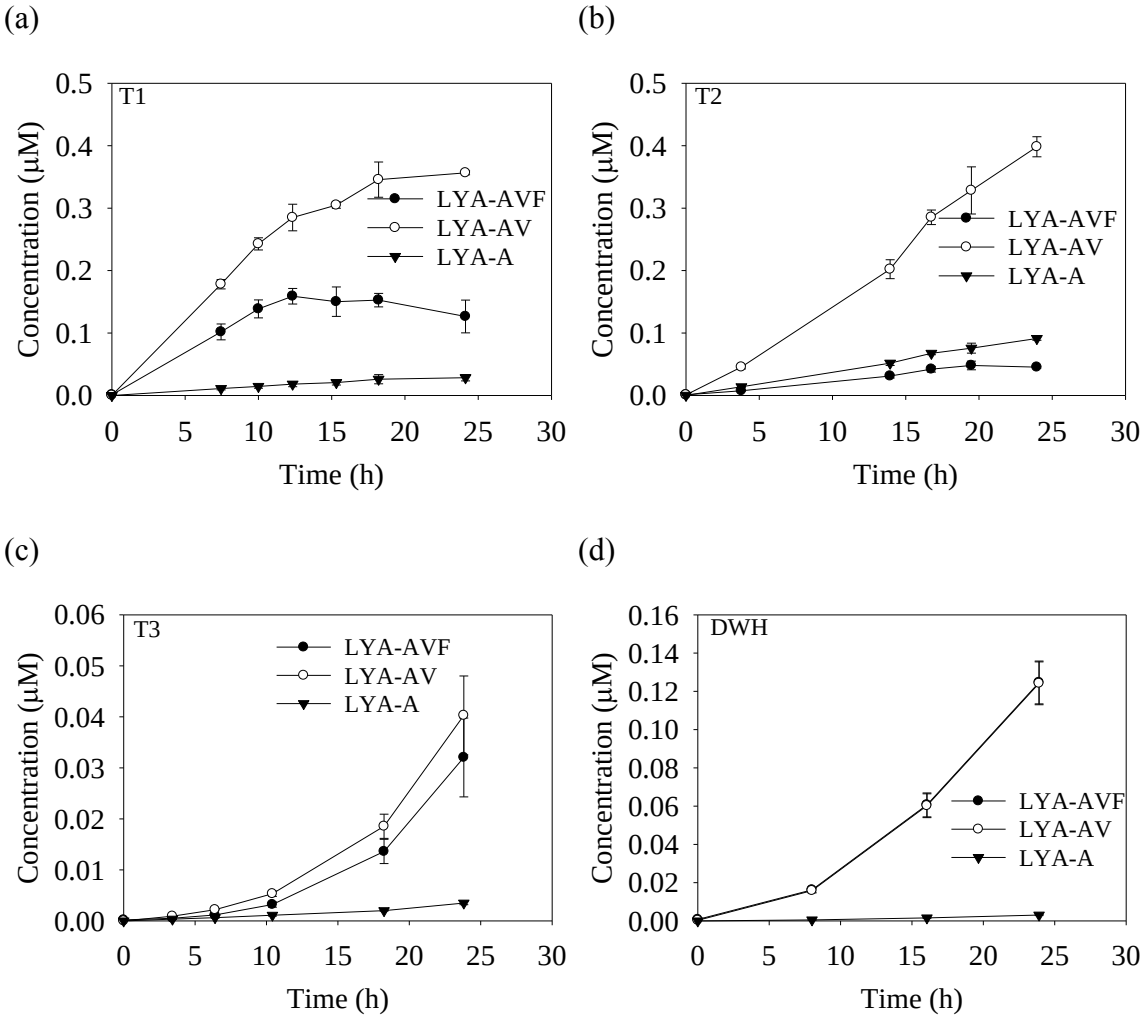

Figure 3.10. Produced peptide fragments (AVF and VFA) and amino acids (A, V and F) from AVFA hydrolysis at Stas. (a) T1, (b) T2, (c) T3, and (d) DWH. Data points are presented as average ± standard deviation of replicate samples.

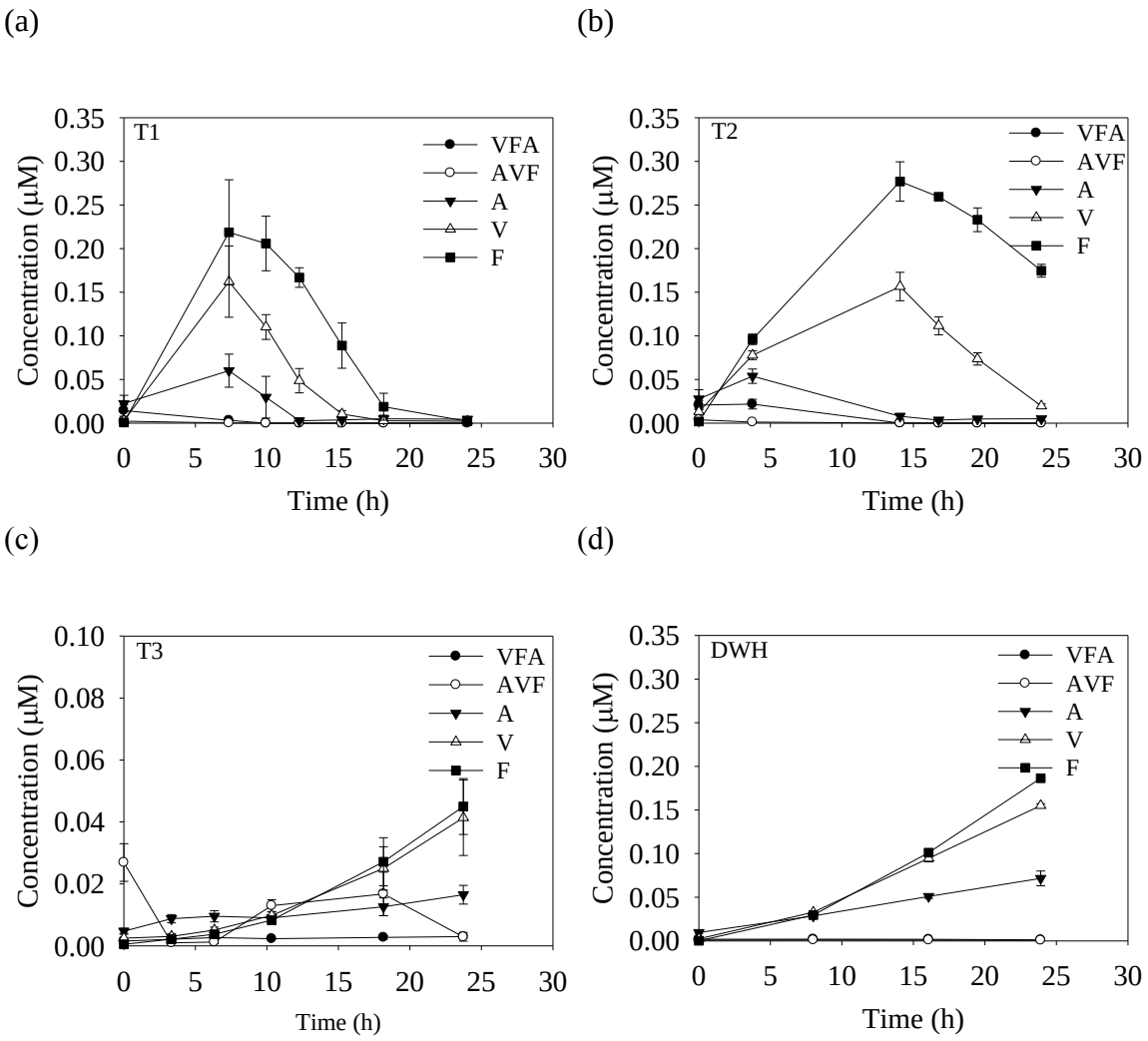

Figure 3.11. Produced peptide fragments (LYA-Ala3, LYA-Ala2, and LYA-Ala) from LYA-Ala4 hydrolysis at Stas. (a) T1, (b) T2, (c) T3, and (d) DWH. Concentrations of LYA-Ala3 and LYA-Ala2 were calculated assuming a same response factor between LYA-Ala4 and LYA-Ala3 or LYA-Ala2 from the fluorescence detection. Data points were presented as average ± standard deviation of replicate samples.

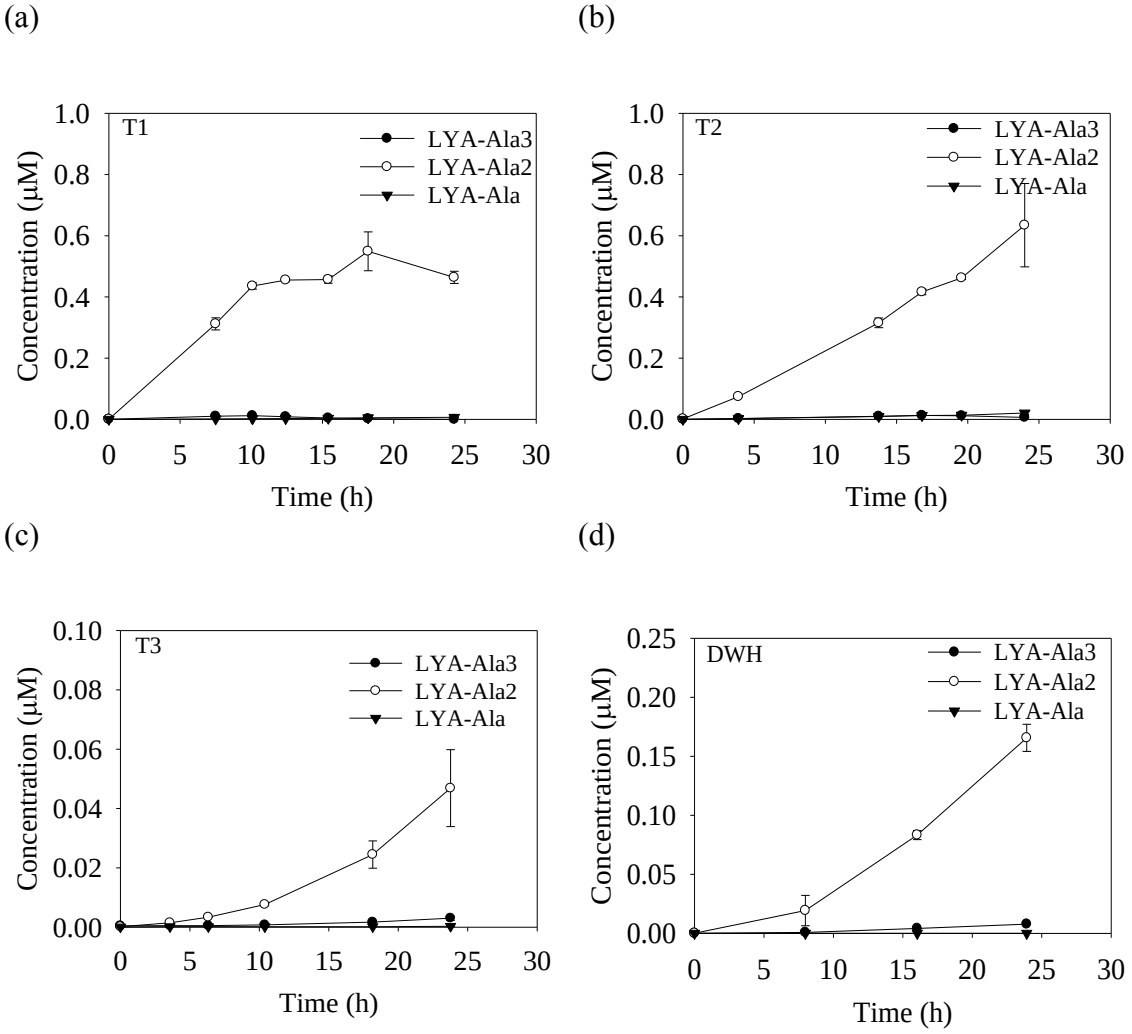

Figure 3.12. Produced peptide fragments (Ala3+Ala2 and Ala) from Ala4 hydrolysis at Stas. (a) T1, (b) T2, (c) T3, and (d) DWH. Concentrations of Ala3+Ala2 might be overestimated due to the overlap of Ala3 and Ala2 in HPLC chromatograms and their concentrations were calculated based on the Ala3 standard that has higher response factor than Ala2. Data points were presented as average ± standard deviation of replicate samples.

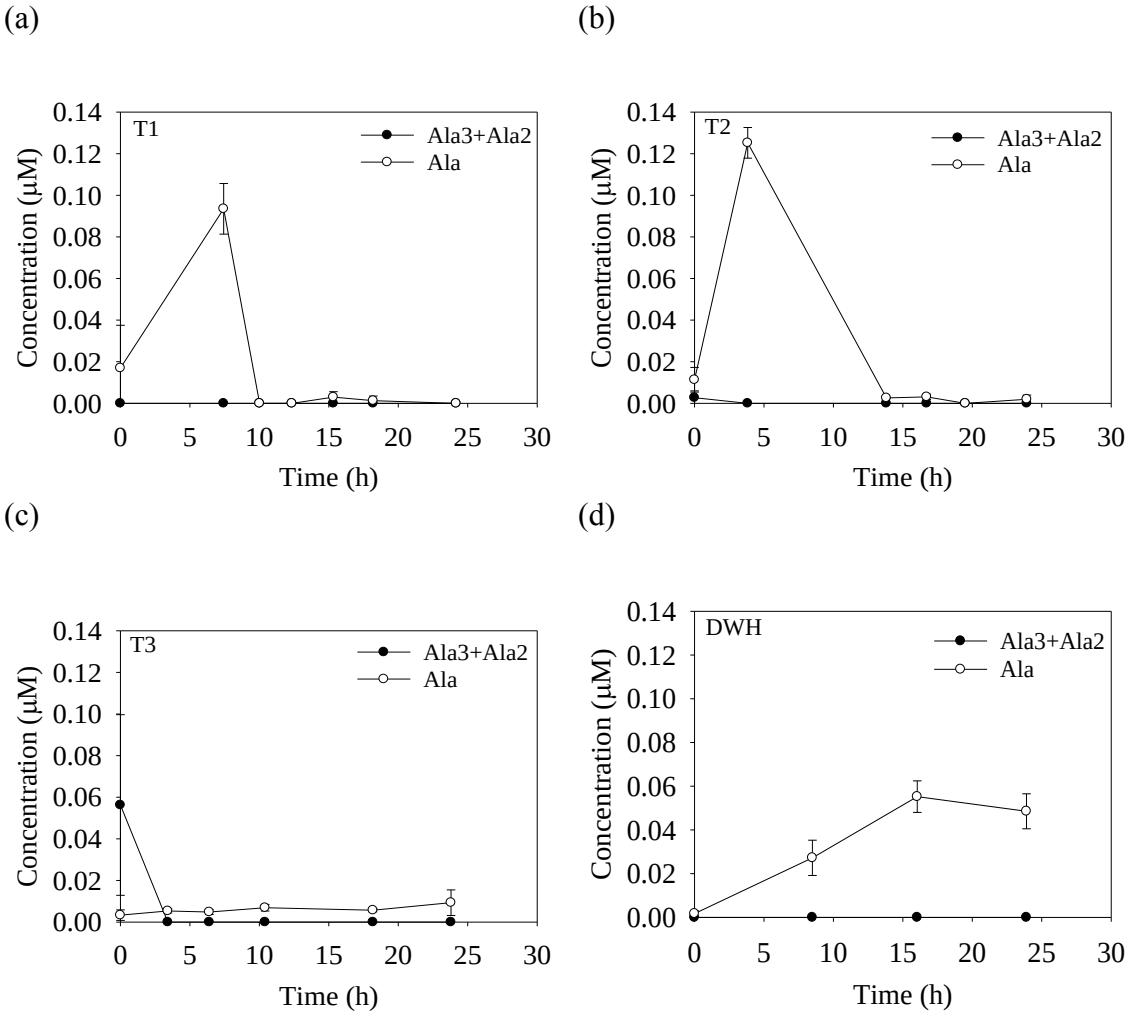

Figure 3.13. Hydrolysis, uptake and undegraded peptide percentage of AVFA with incubation time at Stas. (a) T1, (b) T2, (c) T3, and (d) DWH. Hydrolysis percentage was calculated as the sum of concentrations of VFA, AVF and F divided by the initial amended AVFA concentrations, undegraded percentage was calculated as leftover AVFA concentrations divided by the initial amended AVFA concentrations and uptake percentage was calculated as 100% minus hydrolysis and undegraded percentage. Note hydrolysis percentage may be underestimated due to the uptake of peptide fragments or amino acids.

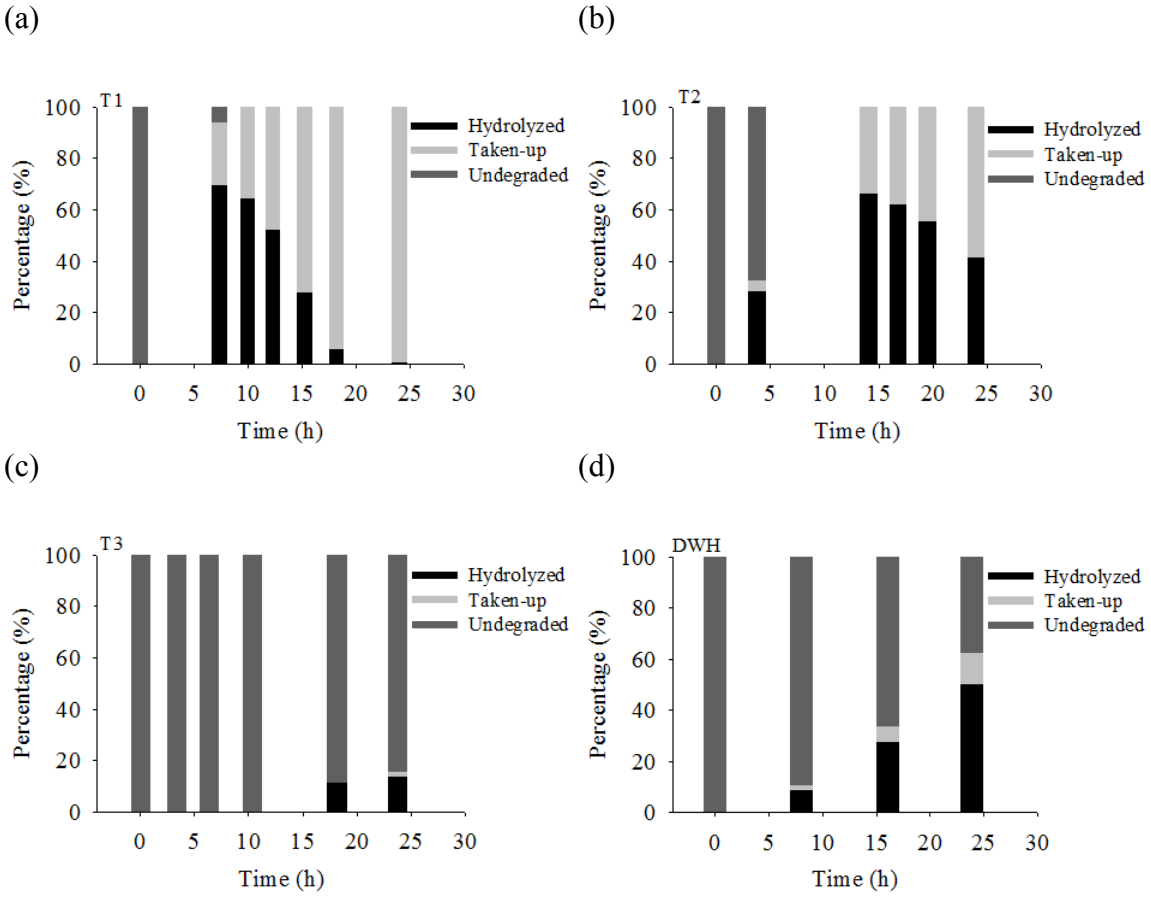

Figure 3.14. Hydrolysis, uptake and undegraded peptide percentage of Ala4 with incubation time at Stas. (a) T1, (b) T2, (c) T3, and (d) DWH. Hydrolysis percentage was calculated as concentrations of Ala divided by the initial amended Ala4 concentrations, undegraded percentage was calculated as leftover Ala4 concentrations divided by the initial amended Ala4 concentrations and uptake percentage was calculated as 100% minus hydrolysis and undegraded percentage. Note hydrolysis percentage may be underestimated due to the uptake of peptide fragments or amino acids.

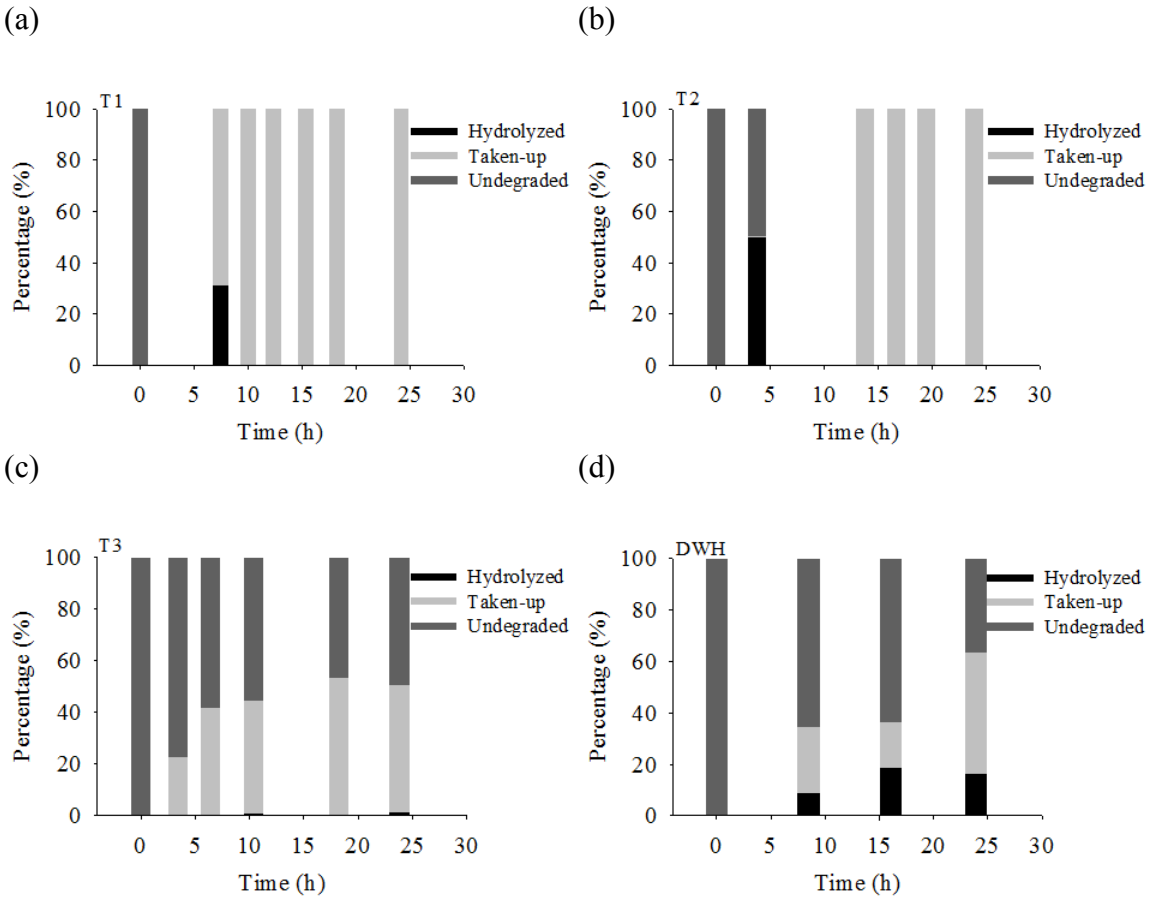

Figure 3.15. Bacterial abundance change with time for peptide analogs and plain peptides incubations at Stas. (a) T1, (b) T2, (c) T3, and (d) DWH. Data points were presented as average ± standard deviation of replicate samples. Note that the y scale for (a) and (b) is one order of magnitude higher than that for (c) and (d).

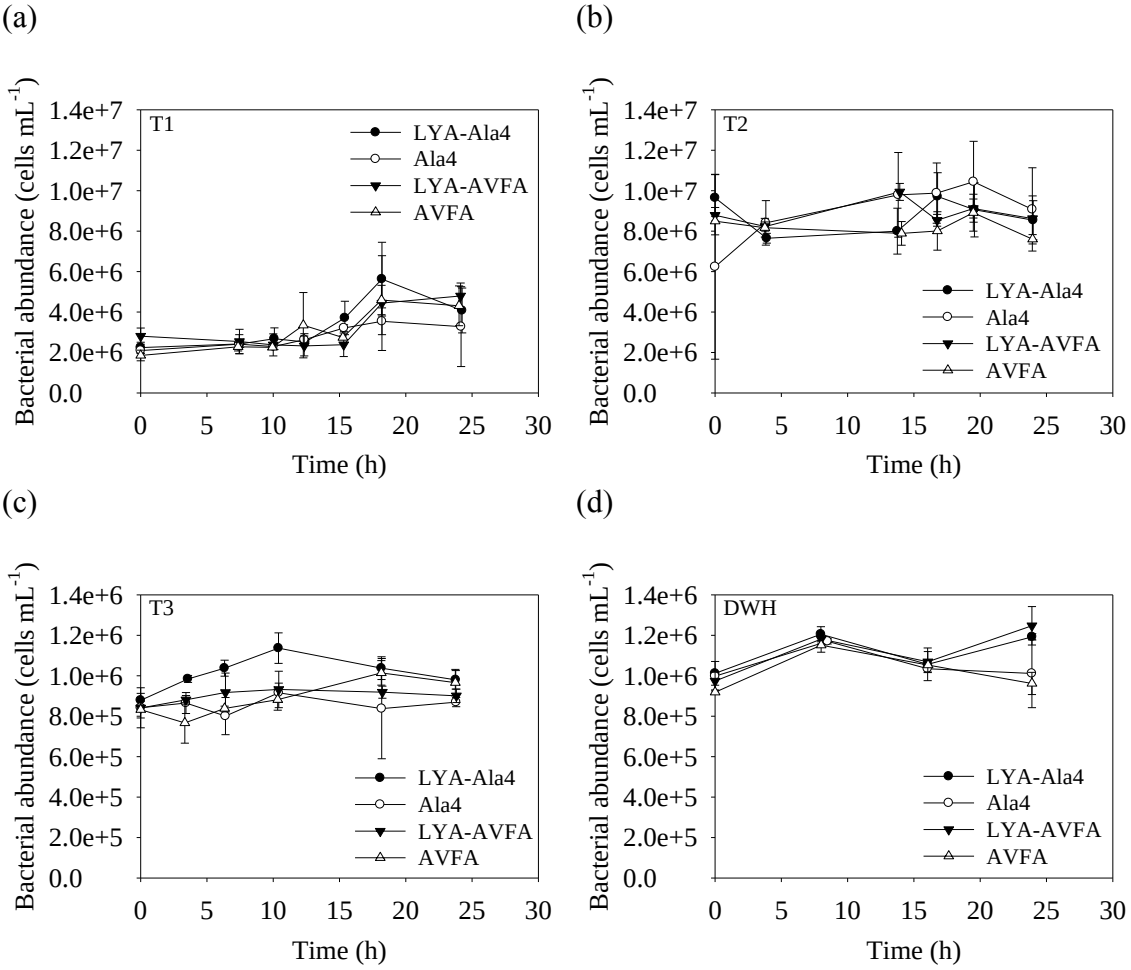

Figure 3.16. AVFA hydrolysis curves (concentration vs. incubation time) at 6 stations (T1, T2, C6, T3, T6, DWH). Data points were presented as average ± standard deviation of replicate samples.

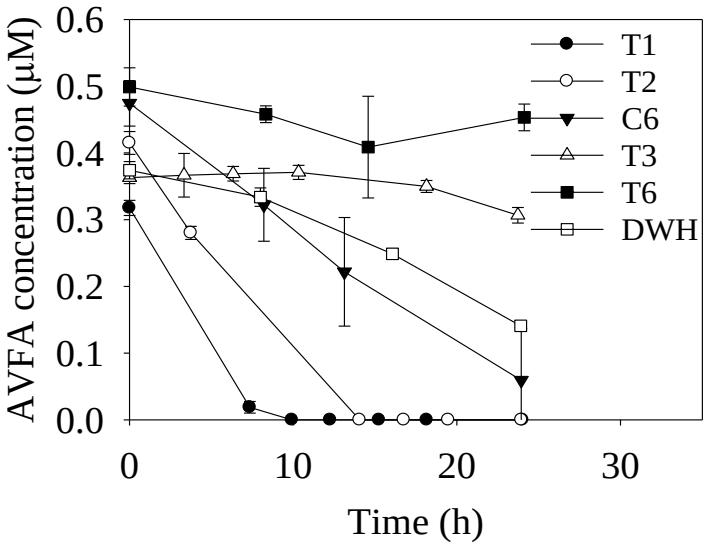

Figure 3.17. Comparison of AVFA hydrolysis rates at 6 stations (T1, T2, C6, T3, T6, DWH). Hydrolysis rates were obtained from the slope of linear regression on peptide hydrolysis curves. Error bars represent standard errors of the slope from linear regression. Letters above the bars indicate significant differences (ANOVA and Bonferroni *t* test, $p<0.05$) of the hydrolysis rates.

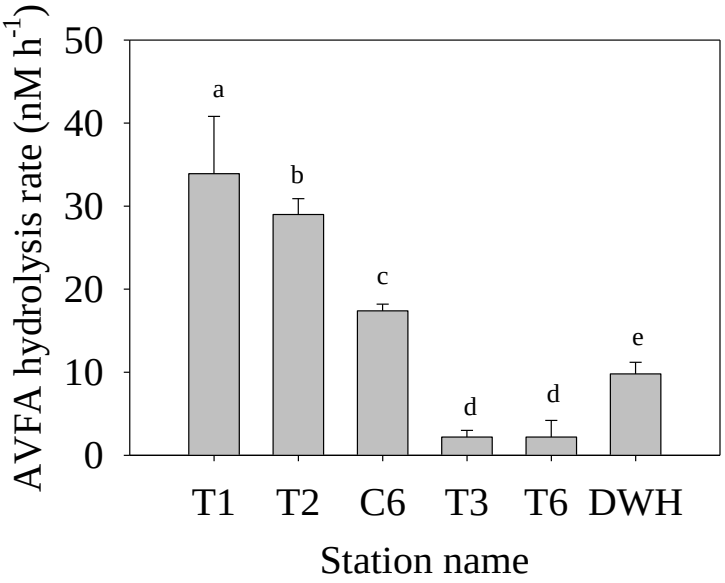

Figure 3.18. AVFA concentration in the killed control incubation at 6 stations (T1, T2, C6, T3, T6, DWH). Data points were presented as average ± standard deviation of duplicate samples.

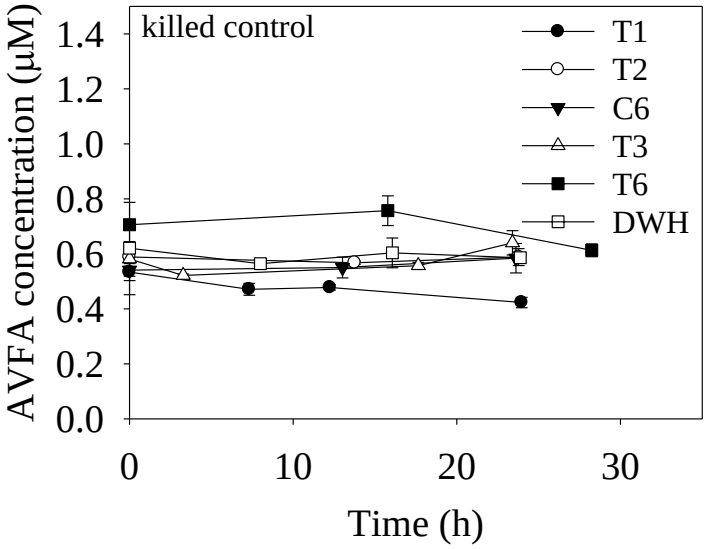

Figure 3.19. Bacterial abundance change with time for AVFA incubations at 6 stations (T1, T2, C6, T3, T6, DWH). Data points were presented as average ± standard deviation of replicate samples.

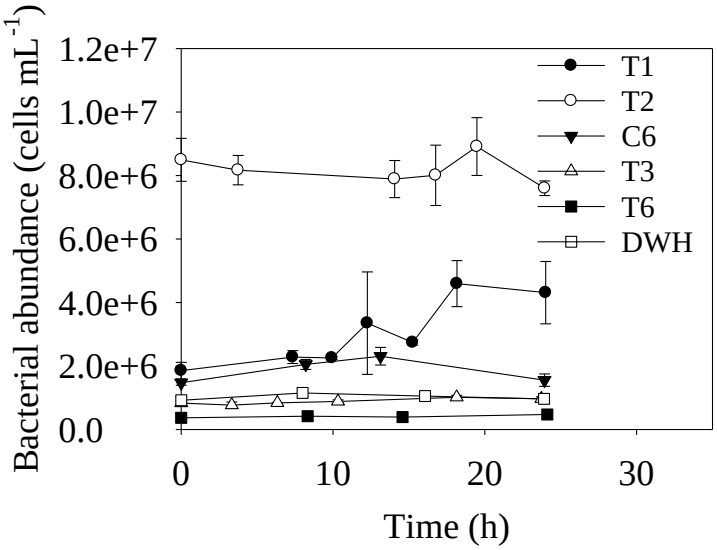

Figure 3.20. Comparison of AVFA hydrolysis rates plotted against salinity at 6 stations (T1, T2, C6, T3, T6, DWH). Hydrolysis rates were obtained from the slope of linear regression on peptide hydrolysis curves. Error bars represent standard errors of the slope from linear regression.

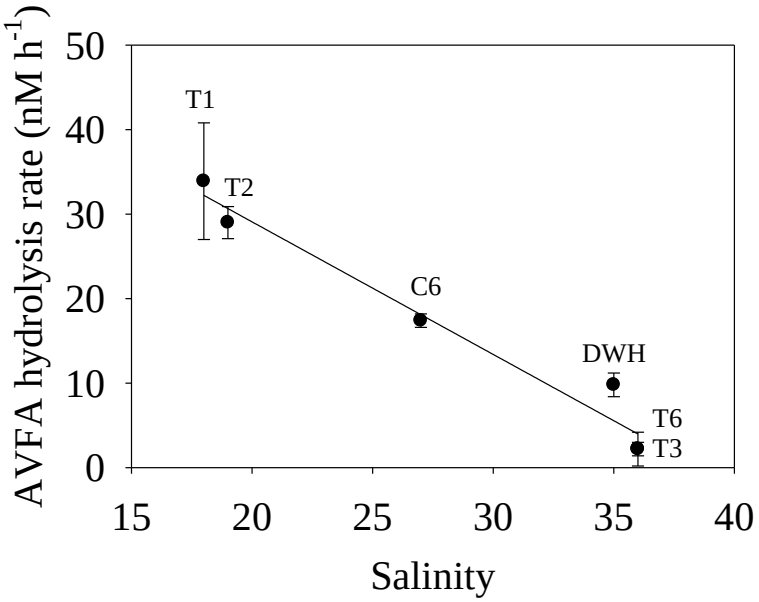

Chapter 4. Effects of chemical structure on hydrolysis pathways of small peptides in the coastal Gulf of Mexico

ABSTRACT

Deciphering peptide hydrolysis pathways is key to understanding the mechanism of peptide hydrolysis, in particular the types of extracellular enzymes that are active in seawater. The role of amino-, carboxy-, and endopeptidases can be estimated quantitatively from the hydrolyzed fragments of small peptides. In this study, we incubated several small peptides with different amino acid compositions in two coastal locations (Sta. SC in the western Gulf of Mexico and Sta. C6 in the northern Gulf of Mexico). The peptide substrates used in this study include alanine-valine-phenylalanine-alanine (AVFA) and its modifications of N-terminal amino acids with serine (S), valine (V), arginine (R) and aspartic acid (D). In both locations, aminopeptidases preferentially hydrolyzed the N terminal amino acids A and R (97-100% of the total peptidases), followed by V (30-90%) and S (37-51%), but were much less accessible to acidic amino acid D (0-1%). This pattern indicates that the N-terminal amino acid in a peptide structure affects how the peptide is hydrolyzed. In particular, for N-terminal amino acids with uncharged side chains, aminopeptidases prefer hydrophobic (A, V) to polar (S) amino acids, and for those with charged side chain, aminopeptidases prefer positive-charged (R) to negative-charged (D) amino acids. This conclusion is supported further through investigating trialanine (AAA) and AVF hydrolysis, and comparing hydrolysis pathways among AVFA, VFA, phenylalanine-alanine-serine-tryptophan-glycine-alanine (FASWGA) and SWGA. Overall, this study provides the first dataset of the relative role of different kinds of peptidases in peptide hydrolysis and its dependence on peptide

chemical structures, demonstrating substrate selectivity of different peptidases in coastal seawater.

INTRODUCTION

Proteins and peptides account for a major fraction of marine biota in seawater, and their hydrolysis is a fundamental process in marine carbon and nitrogen cycles (Pantoja et al., 1997; Findlay and Sinsabaugh, 2003; Nagata, 2008). To be available to bacteria, proteins and peptides need to be hydrolyzed to small peptides (<600 Da) by extracellular enzymes dissolved freely in the water, or by ectoenzymes attached to the cell surface or within the periplasmic space of bacteria (Chróst, 1991; Weiss et al., 1991). Small peptides have been detected as important intermediates during protein and peptide decomposition (Hollibaugh and Azam, 1983; Nunn et al., 2003; Roth and Harvey, 2006). As the first step in peptide decomposition, enzymatic hydrolysis is usually considered to be rate-limiting (Hoppe, 1991; Meyer-Reil and Koster, 1992; Davey et al., 2001), although in certain cases hydrolysis can outpace other factors such as enzyme production (Arnosti, 2004).

The pathway of peptide hydrolysis remains key to understanding the factors controlling hydrolysis and interactions between enzymes and peptides. Hydrolysis pathways also provide insights into the types of peptidases synthesized by microbes, including aminopeptidase, carboxypeptidase and endopeptidase (Chróst, 1991). Aminopeptidases cleave peptides from the N-terminus, carboxypeptidases from the C-terminus, and endopeptidases at internal peptide bonds. The most dominant or active type of peptidases can be inferred through the investigation of peptide hydrolysis pathways. For example, an N-terminus hydrolysis pathway points to the role of aminopeptidases.

Knowing the relative roles of these different peptidases during peptide hydrolysis is a fundamental step needed to understand the controlling mechanisms of enzyme synthesis by microbes, such as at gene levels (Chróst, 1991).

Previous studies on hydrolysis pathways have relied mainly on proteins or peptide analogs with fluorophores that can easily be detected (Hoppe, 1983; Pantoja et al., 1997; Steen and Arnosti, 2013). The dominant role of aminopeptidases, rather than endopeptidases, in peptide hydrolysis was suggested by modeling hydrolysis data of radiolabeled proteins in aquatic environments (Billen, 1991). However, significant contributions of carboxypeptidases and endopeptidases have been observed using a series of targeted peptide analogs (Hashimoto et al., 1985; Obayashi and Suzuki, 2005; Obayashi and Suzuki, 2008). The peptide analogs in these studies targeted specific kinds of peptidases by blocking the peptide N-terminus, C-terminus, or both, making it difficult to compare the relative role of these peptidases simultaneously. In contrast, using plain peptides without fluorogenic tags allows examination of the relative role of the three types of peptidases with all the peptide bonds available. Results from small peptides with similar structures suggested that the hydrolysis by aminopeptidases is the dominant pathway (Liu et al., 2013), but this conclusion was based on only two peptides. When considering the enormous possible structures and amino acid compositions of peptides, there is a need to expand the range of peptides to examine the role of chemical structure in peptide hydrolysis pathways.

Our objective here was to evaluate whether amino acid composition in a peptide affects its hydrolysis pathway. We used several small plain peptides, including trialanine (AAA), alanine-valine-phenyalanine (AVF), VFA, AVFA, VVFA, serine-valine-phenylalanine-alanine (SVFA), arginine-valine-phenylalanine-alanine (RVFA), aspartic acid-valine-phenylalanine-alanine (DVFA), serine-tryptophan-glycine-alanine (SWGA),

and FASWGA that range from a tripeptide to a hexapeptide, to study their hydrolysis pathways in two coastal seawaters.

MATERIALS AND METHODS

Seawater sampling and chemical analysis of initial water

Coastal seawater for incubation was collected from two sampling sites: Sta. SC (27.84ºN, 97.05ºW) in Port Aransas, Texas, in the western Gulf of Mexico and Sta. C6 (28.86ºN, 90.45ºW) in the northern Gulf of Mexico. At Sta. SC, surface seawater was collected manually using a 2-L acid-cleaned polyethylene bottle in March 2013, April 2013, and June 2014. At Sta. C6, surface (2 m) seawater was sampled using Niskin bottles mounted on a conductivity-temperature-depth (CTD) rosette (Seabird 911) in May 2011 and April 2015. Temperature, salinity, dissolved oxygen (DO) and chlorophyll fluorescence were monitored by the CTD device (Table 4.1).

The pH was analyzed through a bench-top pH meter (Thermo Fisher Orion 4-star). Seawater was filtered through a 0.2 μm pore size Nylon filter (25 mm, Whatman) to measure inorganic nutrients, dissolved organic carbon (DOC), total dissolved nitrogen (TDN), dissolved free amino acids (DFAA) and total dissolved amino acids (TDAA). Nitrate, nitrite, ammonium and phosphate were measured using standard protocols (Strickland and Parsons, 1968; Jones, 1984). The inorganic nutrient data for the 2011 Sta. C6 were taken from McCarthy et al. (2013). DOC and TDN were analyzed in a total organic carbon/TDN analyzer (TOC-V/TNM-1, Shimadzu) within 6% error for duplicates. DFAA were measured by HPLC (Shimadzu Prominence) with a fluorescence detector after pre-column *o*-phthaldialdehyde (OPA) derivatization (Lindroth and Mopper, 1979; Lee et al., 2000). TDAA were analyzed in the same way as DFAA but

after hydrolysis by 6 N HCl under nitrogen at 110 ºC for 20 h (Kuznetsova and Lee, 2002). Dissolved combined amino acids (DCAA) were calculated as the difference between TDAA and DFAA. Measurements of replicate samples of DFAA and DCAA had standard deviations of 10-20%.

Peptide incubation

Small peptides (AVFA, VVFA, SVFA, RVFA, DVFA, AAA, D-AAA, VFA, FASWGA, SWGA, AVF) were custom-synthesized by C.S Bio or purchased from Sigma-Aldrich. AVF, VFA, and AVFA are partial structures of ribulose-1, 5 bisphosphate carboxylase oxygenase (RuBisCO). AVFA, VVFA, SVFA, RVFA, and DVFA differed in their N-terminal amino acid, ranging from hydrophobic amino acids (A, V) to polar amino acid (S) and from basic amino acid (R) to acidic amino acid (D). Hydrolysis from the N-terminus of D-AAA (N-terminal alanine as the D isomer) is expected to be blocked by the D-alanine because natural enzymes hydrolyze L-amino acids preferentially (Morozov, 1979). Custom-designed SWGA and FASWGA contain a chromophoric amino acid tryptophan (W), which are easily detectable by fluorescence (Liu et al., 2010). Initial properties of the seawater at Sta. SC and/or Sta. C6 and incubation setup are listed in Table 4.1.

Peptide incubations were initiated immediately onboard or in the laboratory after seawater collection. Individual peptides were added to the seawater with initial concentrations of 3.6-11.5 μmol L^{-1}, which were 3-16 times as high as DCAA that presumably include all hydrolyzable peptides and proteins in the initial seawater (Table 4.1). This high amendment dose is necessary to ensure the detection of hydrolyzed products. Peptides were respectively amended in the 30 mL (Sta. C6-2011), 100 mL (Sta.

SC-Mar 2013, Sta. SC-June 2014, and Sta. C6-2015) or 180 mL (Sta. SC-Apr 2013) seawater in amber round bottles. Duplicate incubations (except for a single incubation at Sta. C6 in 2011) were conducted for each peptide in the dark at room temperature (20-25 ºC), close to the *in-situ* seawater temperature (Table 4.1), for 19-27 h. Aliquots were taken from the duplicate bottles at different time intervals, filtered through 0.2 μm pore size cellulose acetate (CA) or polyvinylidene difluoride (PVDF) syringe filters (13 mm dia., Whatman GD/X), and preserved at -20 ºC until peptide and amino acid analyses. One aliquot (1 mL) was fixed with 3% (final concentration) formaldehyde (AR grade, Mallinckrodt Baker) and preserved at 4 ºC for bacterial abundance analysis at Sta. SC in 2014 and Sta. C6 in 2015. Controls without peptide addition were also included at Sta. SC in 2014 and Sta. C6 in 2015.

Peptide and amino acid analysis

Concentrations of peptides AVF, VFA, AVFA, VVFA, RVFA, SVFA, DVFA and their hydrolyzed fragments were analyzed using HPLC (Shimadzu Prominence) equipped with a photodiode array (PDA) detector scanning from 190 to 800 nm (Liu et al., 2010). Briefly, samples were run through a C_{18} column (Alltima 5 μ, 250 mm x 4.6 mm) that maintained at 40 ºC in a column oven. Two mobile phase solvents were used for gradient elution: solvent A as 0.05 $mol \cdot L^{-1}$ sodium phosphate (monobasic anhydrous, ACS grade) with pH of 4.5 and solvent B as methanol (HPLC grade). The flow rate was 1 mL min^{-1} and the gradient elution program followed the established protocol in Liu et al. (2010). Peptide concentrations were quantified at the wavelength of 206 nm.

AAA, D-AAA and their hydrolysis product dialanine (AA) were analyzed using an HPLC (Shimadzu Prominence) coupled with a post-column derivatization system

(Pickering Lab Pinnacle). AAA and D-AAA samples were eluted in a lithium ion exchange column (Pickering Lab, 4.0 x 100 mm) that provided better separation between AAA and its fragment AA than the C_{18} column (unpublished data). Mobile phases included two lithium eluents, Li275 (pH 2.75) and Li750 (pH 7.50), and one lithium column regenerant RG003. The flow rate was 0.35 mL min^{-1} and the gradient elution program followed the protocol provided by Pickering Lab (amino acid application method 2). The column was kept at 37 ºC. After elution through the column, samples were derivatized by TRIONE® ninhydrin reagent (T100) and detected by Ultraviolet-Visible (UV) detector at 570 nm, after ninhydrin reagent was mixed with the eluted samples at a flow rate of 0.3 mL min^{-1} in a 0.5 mL reactor under 130 ºC.

Peptides SWGA, FASWGA and their fragments including SW, SWG, WGA, ASW, ASWG, FASWG and ASWGA were analyzed using HPLC with a fluorescence detector (Ex: 280 nm, Em: 360 nm). Different elution programs were used for SWGA and FASWGA, respectively. For SWGA and its fragments, solvent B increased from 20% to 40% in the first 15 min, then to 100% at 16 min, and remained at 100% for 1 min. For FASWGA and its fragments, solvent B ramped from 20% to 50% within 25 min, then increased to 100% at 26 min, and kept as 100% from 26 min to 32 min.

Concentrations of amino acids and fragments AV, VF, WG, GA, FASW were measured by HPLC with a fluorescence detector after pre-column OPA derivatization (Lindroth and Mopper 1979). The derivatized samples were eluted through a C_{18} column (Alltima 5 μ, 250 mm x 4.6 mm) by mobile phases consisting of 0.05 mol L^{-1} sodium acetate with 5% tetrahydrofuran (solvent A, pH 5.7) and methanol (solvent B) at a flow rate of 1 mL min^{-1}. Solvent B was ramped from 20% to 60% during the first 40 min, further to 100% in the next 8 min and then kept at 100% for 10 min. Samples were

quantified under excitation and emission wavelengths of 330 nm and 418 nm, respectively.

Bacterial abundance analysis

Bacteria samples were stained with SYBR Green II (Molcular probes, 1:100 v/v) and enumerated under laser excitation with blue light at 488 nm in a flow cytometer (BD Accuri C6) following procedures described in Liu et al. (2013). In brief, bacterial cells were counted in a fixed volume mode with a flow rate below 300 events per second and cell counts were determined in a dot plot of side scatter (SSC-H) versus green fluorescence signal (FL1-H) on a logarithmic scale. Bacterial abundance counting error was about 11% between duplicates.

RESULTS

Hydrolysis of small peptides

Peptides AVFA, VVFA, SVFA, RVFA and DVFA were hydrolyzed generally in a linear mode at rates ranging from 0.017 μmol L^{-1} h^{-1} to 0.071 μmol L^{-1} h^{-1} at Sta. SC in 2014 (Fig. 4.1). The production of VFA, as high as 0.27 μmol L^{-1}, outcompeted other peptide fragments during the AVFA and RVFA hydrolysis (Figs. 4.1a, 4.1d). Amino acid A increased by 0.16 μmol L^{-1} at 4 h and then decreased in the AVFA incubation, and R increased by 0.34 μmol L^{-1} at 12 h followed by a decrease in the RVFA hydrolysis. While VFA was a major fragment in the VVFA and SVFA hydrolysis, its concentration was about half of that of VVF or SVF (Figs. 4.1b, 4.1c). Increase of V (0.11 μmol L^{-1}) was the highest among all amino acids in the VVFA hydrolysis, and A increased by 0.18 μmol L^{-1} and then decreased in the SVFA hydrolysis. In contrast to all above incubations,

VFA did not increase at all during the DVFA hydrolysis and DVF was the dominant fragment (Fig. 4.1e). Amino acid F and V increased by 0.42 μmol L^{-1} and 0.24 μmol L^{-1} respectively at 21 h of the DVFA incubation. In the control at Sta. SC, amino acids D and V remained nearly constant within 21 h and S, R, A, F all decreased with time; concentrations were all below 0.03 μmol L^{-1} throughout the incubation (Fig. 4.2a). Bacterial abundance increased from 1.1-1.6 $\times 10^6$ per mL at 0 h to 1.5-2.2 $\times 10^6$ per mL at 21 h (Fig. 4.2b). The increase of bacterial abundance in the peptide incubation treatments ranged from 8% to 86% during the 21-h incubation. Within this time period, bacterial abundance increased 33% in the control treatment.

At Sta. C6 in 2015, peptide hydrolysis rates resembled those in the Sta. SC seawater, ranging from 0.014 μmol L^{-1} h^{-1} to 0.054 μmol L^{-1} h^{-1} (Fig. 4.3). The production of VFA and FA, as high as 0.31 μmol L^{-1}, outcompeted all other fragments in the AVFA, VVFA and RVFA hydrolysis (Figs. 4.3a, 4.3b, 4.3d). Correspondingly, amino acids V, F and R all increased throughout the three incubations and reached up to 0.18-0.40 μmol L^{-1} at 24 h. In the SVFA hydrolysis, SVF increased by 0.050 μmol L^{-1} at the end while VFA and FA increased by 0.092 μmol L^{-1} and 0.11 μmol L^{-1} respectively (Fig. 4.3c). Amino acid F production was highest among all amino acids in the SVFA incubation. In the DVFA hydrolysis, production of FA and DVF was more than one order of magnitude higher than that of VFA (Fig. 4.3e). F increased by 0.19 μmol L^{-1} at 24 h of the DVFA hydrolysis. Amino acid concentrations decreased with time and remained lower than 0.009 μmol L^{-1} in the controls (Fig. 4.4a). Bacterial abundance changed less than 30% from 4.7-5.3 $\times 10^6$ per mL at 0 h to 3.6-6.1 $\times 10^6$ per mL at 24 h (Fig. 4.4b).

Major hydrolysis pathways of different peptides

The hydrolysis pathways of tested small peptides were deduced from the peptide fragments and amino acids produced during hydrolysis, assuming equivalent bacterial uptake of produced fragments that were used for pathway deduction. Mass balance calculations revealed that hydrolysis products accounted for 71% ± 35% of decreased peptides (Table 4.2), suggesting that ca. 29% of peptide substrates or produced fragments might be taken up during the initial incubation stage. If peptide substrates were taken up as intact molecule without extracellular hydrolysis, this uptake would not affect our deduced hydrolysis pathways. This is also true if peptide substrates were hydrolyzed first and produced fragments were taken up at equivalent amounts. Previous studies showed similar uptake rate of small peptides and amino acids V, F within a short time, while uptake rate of A was higher than that of V or F (Liu et al., 2013). Thus we used peptide fragments containing F (e.g., AVF, VFA, FA) and amino acid F instead of A to deduce hydrolysis pathways. In addition, the amino acids that increased in the peptide incubation were mainly from peptide hydrolysis because their background concentrations were consistently low in the control (Figs. 4.2a, 4.4a). As AVFA, VVFA, SVFA, RVFA and DVFA only differed in their N-terminal amino acids, VFA and FA were common fragments in all five peptides and we can use them to compare hydrolysis of these five peptides by aminopeptidases no matter how the fragments were taken up by bacteria.

The validity of this approach can be demonstrated by VVFA as an example: hydrolyzed products of VVFA differed between the 2014 Sta. SC and 2015 Sta. C6 seawater during the 21-24 h incubation (Figs. 4.1b, 4.3b). At Sta. SC, the production of fragment VVF (0.30 μmol L^{-1}) was almost twice as VFA (0.16 μmol L^{-1}) at the end of incubation (Fig. 4.1a). Other peptide fragments, such as FA and VF, increased less than 0.03 μmol L^{-1} or remained relatively constant throughout the incubation. Amino acid V

increased the most by 0.11 μmol L^{-1}, which was comparable to the increased concentration of VFA, at 21 h among all amino acids. These patterns indicate that the hydrolysis of VVFA in the Sta. SC seawater was mainly as VVFA→VVF+A from C terminus by carboxypeptidases, followed with VVFA→V+VFA from N terminus by aminopeptidases. In contrast, at Sta. C6, the concentration increase of VFA (0.31 μmol L^{-1}) and FA (0.22 μmol L^{-1}) outcompeted that of VVF (0.10 μmol L^{-1}) (Fig. 4.3b), consistent with the high production of V. The production of FA could come from either stepwise hydrolysis from VVFA to VFA and then to FA by aminopeptidases, or cleavage by endopeptidases to produce VV and FA. However, the increase of V (0.64 μmol L^{-1}) was about twice as high as F (0.33 μmol L^{-1}), ruling out the second possibility.

Taken together, these patterns suggest a major pathway of VVFA as VVFA→V+VFA→2V+FA→2V+F+A in the Sta. C6 seawater. Similar analysis of hydrolyzed products was done for all other tested peptides to derive their major pathways in the seawater (Table 4.2, Figs. 4.1, 4.3, 4.5, 4.6). Even though multiple hydrolysis pathways are present for some peptides, the cleavage from the N terminus was always the major hydrolysis pathway for peptides with N-terminal A, V or R, such as AVF, AVFA, VFA, VVFA, and RVFA (Table 4.2). Peptides with N-terminal S were cleaved mainly from the C terminus or cleaved from both termini. DVFA was cleaved mostly from C terminus.

The percentages of hydrolysis by different kinds of peptidases were further calculated based on the proportions of corresponding fragments in all hydrolyzed products. For example, VFA indicated hydrolysis of VVFA by aminopeptidases and VVF indicated hydrolysis by carboxypeptidases at Sta. SC as discussed above. Thus, the percentage of increased VFA among all produced fragments containing F (VFA, VVF, FA, and F) was used as percentage of VVFA hydrolysis by aminopeptidases, that of

increased VVF as by carboxypeptidases, and the rest as by endopeptidases. Whereas for the VVFA hydrolysis at Sta. C6, the sum of VFA, FA and F increase indicated the percentage of VVFA hydrolysis by aminopeptidases, VVF increase represented that by carboxypeptidases, and the rest by endopeptidases.

As produced fragment concentrations changed with incubation time, hydrolysis percentages by different peptidases for each peptide may also differ with time. The percentages by different peptidases were similar throughout the incubation except a few time points in the AVFA, VVFA and DVFA hydrolysis at Sta. SC (Figs. 4.7, 4.8). For instance, hydrolysis percentage of SVFA by aminopeptidases varied slightly from 21 to 37% within 0-21 h, and that of RVFA by aminopeptidases was 79-98% throughout the incubation at Sta. SC (Figs. 4.7c, 4.7d); the hydrolysis percentages of all five peptides changed less than 10% at different time points in the Sta. C6 seawater (Fig. 4.8). Thus, the hydrolysis percentages at the end of incubations were used to compare hydrolysis among peptides below.

The effect of N-terminal amino acid on hydrolysis pathways

When comparing peptides differing only in N-terminal amino acids, hydrolysis by aminopeptidases were highest for AVFA and RVFA (97-100%), followed by VVFA (30-90%) and SVFA (37-51%), and lowest for DVFA (0-1%) at the end of incubation in both seawaters (Fig. 4.9). These differences are statistically significant (ANOVA, $p<0.001$). Bonferroni *t*-test further indicated the significant difference between AVFA and all other peptides except RVFA, and between RVFA and DVFA in both seawaters. Hydrolysis by aminopeptidases of VVFA and SVFA significantly differed at Sta. C6, but not at Sta. SC. In addition, carboxypeptidases contributed substantially (49-100%) to hydrolysis of

VVFA at Sta. SC, of SVFA at both stations, and of DVFA at Sta. SC; endopeptidases accounted for 37% in the DVFA hydrolysis at Sta. C6.

Testing the preference of A by aminopeptidases

The predominant role of aminopeptidases in cleaving N-terminal A was further supported by the comparison between AAA and D-AAA hydrolysis, as a D isomer at the N terminus of peptides may inhibit aminopeptidases. From 0 to 20 h, AAA decreased linearly at a rate of 0.05 μmol L^{-1} h^{-1}, while D-AAA remained relatively constant (Fig. 4.10). From 20 to 24 h, both AAA and D-AAA were hydrolyzed at faster rates, with 0.58 μmol L^{-1} h^{-1} and 0.23 μmol L^{-1} h^{-1}, respectively. Note that AAA hydrolysis was 2.5 times faster than the D-AAA hydrolysis during this time interval. While AAA concentration decreased by 3.37 μmol L^{-1} (71%) over 24 h, D-AAA concentration only decreased by 0.73 μmol L^{-1} (18%) during this time period. The D-isomer on the N-terminus of D-AAA may inhibit the hydrolysis by aminopeptidases, which can explain the lower hydrolysis rate of D-AAA, especially during the initial period (0-20 h) when the concentration of D-AAA remained nearly constant.

The fragments produced during AAA and D-AAA hydrolysis differed. Fragment AA produced from AAA hydrolysis increased from 0.01 μmol L^{-1} to highest concentration of 0.19 μmol L^{-1} at 12 h and then decreased to zero after 20 h (Fig. 4.10a). Similarly, amino acid A increased by 0.14 μmol L^{-1} at 9 h and then decreased to background values at 20 h. In contrast, no AA or D-AA was produced from D-AAA hydrolysis within 24 h, and concentrations of A in the D-AAA hydrolysis samples stayed at low background levels (<0.02 μmol L^{-1}) without measurable increases during the entire incubation, except that the initial concentration was higher (0.14 μmol L^{-1}) (Fig. 4.10b).

The production of AA and amino acid A was only observed in the AAA hydrolysis, suggesting D-AAA was taken up directly as an intact molecule by bacteria. These results indicate that the major hydrolysis pathway of AAA was from the N-terminus.

The role of aminopeptidases in cleaving A was also demonstrated in the AVFA and AVF hydrolysis at Sta. C6 in 2011. With N-terminal A, these two peptides were both hydrolyzed 100% exclusively by aminopeptidases in the Sta. C6 seawater (Figs. 4.5).

Testing preference of hydrophobic to polar uncharged amino acids by aminopeptidases

In addition to the 2014-Sta. SC and 2015-Sta. C6 experiments, hydrolysis between N-terminal hydrophobic and polar uncharged amino acids by aminopeptidases were compared at Sta. SC in 2013. These peptides included AVFA, VFA and FASWGA starting with hydrophobic amino acids, and SWGA with a polar amino acid at the N terminus. About 20-54% of AVFA, VFA and FASWGA were hydrolyzed by aminopeptidases, but only 5% for SWGA (Figs. 4.11, 4.6). ANOVA analysis and bonferroni *t*-test showed that the hydrolysis of AVFA and SWGA by aminopeptidases was significantly different, and so was hydrolysis of VFA and SWGA. A major proportion (46-79%) of AVFA and FASWGA hydrolysis was attributed to endopeptidases, and 59-70% of VFA and SWGA hydrolysis was due to carboxypeptidases.

DISCUSSION

Factors to be considered when deriving peptide hydrolysis pathways

In this study we conducted peptide incubations within a relatively short-time frame (19-27 h). Bacterial abundances increased at different levels (<85%) over 21-24 h (Figs. 4.2b, 4.4b). However, peptide hydrolysis decreased with a linear pattern, indicating their hydrolysis rates were constant throughout the incubation time and not affected much by the bacteria abundance change. The linearity of peptide hydrolysis within 24 h is consistent with previous studies (Liu et al., 2010; Liu et al., 2013).

It is intriguing that appreciable hydrolysis products were present at 0 h during some incubations, such as FASWGA, SWGA, D-AAA, AVFA, VVFA, RVFA, SVFA, and DVFA at Sta. SC (Figs. 4.1, 4.6, 4.10). This initial hydrolysis seems to be instantaneous as the time lag between peptide amendment and the initial sampling point was 2 min at most. The mechanism for this initial instantaneous hydrolysis remains unclear, but perhaps some extracellular enzymes can hydrolyze the amended peptide extremely quickly (Ziervogel et al., 2007). Our preliminary data indicated that this instantaneous hydrolysis was related to extracellular enzymes in cell-free dissolved forms (Appendix I). This instantaneous hydrolysis seems to be present only at the beginning of the incubation because concentrations of hydrolysis products increased gradually after the initial pulse of hydrolysis products. This limited-time effect might be related to the short lifetime or low concentrations of these active extracellular enzymes, or the degradation of these enzymes by other proteases in the seawater (Chróst, 1991). As we used the concentration difference of peptide fragments and amino acids between the target time point and the initial time point, the hydrolysis percentages do not include the instantaneous hydrolysis.

The effects of chemical structure on peptide hydrolysis pathways

For peptides with uncharged N-terminal amino acids, aminopeptidases tend to preferentially cleave A, V, F more than S (Figs. 4.9, 4.11). The hydropathy index of hydrophobic amino acids A, V, and F is 1.8, 4.2, and 2.8, respectively, while that of polar amino acid S is only -0.8 (Kyte and Doolittle, 1982). This result indicates that aminopeptidases prefer hydrophobic amino acids to polar amino acids, and this preference is especially pronounced for A as supported by the different hydrolysis patterns between AAA and D-AAA (Fig. 4.10). This selectivity of N-terminal amino acids by aminopeptidases has also been demonstrated in studies using single bacteria cultures. For instance, a periplasmic aminopeptidase purified from *Escherichia coli* exhibited a high preference for A at the peptide N terminus (Lazdunski et al., 1975).

For the N-terminal amino acids with charged side chains, aminopeptidases preferentially cleave basic and positively charged amino acid such as R rather than acidic and negatively charged amino acid such as D in the seawater (Fig. 4.9). N-terminal glutamic acid (E) and D were consistently resistant to hydrolysis by the extracellular aminopeptidase from the marine bacterium *Aeromonas proteolytica* (Wilkes et al., 1973).

Amino acid preference by aminopeptidases may be related to the degradation index (DI) loading of amino acids. Amino acids with higher DI loading (from Dauwe et al. (1999)), that are removed first from bulk organic matter, corresponded to those susceptible to a broader range of aminopeptidases with high affinity (Steen et al., 2015). However, we observed no correlation between hydrolysis by aminopeptidases and amino acid DI loading (Fig. 4.12), which suggests that other mechanisms should be responsible to the patterns in our results.

Alternatively, the preference of hydrophobic or basic N-terminal amino acids by aminopeptidases may be related to the properties of the enzyme binding site. Bacterial

aminopeptidases can be classified into broad or narrow categories based on their substrate specificity (Gonzales and RobertBaudouy, 1996; Yolanda, 2007). For example, PepA type aminopeptidases (leucine aminopeptidases), one of the most well-characterized aminopeptidases, have broad substrate specificity; they are most effective in removing leucine, but can also cleave most other L-amino acids (Delange and Smith, 1971). N-terminal amino acids with larger and hydrophobic side chains can increase hydrolysis rate by leucine aminopeptidases, whereas hydrolysis of amino acids with smaller, ionic and hydrophilic side chains are slower (Delange and Smith, 1971; Wilkes et al., 1973). The hydrophobic pocket, or active site, of leucine aminopeptidases interact with hydrophobic side chain of substrate amino acids, and metal ions inside enzymes stabilize the enzyme and interact with the α-amino group and amide N to give a complex in the transition state; afterwards the complex undergoes a nucleophilic displacement of amide by an attack with hydroxyl ion (Smith and Spackman, 1955; Taylor, 1993). PepN aminopeptidases, another type of aminopeptidases with broad substrate specificity, also prefer hydrophobic N-terminal amino acids, and can hydrolyze amino acid A rapidly (Lazdunski et al., 1975; Mccaman and Villarejo, 1982). The hydrophobicity feature of the active binding sites of enzymes and hydrophobic interactions between aminopeptidases and substrates may be important in determining the amino acid susceptibility to enzymes. This also explains the preferential cleavage of hydrophobic amino acids at the N-terminus by aminopeptidases we observed. Within the same hydrophobic amino acid group, the preference to hydrolyze these amino acids by aminopeptidases may differ, as indicated by different hydrolysis percentages by aminopeptidases among AVFA, VFA, and FASWGA or between AVFA and VVFA. This observation further suggests subtle difference of substrate susceptibility to aminopeptidases in natural seawater. In addition to aminopeptidases with broad specificity mentioned above, some bacterial aminopeptidases

have strict specificity, such as aminopeptidases P that hydrolyze N-terminal amino acids adjacent to Proline (P), arginine aminopeptidases that are specific to R cleavage, and aminopeptidases A that target on N-terminal acidic D or E (Gonzales and RobertBaudouy, 1996). The high hydrolysis percentage by aminopeptidases in the RVFA hydrolysis observed in our study may be attributed to the active role of either lysine aminopeptidases, the enzyme with broad specificity but especially active at cleaving lysine (K) and R (Arora and Lee, 1992), or arginine aminopeptidases that is specific to R. The small hydrolysis percentage of DVFA by aminopeptidases in the Sta. SC and Sta. C6 seawater indicates that aminopeptidases A were not so active in the two seawaters. The resistance of D to aminopeptidases with broad specificity may be related to its negative charge. A positively charged cysteine derivative was susceptible to aminopeptidases while negatively charged cysteic acid was unable to be attacked by aminopeptidases (Wilkes et al., 1973). Overall, our study provides insights into the active peptidases present in the coastal seawater. In particular, PepA type aminopeptidases (leucine aminopeptidases) and/or PepN aminopeptidases were active in the hydrolysis of N-terminal hydrophobic amino acids, and lysine aminopeptidases and/or arginine aminopeptidases were active in cleaving N-terminal positively-charged amino acids, but aminopeptidases A that cleave negatively-charged amino acids were less active in the coastal seawater we studied.

The susceptibility of substrates to aminopeptidases is not only determined by the amino acid at the N terminus (P1 position), but also by the next amino acids (such as successive P1' and P2' position) in the peptide chain (Delange and Smith, 1971; Gonzales and RobertBaudouy, 1996). For example, the release of S from N-terminus could be reduced if E was present at the P1' position adjacent to the N terminus (Wilkes et al., 1973). Thus, we should be cautious when interpreting the variation of

aminopeptidase hydrolysis among AVFA, VFA and FASWGA at 2013-Sta. SC in our study, as they differ in not only N-terminal amino acids but also the ones next to them.

In addition to the N-terminal amino acid, amino acid in the middle of peptide chain may affect peptide hydrolysis pathways. While the internal amino acid W was present in FASWGA and SWGA, it could fit in the active site of certain endopeptidases, in particular chymotrypsin that preferentially cleaves peptide bonds where the carboxyl side is a large hydrophobic amino acid such as F and W (Appel, 1986). Especially high percentage (79%) of hydrolysis by endopeptidases was shown in the FASWGA hydrolysis at Sta. SC, which might relate to the active role of chymotrypsin in seawater.

Peptide hydrolysis pathways are temporally or spatially dependent

Previous studies found different active peptidases in environments using peptide analogs. For example, aminnopeptidases are active in many systems, such as the Arctic fjord, Baltic Sea fjords, and North Atlantic, revealed through Leucine-Methylcoumarinylamide (Leu-MCA) hydrolysis, while important roles of endopeptidases or carboxypeptidases were shown in the coastal water of Japan (Hoppe, 1983; Hashimoto et al., 1985; Obayashi and Suzuki, 2005), indicating that peptide hydrolysis pathways may be spatially dependent. Our results consistently showed that the major hydrolysis pathways for the same peptide substrate vary in different locations or even in the same location in different seasons. For example, AVFA hydrolysis by aminopeptidases varied from 54% in 2013 to 97% in 2014 at Sta. SC, and VVFA hydrolysis by aminopeptidases ranged from 30% to 90% between Sta. SC and Sta. C6. This variation may be related to the temporal or spatial difference of the enzymatic activities. Ectoenzymes associated with bacterial cells are often the dominant form of extracellular enzymes in peptide

hydrolysis (Chróst et al., 1991). Bacterial species can differ in types and activities of their ectoenzymes (Arrieta and Herndl, 2002; Arnosti et al., 2005; Murray et al., 2007). For instance, 44 isolated pelagic bacteria strains showed a broad range (over 3 orders of magnitude) of aminopeptidase activity (Martinez et al., 1996). As the abundance and activity of peptidases may differ among bacterial groups and bacterial community is not evenly distributed among different seawater (Pommier et al., 2007; Fuhrman and Hagstrom, 2008), the bacterial community may affect the major hydrolysis pathways of small peptides. Alternatively, some protists, including certain phytoplankton and mixotrophic dinoflagellates, can also produce peptidases and utilize organic matter through the osmotrophic nutrition strategy (Glibert and Legrand, 2006; Salerno and Stoecker, 2009; Liu et al., 2015). The different types of protists present or their different nutrition strategies in different seawaters could potentially lead to the different patterns of enzyme activities.

Implications

This study provides the first dataset of relative roles of amino-, endo-, carboxypeptidases in the coastal seawater using plain peptides, and demonstrated the effects of chemical structure on peptide hydrolysis pathways. The results highlight the active role of aminopeptidases hydrolyzing hydrophobic N-terminal amino acids and positive-charged amino acids, such as PepA aminopeptidases, PepN aminopeptidases, lysine aminopeptidases, and/or arginine aminopeptidases, the less active role of aminopeptidases A and resistance of aminopeptidases to negative-charged amino acids in coastal seawater. This finding expands from previous studies using enzymes isolated from single bacteria strains to comparison of different peptidases in natural marine

environments and expand this comparison to more peptidases using plain peptides rather than peptide analogs that target specific peptidases. Through comparing hydrolysis pathways among different substrates, active roles of certain peptidases with broad or specific substrate specificity can be deduced. This approach can be applied to other location to map a relative distribution of different peptidases active in coastal and open oceans, which may be important to understand factors controlling protein and/or peptide hydrolysis patterns and the interactions with microbial community.

Although amino acid composition of a peptide affects its hydrolysis pathway, hydrolysis rates of peptides with N-terminal polar or negative-charged amino acids are comparable to those that are preferentially cleaved by aminopeptidases. This observation suggests that endopeptidases and/or carboxypeptidases become active in the hydrolysis of peptides with N-terminal polar or negative-charged amino acids. In other words, when one kind of peptidases does not fit the substrate, other peptidases may cleave peptides and achieve rapid hydrolysis rates of labile peptides. More studies on peptides with different chemical structures such as ones differing in C-terminal amino acids or internal amino acids, are needed to understand the active role of carboxypeptidases or endopeptidases, evaluate the whole spectrum of extracellular peptidases, and predict hydrolysis patterns of protein or peptides substrates in marine systems.

Table 4.1. Physical and chemical parameters of surface seawater from Sta. ship channel (SC) in Port Aransas, TX and Sta. C6 in the northern Gulf of Mexico, and tested peptide substrates in each sampled seawater.

Time	Station	Temp (ºC)	Salinity (ppt)	DO (mg $\cdot L^{-1}$)	Chl *a* (µg $\cdot L^{-1}$)	pH	NO_3^- (µmol $\cdot L^{-1}$)	NO_2^- (µmol $\cdot L^{-1}$)	NH_4^+ (µmol $\cdot L^{-1}$)	PO_4^{3-} (µmol $\cdot L^{-1}$)	DOC (µmol $\cdot L^{-1}$)	TDN (µmol $\cdot L^{-1}$)	DCAA (µmol $\cdot L^{-1}$)	DFAA (µmol $\cdot L^{-1}$)	Tested peptides
Mar-2013	SC	16.0	33	nm*	nm	8.37	1.89	0.11	1.91	0.62	275	26	1.35	0.30	AAA, D-AAA
Apr-2013	SC	22.5	31	nm	nm	8.06	1.57	0.02	1.82	0.18	208	18	0.99	0.27	AVFA, VFA, FASWGA, SWGA
June-2014	SC	27.0	37	nm	nm	7.96	4.46	ud**	3.38	0.30	nm	nm	0.35	0.08	AVFA, VVFA, SVFA, RVFA, DVFA
May-2011	C6	24.4	27	6.79	0.05	8.37	4.73	0.46	0.46	0.02	175	nm	1.21	0.28	AVF, AVFA
Apr-2015	C6	24.2	25	7.77	4.23	8.38	11.82	ud	2.55	0.05	nm	nm	1.07	0.10	AVFA, VVFA, SVFA, RVFA, DVFA

*nm: not measured; **ud: undetectable.

Table 4.2. Summary of hydrolysis products (percentage as dividing summed increasing concentrations of peptides fragments and amino acids by concentrations of decreasing peptide substrates) at the end of incubations and the major hydrolysis pathways of tested small peptides.

Peptide	Station-Year	Time (h)	Products%	Major hydrolysis pathways
AVFA	SC-2013	19	88	AVFA→A+VFA, AVFA→AV+FA
VFA	SC-2013	19	129	VFA→VF+A, VFA→V+FA
FASWGA	SC-2013	19	131	FASWGA→FASW+GA
SWGA	SC-2013	19	38	SWGA→SWG+A
AVFA	SC-2014	21	37	AVFA→A+VFA
VVFA	SC-2014	21	45	VVFA→VVF+A, VVFA→V+VFA
SVFA	SC-2014	21	42	SVFA→SVF+A→SV+F+A, SVFA→S+VFA
RVFA	SC-2014	21	34	RVFA→R+VFA→R+V+FA→R+V+F+A
DVFA	SC-2014	21	45	DVFA→DVF+A→DV+F+A→D+V+F+A
AVFA	C6-2011	27	72	AVFA→A+VFA→A+V+FA→2A+V+F
AVF	C6-2011	24	69	AVF→A+VF
AVFA	C6-2015	24	92	AVFA→A+VFA→A+V+FA→2A+V+F
VVFA	C6-2015	24	120	VVFA→V+VFA→2V+FA→2V+F+A
SVFA	C6-2015	24	42	SVFA→S+VFA→S+V+FA, SVFA→SVF+A→SV+F+A
RVFA	C6-2015	24	49	RVFA→R+VFA→R+V+FA→R+V+F+A
DVFA	C6-2015	24	110	DVFA→DVF+A→DV+F+A, DVFA→DV+FA

Figure 4.1. Concentrations of AVFA (a), VVFA (b), SVFA (c), RVFA (d), and DVFA (e) with their major hydrolyzed peptide fragments and amino acids during the 21-h incubation using the Sta. SC seawater in 2014. Data points were presented as average ± standard deviation of duplicate samples.

(a) AVFA

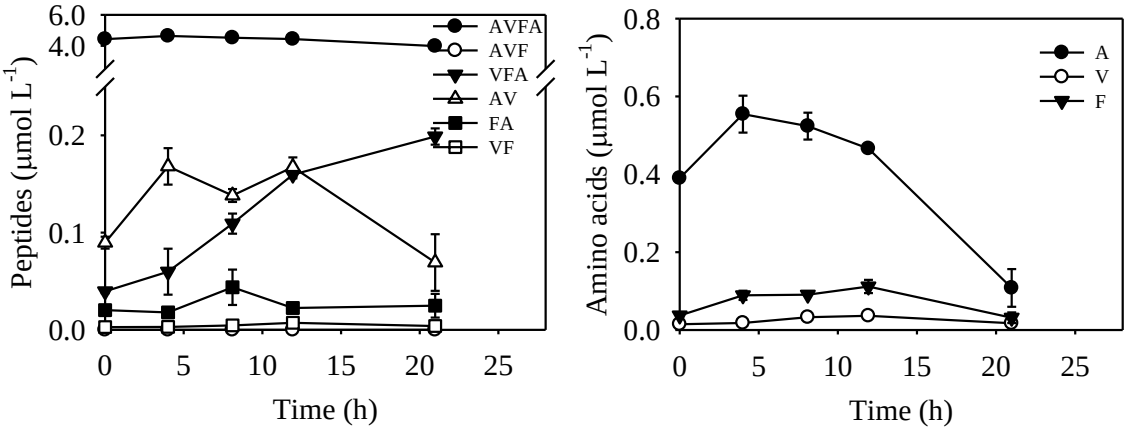

(b) VVFA

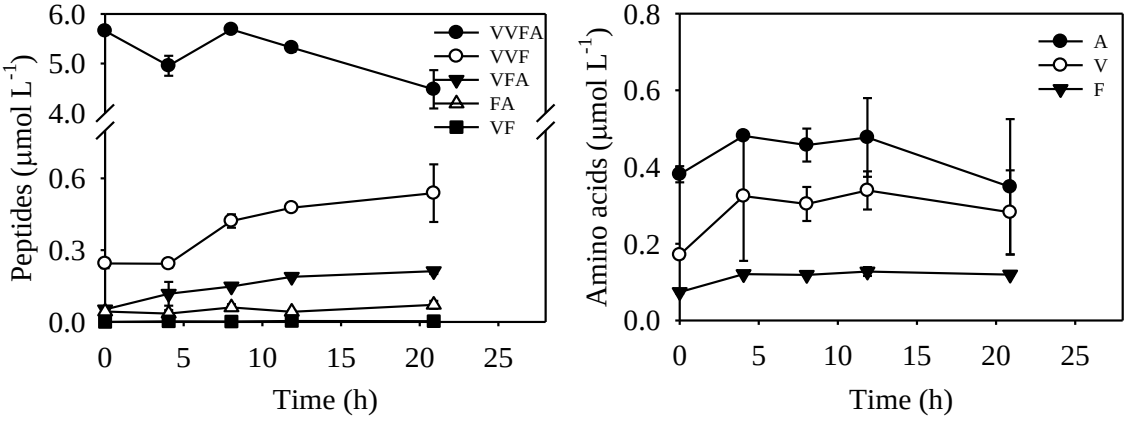

Figure 4.1 (continued)
(c) SVFA

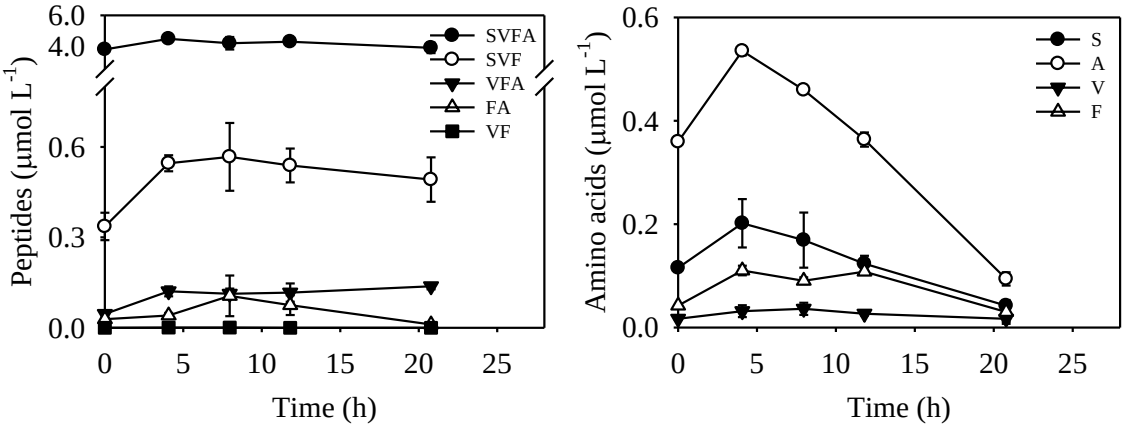

(d) RVFA

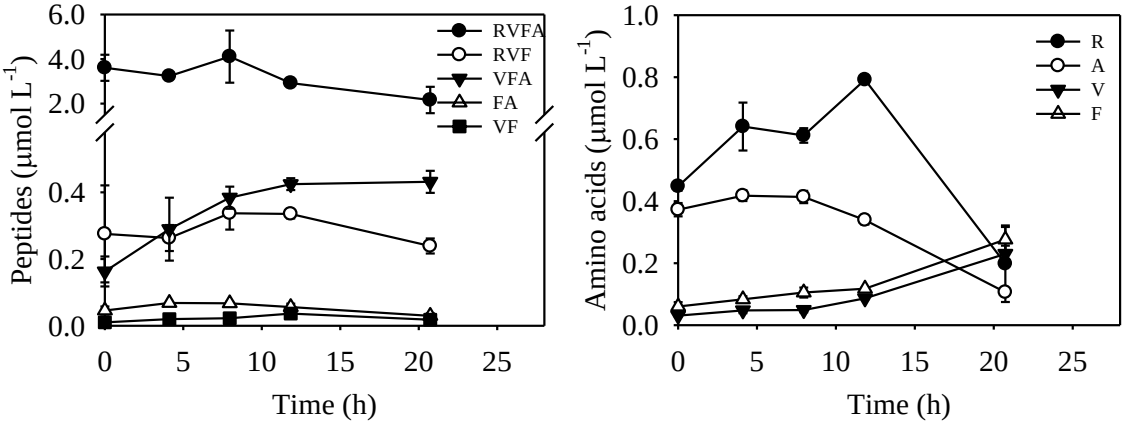

Figure 4.1 (continued)
(e) DVFA

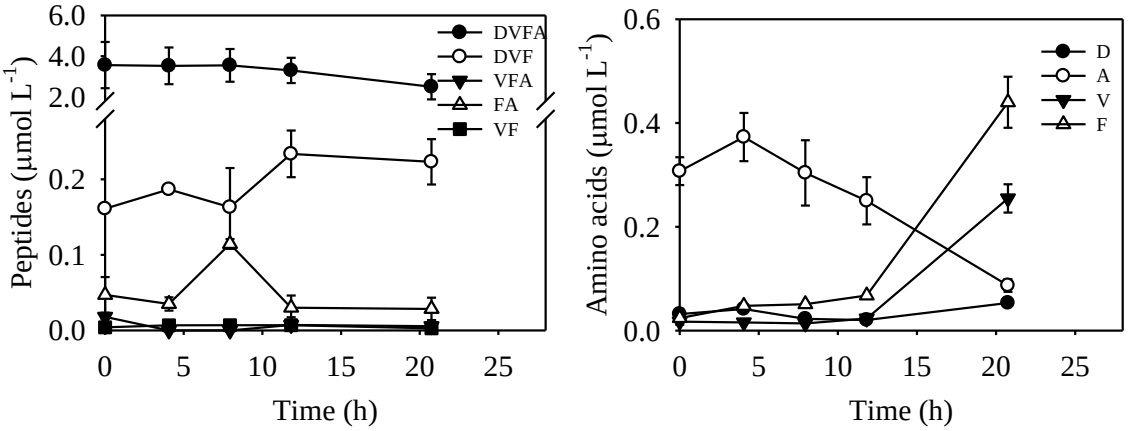

Figure 4.2. Concentrations of DFAA in the control (CTR) without peptide amendment (a), and bacterial abundance in each peptide treatment (b) during the 21-h incubation using the Sta. SC seawater in 2014. Data points were presented as average ± standard deviation of duplicate samples.

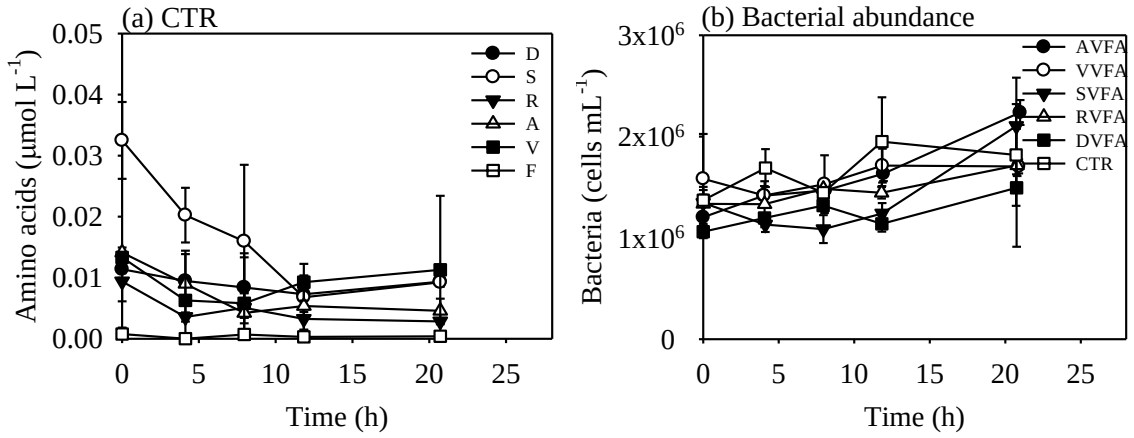

Figure 4.3. Concentrations of AVFA (a), VVFA (b), SVFA (c), RVFA (d), and DVFA (e) with their major hydrolyzed peptide fragments and amino acids during the 24-h incubation using the Sta. C6 seawater in 2015. Data points were presented as average ± standard deviation of duplicate samples.

(a) AVFA

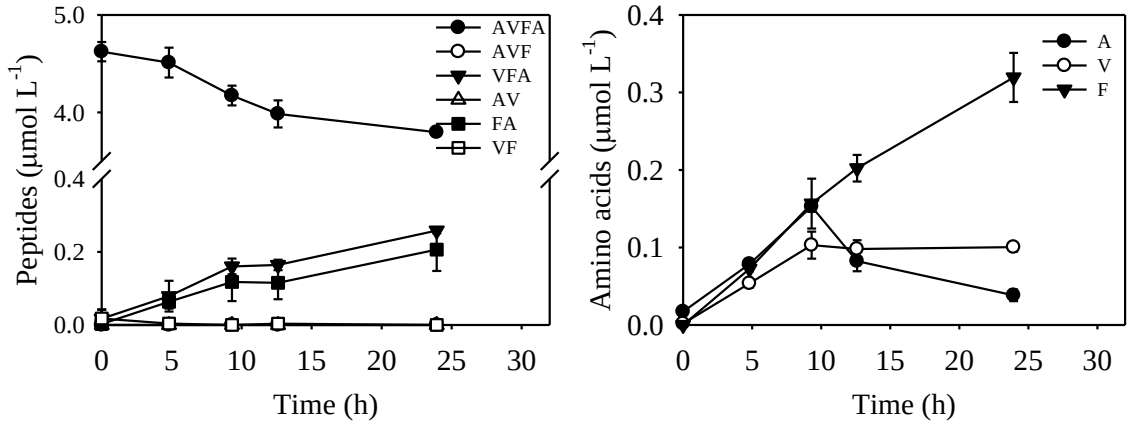

(b) VVFA

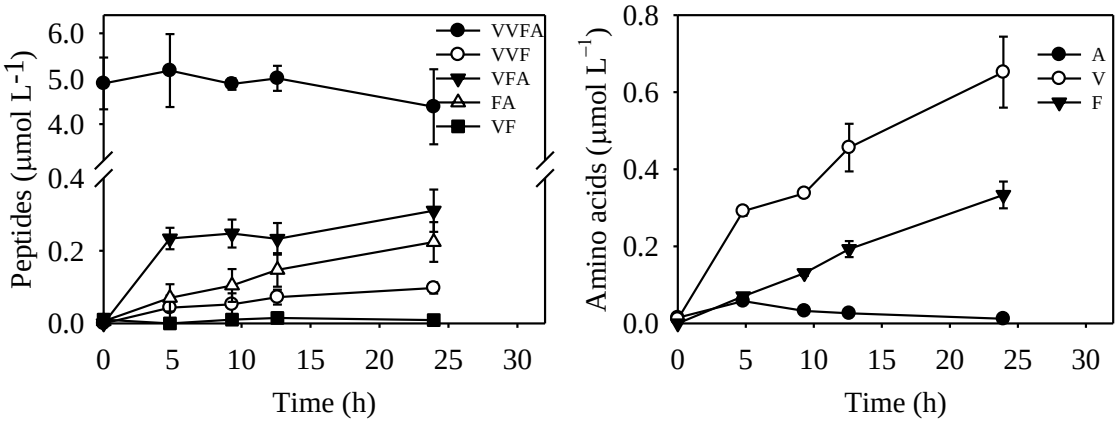

Figure 4.3 (continued)
(c) SVFA

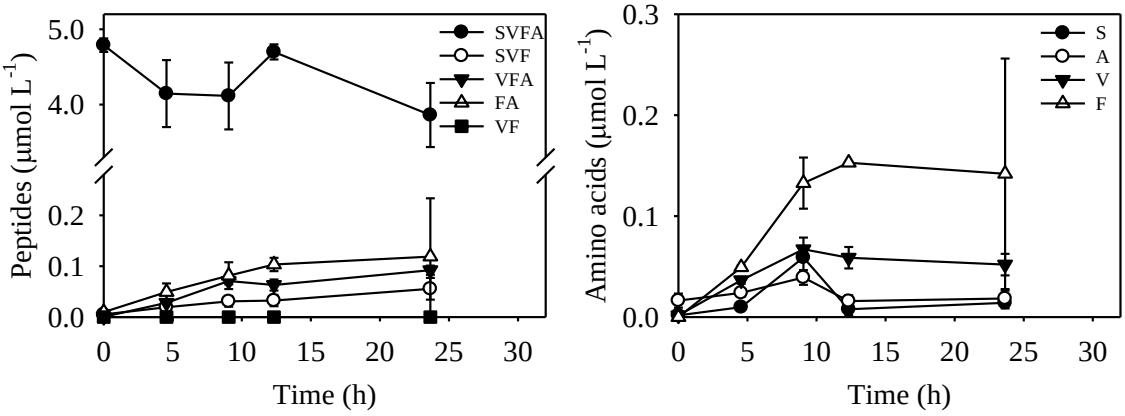

(d) RVFA

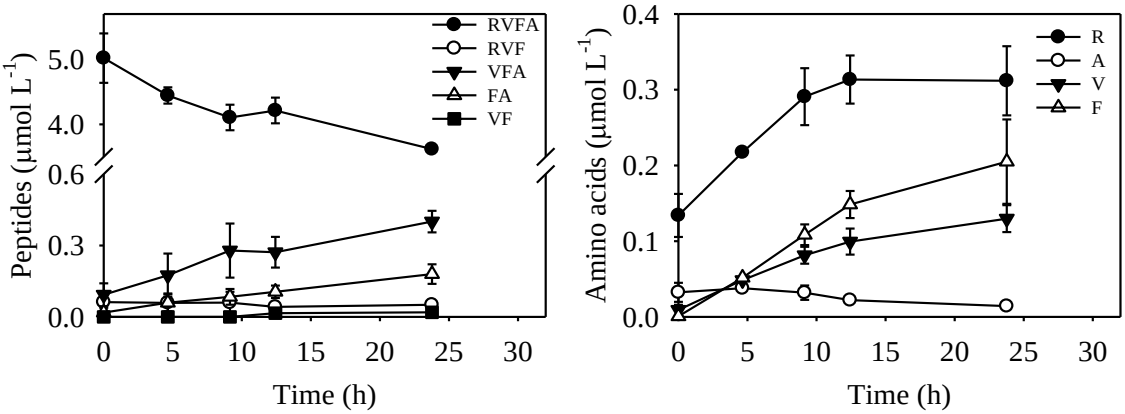

Figure 4.3 (continued)
(e) DVFA

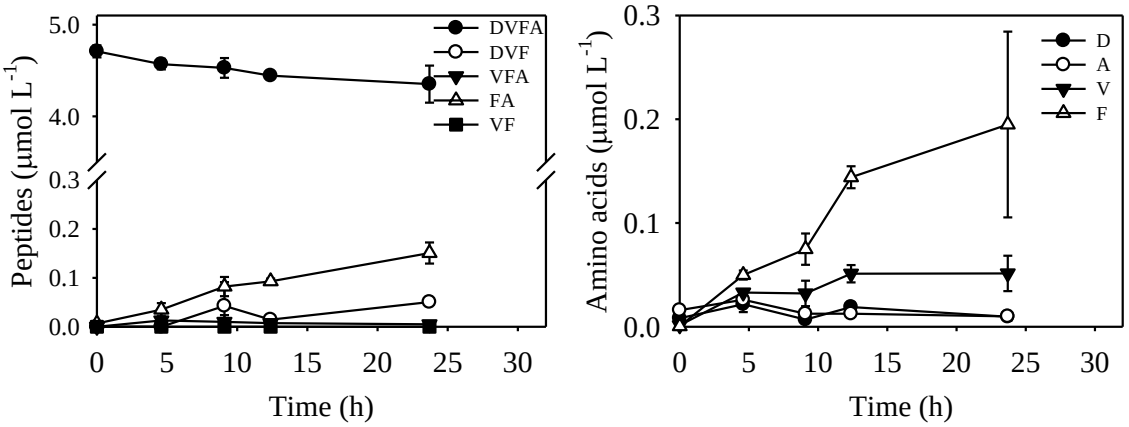

Figure 4.4. Concentrations of DFAA in the control (CTR) without peptide amendment (a), and bacterial abundance in each peptide treatment (b) during the 24-h incubation using the Sta. C6 seawater in 2015. Data points were presented as average ± standard deviation of duplicate samples.

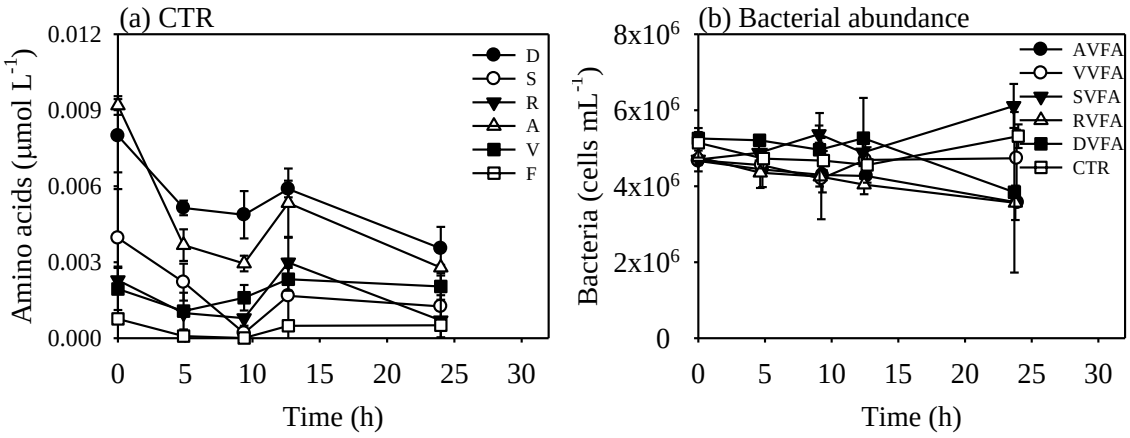

Figure 4.5. Concentrations of AVFA (a) and AVF (b) with their major hydrolyzed peptide fragments and amino acids during the 24-27 h incubation using the Sta. C6 seawater in 2011.

(a) AVFA

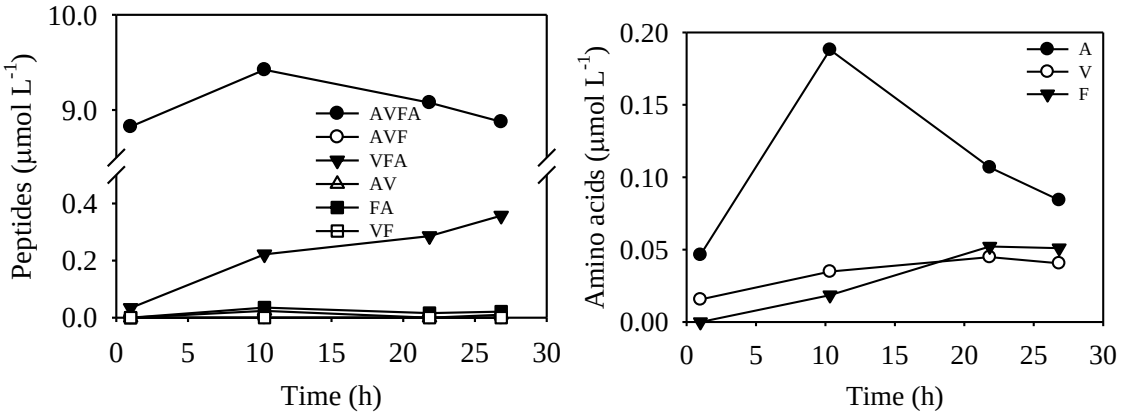

(b) AVF

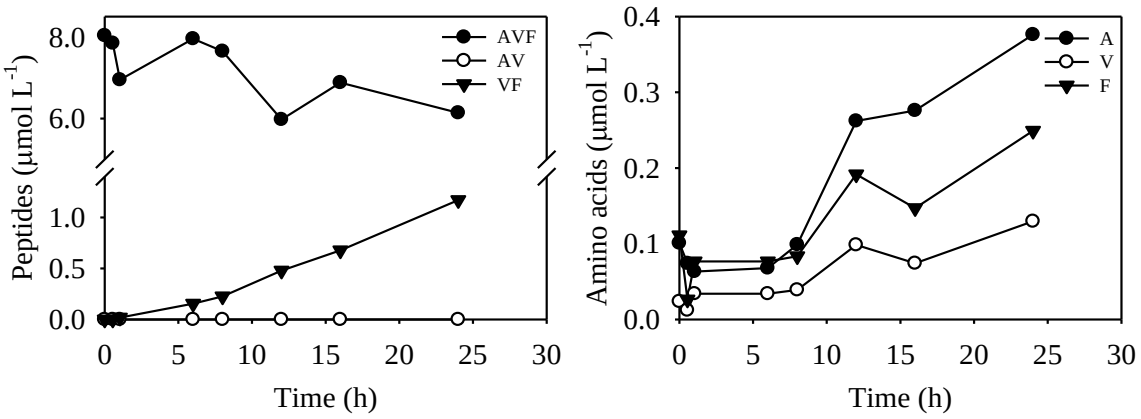

Figure 4.6. Concentrations of AVFA (a), VFA (b), FASWGA (c), and SWGA (d) with their major hydrolyzed peptide fragments and amino acids during the 19-h incubation using the Sta. SC seawater in 2013. Data points were presented as average ± standard deviation of duplicate samples.

(a) AVFA

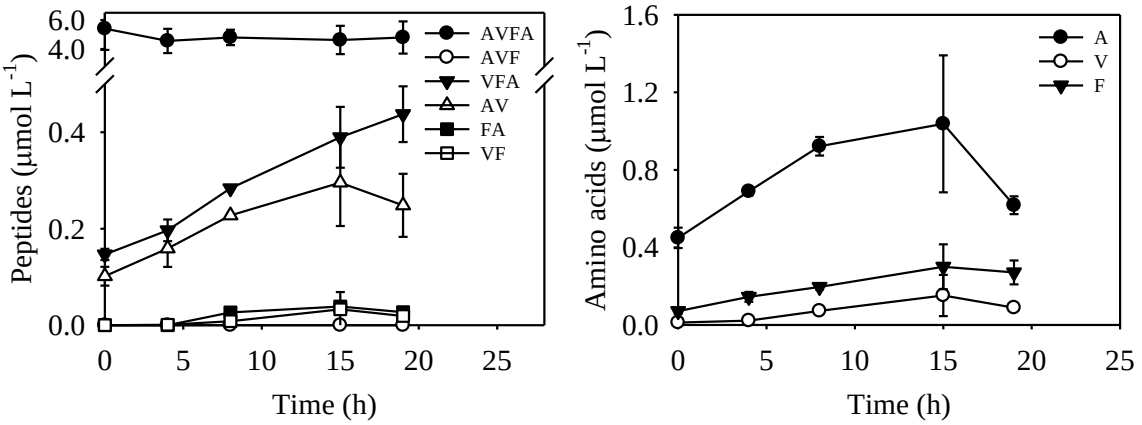

(b) VFA

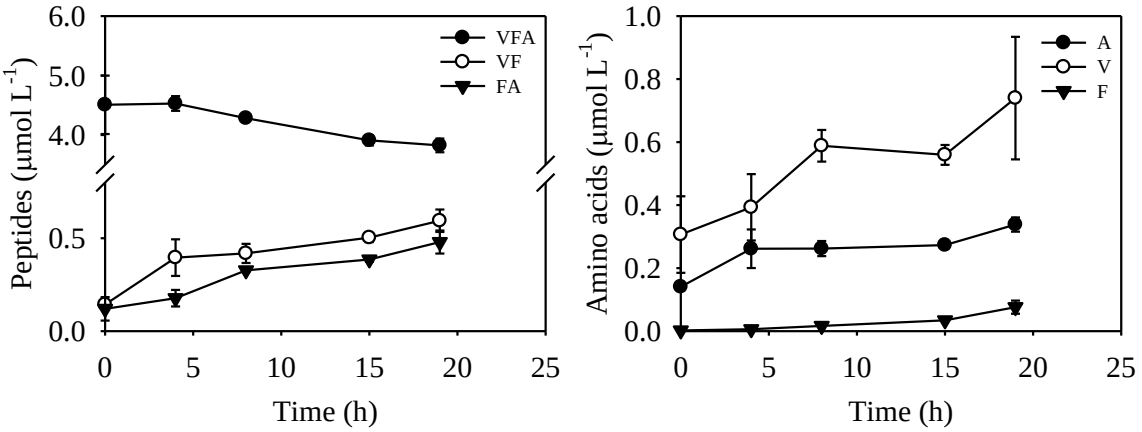

Figure 4.6 (continued)
(c) FASWGA

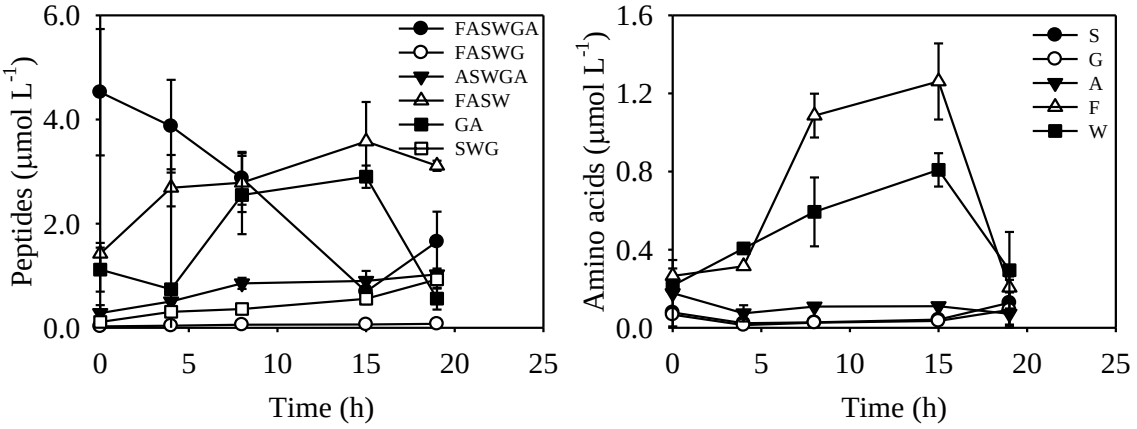

(d) SWGA

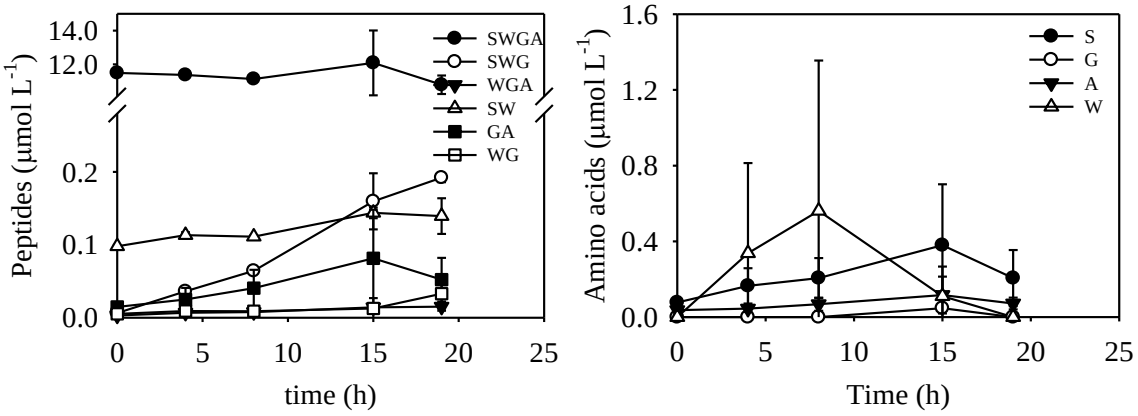

Figure 4.7. Percentages of hydrolysis by aminopeptidases, carboxypeptidases, and endopeptidases at each time point during the AVFA (a), VVFA (b), SVFA (c), RVFA (d), and DVFA (e) incubations using the Sta. SC seawater in 2014.

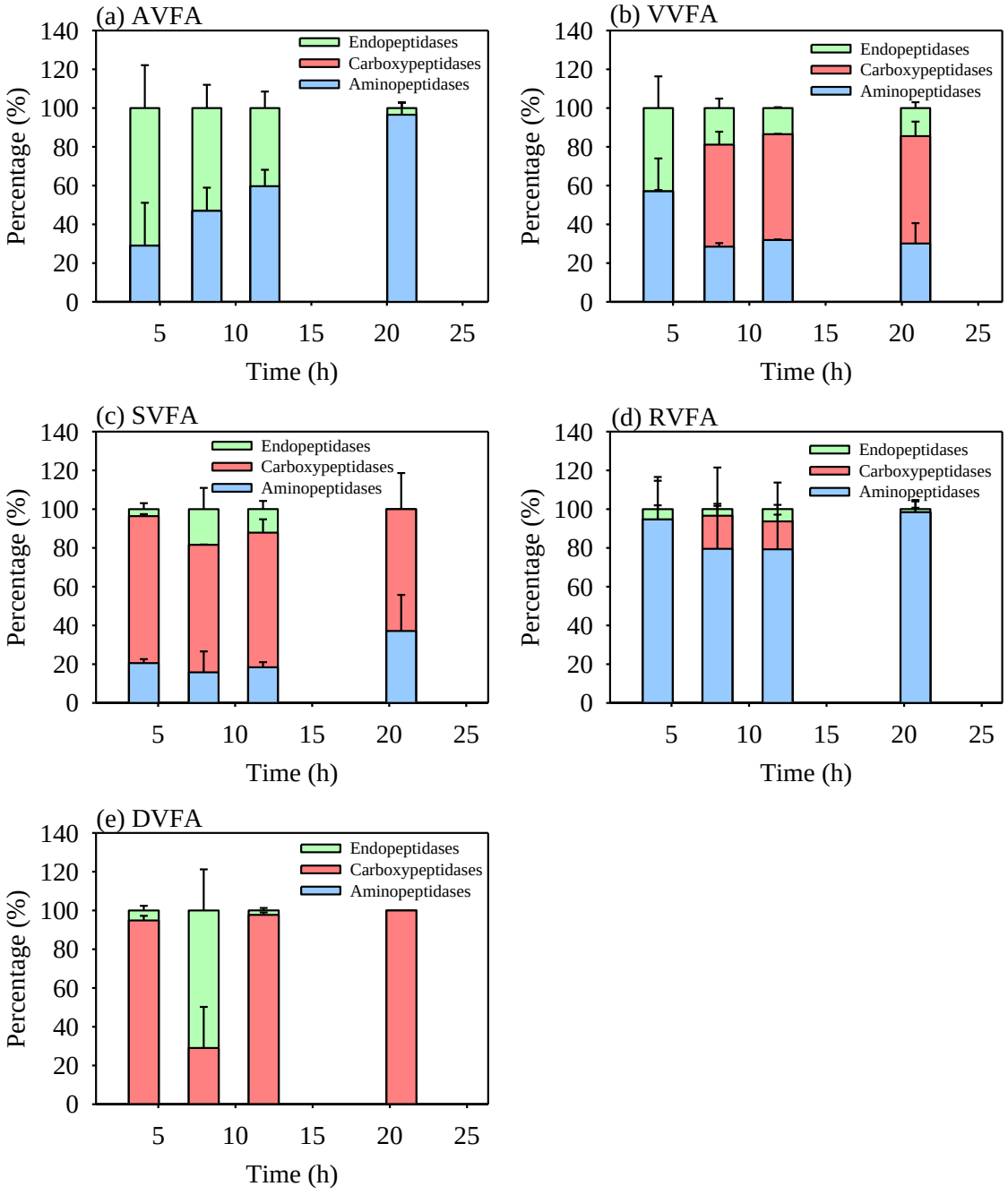

Figure 4.8. Percentages of hydrolysis by aminopeptidases, carboxypeptidases, and endopeptidases at each time point during the AVFA (a), VVFA (b), SVFA (c), RVFA (d), and DVFA (e) incubations using the Sta. C6 seawater in 2015.

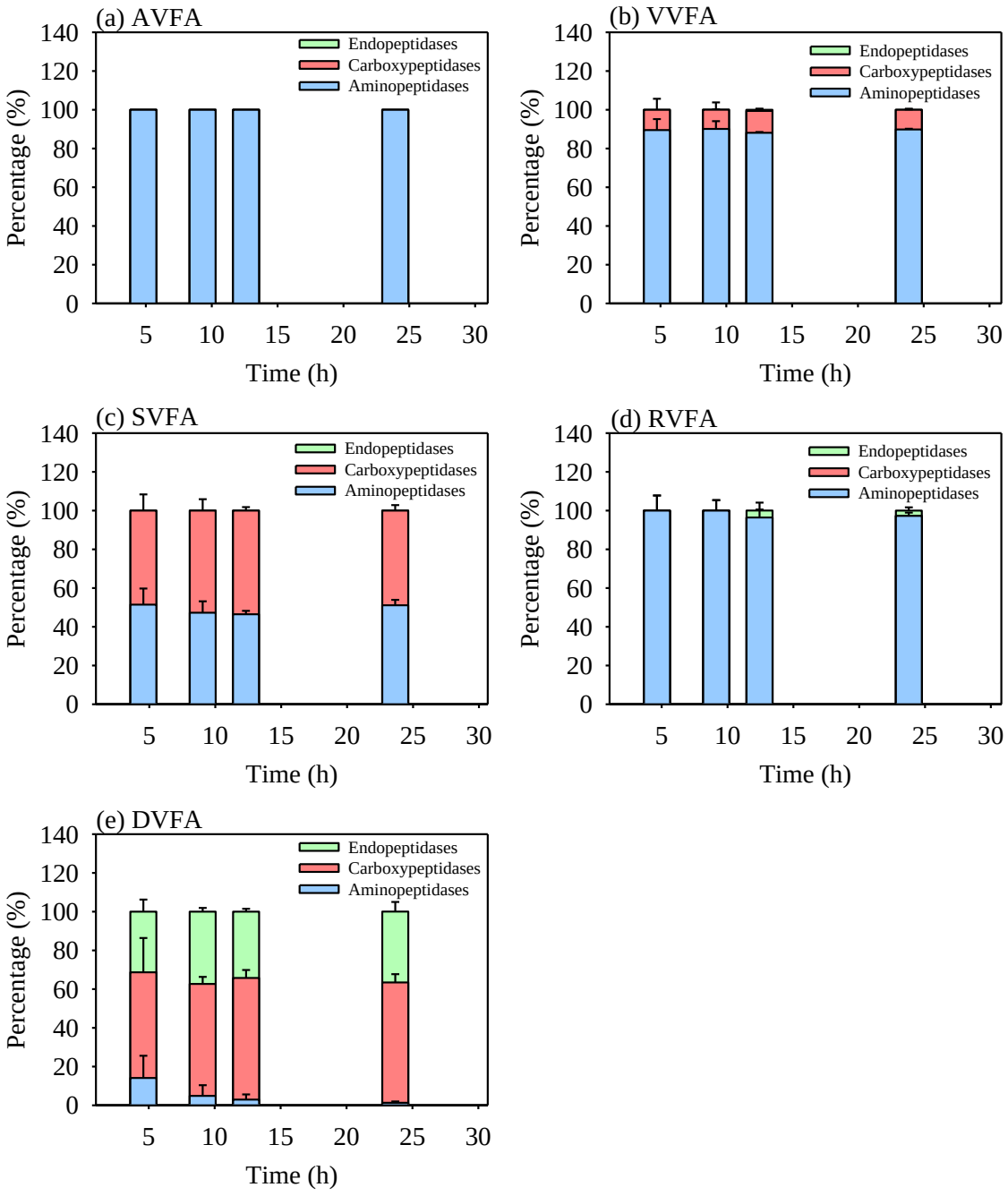

Figure 4.9. Percentages of hydrolysis by aminopeptidases, carboxypeptidases, and endopeptidases at the end time point (21-24 h) in the AVFA, VVFA, SVFA, RVFA and DVFA incubations using Sta. SC seawater in 2014 (a) and Sta. C6 seawater in 2015 (b). Error bars represented standard deviation of duplicate samples.

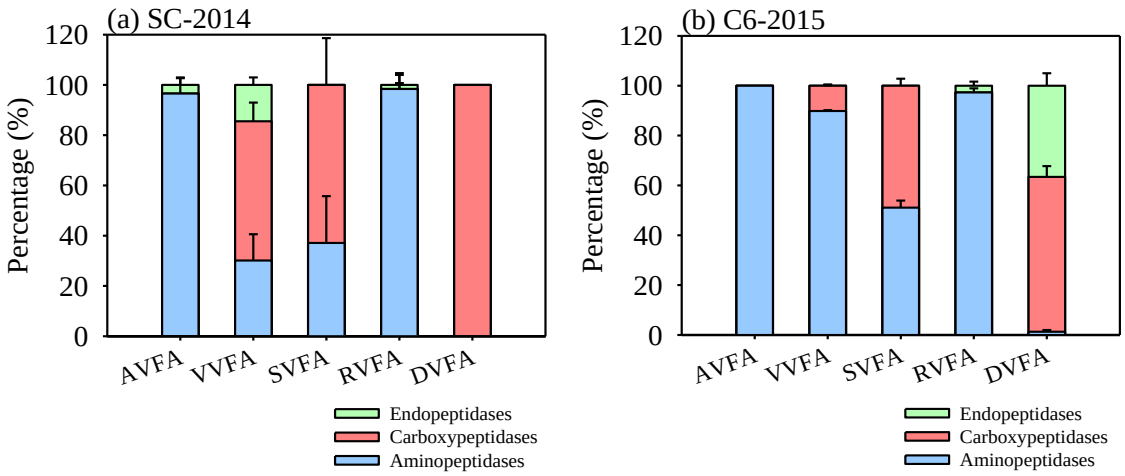

Figure 4.10. Concentrations of AAA (a) and D-AAA (b) with their hydrolyzed products during the 24-h incubation in the Sta. SC seawater. Data points were presented as average ± standard deviation of duplicate samples.

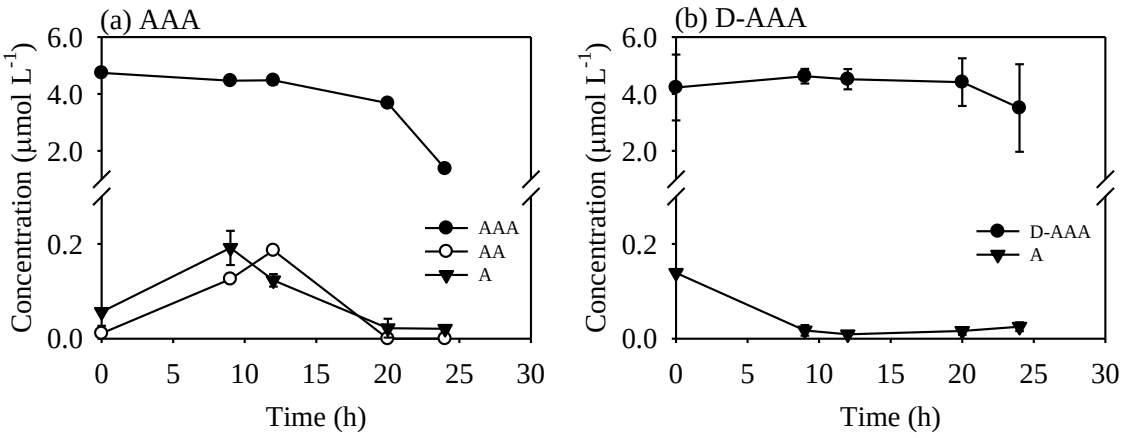

Figure 4.11. Percentages of hydrolysis by aminopeptidases, carboxypeptidases, and endopeptidases at the end time point (19 h) in the AVFA, VFA, FASWGA and SWGA incubations using Sta. SC seawater in 2013. Error bars represented standard deviation of duplicate samples.

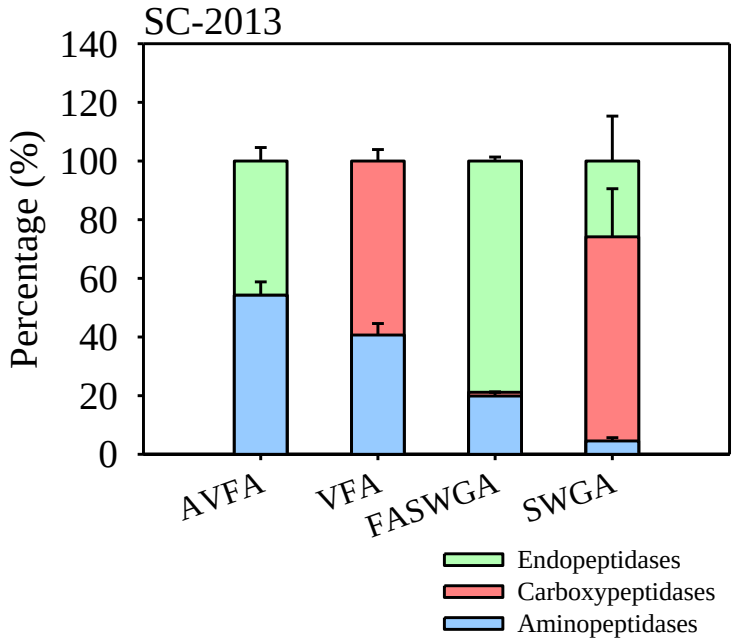

Figure 4.12. Percentages of hydrolysis by aminopeptidases vs. degradation index (DI) loading of N-terminal amino acids (from Dauwe et al. (1999)) for the peptide incubations at Sta. SC in 2014 (a), at Sta. C6 in 2015 (b), and Sta. SC in 2013 (c).

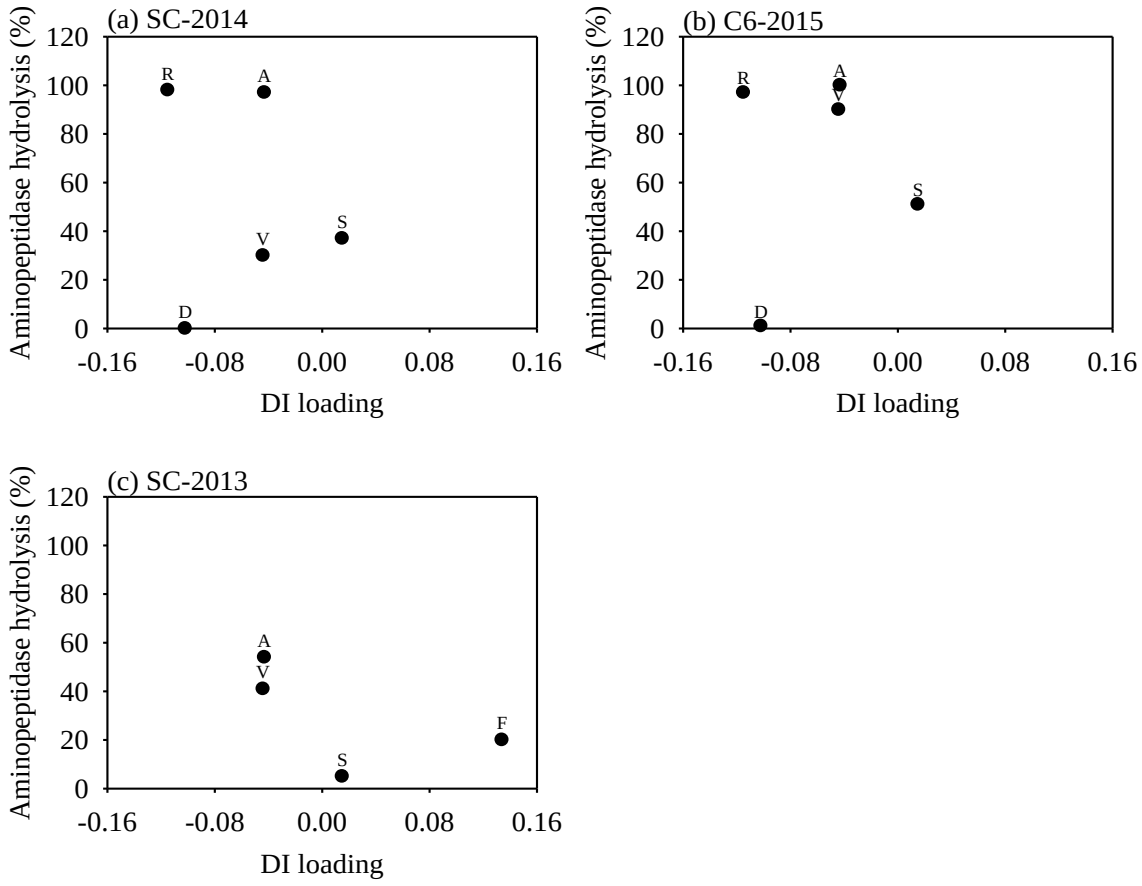

Chapter 5. Linking peptide decomposition and bacterial communities in the northern Gulf of Mexico normoxic and hypoxic waters using DNA stable isotope probing

ABSTRACT

Proteins and peptides are key components of the labile dissolved organic matter (LDOM) pool in marine environments. Knowing which types of bacteria metabolize peptides is necessary to understand the factors that govern peptide decomposition and further carbon and nitrogen remineralization in marine environments. A ^{13}C-labeled tetrapeptide, alanine-valine-phenylalanine-alanine (AVFA), was added to both surface (normoxic) and bottom (hypoxic) seawater from a coastal station in the northern Gulf of Mexico for a two-day incubation experiment, and bacteria that incorporated the peptide were identified using DNA-stable isotope probing (DNA-SIP). The decomposition rate of AVFA in the bottom hypoxic seawater (0.018-0.035 μM h^{-1}) was twice as fast as that in the surface normoxic seawater (0.011-0.017 μM h^{-1}). Bacterial community structure changed differently between the surface and bottom water incubations. DNA-SIP data consistently showed that incorporation of ^{13}C-AVFA was highest for *Flavobacteria*, *Sphingobacteria*, *Alphaproteobacteria*, *Cyanobacteria*, and *Actinobacteria* in the surface water, while highest for *Alphaproteobacteria* and *Gammaproteobacteria* in the bottom water. High ^{13}C enrichment was observed in three genera (*Thalassococcus*, *Rhodobacteraceae*, *Ruegeria*) belonging to *Alphaproteobacteria* and five genera (*Colwellia, Balneatrix*, *Thalassomonas*, *Pseudoalteromonas*, *Neptuniibacter)* belonging to *Gammaproteobacteria* in the bottom water, suggesting that these bacteria may have high capabilities in metabolizing dissolved peptides in marine systems and contribute to faster peptide decomposition in the bottom water. Taken together, this study offers

insights into the types of bacteria that can metabolize labile organic matter in hypoxic vs. normoxic coastal waters of the northern Gulf of Mexico.

INTRODUCTION

Proteins and peptides are key components of labile dissolved organic matter (LDOM) that supports bacterial growth (Azam, 1998). Small peptides (ca. <600 Da) are key immediate products of microbial protein decomposition owing to the size constraints of bacterial cell membrane transport systems, i.e., porins (Weiss et al., 1991). After proteins are degraded to small peptides, these small peptides can be either taken up directly by bacteria as intact substrates, or hydrolyzed further to individual amino acids via extracellular enzymes with subsequent uptake of amino acids by bacteria. The interaction between peptide decomposition and bacteria plays an important role in the cycling of carbon and nitrogen, regeneration of nutrients, and preservation of refractory dissolved organic nitrogen (DON) (Aluwihare et al., 2005; Nagata, 2008).

Our previous studies have demonstrated that small peptides decompose more quickly in bottom hypoxic than in surface normoxic (normal oxygen-saturated) waters in the northern Gulf of Mexico (nGOM), and that certain bacterial genera, such as *Neptuniibacter*, *Pseudoalteromonas*, *and Roseobacter*, grew exceptionally well in the bottom hypoxic water with added peptides (Liu et al., 2013; Liu and Liu, 2016). These results suggest that some bacterial groups may be particularly effective at metabolizing peptide-derived organic matter in hypoxic seawater, but direct evidence of linkage between bacterial communities and peptide decomposition is needed. Knowing which types of bacteria metabolize peptides in the hypoxic seawater is also important to

understanding the factors controlling hypoxia formation, as decomposition of labile organic matter leads to rapid consumption of dissolved oxygen (Liu et al., 2013).

Previous studies have demonstrated that some bacterial groups can outcompete others during the utilization of labile DOM (Eilers et al., 2000; Teske et al., 2011; Liu et al., 2015). For instance, the bacterial community shifted to *Alphaproteobacteria* and *Betaproteobacteria* dominated phylotypes in mesocosm tanks with diatom blooms that produced labile proteins, peptides and polysaccharides exudates (Murray et al., 2007). After bovine serum albumin (BSA) amendment, *Gammaproteobacteria* became the dominant bacterial class in the Chesapeake Bay water, while *Bacteroidetes* became dominant in the lower Delaware Bay water (Harvey et al., 2006). However, requisite phylogeny-based incubation studies provide only indirect evidence of the role of different bacterial groups play in labile DOM mineralization, and only a few studies to date have linked specific bacteria groups with labile DOM decomposition directly using radioisotope-labeled substrate and microautoradiography combined with fluorescent *in situ* hybridization (MAR-FISH) technique (Tabor and Neihof, 1982). For example, Cottrell and Kirchman (2000) identified that *Bacteroidetes* and *Gammaproteobacteria* actively utilized ^{3}H-labeled protein in two estuary waters.

While powerful, hybridization techniques such as MAR-FISH are a targeted approach. Unique probes are applied in order to detect individual phylogenetic groups. These techniques, however, often do not allow the identification of active bacteria beyond limited taxonomic depth due to probe hybridization constraints. In contrast, DNA-stable isotope probing (SIP) technique, combined with next generation sequencing approaches, provides an opportunity to interrogate activity *in situ* and to identify bacteria at fine phylogenetic levels without a priori selection of specific phylotypes. Historically, the DNA-SIP technique has been applied to identify bacteria that can degrade one-carbon

(C_1) compounds or specific pollutants in many environmental studies, such as discovering novel bacteria that degrade methanol, toluene, or alkanes in the soil, sediments or marine seeps (Radajewski et al., 2000; Neufeld et al., 2007b; Luo et al., 2009; Redmond et al., 2010; Kleindienst et al., 2014). More recently, the application of DNA-SIP has been extended to marine environments to investigate C and N cycles, such as studying urea uptake by marine pelagic bacteria and archaea in Arctic water, comparing bacteria incorporating glucose and *Cyanobacteria* exudates in the Sargasso Sea, and exploring acetate-utilizing bacteria at the oxic-anoxic interface in the Baltic Sea (Gihring et al., 2009; Wawrik et al., 2009; Nelson and Carlson, 2012; Wawrik et al., 2012a; Berg et al., 2013; Connelly et al., 2014).

The objective of this study was to gain insight into bacterial types utilizing peptides in the nGOM normoxic and hypoxic seawater. This information is important because our preliminary studies showed that certain bacterial genera outcompeted others and might be responsible for rapid peptide decomposition in the hypoxic zone, as discussed above. As a model for small peptides, the ^{13}C-labeled tetrapeptide alanine-valine-phenylalanine-alanine (AVFA) was incubated in both surface normoxic and bottom hypoxic seawater in the nGOM. The AVFA sequence is within the ribulose-1,5-biphosphate carboxylase/oxygenase (RuBisCO) enzyme that is ubiquitous in photosynthesis and has been used to investigate peptide hydrolysis (Liu et al., 2010; Liu and Liu, 2014; Liu and Liu, 2015; Liu et al., 2015). Although individual peptides are often undetectable in natural seawater due to their rapid turnover, they support bacterial growth as intermediates released from sloppy-feeding or lysis of cells (Bronk, 2002; Nagata, 2008). This study identified different bacterial taxa utilizing the added AVFA in the normoxic and hypoxic seawater and directly linked bacterial communities to peptide decomposition.

MATERIALS AND METHODS

Seawater sampling

Surface (2 m) and bottom (16 m) seawater were collected at Sta. C6 (28°52'N, 90°30'W) in the nGOM during a May 2013 cruise on the R/V *Pelican*. This station, with a depth of 18 m and ca. 20 km offshore, is heavily influenced by Mississippi River discharge and often subjected to hypoxia during summer (Rabalais et al., 2001). Seawater was sampled using 10 L Niskin bottles mounted on a conductivity-temperature-depth (CTD) rosette (Seabird 911). Temperature, salinity, dissolved oxygen (DO) and chlorophyll *a* of seawater were monitored through the CTD device (Table 5.1). Seawater was filtered immediately onboard through a 0.2 μm Nylon filter (dia. 47 mm, Whatman) and preserved under -20 °C for the analysis of dissolved organic carbon (DOC), total dissolved nitrogen (TDN), total dissolved amino acids (TDAA), dissolved combined amino acids (DCAA), dissolved free amino acids (DFAA) and nutrients.

Peptide incubation

Peptides ^{12}C-AVFA and ^{13}C-AVFA were custom-synthesized (C.S Bio, CA), and had a >95% compound purity (Liu et al., 2013). In ^{13}C-AVFA, 17 out of total 20 carbon atoms were labeled isotopically (all three carbons in A, all five carbons in V and six carbons of the aromatic ring in F). AVFA was incubated onboard in the surface normoxic and bottom hypoxic seawater. Briefly, either ^{12}C-AVFA or ^{13}C-AVFA was respectively amended in a series of 125 mL amber bottles filled with 120 mL seawater at a final concentration of 0.25-0.47 μM. Duplicate incubations were conducted in the dark for 48

h at 24 °C, close to the ambient seawater temperature (Table 5.1). At different time points (0, 8, 13, 24, and 48 h), 1 mL aliquot of unfiltered water was collected and fixed with formaldehyde at a final concentration of 3% and stored at 4 °C for bacterial abundance analysis; the remaining 119 mL were filtered through the 0.2 μm Nylon filter and preserved at -20 °C for the analysis of peptides, amino acids, ammonium and phosphate (P_i). The filters were preserved in 1×STE (10 mM Tris-HCl [pH 8.0], 0.1 M NaCl, 1 mM EDTA [pH 8.0]) buffer at -20 °C for DNA extraction and sequencing. Dissolved oxygen (DO) was not monitored throughout the incubation, but the parallel incubation experiment showed that it remained relatively constant throughout the 72 h (Liu and Liu, 2016).

Two kinds of control were included for the incubation experiment: a seawater control without peptide amendment and a killed control with 0.48-0.58 μM ^{12}C-AVFA and 180 μM $HgCl_2$ to inhibit bacterial activity (Lee et al., 1992). The incubation and aliquot sampling for the controls followed the same procedures as described above, but only AVFA was analyzed in the killed control.

Chemical analyses

DOC and TDN of the filtered initial seawater were analyzed using a Shimadzu total organic carbon (TOC-V) analyzer coupled with a TNM-1 TDN analyzer with <6% error between duplicates (Table 5.1). DFAA were analyzed in a high performance liquid chromatography (HPLC, Shimadzu Prominence) equipped with a fluorescence detector after pre-column *o*-phthaldialdehyde (OPA) derivatization (Lindroth and Mopper, 1979; Lee et al., 2000). TDAA were analyzed in the same way as DFAA but after hydrolysis in 6 N HCl under nitrogen at 110 °C for 20 h (Kuznetsova and Lee, 2002). DCAA were

calculated as TDAA subtracting DFAA. Nitrate, nitrite and phosphate (P_i) were measured following established protocols (Strickland and Parsons, 1968; Jones, 1984).

AVFA was analyzed in an HPLC-mass spectrometry (HPLC-MS) system (Shimadzu Prominence) following the method in Liu and Liu (2014). In brief, the mobile phase A was 10 mM ammonium acetate and mobile phase B was methanol. Samples were eluted through a C_{18} column (Alltima 5 μm, 150 mm × 4.6 mm) and a 6-way valve was programmed to direct the sea salt peak to waste before introducing the AVFA peak to the MS detector that is equipped with an electrospray ionization (ESI) source and a quadrupole mass analyzer. ^{12}C-AVFA and ^{13}C-AVFA were quantified in positive ion mode under selective ion monitoring (SIM) at m/z = 407 and 424, respectively.

AVFA hydrolysis products including peptide fragments (AV, VF, FA, VFA) and amino acids (A, V, F) were analyzed by HPLC after pre-column OPA derivatization (Liu et al., 2013). Standard deviations of amino acid analysis among replicates were 10-20%. Ammonium, a main metabolite of AVFA, was analyzed using HPLC with post-column OPA derivatization (Gardner and St. John, 1991). P_i concentrations were also monitored throughout the incubation.

Bacterial abundance analysis

Bacterial cells in the formaldehyde-preserved samples were stained with SYBR Green II (Molecular Probes, 1:100 v/v) and enumerated in a flow cytometer (BD Accuri C6) under blue laser excitation at 488 nm (Marie et al., 1997; Liu et al., 2013). Bacterial cells were counted in a fixed volume mode with a flow rate below 300 events per second and cell counts were determined in a dot plot of side scatter (SSC-H) versus green fluorescence signal (FL1-H) on a logarithmic scale.

DNA extraction and ultracentrifugation in CsCl gradients

DNA was extracted from filtered cells using MoBio PowerSoil® DNA isolation kits (MoBio Laboratories, Carlsbad, CA). The extracted DNA was quantified in both a Nanodrop 1000 Spectrophotometer (Thermo Scientific) and a Qubit® 2.0 Fluorometer (Life Technologies). A subsample (ca. 10 μL) at each incubation time point was saved for microbial community structure analysis, and the remainder (ca. 80 μL) was for the ultracentrifugation in CsCl gradients. All duplicate DNA samples from three time points (13h, 24h, and 48 h) were pooled for surface and bottom seawater incubations to obtain sufficient DNA for ultracentrifugation and later fractionation. The impact of pooling was considered acceptable, given minimal changes in community structure from 13 h to 48 h during incubation (see Results). The pooled DNA was precipitated using isopropanol, and the DNA pellet was then re-suspended in 50 μL TE buffer (50 mM Tris-HCl, 15 mM EDTA [pH 8.0]) as previously described (Wawrik et al., 2009). Four pooled DNA samples (^{12}C-AVFA surface, ^{13}C-AVFA surface, ^{12}C-AVFA bottom, ^{13}C-AVFA bottom) were prepared for ultracentrifugation.

DNA ultracentrifugation in CsCl gradients and fractionation followed protocols as described previously (Buckley et al., 2007; Luo et al., 2009; Wawrik et al., 2009; Wawrik et al., 2012a). In brief, ca. 61-170 ng DNA was mixed with 0.26 mL TE buffer and 4.45 mL of 1.295 g mL^{-1} CsCl in gradient buffer A (15 mM Tris-HCl [pH 8.0], 15 mM KCl, 15 mM EDTA [pH 8.0], 2 mg mL^{-1} ethidium bromide) in 4.7 mL polyallomer Optiseal tubes (Beckman). The tubes were centrifuged in a Beckman rotor VTi 65.2 at ca. 140,000 × g for 72 h. After ultracentrifugation, thirty 150 μL fractions were collected from each tube in a Beckman fraction recovery system by replacing samples with mineral oil on top of the tubes at a constant rate using a peristaltic pump. The density of each fraction was

calculated based on the refractive index that was measured in a Reichert AR200 refractometer (Wawrik et al., 2009). DNA was purified from each CsCl fraction by isopropanol precipitation and dissolved in 50 μL sterile nuclease-free water.

Quantitative PCR (qPCR) of 16S rRNA gene

The purified DNA from each SIP fraction was used to determine 16S rRNA gene copy numbers of bacteria and archaea via qPCR. Primers were 27F (5'-AGA GTT TGA TCM TGG CTC AG-3') and 519R (5'-GWA TTA CCG CGG CKG CTG-3') for bacteria and A8F (5'-TCC GGT TGA TCC TGC C-3') and A344R (5'-TCG CGC CTG CTG CIC CCC GT-3') for archaea. Every 30 μL reaction mix for qPCR included 13.9 μL 1X Power SYBR Green PCR master mix (Applied Biosystems), 13.9 μL nuclease-free water, 200 nM (final concentration) of each primer, and 2 μL DNA template. qPCR was conducted in a real-time PCR system (Applied Biosystems, ABI 7300) followed the program: 2 min at 50 °C, 8 min at 95 °C, 40 cycles of 30 s at 95 °C, 1 min at 55 °C and 1 min at 72 °C. Genomic DNA of *Roseobacter denitrificans* Och 114 (DSMZ 7001) was used as the standard DNA for bacteria and a linearized plasmid with the 16S rRNA gene of *Methanospirillum hungatei* JF-1 for archaea. Since archaeal qPCR results were mostly below the detection limit, only bacterial results are presented here.

PCR, barcoding, and Illumina sequencing

Partial 16S rRNA genes of DNA from each incubation time point and purified DNA from SIP gradients were amplified by PCR using Phusion high-fidelity DNA polymerase (Thermo Scientific) and barcoded for Illumina sequencing. For every 30 μL PCR reaction, 6 μL Phusion HF buffer, 0.6 μL 10 mM dNTPs, 0.15 μL 100 mM (final

concentration of 0.5 μM) universal forward primer M13-519F with a 5' M13 tag on it (5'-GTA AAA CGA CGG CCA GCA CMG CCG C-3'), 0.15 μL reverse primer Bac-785R (5'-TAC NVG GGT ATC TAA TCC-3'), 0.3 μL Taq polymerase (final concentration of 0.02u μL^{-1}), 20.8 μL nuclease-free water, and 2 μL DNA template were mixed (Klindworth et al., 2013). PCR started with 94 °C for 2 min, followed by 28 or 32 cycles (32 cycles for surface SIP gradient samples, 28 cycles for bottom SIP gradient samples and samples at individual incubation time point) of 95 °C for 30 s, 52.8 °C for 30 s, and 72 °C for 30 s, then 72 °C for 5 min. The number of PCR cycles was determined based on qPCR results and agarose gel check of PCR products to make sure enough PCR products were obtained but not reaching PCR plateau. Water, instead of DNA template, was used as negative control.

PCR products were purified by QIAquick PCR purification kit (Qiagen) and barcoded with a different 8-bp forward primer for every sample by loading 2 μL cleaned PCR products in the 30 μL Phusion polymerase reaction mix (Wawrik et al., 2012b). Barcode tagging was conducted through a short 6-cycle PCR and checked by gel electrophoresis. Barcoded samples were sent to the Oklahoma Medical Research Foundation for MiSeq Illumina sequencing. Adapter and primer of raw Illumina sequences were first removed and then overlapping forward and reverse reads were stitched. Processed sequences were clustered into OTUs using UCLUST, checked for chimeras using USEARCH and classified into taxonomy through the QIIME pipeline (Caporaso et al., 2010b). A randomly-chosen set of representative sequences from each OTU was aligned to the SILVA small-subunit rRNA reference alignment (www.arb-silva.de) using the PyNAST algorithm (Caporaso et al., 2010a). Sequences were assigned to the genus level at the 95% identity as a compromise between resolution and conservative interpretation due to the short reads (250 bp) used here (Connelly et al.,

2014). Sequences were deposited in National Center for Biotechnology Information (NCBI) GenBank under BioProject accession number PRJNA297372.

Bacterial community structures (% genus) of samples from each incubation time point were compared by non-metric multidimensional scaling (nMDS) using Matlab®. Analysis of similarity (ANOSIM) was applied to compare the bacterial community structures between surface and bottom seawater samples using vegan package in R (Oksanen et al., 2016).

Calculating percentage enrichment of each bacterial taxa in the ^{13}C-AVFA samples relative to the ^{12}C-AVFA SIP samples followed the protocol of Bell et al. (2011). In brief, 16S rRNA gene copy numbers for each SIP fraction were quantified through qPCR. Then the proportion of each bacterial taxonomic group sequences in a given density range was multiplied by the 16S rRNA gene copy number in that same density range, and the derived relative copy number of each bacterial taxonomic group was corrected for the slight difference in total DNA between the ^{12}C-AVFA and ^{13}C-AVFA samples. Percentage enrichment of a certain bacterial taxonomic group was defined as dividing the difference of the relative copy number summed in the heavy density fractions between the ^{13}C-AVFA samples and the ^{12}C-AVFA samples by the relative copy number in the ^{12}C-AVFA samples within the same density range, i.e.,

$$Percentage\ enrichment\ in\ heavy\ fractions\ for\ bacteria\ i = \frac{\sum 13C - AVFA\ relative\ copy\ number\ of\ i - \sum 12C - AVFA\ relative\ copy\ number\ of\ i}{\sum 12C - AVFA\ relative\ copy\ number\ of\ i}$$

RESULTS

Peptide decomposition

The ^{12}C- and ^{13}C-AVFA decomposition patterns were nearly identical during the 48 h incubation, as expected (Fig. 5.1). The AVFA concentrations decreased linearly with time in both the surface 2 m and bottom 16 m seawater, but the decomposition rate in the bottom seawater (0.018-0.035 μM h^{-1}) was twice as high as in the surface seawater (0.011-0.017 μM h^{-1}). AVFA was completely degraded within 24-48 h in the surface water and within 13-24 h in the bottom water. In contrast, AVFA concentrations in the killed control remained nearly unchanged during the 48 h incubation (Fig. 5.1c), indicating that the peptide disappearance in the seawater was due to microbial activity.

AV, FA, VF and VFA produced during hydrolysis of AVFA (Liu et al., 2013) varied at levels <0.012 μM throughout the incubation, but more amino acids and peptide fragments were produced in the surface than in the bottom waters (Fig. 5.2). Concentrations of free amino acids (A, V, and F) were 2-30 times greater than those of peptide fragments. F was the dominant amino acid, reaching up to 0.17 μM in the surface at 24 h and 0.082-0.11 μM in the bottom at 8 h, and then decreased to the background level at the end of the incubation. V and A followed a similar pattern to F, but with smaller changes. Compared to the AVFA treatment, concentrations of amino acids in the control without peptide amendment remained relatively low (<0.011 μM) and constant throughout the incubation.

During the first 24 h in the surface seawater incubation, ammonium concentrations increased by 0.66-1.45 μM in the ^{12}C- and ^{13}C-AVFA samples (Fig. 5.3). In contrast, ammonium concentrations in the bottom seawater changed little before AVFA was completely degraded (0-13 h). After 13 h, ammonium concentrations kept increasing to 2.6-2.9 μM in the surface incubation and remained constant at about 2.8 μM

or increased by 1.5 μM to reach 4.1 μM in the bottom incubation. In the control without AVFA, ammonium concentrations increased by 0.97 μM in the surface seawater and decreased by 0.63 μM in the bottom seawater during the 48 h. P_i concentrations remained relatively constant throughout the 48-h incubation in both the peptide and control treatments (Fig. 5.4). P_i concentrations in the bottom water (1.1-1.5 μM) were more than one order of magnitude higher than those in the surface water (0.02-0.09 μM).

Bacterial abundance and community structure

In the surface ^{12}C- and ^{13}C-AVFA incubations, bacterial abundance increased by 31-57% within the initial 8-13 h, and then decreased afterwards, while in the bottom, bacterial abundance increased by 44-45% during the initial 24 h and then decreased afterwards (Fig. 5.5). Bacterial abundances in the control either decreased over time in the surface seawater or remained nearly constant in the bottom seawater (Fig. 5.5c).

Ambient surface water bacterial communities were dominated by *Synechococcus* (15-49%), whereas bottom samples were more evenly populated by *Rhodobacteraceae* (11-13%), *Acidimicrobiaceae* OCS155 marine group (3-8%), *Saprospiraceae* (5-7%), *Planctomycetaceae* (2-7%), SAR11 clade Surface 1 (3-6%), and *Acidimicrobiales* TM214 (3-5%) (Figs. 5.6a, b). By 24 h, the relative abundance of *Rhodobacteraceae*, *Thalassococcus*, and *Ruegeria* increased by 8-18%, 7-13%, and 2-3%, respectively, in both surface and bottom seawater, while other bacterial genera developed differently in the surface and bottom seawater incubations. For instance, OTUs classified within the *Roseovarius* clade increased by 5% only in the surface incubation, whereas *Colwellia* increased by 2-3% only in the bottom incubation. The surface and bottom bacterial community structures were well separated in the nMDS plot (Fig. 5.6c); ANOSIM

showed significant difference between the surface and bottom bacterial community structures ($p = 0.001$), further suggesting that bacterial community structures developed differently between the two water layers.

Identifying bacteria that incorporated peptides through DNA-SIP

qPCR of SIP fractions indicates that the DNA fractions of the ^{13}C-AVFA samples shifted to heavier densities as compared to the ^{12}C-AVFA samples in both the surface and bottom incubations (Figs. 5.7a, b). 16S PCR products from respective fractions were bar-coded and sequenced using Illumina Miseq to generate sequence libraries. A positive percentage enrichment is an indicator of the bacterial capability in incorporating ^{13}C (Bell et al., 2011). Peptide uptake was more evenly distributed among the bacterial classes in the surface seawater than in the bottom seawater (Figs. 5.7c, 5.7d). *Flavobacteria*, *Sphingobacteria*, *Alphaproteobacteria*, *Cyanobacteria*, and *Actinobacteria* showed highest enrichment ranging from 147% to 305% in the surface water, whereas *Alphaproteobacteria* and *Gammaproteobacteria* highest ranging from 176% to 278% in the bottom water.

Communities taking up ^{13}C-AVFA in the surface and bottom seawater also differed at the level of dominant genera (> 0.1% of the total bacterial community) (Figs. 5.8). In the surface seawater, sequences classified within genera belonging to the *Saprospiraceae*, *Tropicibacter*, *Rhodobacteraceae*, *Thalassococcus*, *Roseovarius*, *Owenweeksia*, *Flavobacteria* NS4 marine group, *Acidimicrobiaceae*, *Microbacteriaceae* SV1-8 and *Synechococcus* dominated the ^{13}C uptake. In the bottom samples, major ^{13}C enriched groups included the genera *Ruegeria*, *Colwellia*, *Balneatrix*, *Thalassomonas*, *Pseudoalteromonas*, and *Neptuniibacter*. Several taxa, including *Thalassococcus* and

Rhodobacteraceae, displayed similar patterns in surface and bottom incubations. The extent of taxonomic enrichment varied widely among different bacterial genera, ranging from 101% to 565% in the surface incubation and from 4% to 642% in the bottom incubation. Within the same class, the enrichment of *Roseovarius* and *Thalassococcus* was almost twice as high as that of other *Alphaproteobacteria*, and the enrichment of *Colwellia* was more than three times higher than that of other *Gammaproteobacteria*.

DISCUSSION

Factors to be considered for the DNA-SIP approach

A successful DNA-SIP experiment depends on the amount of isotopically-labeled substrate being assimilated and the length of the incubation time (Radajewski et al., 2003; Neufeld et al., 2007a). The substrate concentration must be high enough to ensure sufficient isotopic labeling of nucleic acids relative to unlabeled background substrates that are relatively abundant. However, if the substrate concentrations are too high, the incubation may deviate from the *in situ* situation. In our incubations, we added relatively low concentrations (0.25-0.47 μM) of AVFA to mimic *in situ* condition. qPCR results support the notion that sufficient isotope was incorporated into bacterial DNA. Several other pieces of evidence further suggested the successful uptake of peptide by bacteria, including increased bacterial abundance in peptide treatments compared to control (Fig. 5.5), and a 2-30 fold increase of certain bacterial genera in the peptide treatment relative to the control (Fig. 5.6). Even though bacterial community structures in the control samples might have potentially been shaped by bottle effects and grazing pressure during incubation (Ferguson et al., 1984; Pomeroy et al., 1994), the difference between the peptide treatment and control samples is more likely attributable to the peptide utilization

by bacteria. Longer incubation time often results in greater isotope incorporation, but may also lead to cross-feeding, such as bacterial assimilation of labeled byproducts, intermediates or dead cells, produced from substrate metabolism (Neufeld et al., 2007a; Neufeld et al., 2007c; Wang et al., 2015). To reduce cross-feeding, relatively short incubation time (48 h) that was nonetheless sufficient to allow complete peptide degradation was applied in this study.

A potential limitation of the DNA-SIP approach is that the buoyance density of DNA varies with G+C content and that this property may vary among different bacteria. This pattern may result in a loss of power to identify bacteria that have incorporated the labeled substrate based on density shift (Buckley et al., 2007). However, it is more problematic for ^{15}N than for ^{13}C substrates given the greater buoyant density differential for nucleic acids labeled with ^{13}C. The density shift in our results was > 0.01 g mL^{-1}, equating to ca. 28% of ^{13}C incorporation, which is more than the minimum percentage (20%) that is typically required for separating ^{13}C and unlabeled organisms (Uhlik et al., 2009). Note that the overall buoyance density differed somewhat between the surface and bottom DNA fractions (Figs. 5.7a, b). It is unclear why this difference was observed, but may be related to the different bacterial community composition in the surface and bottom incubations, as %G+C contents of DNA vary among different bacterial taxa and higher %G+C leads to heavy density (Buckley et al., 2007; Holben, 2011). However, it is presumed that this density difference will not affect our ability to identify bacteria incorporating peptides, because the taxonomic percentage enrichment was derived relative to the corresponding ^{12}C-AVFA incubations within the surface or bottom samples.

DNA from three incubation time points (13, 24, 48 h) were pooled (see methods). This approach might have caused some ‘smearing’ of the signal by spreading the DNA of

active bacterial taxa across the density range to a greater degree than for a single time point. However, this smearing should not be problematic with respect to the objectives of this study, because major bacterial taxa in the bacterial community structure were similar at all time points (Fig. 5.6). While the exact degree of isotopic labeling may therefore not be attainable from our experiments, the high degree of enrichment observed for some bacteria (Figs. 5.7c, d, 6) supports the notion of active ^{13}C incorporation. Hence, the focus of the subsequent discussion is primarily on the bacterial taxa with large percentage enrichment values, to minimize potential uncertainties that result from sample pooling and pooling likely did not significantly affect our conclusion.

Faster AVFA decomposition in the hypoxic than in the normoxic seawater

Peptide decomposition rate was twice faster in the bottom incubation as compared to the surface incubation (Fig. 5.1). AVFA decomposition produced more hydrolyzed fragments, including amino acids and peptides, in the surface than bottom incubations (Fig. 5.2), indicating extracellular hydrolysis in the surface water but direct uptake or tightly coupled hydrolysis-uptake in the bottom water. In contrast to previous studies, which used relatively high concentrations of amended peptides (5-10 μM) (Liu et al., 2013; Liu and Liu, 2016), the much lower concentrations of AVFA (0.25-0.47 μM) added here accounted for 14-84% of ambient DCAA (Table 5.1). The low concentration amendments conducted here resulted in uptake patterns generally consistent with previous studies (Liu et al., 2013; Liu and Liu, 2016).

The peptide decomposition mechanism can be interrogated through a mass balance of the fate of added nitrogen, which may include: (1) extracellular hydrolysis to produce peptide fragments and amino acids, (2) remineralization to ammonium, and (3)

incorporation into bacterial biomass. The percentage of extracellular hydrolysis can be estimated using the amino acid F and peptide fragments containing F, as bacterial uptake of F is limited within 24 h (Liu et al., 2013). The degree of remineralization can be estimated via changes in ammonium concentrations in peptide treatments compared to controls, assuming nitrification is negligible during the 24 h (Liu et al., 2013). To calculate the incorporation percentage to microbial biomass, we assume a carbon conversion value of 20 fg C per bacterial cell and a C/N ratio of 4 for bacteria (Lee and Fuhrman, 1987). Based on these parameters, extracellular hydrolysis (40-56%) dominated the decomposition of AVFA in the surface water, whereas biomass production (4-20%) dominated in the bottom water throughout the incubation, leaving a major fraction (29-81%) of the AVFA nitrogen uncounted for in both layers, possibly in other forms of DON (Table 5.2). For example, at 24 h, ca. 40% of decrease in AVFA in the surface seawater was hydrolyzed to peptide fragments and amino acids, ca. 6% was converted to ammonium, 2-11% to bacterial biomass (8.1×10^4-3.3×10^5 cells per mL), and about 50% to other DON. In contrast, in the bottom seawater, less than 5% was hydrolyzed to peptide fragments and amino acids, hardly any ammonium was produced, and 18-28% was incorporated into bacterial biomass (7.7×10^5-9.0×10^5 cells per mL) at 13 h when AVFA disappeared, resulting in about 70-80% of AVFA nitrogen as DON. This contrasting pattern suggests that the fast disappearance of AVFA in the bottom water incubation may relate to the higher percentage of peptide incorporation into bacterial biomass, i.e., bacterial growth. The efficiency of AVFA decomposition may depend on the fraction of nitrogen allocated to those fast-growing bacteria.

Uptake of peptide in the normoxic vs. hypoxic seawater

In the surface seawater incubation, the incorporation of ^{13}C peptide was greatest for *Flavobacteria*, *Sphingobacteria*, *Alphaproteobacteria*, *Cyanobacteria*, and *Actinobacteria* (Fig. 5.7c). At the genus level, *Saprospiraceae* (*Sphingobacteria*), *Tropicibacter*, *Roseovarius* (*Alphaproteobacteria*), *Owenweeksia*, *Formosa*, *Flavobacteria* NS4 marine group (*Flavobacteria*), and *Microbacteriaceae* SV1-8 (*Actinobacteria*) took up the most peptide in the surface seawater (Fig. 5.8a). *Sphingobacteria* showed a responsive role during peptone incubation in the seawater (Simon et al., 2012). As members of *Roseobacter* clade, *Tropicibacter* and *Roseovarius* were hypothesized to be opportunistic in nutrient exploitation and are often associated with plankton aggregates (Moran et al., 2007; Teeling et al., 2012; Yau et al., 2013). Therefore, the observation that requisite populations can utilize the amended peptide is expected. *Flavobacteria* are often effective in degrading high-molecular-weight DOM including proteins (Cottrell and Kirchman, 2000). Some *Actinobacteria* can produce a wide range of bioactive metabolites including extracellular peptidases that are sometimes involved in pathogenic processes (Ventura et al., 2007; Chen et al., 2012), suggesting their potential in peptide utilization. Consistent with our results, diverse bacterial taxa, such as *Flavobacteria*, *Verrucomicrobia*, *Gammaproteobacteria*, *Alphaproteobacteria*, *Actinobacteria*, and *Planctomycetes*, used added dissolved proteins in coastal California waters (Orsi et al., 2016). The widespread of bacterial classes incorporating peptides in this study agrees with ecological theory and previous studies indicating that heterogeneity of the coastal oceans favor generalist bacteria in DOC utilization (Mou et al., 2008). Alternatively, this diverse bacterial pattern may result from the significant production of individual amino acids from extracellular hydrolysis (Fig. 5.2a, c). Since uptake of amino

acids is generally constitutive among marine bacterial taxa (Payne and Gilvarg, 1971; Poretsky et al., 2010), bacterial groups possessing the ability to take up amino acids A, V, and F should be widespread, thus increasing the range of bacteria taxa showing positive percentage enrichment in the surface seawater.

In contrast to the surface seawater incubation, bacteria incorporating the peptide in bottom waters were associated with fewer taxonomic groups, primarily belonging to the *Alphaproteobacteria* and *Gammaproteobacteria* (Fig. 5.7d). The bacteria that metabolized the peptide differed between the surface normoxic and bottom hypoxic seawater, which corresponds well with the overall different bacterial community structures between the two water layers (Fig. 5.6). The dominant percentage enrichment of *Alphaproteobacteria* and *Gammaproteobacteria* in the bottom seawater suggested their high capability of incorporating AVFA thus leading to faster decomposition of the peptide in the bottom seawater. This result is consistent with previous studies in DOM utilization, which quantified this process either directly through tracing radioisotope incorporation by bacteria or indirectly via analyzing changes of bacterial community structure (Gihring et al., 2009; McCarren et al., 2010; Carney et al., 2015). For example, the percentage of *Gammaproteobacteria* consuming proteins among all bacterial phylogenetic groups was higher than their abundance percentage in estuarine and coastal environments, indicating their high capability of metabolizing proteins (Cottrell and Kirchman, 2000). *Alphaproteobacteria* or *Gammaproteobacteria* can dominate the bacterial community during DOM incubation in certain marine environments, indicating they can outcompete other bacteria in using DOM substrates (Harvey et al., 2006).

At the genus level, the highest percentage enrichment in the bottom seawater occurred to the *Thalassococcus*, *Rhodobacteraceae*, *Ruegeria* (*Alphaproteobacteria*), *Colwellia*, *Balneatrix*, *Thalassomonas*, *Pseudoalteromonas, and Neptuniibacter*

(*Gammaproteobacteria*) (Fig. 5.8b). *Thalassococcus* were capable of utilizing phthalate (Iwaki et al., 2012), but its ability to metabolize peptides, as suggested here, has not yet been explored. Previous studies have shown that *Rhodobacterales* are often one of the dominant groups in coastal seawaters, accounting for as high as 75% of the *Alphaproteobacteria* (Dong et al., 2014). Their abundance is thought to relate to DOC concentrations in nutrient-enriched habitats and they are frequently involved in taking up labile organic molecules, such as peptides and amino acids, as detected by metaproteomics (Dong et al., 2014; Fodelianakis et al., 2014). Our previous study also showed that populations of *Ruegeria*, *Thalassomonas*, *Pseusoalteromonas* and *Neptuniibacter* grow rapidly when AVFA was amended to the same Sta. C6 bottom water (Liu et al., 2013). These genera may be mostly *r*-selected bacteria that use labile organic matter in nutrient-enriched environments, contrasting them to those *K*-selected bacteria that maintain efficient metabolism and grow slowly using complex refractory substrates (Fierer et al., 2007; Wang et al., 2015). These *r*-selected bacteria, such as *Ruegeria*, *Vibrio*, *Alteromonas* and *Colwellia*, grow rapidly when substrates become available while maintain growth potential under starvation using one ecological strategy called "feast or famine", thus they can adapt to changing environments quickly (Eilers et al., 2000; Christie-Oleza et al., 2012). Their high capability to assimilate peptide is thus consistent with their ecology strategy. The growth of *Pseudoalteromonadaceae* and *Colwellia* increased when peptone was incubated in the Southern Ocean seawater (Simon et al., 2012). Consistently, opportunistic bacteria, such as *Vibrio*, *Roseobacter*, *Pseudoalteromonas*, *Photobacterium*, *Marinomonas*, *Marinobacter*, and *Alteromonas*, dominated the incorporation of DOC sources from *Synechococcus* exudate or lysate in seawater culture incubations (Nelson and Carlson, 2012). Particle-attached *Colwellia* and *Pseudoalteromonas* also showed high incorporation of proteins in marine microcosms

(Mayali et al., 2015). DOC-related transporter genes, such as amino acids, oligopeptides, carbohydrates, carboxylic acids, polyamines, and lipids transporters, in coastal seawater were associated with *Rhodobacterales* (primarily *Roseobacter*), *Rickettsiales* (primarily SAR11), *Flavobacteriales*, and five orders of *Gammaproteobacteria*, including *Alteromonadales*, *Oceanospirallales*, *Pseudomonadales*, *Vibrionales*, and an uncharacterized taxon related to sulfur-oxidizing symbionts (Poretsky et al., 2010). Most of these bacteria also assimilated the peptide used in our study.

It should be pointed out that bacterial taxa with higher percentage enrichment are not necessarily the most abundant within communities. For instance, *Escherichia-Shigella*, *Balneatrix*, and *Thalassomonas* accounted for <2% of communities while their enrichment was 100%-200%. *Microbacteriaceae* remained below 5% and did not greatly increase with peptide incubation time, while their SIP-based percentage enrichment was estimated at >500% in the surface seawater. Similar observations are reported elsewhere (Zemb et al., 2012), and indicate that some bacteria can be highly enriched in ^{13}C, but they may represent only a small proportion of the overall community. These rare bacteria may have long generation time, which varied from about 12 h to 24 h or more (Brock, 1971, Eilers et al., 2000). During our short 48 h incubation, certain bacteria might be at their lag phase of growth, which changed little in the community structure. For example, if these rare bacteria only doubled once during 48 h, their increase from ca. <1% to ca. <2% would not contribute much the overall community structure. Alternatively, these rare bacteria might have utilized the assimilated peptides mostly for respiration instead of for biomass building, leading to the mismatch between abundance and SIP incorporation. These data showed the potential role of some rare and unculturable bacteria in peptide utilization, which is often overlooked based on bacterial community structure analysis.

Factors leading to the development of different bacterial communities

It is intriguing that bacterial communities that metabolized the added peptide differed in surface and bottom incubations. The two layers also differed in chemical and biological parameters (Table 5.1, Figs. 5.5, 5.6), such as DO, DOC, and initial bacterial community structure, which probably contributed to the development of different bacterial communities, but the role of these factors seems to be limited (Liu et al., 2013; Liu and Liu, 2016). Other than these parameters, high levels of P_i (>0.4 μM) in the bottom seawater may stimulate the growth of fast-growing bacteria with high RNA content (Liu and Liu, 2016), such as *Alphaproteobacteria* and *Gammaproteobacteria*, consistent with the Growth Rate Hypothesis (Elser et al., 2000; Makino et al., 2003). The fast-growing bacteria may lead to faster peptide decomposition observed in the bottom than in the surface seawater. Assuming 0.2 pg dry mass bacterial cells and a P content of 1.3% (Sterner and Elser, 2002), the bacterial abundance increase observed here would have required 0.01-0.08 μM P_i. These small values are close to the standard deviation (ca. 0.02 μM) of P_i measurement, which may explain why no obvious decrease of P_i was observed during our incubations (Fig. 5.4). On the other hand, these results further suggest that it is the level of P_i, rather than its absence, that is the key factor limiting the development of fast-growing bacteria. The unique development of certain *Alphaproteobacteria* and *Gammaproteobacteria* genera may also explain much lower production of AVFA fragments during the bottom water incubation (Figs. 5.2b, d). Either these bacteria directly took up the peptide (Appendix II), or the hydrolysis and subsequent uptake of the fragments were coupled tightly (Fuhrman, 1987; Kuznetsova and Lee, 2002; Liu et al., 2013). These two processes cannot be differentiated with these

data, but regardless, both pathways differ from that of the surface incubation, where hydrolysis and the uptake seem uncoupled.

CONCLUSION

A variety of bacterial groups responsible to peptide decomposition was identified in surface and bottom waters in the hypoxic region of northern Gulf of Mexico using DNA-SIP approach. Bacterial groups metabolizing peptide appear to differ between the surface normoxic and bottom hypoxic seawater. Certain *Alphaproteobacteria* (*Thalassococcus*, *Rhodobacteraceae*, *Ruegeria*) and *Gammaproteobacteria* (*Colwellia*, *Balneatrix*, *Thalassomonas*, *Pseudoalteromonas, Neptuniibacter*) in the bottom seawater had high capability of utilizing peptide. Although this work only studied bacterial groups incorporating peptides in one station at one sampling time, the pattern is in consistent with our previous work from different years at this station and other stations (Liu et al., 2013; Liu and Liu, 2016), which consolidates the conclusion of this study. This study expands our understanding of linkage between peptide decomposition and bacterial communities, especially with low concentrations of peptide amendment, and further implies that certain bacteria taxa capable of rapid peptide decomposition can develop rapidly under high P_i concentrations in the hypoxic seawater. With more similar SIP work at other coastal and oligotrophic regions, a comprehensive picture of labile organic matter decomposition linked with microbial communities may be achieved in the future.

Table 5.1. Chemical parameters of initial surface (2 m) and bottom (16 m) seawater at Sta. C6.

Depth	Temp (℃)	Salinity (ppt)	DO ($mg \cdot L^{-1}$)	Chl *a* ($\mu g \cdot L^{-1}$)	DOC (μM)	TDN (μM)	DCAA (μM)	DFAA (μM)	NO_3^- (μM)	NO_2^- (μM)	Pi (μM)
2 m	25.5	27	7.9	1.51	233.3	14.3	1.79	0.18	0.54	ud	0.11
16 m	22.3	35	0.4	0.63	200.0	10.7	0.56	0.07	6.85	0.54	0.89

ud: under detection limit (ca. 0.03 μM).

Table 5.2. An example of mass balance (including percentages of decreased peptide due to hydrolysis, remineralization to ammonium, incorporation into bacterial biomass and other unaccounted transformation to DON) throughout the ^{12}C-AVFA decomposition in the surface (2 m) and bottom (16 m) seawaters.

Depth	Time	Hydrolysis%	Remineralization %	Incorporation%	Other DON%
2 m	8 h	56	0	11	33
	13 h	53	2	16	29
	24 h	40	6	2	52
16 m	8 h	24	0	4	72
	13 h	0.2	0	18	80.8
	24 h	0	37	20	43

Figure 5.1. AVFA concentrations with incubation time in the surface 2 m and bottom 16 m seawater of (a) ^{12}C-AVFA, (b) ^{13}C-AVFA, and (c) killed control samples. Data points were presented as average ± absolute error of duplicate samples except control samples.

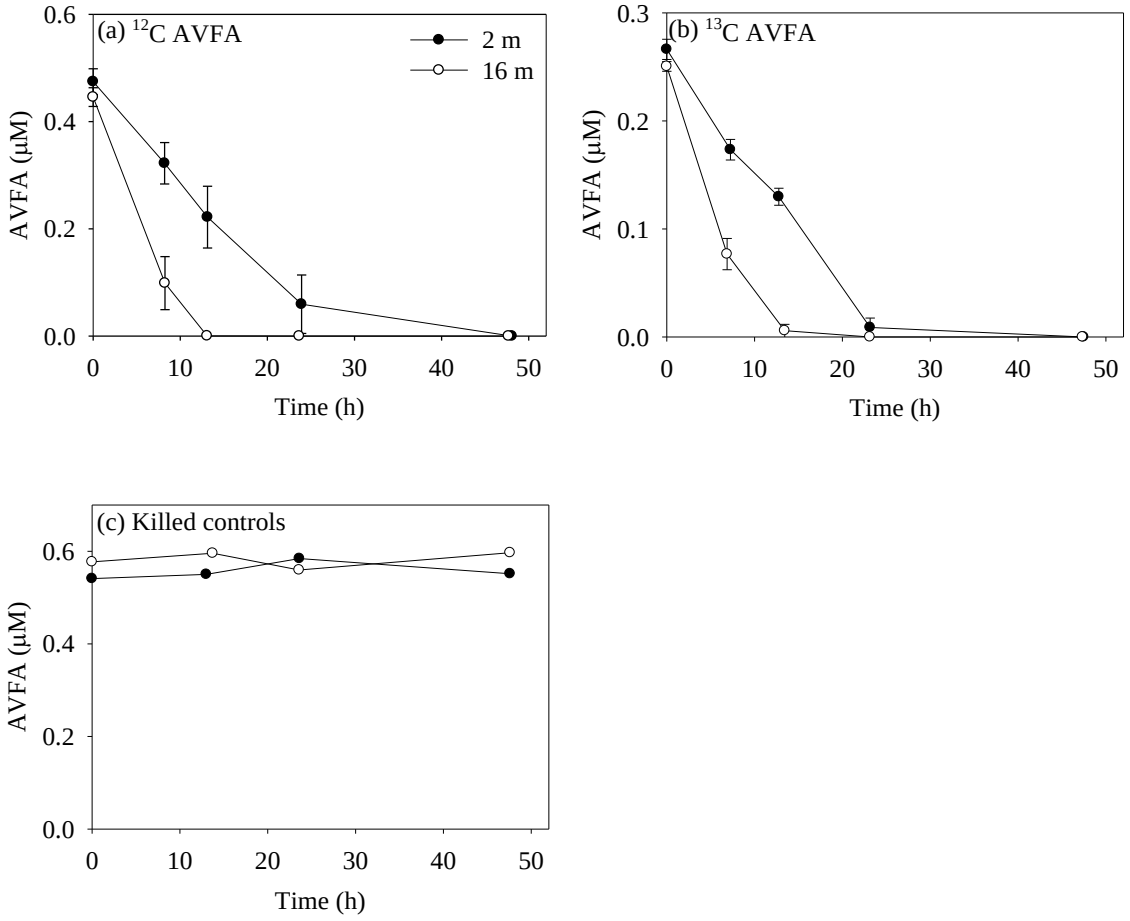

Figure 5.2. Concentrations of produced amino acids and peptide fragments with incubation time in the (a) surface 2 m seawater of ^{12}C-AVFA incubation, (b) bottom 16 m seawater of ^{12}C-AVFA incubation, (c) surface 2 m seawater of ^{13}C-AVFA incubation, (d) bottom 16 m seawater of ^{13}C-AVFA incubation samples, and amino acid concentrations with time in the (e) surface 2 m seawater of no-AVFA control and (f) bottom 16 m seawater of no-AVFA control samples. Data points were presented as average ± absolute error of duplicate samples except control samples.

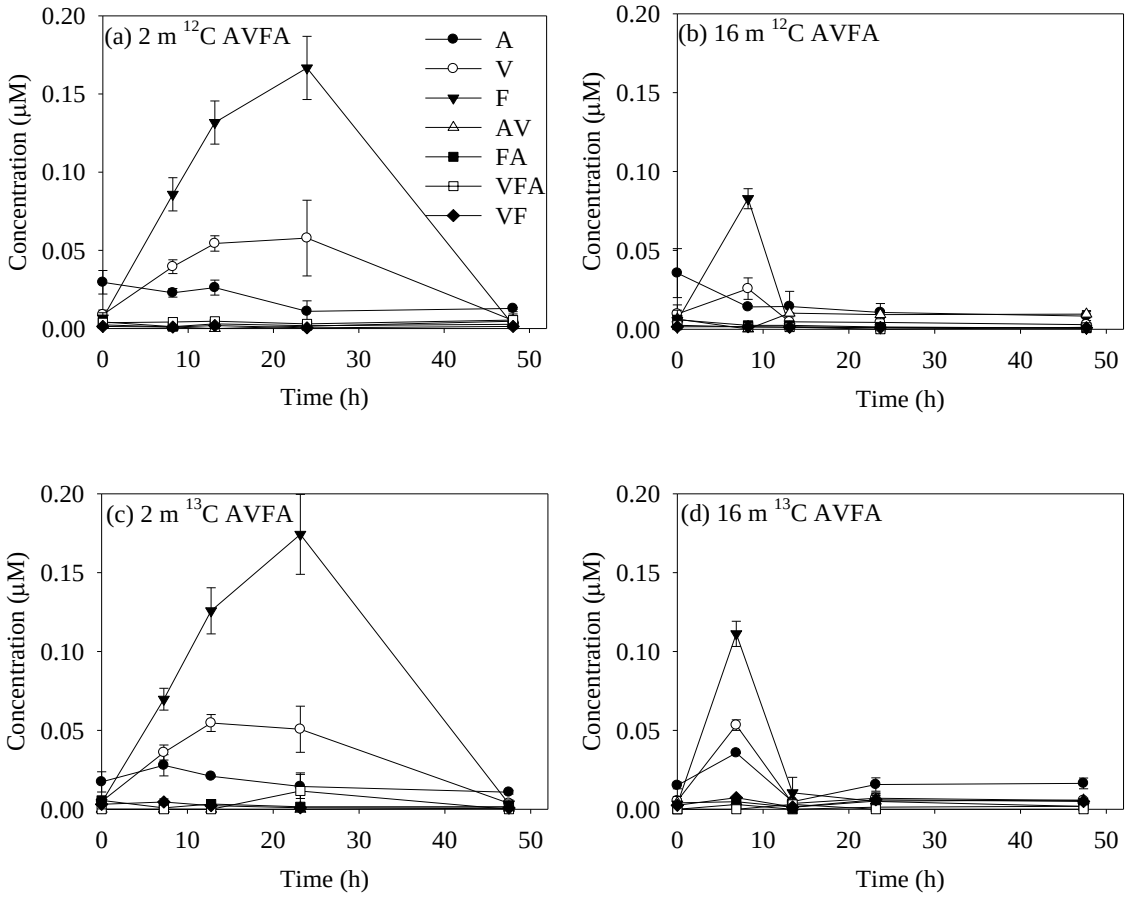

Figure 5.2 (continued)

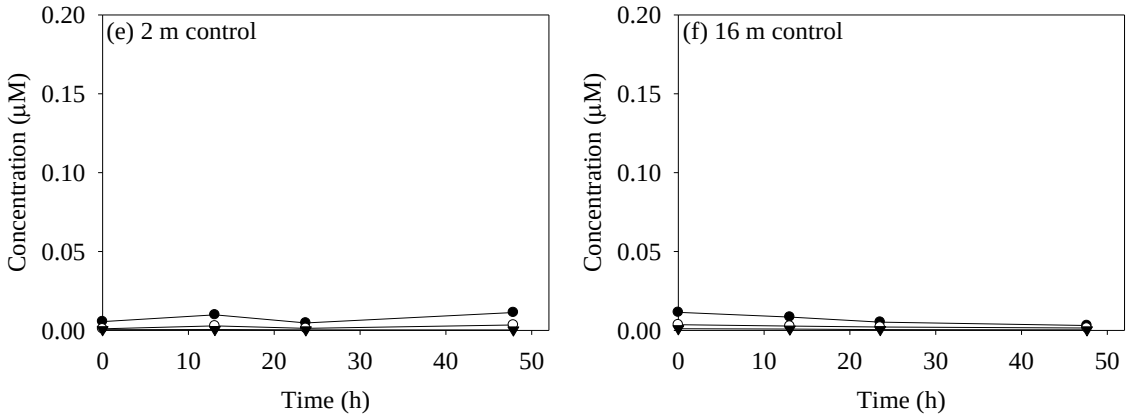

Figure 5.3. Ammonium concentrations with incubation time in the surface 2 m and bottom 16 m seawater of (a) ^{12}C-AVFA, (b) ^{13}C-AVFA and (c) no-AVFA control samples. Data points were presented as average ± absolute error of duplicate samples except control samples.

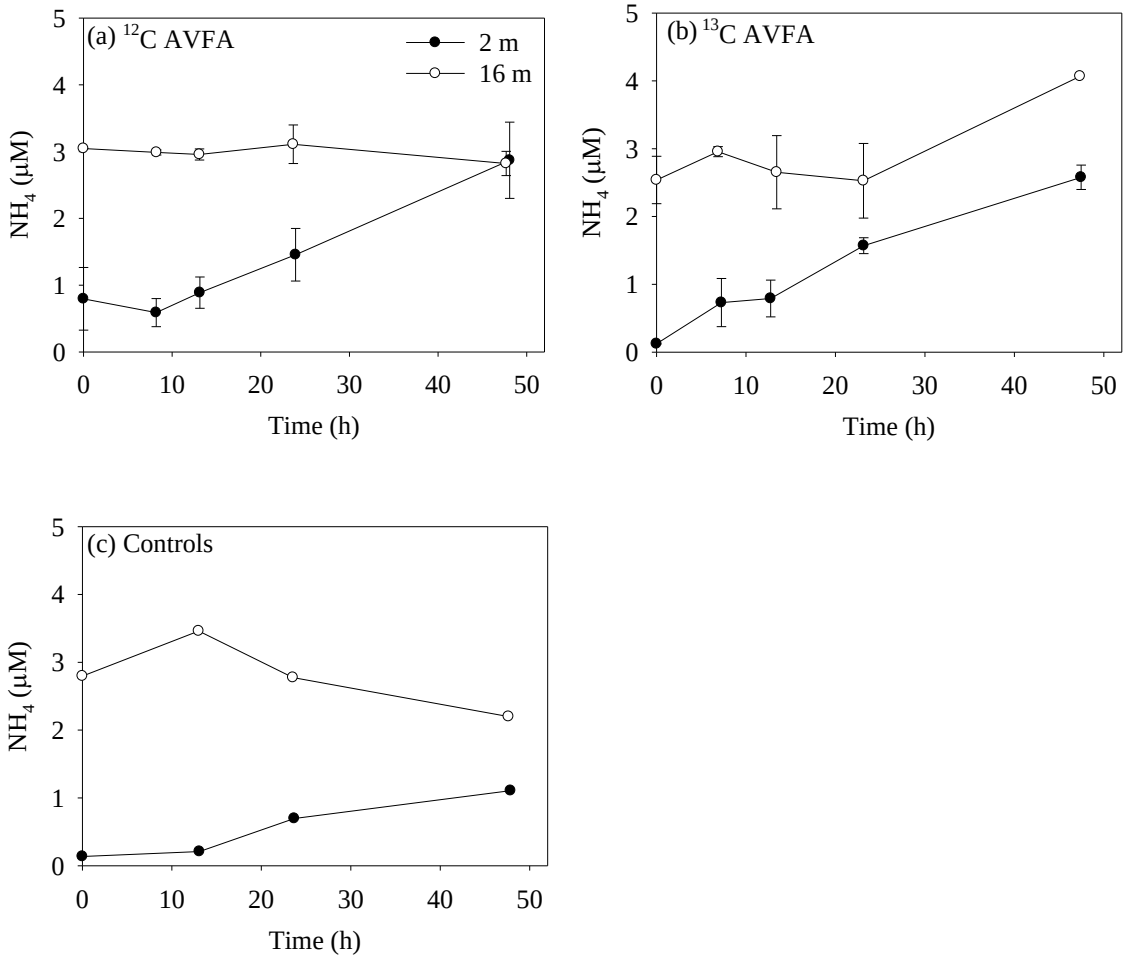

Figure 5.4. P_i concentrations with incubation time in the surface 2 m and bottom 16 m seawater of (a) ^{12}C-AVFA, (b) ^{13}C-AVFA and (c) no-AVFA control samples. Data points were presented as average ± absolute error of duplicate samples except control samples.

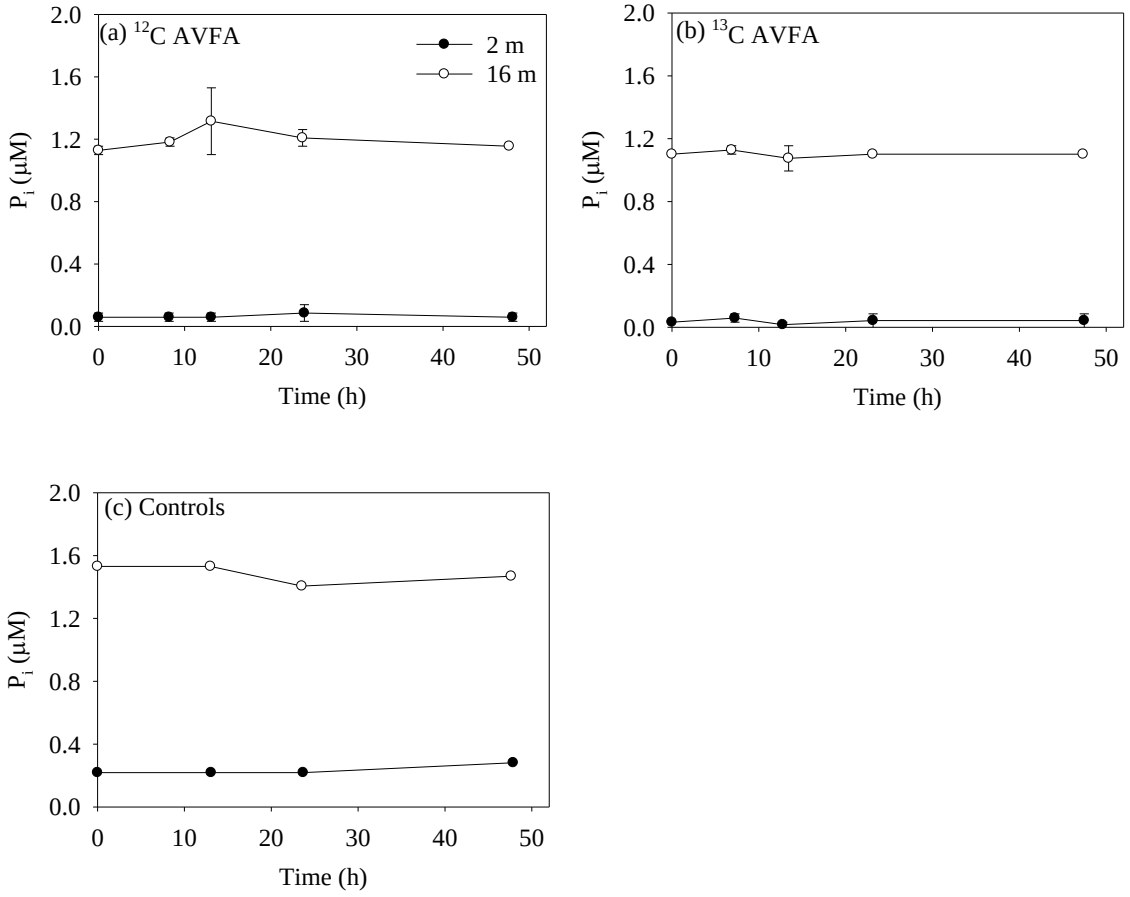

Figure 5.5. Bacterial abundance with incubation time in the surface 2 m and bottom 16 m seawater of (a) ^{12}C-AVFA, (b) ^{13}C-AVFA, and (c) no-AVFA control samples. Data points were presented as average ± absolute error of duplicate samples except control samples.

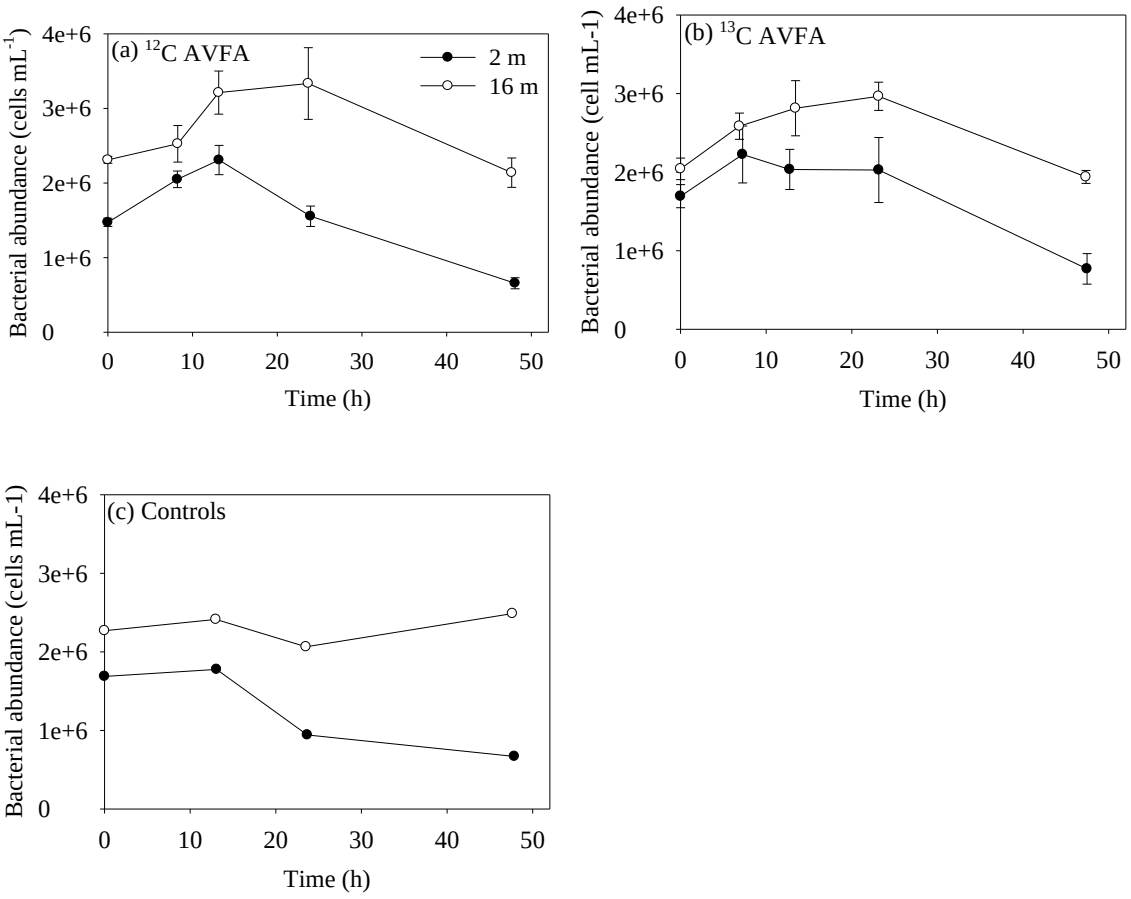

Figure 5.6. Changes of bacterial community structure (% genus) with time during ^{12}C-AVFA, ^{13}C-AVFA and no-AVFA control (CTR) incubation in the (a) surface 2 m and (b) bottom 16 m seawater; percentages were average of duplicate samples except control, 2 m 0 h and 16 m 0 h samples; (c) non-metric multidimensional scaling (nMDS) on the bacterial compositions at genera level in all the above samples; S12, surface 2 m ^{12}C-AVFA samples; S13, surface 2 m ^{13}C-AVFA samples; SC, surface 2 m no-AVFA control samples; B12, bottom 16 m ^{12}C-AVFA samples; B13, bottom 16 m ^{13}C-AVFA samples; BC, bottom 16 m no-AVFA control samples.

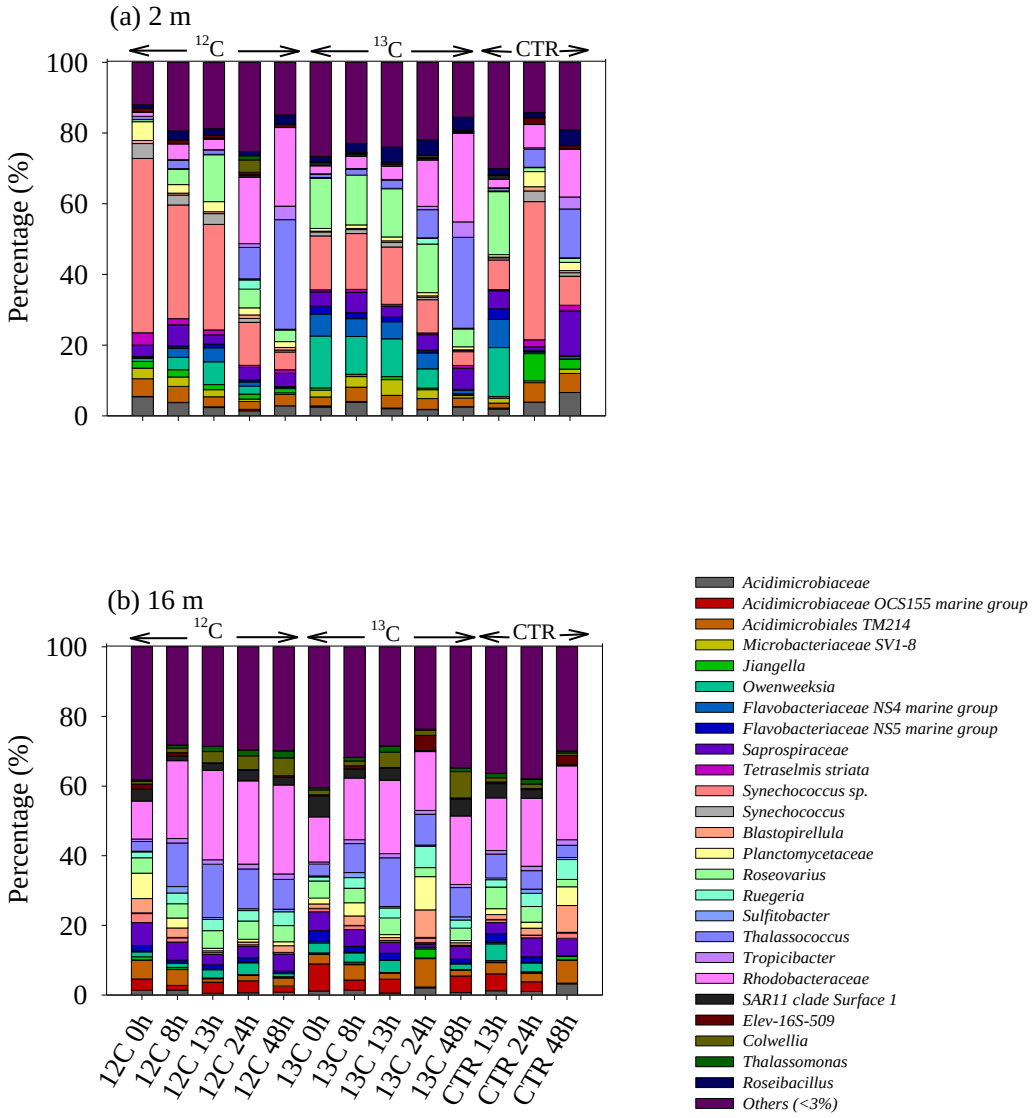

Figure 5.6 (continued)

(c)

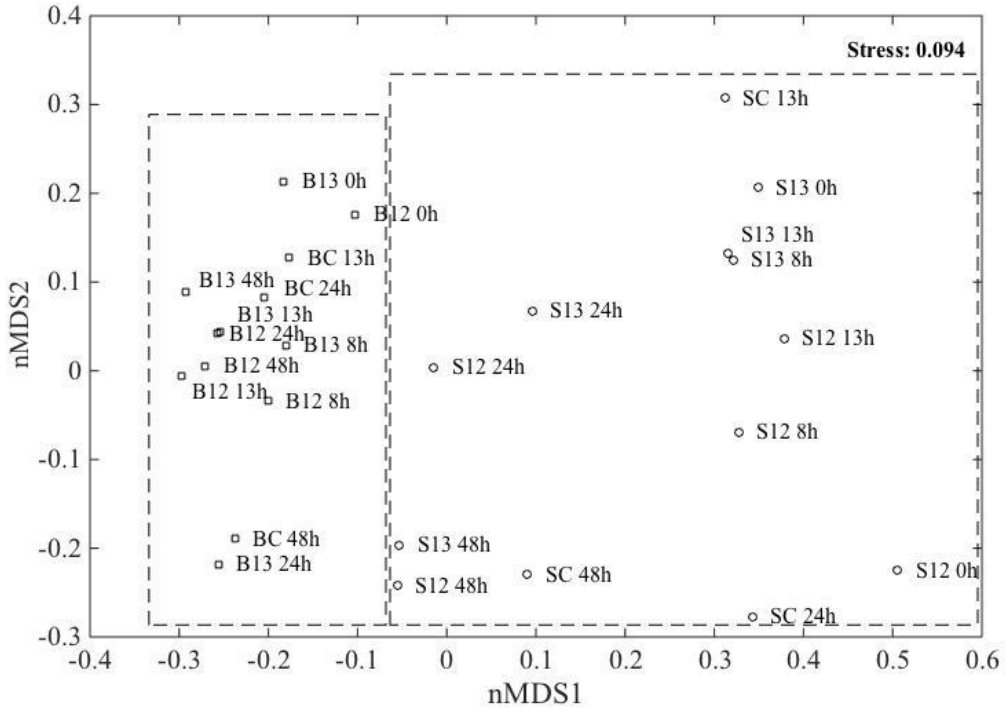

Figure 5.7. (a-b) qPCR analysis results shown as relative quantities versus density of SIP gradient fractions for bacterial 16S rRNA gene copies in the surface 2 m and bottom 16 m samples. The ratio of quantities was normalized to the highest quantities observed. Data points were presented as average ± standard deviation of three replicate qPCR measurements. Grey bars indicate heavy density ranges used for percentage enrichment calculations in (c) and (d). (c-d) Uptake of peptides shown as percentage enrichment of major bacterial classes in the heavy density range in the ^{13}C-AVFA SIP fractions compared to the ^{12}C-AVFA SIP fractions. Bacterial class chosen were at least 0.1% abundance of the community. *Flavo*, *Flavobacteria*; *Sphingo*, *Sphingobacteria*; *Alpha*, *Alphaproteobacteria*; *Acidi*, *Acidimicrobiia*; *Verruco*, *Verrucomicrobiae*; *Cyano*, *Cyanobacteria* subsectionI; *Actino*, *Actinobacteria*; *Beta*, *Betaproteobacteria*; *Plancto*, *Planctomycetacia*; *Gamma*, *Gammaproteobacteria.*

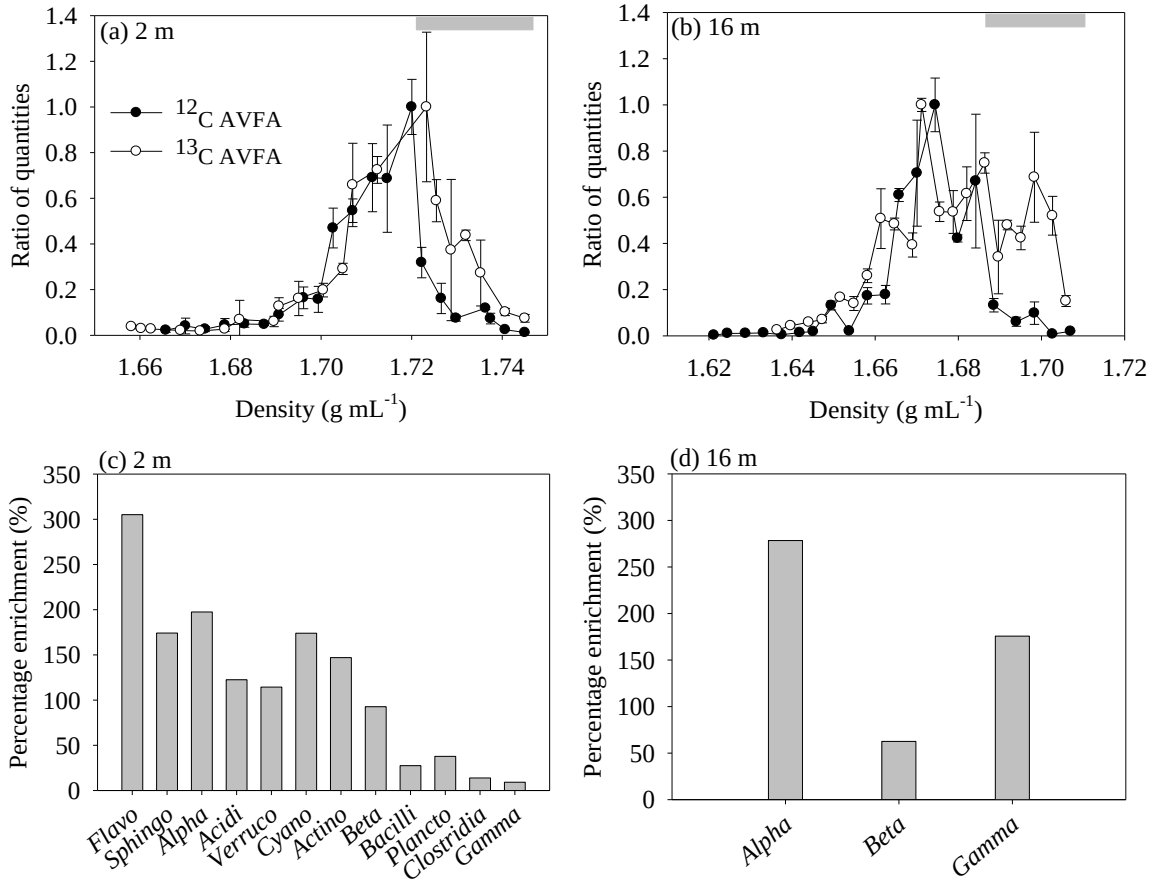

Figure 5.8. Uptake of peptides shown as percentage enrichment of major bacterial genera within each class (listed above the bars) in the heavy density range of the ^{13}C AVFA sample SIP fractions compared to the ^{12}C AVFA sample SIP fractions in the (a) surface 2 m and (b) bottom 16 m seawater. Bacterial genera chosen were at least 0.1% abundance of the community. Bacterial class abbreviation was same as that in Figure 5.7.

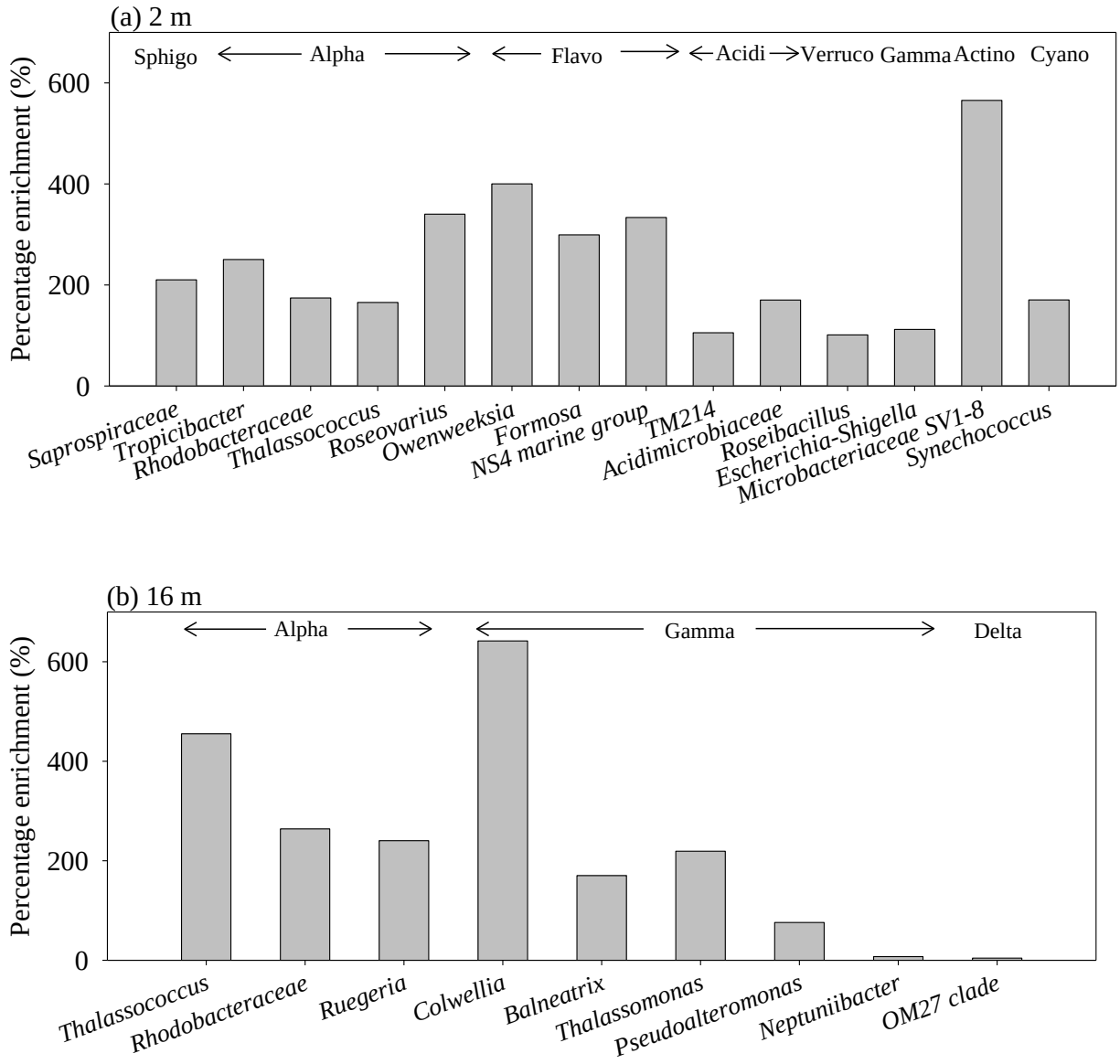

Chapter 6. Differentiating the role of different-sized microorganisms in peptide decomposition during incubations using size-fractioned coastal seawater

(Published in Journal of Experimental Marine Biology and Ecology 472 (2015): 97-106)

ABSTRACT

Peptide decomposition by different-sized microorganisms was compared by incubating tetrapeptide alanine-valine-phenylalanine-alanine (AVFA), a fragment of RuBisCO, in coastal seawater after size-fraction by filtration. The size-fractioned seawater included <0.8-μm filtered (free-living bacteria), <5-μm filtered (free-living bacteria + heterotrophic nanoflagellates), <20-μm filtered (free-living and particle-attached bacteria + heterotrophic nanoflagellates + other small protists), and unfiltered whole water collected from Texas coast in the western Gulf of Mexico. Decomposition rates of AVFA in the <20-μm and unfiltered seawater were significantly higher than those in the <0.8-μm and <5-μm seawater in the December 2011 incubation. The higher decomposition rate in the large size fractions can be attributed to activities of particle-attached bacteria and/or large-size microorganisms, such as osmotrophic protists. However, the role of particle-attached bacteria in explaining this decomposition difference might be limited, as bacterial abundance and community structure did not differ much among the 4 treatments. Consistently, the June 2013 incubation indicated that AVFA decomposed most rapidly in the unfiltered seawater with >20-μm microorganisms. This study provides insights into the relative role of different-sized microorganisms in regulating the recycling of labile organic matter in coastal waters.

INTRODUCTION

Proteins and peptides, accounting for 25-70% of plankton biomass (Emerson and Hedges, 2008), serve as an important link in the microbial loop in marine environments. The decayed plankton matter is metabolized by different-sized microorganisms in seawater. In the small non-particulate fractions (<3-5 μm) (Hoppe, 1991; Bidle and Fletcher, 1995; Šimek et al., 1999), proteins and peptides are primarily decomposed by free-living heterotrophic bacteria (Sussman and Gilvarg, 1971; Hoppe, 1983; Pantoja et al., 1997). In the large particulate fractions (>3-5 μm), particle-attached bacteria can be one major decomposer of proteins and peptides (Hoppe, 1991). Free-living bacteria predominate total bacterial abundance and often account for a major fraction (40-70%) of dissolved organic matter hydrolysis or decomposition in seawater (Hoppe, 1991; Unanue et al., 1992), but particle-attached bacteria are often more active than free-living bacteria per cell basis and can contribute to a significant proportion of organic matter hydrolysis or decomposition in certain environments (Kirchman and Mitchell, 1982; Griffith et al., 1994).

Recent studies showed that a significant fraction of labile organic matter, such as peptides, is processed by protists in the >3-5 μm seawater (Karner et al., 1994; Berg et al., 2002; Bradley et al., 2010). As single-cell eukaryotes, protists include autotrophic phytoplankton, heterotrophic flagellates, microzooplanktonic ciliates and mixotrophic microbes (Kirchman, 2008). Their sizes range from 2 to 20 μm for nanoflagellates such as *Gymnodinium,* to 200-2000 μm for dinoflagellates such as *Noctiluca*. Besides grazing on bacteria or other protists of similar size (Šimek et al., 1999; Park and Cho, 2002; Pernthaler, 2005), some heterotrophic and mixotrophic protists can take up organic compounds directly by an "osmotrophic" nutrient strategy, particularly under

environmental conditions of limited light, depleted nutrients or high concentrations of organic matter (Stoecker, 1999; Glibert and Legrand, 2006; Salerno and Stoecker, 2009). Osmotrophic protists have several pathways of utilizing organic matter, including direct uptake, extracellular oxidation and hydrolysis, or pinocytosis that involves engulfing and transporting molecules into the cells via vesicle formation (Antia et al., 1991). These osmotrophic protists may contribute to peptide decomposition in the large-size fraction of seawater.

Several studies have shown that some protists can hydrolyze peptides extracellularly (Karner et al., 1994; Mulholland et al., 2002; Salerno and Stoecker, 2009). For instance, mixotrophic dinoflagellate *Prorocentrum minimum*, benthic protist thraustochytrids, axenic cultures of algae *Aureococcus anophagefferens*, *Alexandrium tamarense*, and *Heterocapsa triquetra* can release aminopeptidases to hydrolyze peptides, sometimes at a higher hydrolysis rate than bacteria (Berg et al., 2002; Stoecker and Gustafson, 2003; Bongiorni et al., 2005). However, most studies have focused on single protist species, and only a few studies have investigated peptide decomposition by natural protist assemblages in seawater (Karner et al., 1994; Salerno and Stoecker, 2009; Thao et al., 2014). The relative roles of different-sized microorganisms in decomposing small peptides, ranging from free-living bacteria to particle-attached bacteria and protists, have not been thoroughly examined. Large microorganisms, such as protists, may be important in organic nitrogen remineralization and nutrient regeneration, but this possibility has only been investigated in a few studies and often overlooked in the traditional microbial loop model (Azam et al., 1983).

Previous studies on peptide hydrolysis have mostly relied on peptide analogs, such as L-leucine 7-amido-4-methyl coumarin (leu-MCA), as a proxy to measure aminopeptidase activity due to the simplicity of this technique (Hoppe, 1983; Chróst,

1991). These peptide analogs offer advantage of providing unambiguous rates of extracellular enzyme activities in different environments. However, the large fluorophore on the chemical structures of these small analogs may affect hydrolysis rate due to the potential steric effect (Pantoja and Lee, 1999; Mulholland et al., 2003; Obayashi and Suzuki, 2008; Liu et al., 2010). Using leu-MCA may also underestimate the hydrolysis rate because this analog only measures aminopeptidases, excluding carboxypeptidases and endopeptidases (Hashimoto et al., 1985; Pantoja et al., 1997; Steen and Arnosti, 2013). In addition, peptide analogs with large fluorophores cannot be taken up directly by microbes, so the measured rates do not include uptake, which may be significant in certain scenarios (Liu et al., 2013). In contrast, studies with small peptides without fluorogenic tags can provide information on their hydrolysis and microbial decomposition rates in a more realistic way, and the hydrolyzed fragments of small peptides can also be used to pinpoint the hydrolysis pathway (Kirchman and Hodson, 1984; Mulholland and Lee, 2009; Liu et al., 2010; Liu et al., 2013; Liu and Liu, 2014; Liu and Liu, 2015). The decomposition pathways of small peptides include both extracellular hydrolysis with subsequent uptake for further metabolism and direct uptake for intracellular hydrolysis (Weiss et al., 1991; Payne and Smith, 1994; Cunha, 2010). Thus, the use of small peptides without fluorogenic tags targets on a complete decomposition process including peptide hydrolysis, uptake and transformations by microorganisms.

In this study, peptide decomposition patterns and rates were compared among different-sized microorganisms ranging from free-living bacteria, heterotrophic nanoflagellates (HNF) to particle-attached bacteria and other large protists in coastal seawater. Tetrapeptide alanine-valine-phenylalanine-alanine (AVFA), a fragment of Ribulose-1,5-bisphosphate carboxylase/oxygenase (RuBisCO), was incubated using size-

fractioned coastal seawater. The results suggest the importance of microorganisms in large-sized fractions, such as particle-attached bacteria and/or protists, in metabolizing labile organic nitrogen in coastal seawaters.

MATERIALS AND METHODS

December 2011 peptide incubation

Surface seawater for peptide incubation was collected using 2 L acid-cleaned polyethylene bottles at the Port Aransas ship channel (27.84ºN, 97.05ºW) in Texas coast of the western Gulf of Mexico in December 2011. Seawater were size-fractioned with gentle filtration (<5 mm Hg) according to the protocol of Šimek et al. (1999), including seawater through (1) a 0.8-μm nylon filter (47 mm dia., Magna), containing free-living bacteria only, (2) a 5-μm nylon filter (47 mm dia., Isopore^{TM}), containing mainly free-living bacteria and HNF, (3) a 20-μm nylon filter (47 mm dia., Magna), containing free-living and particle-attached bacteria, HNF, and other small protists, and (4) the whole unfiltered seawater, containing the full spectrum of microbial assemblages. A series of duplicate 60 mL amber bottles (Wheaton) with 50 mL of seawater was set up for each treatment. Stock solution of AVFA, synthesized by a solid phase synthesizer (C S Bio) (Liu et al., 2010), was amended to every bottle to reach a final concentration of 10 μmole·L^{-1}, ca. 3 times higher than the background concentration of dissolved combined amino acids (DCAA) that presumably include peptides and proteins (Table 6.1). This concentration is necessary for detection of the peptide and its hydrolysis fragments (Liu et al., 2013).

The incubation lasted 65 h at room temperature (23 ºC) under dark. One bottle of each treatment was sacrificed at each time point (0, 22, 30, 46, 54, and 65 h) for sample

collection. Duplicate water samples (each 1.5 mL) from the bottle were filtered through 0.22 μm syringe filters (PVDF, 13mm dia., Whatman) and stored under -20 ºC until analyses for peptide, amino acids and ammonium. An aliquot (1 mL) from each bottle was preserved in 3% formaldehyde under 4 ºC for bacterial enumeration. An aliquot (15 mL) was filtered through 0.22 μm Nylon filter (25mm dia., Magna) and the filters were stored under -20 ºC for bacterial community structure analysis. The rest of water in bottles was preserved with formaldehyde to achieve a final concentration of 5% and then stored at 4 ºC under dark for protist counting within a week.

June 2013 peptide incubation

The incubation of AVFA in June 2013 followed the same procedure as described above, except that the protocol of protist preservation was modified to extend the preservation time. Briefly, 5 μL alkaline Lugol's solution was added to fix 10 mL of water sample, and then 0.25 mL sodium borate-buffered formaldehyde was immediately amended, followed by addition of 10 μL 3% sodium thiosulfate to bleach out the iodine color (Sherr and Sherr, 1993). The fixed samples were stored at 4 ºC under dark until analysis. Controls without peptide amendments were also included, with 4 separate 125 mL amber bottles filled with 100 mL size-fractioned seawater. Aliquots from controls were taken at 0, 11, 29, and 49 h, respectively.

Chemical measurements

Chemical properties of the initial seawater for incubation were monitored (Table 6.1). Temperature and salinity were measured with thermometer and refractometer, respectively. The pH was measured with a bench-top pH meter (Thermo Fisher Orion 4-

star). Dissolved oxygen (DO) was analyzed by an oxygen microsensor (Unisense) with a two-point calibration, 100% point with air-purged seawater and 0% with N_2-purged seawater. Seawater was filtered through a 0.22 μm nylon filter for measuring concentrations of nutrients, dissolved organic carbon (DOC), total dissolved nitrogen (TDN), dissolved free amino acids (DFAA) and total dissolved amino acids (TDAA). Nitrate, nitrite, and soluble reactive phosphate concentrations were analyzed in a UV-Vis spectrophotometer (Evolution 160, Thermo Scientific) following established procedures (Strickland and Parsons, 1968; Jones, 1984). Concentrations of DOC and TDN were analyzed in a Shimadzu total organic carbon (TOC-V) analyzer coupled to a TNM-1 TDN analyzer with error within 6% between duplicates. Concentrations of DFAA were measured by high performance liquid chromatography (HPLC) equipped with a fluorescence detector (Shimadzu Prominence) after pre-column *o*-phthaldialdehyde (OPA) derivatization (Lindroth and Mopper, 1979; Lee et al., 2000). Concentrations of TDAA were measured in a same way as DFAA after samples were hydrolyzed into individual amino acids with 6 mol·L^{-1} HCl under nitrogen at 110 ºC for 20 h (Kuznetsova and Lee, 2002). Concentrations of DCAA were calculated as the difference between TDAA and DFAA. Measurements of DFAA and DCAA in replicate samples had relative standard deviations (RSDs) of 10–20%.

Concentrations of AVFA in incubation samples were measured using HPLC (Shimadzu Prominence) with photodiode array (PDA) detection (Liu et al., 2010). Briefly, the HPLC system was equipped with a C_{18} column (Alltima 5 μ, 250 mm × 4.6 mm) and two mobile phase solvents for gradient elution, solvent A as 0.05 mol·L^{-1} sodium phosphate (monobasic, ACS grade, VWR) with pH of 4.5 and solvent B as methanol (HPLC grade, Fisher Scientific). Peptide concentrations were quantified in gradient elution using external standards at the wavelength of 206 nm. Concentrations of

individual amino acids (A, V and F) and peptide fragments (VFA and FA) from AVFA hydrolysis were measured by HPLC with a fluorescence detector after pre-column OPA derivatization (Lindroth and Mopper, 1979; Liu et al., 2013). Ammonium was analyzed using HPLC with post-column OPA derivatization (Gardner and St. John, 1991).

Bacterial abundance

Bacterial cells were enumerated with a flow cytometer (BD Accuri C6) under laser excitation of blue light at 488 nm (Marie et al., 1997). For a 500 μL sample, a 5 μL SYBR Green II (Molecular probes) working solution (1:100 v/v) was added and kept in dark for at least 15 min before analysis. Dyed samples were analyzed with a fixed intake volume of 30 μL at the same flow rate below 300 events per second in a logarithmic mode. Validation beads (Polysciences) were used as calibration reference daily. Bacteria cell counts were detected on a two-dimensional dot plot of side scatter (SSC-H) versus fluorescence signal (FL1-H) on a log scale. Data analysis was performed with CFlow Plus software associated with the instrument. Counting error of bacterial abundance was ca. 11% for duplicate samples.

Flow cytometry may underestimate the total bacterial abundance if some particle-attached bacteria are buried within the particles and not counted. To assess this possibility, seawater collected from ship channel in April 2014 was size-fractioned using the procedure described above and counted in the flow cytometer. Bacterial abundance in each size fraction was compared with vs. without sonication. For the sonication samples, formaldehyde fixed bacteria samples were sonicated at the power level of 100 W (FS60, Fisher Scientific) for 30 s to disperse bacteria from particles before the SYBR Green staining (Velji and Albright, 1993).

Bacterial community structure

The 2011 filter samples were sent to the Research and Testing lab (Lubbock, TX) for DNA extraction and pyrosequencing, following the procedures described in Liu et al. (2013). Community structure analyses were based on bacterial tag-encoded FLX amplicon pyrosequencing (bTEFAP). The 16S universal Eubacterial primers Gray28F 5'TTTGATCNTGGCTCAG and Gray519r 5'GTNTTACNGCGGCKGCTG were used for PCR with 30 cycles (Dowd et al., 2008; Smith et al., 2010). Using a Roche 454 FLX instrument with titanium reagents, the pyrosequencing was based on RTL protocols (www.researchandtesting.com). The sequencing data were processed through the pipeline consisting of quality checking, denoising, and microbial diversity analysis. Sequences with identity scores between 90% and 95% were resolved at the genus level and between 80 and 85% at the class level. Bacteria sequences were deposited in National Center for Biotechnology Information (NCBI) GenBank under BioProject accession number PRJNA223070.

Protist counting

The 2011 protist samples were analyzed within one week after formaldehyde preservation and the 2013 samples within three weeks after Lugol's fixation. The preserved sample (1 mL) was stained with fluorescein isothiocyanate (FITC, 90% pure, Acros organics) and incubated in dark for 5-10 min to distinguish autotrophs (and mixotrophs) and heterotrophs (Sherr et al., 1993). The FITC stained heterotrophic protist cells showed green fluorescence, while autotrophic and mixotrophic protists showed red to yellowish autofluorescence. Stained samples were filtered through 0.22 μm black

polycarbonate filters (25 mm dia.) with GF/C as backing filters (1.2 μm, Whatman). Filtration was performed under a gentle vacuum of 5 mm Hg to maintain the shape of protists, and the filter was rinsed twice with 10 mL cold 0.5 $mol \cdot L^{-1}$ sodium carbonate buffer (pH 9.5). The black filter was mounted on a microscope glass slide with a drop of FA mounting fluid (pH 9, VMRD Inc.), and examined with an epifluorescence microscope under blue light excitation and 400 times magnification. Protists were counted mostly on one of the duplicate samples due to the large number of samples, long sample counting time, and short effective time of protist preservation. Counting from a few duplicate samples indicated a deviation of ca. 29%.

Statistical analysis

Decomposition rates of AVFA were calculated from linear regressions of the decomposition curves for each treatment (multiple regressions were done for different stages of 2013 data as shown later). Ammonium release rates were calculated from linear regression of the curves of ammonium concentration with time. Difference of AVFA decomposition rates or ammonium releasing rates among treatments was evaluated using two-sample *t*-test ($\alpha = 0.05$), and variance difference assessment was based upon F test ($\alpha = 0.05$). Principal component analysis (PCA) and cluster analysis based on Bray-Curtis dissimilarity was applied on bacterial composition (% genera) data using MATLAB® (Xue et al., 2011).

RESULTS

Peptide decomposition during the incubation

In the December 2011 incubation, AVFA concentrations (normalized to initial concentrations of 10.29 ± 0.05 $\mu mol \cdot L^{-1}$) in the <0.8 μm and <5 μm seawater decreased steadily at rates of 0.13 and 0.14 $\mu mol \cdot L^{-1} \cdot h^{-1}$, respectively (Fig. 6.1a). In contrast, concentrations of AVFA in the <20 μm and unfiltered seawater decreased to almost zero at a faster rate of 0.19-0.20 $\mu mol \cdot L^{-1} \cdot h^{-1}$ within the 65 h. The decomposition rates in the <20 μm and unfiltered seawater were significantly higher than those in the <0.8 μm and <5 μm seawater (*t*-test, $p < 0.05$, assuming equal variance after F test). This difference was more evident after 22 h.

Decomposition of AVFA showed a two-stage pattern in the June 2013 incubation (Fig. 6.1b). Time intervals of the first stage differed among the four incubations, 0-34 h for the <0.8 μm, 0-22 h for the <5 μm and <20 μm, and 0-11 h for the unfiltered treatment. During the first stage, AVFA decreased slowly in the four treatments at a rate of 0.071 $\mu mol \cdot L^{-1} \cdot h^{-1}$. In contrast, AVFA decomposed much faster at 0.39-0.75 $\mu mol \cdot L^{-1} \cdot h^{-1}$ during the second stage from 11-34 h to the end of incubation. The decomposition rate during the 11-28 h was significantly higher in the unfiltered seawater than those in the other three treatments (*t*-test, $p < 0.05$, assuming equal variance after F test). Decomposition rates of AVFA were similar in the <20 μm seawater and <5 μm seawater, and the rate was the lowest in the <0.8 μm seawater.

Production of peptide fragments and amino acids in the peptide incubation

As extracellular hydrolysis fragments of AVFA (Liu et al., 2013), peptides FA and VFA were monitored throughout the incubation. Concentrations of FA remained low

in all four treatments throughout the incubation (<0.03 μmol·L^{-1} in 2011 and <0.06 μmol·L^{-1} in 2013, Figs. 6.2 and 6.3). In contrast, VFA concentrations in the 2011 incubation reached 0.15-0.19 μmol·L^{-1} in the <0.8 μm and <5 μm incubation, 3-5 times higher than those in the <20 μm or unfiltered seawater incubation (0.04-0.05 μmol·L^{-1}) (Fig. 6.2). In the 2013 incubations, VFA reached 0.25-0.45 μmol·L^{-1}, and the highest VFA concentration (0.45 μmol·L^{-1}) occurred in the <0.8 μm incubation.

Either AVFA or the hydrolyzed peptide fragments can be further hydrolyzed to individual amino acids. Background concentrations of A, V and F in the 2011 seawater were 0.023, 0.0047 and 0.0021 μmol·L^{-1}, respectively. Concentrations of V and F throughout the <5 μm, <20 μm and unfiltered incubations (<0.05 μmol·L^{-1}) were about one order of magnitude higher than the background values (Figs. 6.2b, c, and d). Concentrations of A remained within the background level in these three treatments during the incubation, except that its concentration reached 0.2-0.3 μmol·L^{-1} at the initial time point. Overall, more amino acids were released in the <0.8 μm incubations than in other incubations (Fig. 6.2a). Consistently, the amounts of amino acids released were the highest in the <0.8 μm seawater during the 2013 incubation, with A as high as 1.08 μmol·L^{-1} and F as high as 0.18 μmol·L^{-1} (Fig. 6.3a). In the <5 μm, <20 μm and unfiltered incubations, the A concentration was below 0.46 μmol·L^{-1}, but almost 4 times higher than V and F concentrations (Figs. 6.3b, c, and d).

Production of ammonium during the peptide incubation

Ammonium is a major metabolite of microorganisms after AVFA and its fragments are taken up (Liu et al., 2013). The change of ammonium concentration with time showed a two-stage pattern during the 2011 incubation (Fig. 6.4a). From 0 to 22 h,

ammonium concentrations increased slightly from 1.1-2.7 μmol·L^{-1} to 2.1-4.7 μmol·L^{-1}, whereas from 22 to 65 h, the concentrations increased rapidly to 7.7-16.8 μmol·L^{-1} in the <0.8 μm and <5 μm incubations, and 21.8-22.8 μmol·L^{-1} in the <20 μm and unfiltered incubations. The ammonium release rates during the second stage (22-65 h) were significantly higher in the <20 μm and unfiltered seawater than those in the other two treatments (*t*-test, $p < 0.05$, assuming unequal variance after F test), corresponding well with the respective AVFA decomposition patterns (Fig. 6.1a). In comparison, the ammonium release showed a three-stage pattern in the 2013 incubation (Fig. 6.4b). During the initial 11 h, ammonium concentrations remained at the background level of 1.8 μmol·L^{-1} in all treatments. From 11 to 28 h, the release rate of ammonium was highest in the unfiltered seawater (0.53 μmol·L^{-1}·h^{-1}) among the four treatments, concomitant with the rapid AVFA decomposition (Fig. 6.1b). This release rate was about 2.5 times higher than those in the <0.8 μm, <5 μm and <20 μm incubations from 11 to 28 h. After 34 h, ammonium concentrations were similar in the <5 μm, <20 μm and unfiltered incubations, and increased at a lower rate of ca. 0.25 μmol·L^{-1}·h^{-1}. Ammonium concentrations were consistently lower in the <0.8 μm seawater than in other treatments throughout the incubation. Controls without peptide amended showed that ammonium concentrations decreased slightly with time and remained below 2.1 μmol·L^{-1} throughout the incubation (Fig. 6.4b), suggesting that the ammonium in peptide incubations was produced by AVFA decomposition, not from the background organic matter.

Bacterial abundance in the peptide incubation

Total bacterial abundances before and after sonication differed by less than 2.1% for each size fraction (data not shown), indicating that bacterial abundance, measured by

flow cytometry, included both free-living and particle-attached bacteria, or that the fraction of particle-attached bacteria is negligible in the ship channel water. Initial bacterial abundances in the 2011 incubation were similar among all treatments (RSD = 23%), ca. 2.6×10^6 cells·mL^{-1}, except the <0.8 μm treatment. Bacterial abundance increased 2-4 times with incubation with the peak at 46-54 h, and then decreased slightly (Fig. 6.5a). Bacterial abundance in the <20 μm incubation increased the most from 0 to 46 h, followed by the <5 μm incubation. In contrast, bacterial abundance increased at a lower rate in the unfiltered seawater.

The low initial bacterial abundance in the <0.8 μm incubation was caused by the exclusion of large bacteria (>0.8 μm) or those attached to particles by the 0.8 μm filtration (Rego et al., 1985; Schut et al., 1997). About 53% of bacteria were retained on the 0.8 μm filter relative to other large size-fractioned seawater. The overall change of bacterial abundance with incubation time in the <0.8 μm treatment was similar to other treatments, except that the growth rate was the highest during 0 to 46 h (Fig. 6.5a). The bacterial abundance in the <0.8 μm incubation reached the level of other treatments at 30 h. This fast-growing pattern was likely due to the elimination of protists, the bacterial grazers (Beardsley et al., 2003).

Consistent with the 2011 incubation, initial bacterial abundances were similar among the <5 μm, <20 μm and unfiltered treatments in the 2013 incubation, with an average of 8.1×10^5 cells·mL^{-1}; 83% of bacteria were filtered out in the <0.8 μm treatment (Fig. 6.5b). Bacterial abundance in all treatments increased 4-12 times from 0 h to 34-44 h, and decreased afterward for the <5 μm and unfiltered incubations but remained relatively constant for the <0.8 μm and <20 μm incubations. During 0-34 h, bacterial abundance in the <20 μm seawater increased the most (8 times), and those in the <5 μm and unfiltered seawater increased 4 times. In the control without peptide

amendment, bacterial abundance increased slightly and remained under 2.2×10^6 cells·mL^{-1} over 49 h in all four treatments (Fig. 6.5c), suggesting that the rapid increase of bacterial abundance in the size-fractioned treatments was caused by the AVFA decomposition.

Bacterial community structure in the Dec 2011 incubation

Initial bacterial communities in the 2011 incubation were analyzed only for <0.8 μm and <20 μm treatments, assuming that they were the same among the <5 μm, <20 μm and unfiltered seawater treatments. This assumption is reasonable because the initial bacterial abundances were similar among the three treatments. *Alphaproteobacteria* (52.6%), *Cyanobacteria* (18.6%), *Gammaproteobacteria* (11.5%), *Flavobacteria* (6.1%), and *Sphingobacteria* (4.5%) were the major bacterial classes in the <20 μm treatment at the initial time point (Fig. 6.6c). In contrast, the <0.8 μm seawater was dominated by *Sphingobacteria*, *Cyanobacteria* and *Opitutae* with similar proportions (33%), suggesting that a major fraction of large bacteria including *Alphaproteobacteria*, *Gammaproteobacteria* and *Flavobacteria* was filtered out (Fig. 6.6a).

Bacteria community structure in the <0.8 μm treatment developed differently at the beginning, but converged with other treatments over time. In the <0.8 μm incubation, *Gammaproteobacteria* developed rapidly from 0% at 0 h to 80.6% at 65 h; the proportion of *Alphaproteobacteria* increased from 0% to 53.7% during 0-30 h but decreased to 11% during 30-65h. In contrast, *Gammaproteobacteria* developed more rapidly, increasing from 11.5% at 0 h to 82.1%, 79.0% and 88.7% at 46 h in the <5 μm, <20 μm and unfiltered incubations, respectively. *Alphaproteobacteria* decreased from 52.6% at 0 h to 10.2%-19.2% at 46 h in these three incubations. From 46 h to 65 h, the proportion of

Alphaproteobacteria increased to 38.3% and 27.7% in the <20 μm and unfiltered incubations, respectively, but remained relatively constant in the <5 μm seawater. Other bacterial classes together accounted for minor proportions (<4.2%) in the <5 μm, <20 μm and unfiltered treatments during 30-46 h.

The rapidly-developed bacterial genera (out of total 226 genera) included 7 *Gammaprotoebacterial* genera (*Marinomonas*, *Alteromonas*, *Neptunomonas*, *Vibrio*, *Marinobacterium*, *Chromohalobacter*, *Neptuniibacter*), 3 *Alphaproteobacterial* genera (*Nautella*, *Phaeobacter*, *Ruegeria*), and 1 *Actinobacterial* genus (*Ponticoccus*). These bacteria accounted for 54% to 92% of the bacteria community in all samples except those at 0 h. Bacterial community compositions of all samples were further compared using PCA (Fig. 6.7). The converged group (the circle in Fig. 6.7) included the <0.8 μm sample at 65 h, <5 μm samples from 30 to 65 h, <20 μm samples from 30 to 46 h, and unfiltered samples from 30 to 65 h; these samples were enriched with *Alteromonas* (40.1 - 61.8%), *Marinomonas* (8.1 - 14.1%) and *Vibrio* (5.1 - 21.7%). The <0.8 μm samples at 30 h and 46 h were not in the group because again the initial filtration modified the bacterial community structure, but the structure did converge with other samples by 65 h.

Protist abundance in the peptide incubation

The initial seawater contained heterotrophic protists in different sizes and abundances. From the microscopic observation, the <0.8 μm seawater did not contain protists, and large heterotrophic protists, such as protoperidinium and ciliates, were present only in the <20 μm and/or the unfiltered seawater. In the 2011 incubation, the initial protist abundances in <5 μm, <20 μm and unfiltered seawater were 413, 592 and 825 cells·mL^{-1}, respectively (Fig. 6.8a). Their abundances in these three treatments

decreased by 5-6 times by 30- 46 h of incubations, followed by an increase at the end of incubation. The abundances of heterotrophic protist in the <20 μm and unfiltered seawater were 1.1-2 times as high as those in the <5 μm seawater throughout the incubation.

The initial protist abundance in the 2013 unfiltered seawater (732 cells·mL^{-1}) was 2-4 times higher than those in the <5 μm and <20 μm seawater (Fig. 6.8b). The abundances in all the 2013 treatments decreased from 0 to 11 h. After the initial decrease, the abundance doubled in the unfiltered seawater at 48 h, and tripled in the <5 μm and <20 μm treatments at the end of incubation. Protist abundance in the unfiltered seawater was 2-4 times higher than the other two treatments at 0 and 11 h, but no consistent pattern was observed among the three treatments afterwards.

DISCUSSION

Factors contributing to the peptide disappearance

Possible fates of the amended peptide include biological decomposition and physical sorption to glass wall and/or particles. Previous studies showed that peptide sorption on glass or particles are negligible (Liu and Lee, 2006; Liu et al., 2010). Although killed controls were not included in this study, previous results showed that AVFA concentrations changed little when $HgCl_2$ was added to the incubation to inhibit microbial activity (Liu et al., 2010; Liu and Liu, 2014). Thus, peptide disappearance during the incubation was attributed mainly to biological processes. Significant production of ammonium during the AVFA incubations, but not the controls, further confirms that the amended AVFA was metabolized by microbes (Fig. 6.4).

Filtration is a simple approach to separate the organisms into different size fractions and quantify the ecological role of microbial communities in each size fraction (Somville and Billen, 1983; Karner et al., 1994; Šimek et al., 1999; Stoecker and Gustafson, 2003). Filtration may introduce certain artifacts in enzymatic studies, such as enzyme liberation due to cell lysis and/or enzyme adsorption on filters. However, these artificial processes play only a minor role in the assessment of extracellular enzyme activity (Karner and Rassoulzadegan, 1995; Salerno and Stoecker, 2009). Additionally, no significant differences in peptide decomposition were found between <0.8 μm and <5 μm or between <20 μm and unfiltered seawater in the 2011 incubation despite the different filtration strength, indicating that enzyme activity was not significantly affected by filtration.

Particle-attached extracellular enzymes (referring to enzymes outside bacteria in contrast to particle-attached bacteria discussed later) did not seem to be significant for the AVFA hydrolysis in this study. A reported lifetime of several weeks for particle-attached enzymes (Karner et al., 1994) would be sufficient to decompose peptides in the 65-69 h incubation. However, if these enzymes had led to the peptide decomposition differences observed among the 4 treatments, higher amounts of hydrolyzed amino acids or peptide fragments should have occurred in the <20 μm and unfiltered seawater in the 2011 incubation and in the unfiltered seawater in the 2013 incubation. However, both peptide fragments and amino acids remained at low levels throughout the <20 μm and unfiltered incubations in 2011, and in the unfiltered incubation in 2013 (Figs. 6.2c, d and 6.3d), indicating a limited role of the particle-attached extracellular enzymes in peptide decomposition. More ammonium release from these large-size fractions further suggests that AVFA was metabolized mainly by microbes rather than just being extracellularly hydrolyzed. It is concluded that different-sized microorganisms including bacteria (both

free-living and particle-attached) and protists were the key players in decomposing AVFA.

Mass balance and peptide decomposition pathways

Mass balance calculations can help quantify fates of the decomposed peptide. Decomposition of AVFA was complete within 3 d in both 2011 and 2013 incubations. Of the amino acids released from AVFA extracellular hydrolysis, V is more resistant to bacterial uptake than A and F (Liu et al., 2013), so V was assumed to represent the amino acids released from AVFA, conservatively because amino acid uptake was not considered. The released ammonium was assumed to be the metabolite from AVFA that contains four nitrogen atoms per molecule, because the ammonium levels did not increase in the control without peptide amendment (Fig. 5.4b). And minimal nitrification was expected within this short time scale, as indicated from the previous study (Liu et al., 2013). Based on these assumptions, less than 1% of the AVFA in the <20 μm and unfiltered treatments in the 2011 incubation was hydrolyzed into V and VFA, 49% was remineralized to ammonium, and the rest 50% may have been incorporated into bacteria and/or protists biomass or transformed to other DON form at 65 h. In contrast, 2-4% of AVFA in the <0.8 μm and <5 μm treatments was hydrolyzed to amino acids and VFA, 32% to ammonium and 64-66% to the biomass or other DON (Figs. 6.2 and 6.4a). Similarly, only a small amount of peptide (4-5%) in the 2013 incubation was hydrolyzed to amino acids and peptide fragments (Fig. 6.3), 38-54% decomposed to ammonium (Fig. 6.4b) and the rest (41-58%) being combined into biomass or transformed to other DON. This high efficiency of assimilation is consistent with a previous study in the Mississippi River plume (Liu et al., 2013). It was also intriguing to observe high concentrations of A

and VFA at the initial time point right after AVFA was amended, such as in the <0.8 μm and <5 μm treatments (Figs. 6.2 and 6.3). Preliminary results suggested that this initial rapid hydrolysis was caused by certain active extracellular enzymes that can immediately hydrolyze the amended peptide (Appendix I).

Peptide decomposition pathway can be derived from above mass balance calculation. Small peptides can be either hydrolyzed extracellularly with subsequent amino acid uptake or taken up as intact peptides by microorganisms directly. The minor release of amino acids and peptide fragments (1-5%) in all treatments indicates that a major fraction of AVFA was directly taken up by microorganisms. Alternatively, extracellular hydrolysis of AVFA and subsequent uptake of hydrolyzed products were coupled tightly. Direct uptake of peptide was through peptide transporters across the cell membranes, which are ubiquitous in both prokaryotes and eukaryotes including protists (Daniel et al., 2006; Saier, 2000). For example, different peptide transporter systems have been well-studied in bacteria such as *Escherichia coli* and *Salmonella typhimutium* (Payne and Gilvarg, 1971; Payne, 1980). Several genes involved in oligopeptide transport have also been discovered in protist *Micromonas* (McDonald et al., 2010). These peptide transporters may play an important role in determining the peptide decomposition pathway. Alternatively, protists may engulf the intact peptide through pinocytosis without production of amino acids or peptide fragments. For example, *Prorocentrum micans* and *Alexandrium catenella* can accumulate organic molecules in small vesicles within their cells (Klut et al., 1987, Legrand and Carlsson, 1998).

The role of different-sized microorganisms in peptide decomposition

Potential decomposers of peptides include free-living bacteria in the small-size (<5 μm) fractions, particle-attached bacteria, and protists in the large-size fractions (>5 μm). Bacteria are key decomposers of labile organic matter in marine environments (Azam et al., 1983, Kirchman, 2008). The proportion of *Gammaproteobacteria*, dominated by *Alteromonas*, increased to >70% during the AVFA incubation (Fig. 6.7). This pattern indicates that AVFA may have been metabolized mainly by *Alteromonas*, which is known to be important in organic matter utilization, such as phytodetritus degradation and nucleic acid uptake (Gihring et al., 2009, Mayali et al., 2012). Although bacterial community structure in the control samples without peptide amendment was not analyzed, similar peptide incubation experiments with controls showed that this dramatic bacterial community shift was caused by peptide amendment (Liu et al., 2013). Consistent with these results, significant shifts of bacterial community structure were observed after amendment of different labile organic substrates in aquatic environments (Eilers et al., 2000; Harvey et al., 2006; Murray et al., 2007; Teske et al., 2011; Liu et al., 2013).

Particle-attached bacteria in the large-size fractions may have contributed to faster peptide decomposition. Several studies have shown the importance of particle-attached bacteria in organic matter decomposition (Kirchman and Mitchell, 1982; Hoppe, 1991). However, similar bacteria abundances with or without sonication, together with the similar initial bacterial abundances among the <5 μm, <20 μm and unfiltered treatments in the 2011 incubation or among the <5 μm and unfiltered treatments in the 2013 incubations (Fig. 6.5), indicate that particle-attached bacteria only accounted for a small fraction of the total bacteria in the seawater. Free-living bacteria are predominant in total bacterial numbers with >90% in most oligotrophic and mesotrophic marine environments

(Unanue et al., 1992; Bidle and Fletcher, 1995). Consistently, based on the nutrient concentrations (Table 6.1), the seawater used in this study can be classified as oligotrophic to mesotrophic condition (Vollenweider et al., 1992). In addition, bacterial abundance in the large-size fraction was similar or even smaller than that in some small-size fractions during the entire incubation time (Fig. 6.5). This observation, together with the overall similar bacterial community structures among the four treatments (Fig. 5.6), suggests that the role of the particle-attached bacteria was limited in metabolizing the amended peptide.

Larger microorganisms such as the osmotrophic protists in the large-size fractions may help explain the differences in peptide decomposition rates among treatments. Higher abundances of heterotrophic protist, together with higher peptide decomposition rates, in the unfiltered seawater in both the 2011 and 2013 incubations indicate that the presence of protists can possibly enhance peptide decomposition. Peptide decomposition rates were similar between <20 μm and unfiltered seawater treatments in the December 2011 incubation, so the protists involved in the peptide decomposition were within the 5-20 μm size range. In June 2013, higher AVFA decomposition rate was only observed in the unfiltered seawater, indicating that the larger-sized protists (>20 μm) were involved in the peptide decomposition. Higher temperature in summer 2013 than winter 2011 (Table 6.1) may have caused faster growth and larger cell volume of protists (Auer and Arndt, 2001; Dupuy et al., 2007). Alternatively, specific types of protists that can utilize peptides may differ between winter and summer. In addition to heterotrophic protists, certain mixotrophic protists may have released hydrolytic enzymes or been involved in peptide uptake (Stoecker and Gustafson, 2003; Glibert and Legrand, 2006; Salerno and Stoecker, 2009). However, it is difficult to differentiate autotroph and mixotroph due to the limitation of the counting method (Fig. 6.9). It should be noted that the initial

decrease of protist abundance (Fig. 6.8) may be caused by bottle containment, grazing by large zooplankton or pathogenic bacterial infection on protists such as through releasing toxin (Görtz and Maier, 1991; Brüssow, 2007; Weber et al., 2012), but the abundance of heterotrophic protists nearly doubled from 46 to 65 h in 2011 and from 11 h to 48 h in 2013, as expected from their generation time of several days (Kisand and Zingel, 2000). Although the change of total protist abundance did not correlate exactly with peptide decomposition, perhaps only a small fraction of total protists was responsible for peptide decomposition. Further studies are needed to investigate specific types of protists utilizing peptides, such as using 18S rRNA sequencing analysis (Lin et al., 2012).

The osmotrophic nutrition strategy by protists may be favored in organic-enriched environments but with depleted inorganic nutrients (Carlsson and Graneli, 1998). For example, peptide hydrolysis in the 1.2-5-μm fraction that contains protists was at a comparable rate to that in the bacteria fraction in Quantuck Bay, where inorganic N was limited and organic N was abundant (Mulholland et al., 2002). The aminopeptidase activity decreased in *Prorocentrum minimum* cultures after addition of ammonium (Salerno and Stoecker, 2009). In this study, seawater was collected from the coastal area with relatively high concentration of organic matter but possibly depleted in nutrients (Table 6.1). The N:P ratio was less than the Redfield ratio 16 in both incubations, indicating possible nitrogen limitation. In comparison, the decomposition rates of AVFA did not differ among size-fractioned surface seawater in a similar peptide incubation experiment at a coastal station (C6) in the northern Gulf of Mexico with N:P above 16 (data not shown) in the surface water (Figs. 6.10 and 6.11). The N limitation in the ship channel seawater may have triggered the osmotrophic protists to decompose peptides that contain both carbon and nitrogen sources for nutrition at the early stage of the incubation. However, this nutrient limitation analysis based upon comparisons with Redfield ratio

has large uncertainty since this ratio varies with different species compositions and environmental conditions (Sterner et al., 2008), so more studies are needed to further explore the exact environmental mechanisms triggering the osmotrophic nutrition strategy of protists.

CONCLUSIONS

This study suggests that peptide decomposition by a combination of all different-sized organisms is more efficient than bacteria alone. In addition to free-living bacteria, microorganisms in the large-size fractions (5-20 μm or >20 μm), such as particle-attached bacteria and/or some osmotrophic protists, may be important in decomposing labile organic compounds directly and thus enhancing DOM degradation and nutrient cycles in the coastal environment. This bottom-up osmotrophic nutrition strategy of protists needs to be considered in biogeochemical C and N cycles, emphasizing the link between organic matter and protists in the classical microbial loop. However, more coastal systems and other types of DOM substrates need to be examined to further understand the link between DOM and different-sized microorganisms. Future studies are also needed to differentiate the role of particle-attached bacteria and protists in labile organic matter decomposition, and particularly the need to evaluate protists to metabolize peptides. This study suggests that among all bacteria utilizing peptides *Alteromonas* may play the dominant role in taking up small peptides in coastal waters. Taken together, using the small peptide without the fluorogenic tag as the substrate, this study extends from peptide hydrolysis to the whole decomposition process and provides insights into the relative role of different-sized microorganisms in regulating the recycling of labile organic matter in coastal waters.

Table 6.1. Chemical parameters of the ship channel surface seawater collected in Port Aransas, Texas on Dec 6th, 2011 and June 18th, 2013.

Time	Temp (ºC) [a]	Salinity (ppt)	pH	DO ($mg \cdot L^{-1}$)	NO_3^- ($\mu mol \cdot L^{-1}$)	NO_2^- ($\mu mol \cdot L^{-1}$)	PO_4^{3-} ($\mu mol \cdot L^{-1}$)	DOC ($\mu mol \cdot L^{-1}$)	TDN ($\mu mol \cdot L^{-1}$)	DCAA ($\mu mol \cdot L^{-1}$)	DFAA ($\mu mol \cdot L^{-1}$)
2011	21.5	37	8.19	7.03	0.80	ud[b]	0.28	nm[c]	nm	2.67	0.35
2013	26.0	35	7.95	nm	3.64	0.39	0.91	150	18	0.93	0.06

[a] Temp, temperature; DO, dissolved oxygen; DOC, dissolved organic carbon; TDN, total dissolved nitrogen; DCAA, dissolved combined amino acids; DFAA, dissolved free amino acids.

[b] Under detection limit ($NO_2^- < 0.03 \ \mu mol \cdot L^{-1}$).

[c] Not measured.

Figure 6.1. Tetrapeptide AVFA decomposition curves in (a) Dec 2011 and (b) June 2013 during 65-69 h incubation under dark with initial amended concentration of ca. 10 μM in four treatments including seawater filtered through 0.8 μm, 5 μm, 20 μm nylon filters, and unfiltered seawater. Data points are presented as average ± absolute error of duplicate samples.

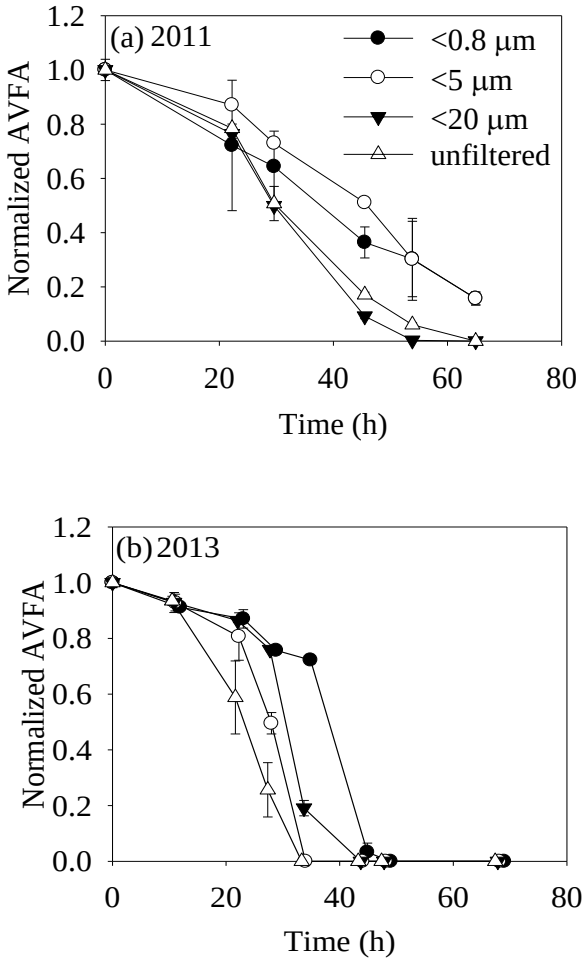

Figure 6.2. Concentration changes of amino acids (A, V, F) and hydrolyzed small peptides (VFA, FA) during 2011 AVFA incubation in seawater filtered through (a) 0.8 μm nylon filter, (b) 5 μm nylon filter and (c) 20 μm nylon filter, and (d) in unfiltered seawater. Data points are presented as average ± absolute error of duplicate samples.

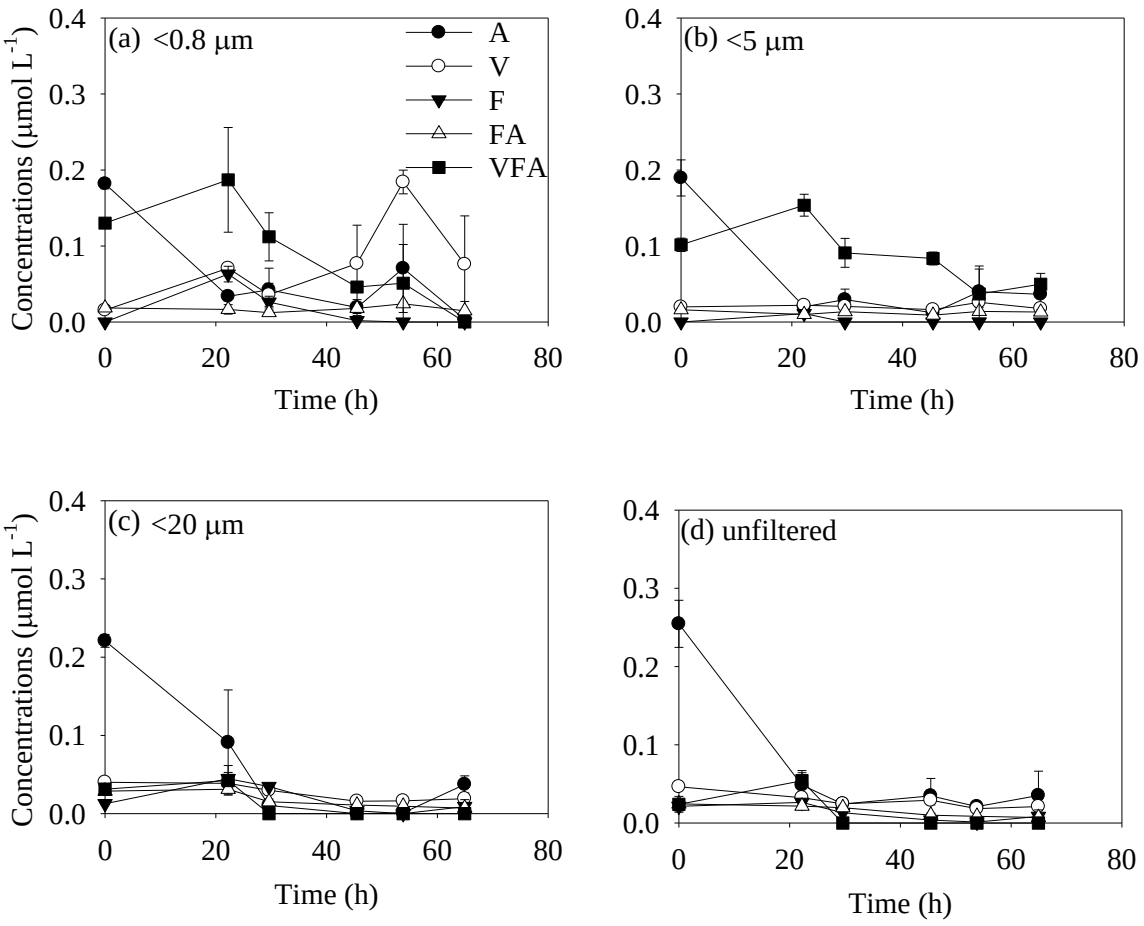

Figure 6.3. Concentration changes of amino acids (A, V, F) and hydrolyzed small peptides (VFA, FA) during 2013 AVFA incubation in seawater filtered through (a) 0.8 μm nylon filter, (b) 5 μm nylon filter and (c) 20 μm nylon filter, and (d) in unfiltered seawater. Data points are presented as average ± absolute error of duplicate samples.

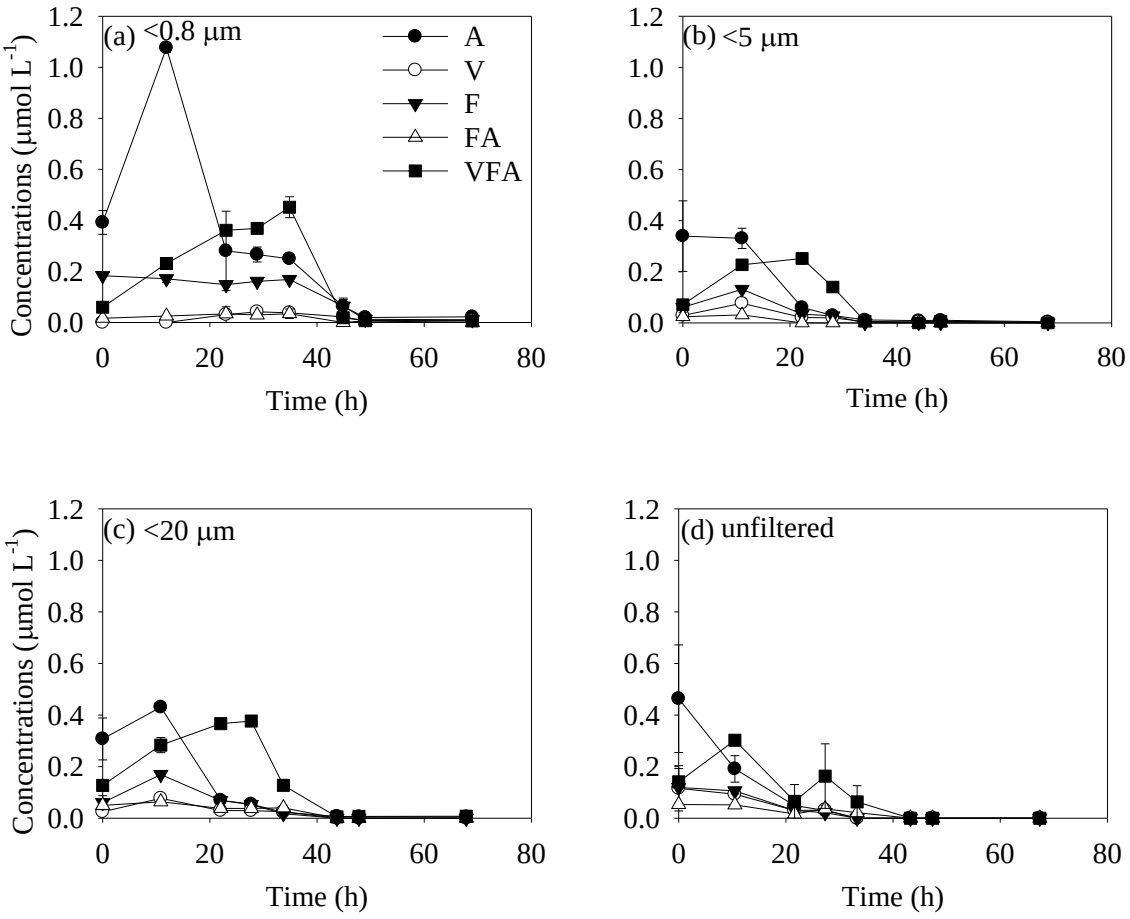

Figure 6.4. Ammonium concentration changes during (a) 2011 AVFA, (b) 2013 AVFA and control without AVFA incubation in four seawater treatments including seawater filtered through 0.8 μm, 5 μm, and 20 μm nylon filters, respectively, and unfiltered seawater. Data points for AVFA incubations are presented as average ± absolute error of duplicate samples.

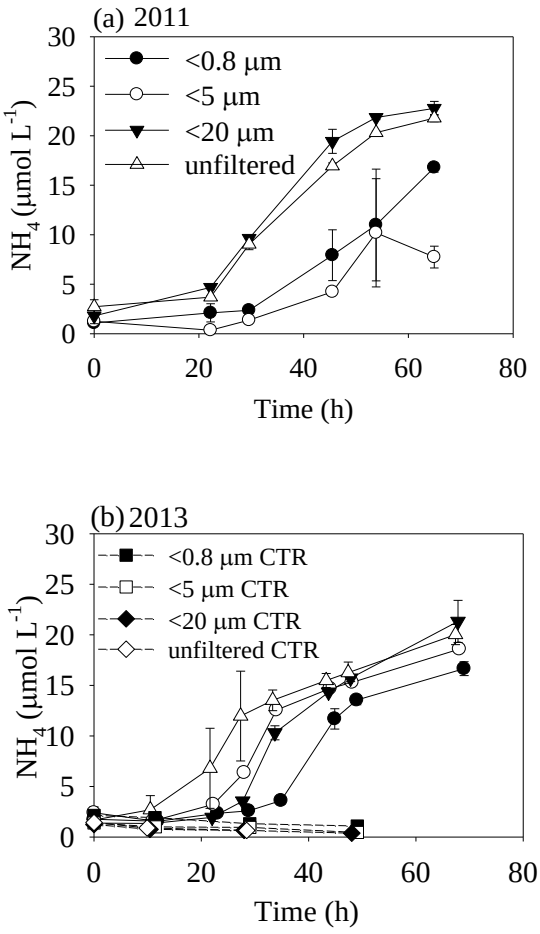

Figure 6.5. Changes of bacteria abundance during (a) 2011 AVFA, (b) 2013 AVFA and (c) 2013 control without AVFA incubation in four seawater treatments including seawater filtered through 0.8 μm, 5 μm, and 20 μm nylon filter and unfiltered seawater. Data points for AVFA incubations are presented as average ± absolute error of duplicate samples.

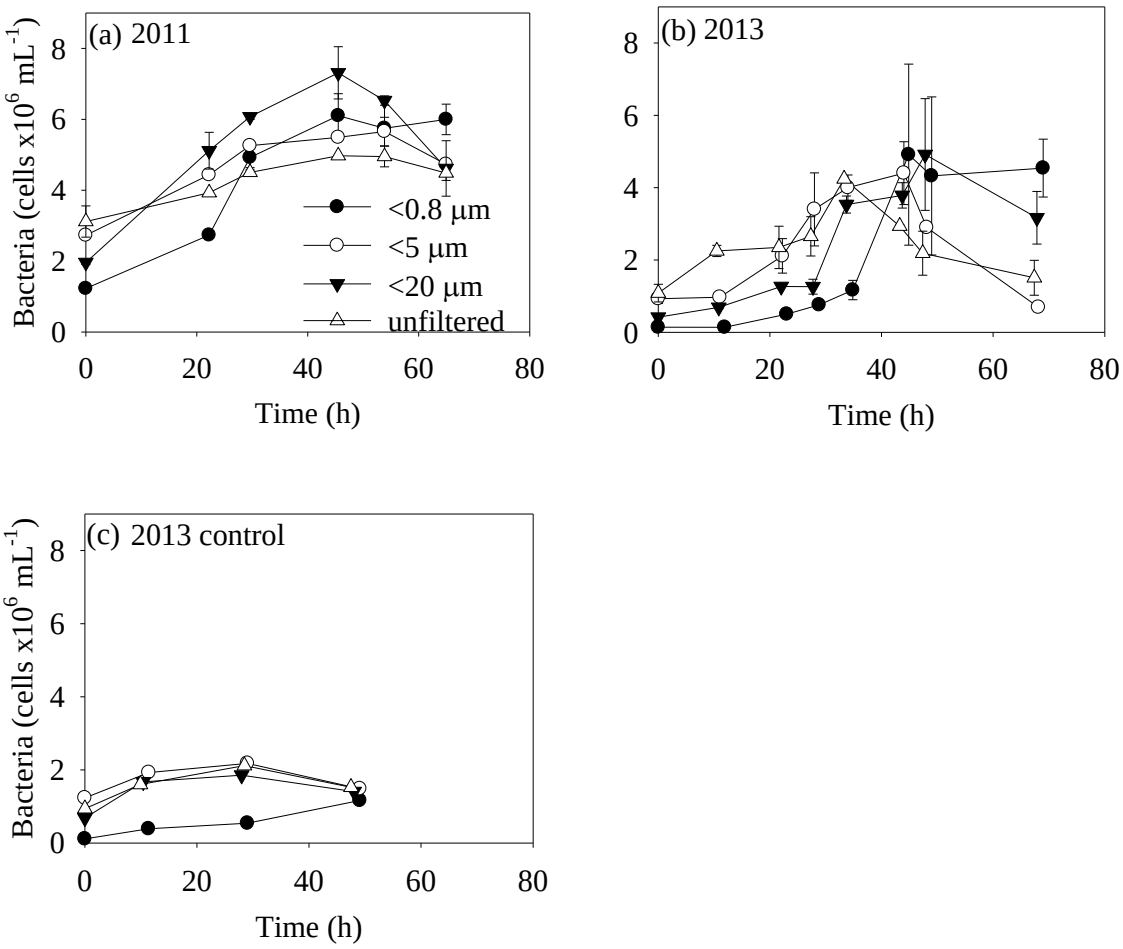

Figure 6.6. Changes of bacterial community structure (% class) during 2011 AVFA incubation at 0, 30, 46, and 65h in four seawater treatments including seawater filtered through (a) 0.8 µm nylon filter, (b) 5 µm nylon filter, (c) 20 µm nylon filter, and (d) unfiltered seawater. *Gamma, Gammaproteobacteria; Alpha, Alphaproteobacteria; Flavo, Flavobacteria; Actino, Actinobacteria; Sphingo, Sphingobacteria; Verruco, Verrucomicrobiae; Cyano, Cyanobacteria.* Others represent bacteria classes less than 1% in all treatments during incubation.

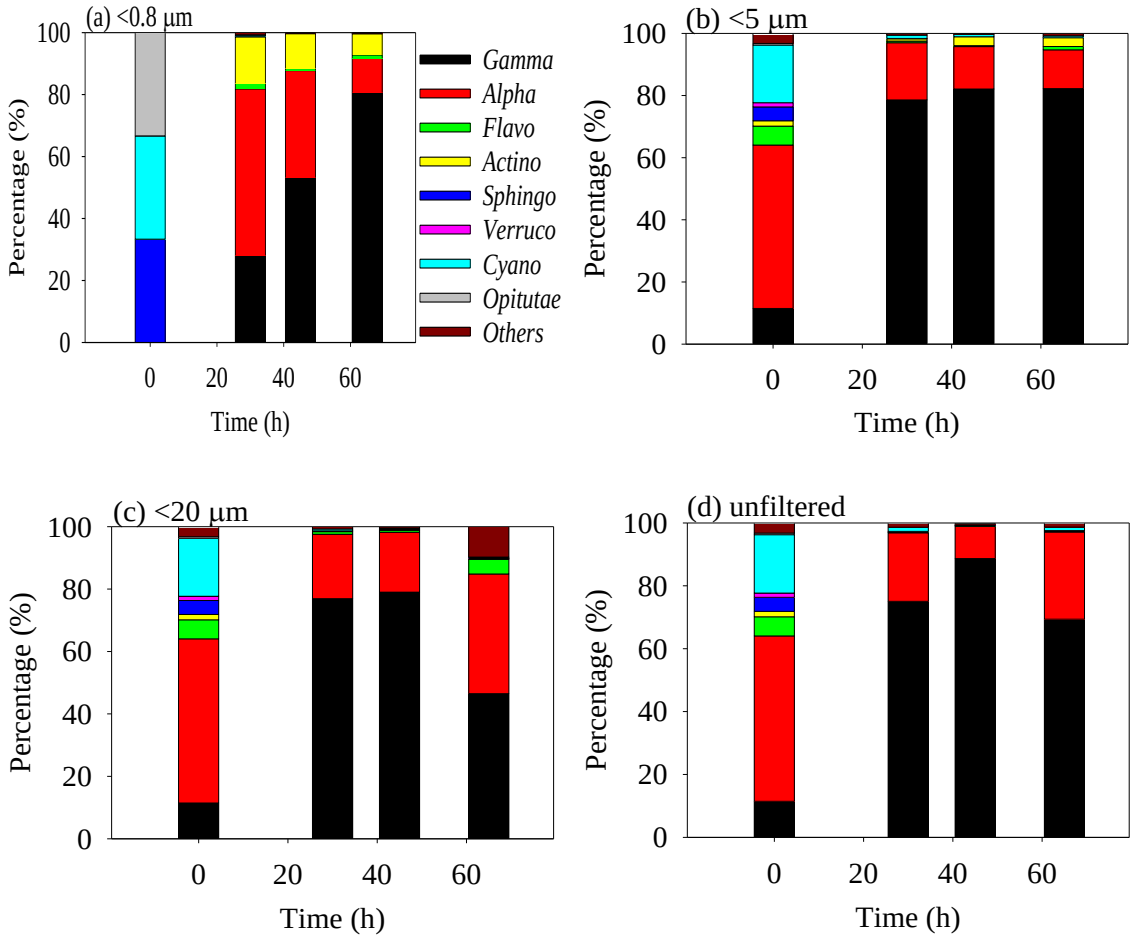

Figure 6.7. Principlal component analysis (PCA) on the compositions of major rapid-growth bacteria at genera level during 2011 AVFA incubation at 0, 30, 46, and 65 h in four seawater treatments including <0.8 μm, <5 μm, <20 μm and unfiltered (UNF) seawater. Bacterial genera names were in cross and sample names were in dot. PC1 explained 79% variance of the data matrix and PC2 12%. The incubation samples with similar bacterial composition were clustered together in the circle based on Bray-Curtis dissimilarity analysis.

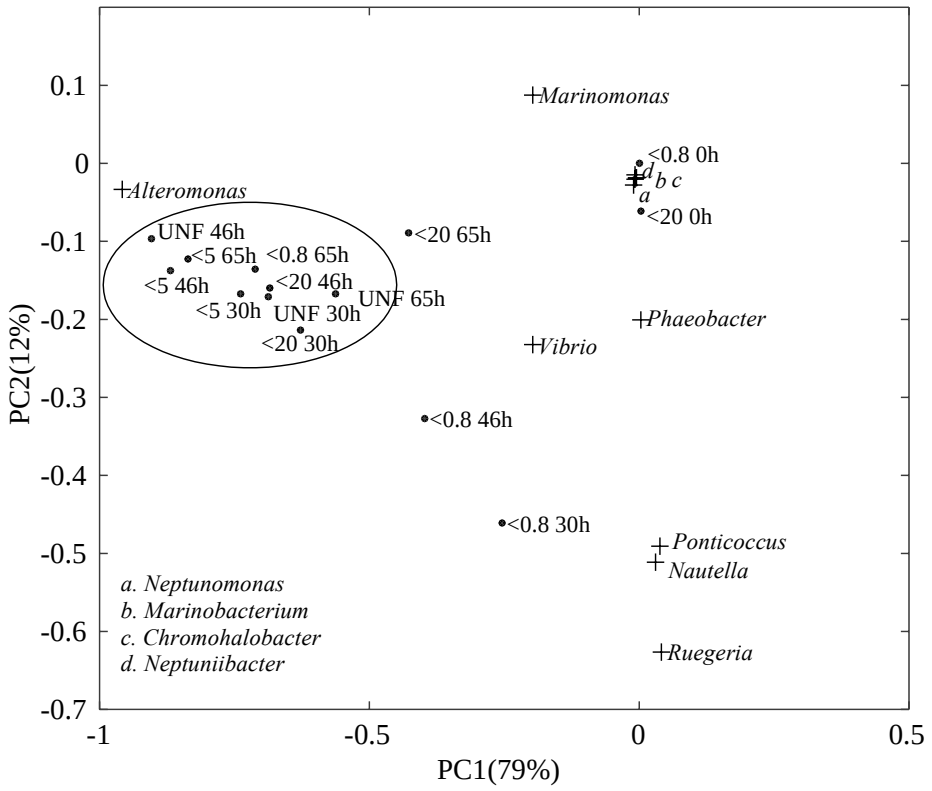

Figure 6.8. Changes of heterotrophic protists number with time during (a) 2011 AVFA incubation at 0, 22, 30, 46, and 65 h and (b) 2013 AVFA incubation at 0, 11, 22, 28, 34, 44, 48, 69 h in three seawater treatments including seawater filtered through 5 μm, 20 μm nylon filters, respectively, and unfiltered seawater.

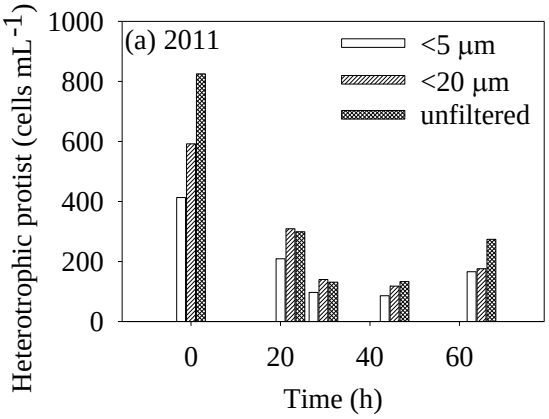

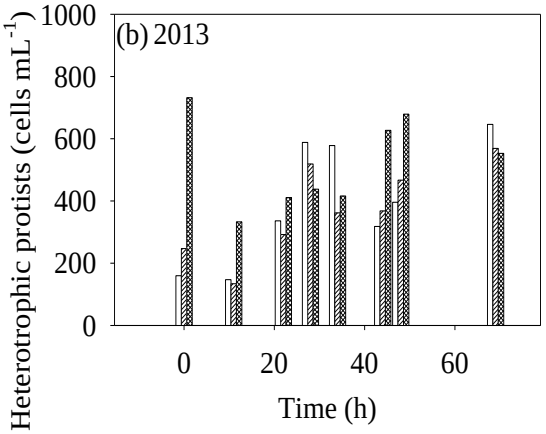

Figure 6.9. Changes of autotrophic and mixotrophic protists number with time during (a) 2011 AVFA incubation at 0, 30, 46, and 65 h and (b) 2013 AVFA incubation at 0, 11, 22, 28, 34, 44, 48, 69 h in three seawater treatments including seawater filtered through 5 μm, 20 μm nylon filter and unfiltered seawater.

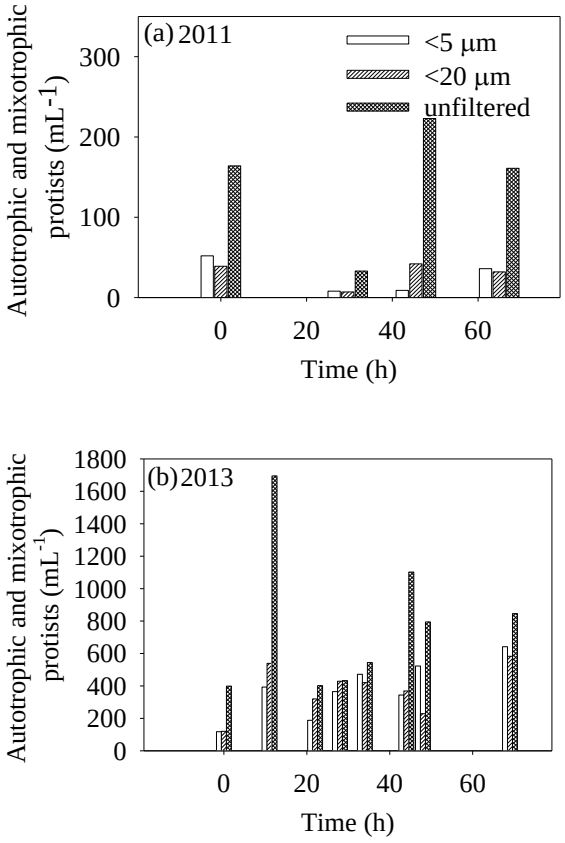

Figure 6.10. AVFA decomposition curve at C6 station of the northern Gulf of Mexico during 75 h incubation under dark with initial amended concentration of ca. 5 μM in four surface (1 m) seawater treatments including seawater filtered through 0.8 μm, 5 μm, 20 μm nylon filter and unfiltered seawater. Data points were presented as average ± standard deviation of replicate samples (n=4).

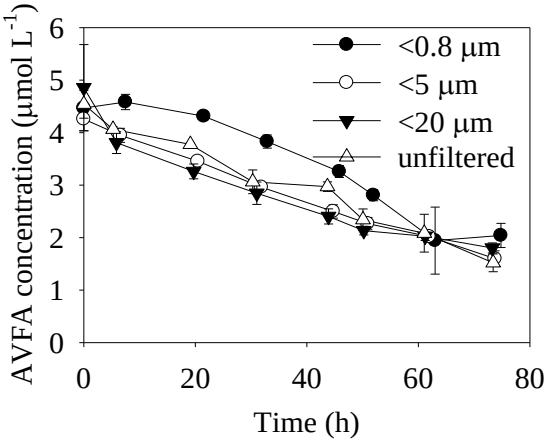

Figure 6.11. Changes of (a) heterotrophic and (b) autotrophic and mixotrophic protists number with time during AVFA incubation at C6 station of the northern Gulf of Mexico at 0, 6, 20, 31, 44, 51, 62, 74 h in three surface seawater treatments including seawater filtered through 5 μm, 20 μm nylon filter and unfiltered seawater.

(a)

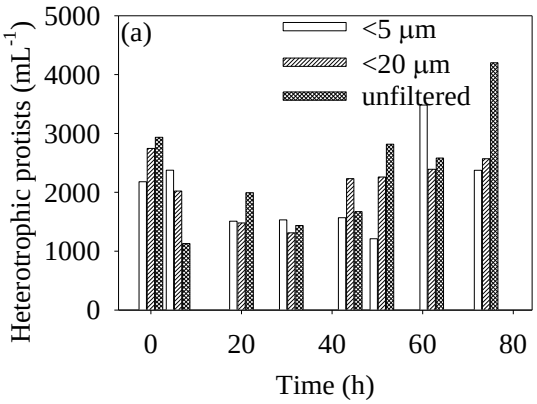

(b)

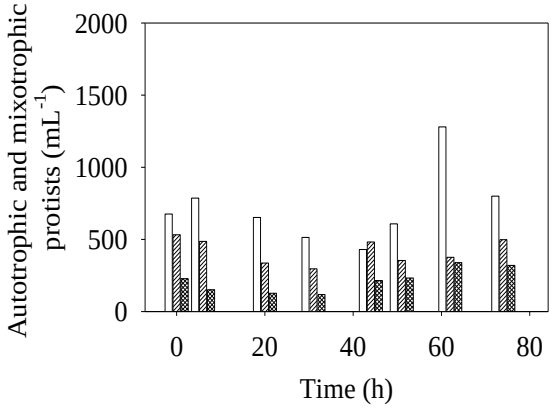

Chapter 7. Conclusions and implications

In this dissertation peptide hydrolysis and decomposition are examined in terms of their overall rates, pathways in different marine environments, and interactions with different microorganisms. This work ranges from bulk analysis of peptide degradation rates to detailed mechanisms, including enzyme functions and microbial linkages.

From the chemistry perspective, we showed that peptide hydrolysis pathways are affected by the fluorogenic tags in commonly used peptide analogs (Chapter 3). This indicates that previous peptide studies using peptide analogs should be interpreted with caution, and also highlights the need to expand our understanding of peptide decomposition using natural peptides. For natural peptides measurements, there is a need to develop more sensitive analytical methods for detecting ambient low-concentration plain peptides. When using these various modeled peptide substrates, we need to understand what we are actually measuring, which is important in interpreting the data and to make sure we do not extrapolate too far from the data. For example, we need to consider questions, such as What fraction of extracellular enzymes did we capture using peptide analogs? Can we say that we include the whole spectrum of peptidases using small plain peptides? Is there bias of certain peptide substrate on enzyme selection? How well can the results from one small peptide tell us about the hydrolysis pattern of other small peptides or big proteins in natural seawater? With these questions in mind, we then can get appropriate conclusions and know how to approach further in the future research.

We demonstrated that peptide hydrolysis and/or decomposition rates differed among environments such as along salinity gradients or across varying water depths (Chapter 3 and Chapter 5). These results provide information on spatial variation of enzymatic activities and are helpful to map geographic patterns of labile organic matter

decomposition that is one essential component in carbon and nitrogen cycles (Arnosti, 2010). The variation of hydrolysis and/or decomposition rates in different environments also suggests that certain environmental factors may control the enzyme activities and contribute to the pattern. Our results showed that high phosphate concentration might facilitate the rapid peptide decomposition in deep waters (Liu and Liu, 2016). More data across larger spatial gradients are needed to confirm the important role of phosphate in peptide decomposition at larger scale, assess more potential factors controlling the rate difference, and tease out the co-varying environmental parameters to identify the exact mechanisms determining spatial variation of peptide hydrolysis and/or decomposition.

Through mass balance calculation, we estimated the percentage of peptide decomposition attributed to hydrolysis, remineralization, incorporation into microbial biomass, and conversion to other DON (Chapter 5 and Chapter 6). This derived fate of peptide decomposition can help to elucidate the carbon and nitrogen flux in a quantitative way and be used to construct models in assessing this flux. For example, the large percentage converted to other DON during labile peptide decomposition indicates the important role of microbial activity in generating semi-labile or refractory DOM and offers insights into the natural DOM formation process in seawater. Previous studies mostly focus on fate of general DOM pool, such as phytoplankton exudate substrate or primary production (Larsson and Hagstrom, 1979; Azam et al., 1983). However, the complex DOM pool consists of different groups of compounds such as labile, semi-labile, and refractory DOM, fate of different components may vary greatly and contribute to C and N cycles at different time scale (Carlson, 2002). Assessing the fate of individual substrate such as peptides is necessary to understand detailed decomposition steps and provide a basis on building accurate global C and N cycle models.

In addition, our results demonstrated that the amino acid composition of a peptide affects its susceptibility to peptidases (Chapter 4). The results provide insight into the resistance of amino acids in the labile organic matter, such as proteins. Hydrolysis process may affect amino acid compositions and DON preservation in seawater. In particular, acidic amino acids resistance to aminopeptidases may have implications in the refractory DOM formation, as labile organic matter can be converted to refractory organic matter by bacteria (Hedges et al. 2000; Ogawa et al. 2001; Eglinton 2004). High molecular weight DOM in natural seawater is composed of mainly refractory acylpolysaccharides (ASP) and protein homologues because of the abundant carboxyl, akyl and amide functional groups from the NMR spectra of DOM (Aluwihare and Repeta, 1999; Zang et al., 2001; Hertkorn et al., 2006; Meador et al., 2007). The amide bond present in refractory organic matter implies that peptides may be the precursor for refractory organic matter formation, although it is still unknown whether the amide bond of refractory organic matter is from the original amide bond of proteins and peptides and/or newly formed after peptide bonds are totally metabolized (Hedges et al., 2000; Eglinton, 2004; Liu et al., 2009). A major refractory component of marine DOM is characterized as carboxyl-rich alicyclic molecules (CRAM). Whether the carboxyl group in acidic amino acids result to their resistance to enzymes and whether this is related to the formation of CRAM with low bioavailability require more investigation.

While amino acid composition selects different peptide hydrolysis pathways, it did not seem to affect overall peptide hydrolysis rates (Chapter 4). This result indicates that when one kind of peptidases fails to cleave a peptide, other kinds of peptidases can take over. Whether these different enzymes are constitutively present in the seawater or they are induced through time based on different peptide substrates is unclear yet. Enzyme expression and genomic information on microbes need to be studied further.

From the biology perspective, we linked the bacterial communities to peptide decomposition in normoxic and hypoxic coastal seawater in the northern Gulf of Mexico (Chapter 5) and highlighted the possible role of protists in peptide decomposition (Chapter 6). There are many implications for C and N cycles from these studies. First, linking microbial communities to their metabolic functions in biogeochemical processes in ecosystem has long been challenging in the field of microbial ecology. DNA-SIP technique provides us a means to link functions of microbial groups to their phylogenetic identities without isolating them in cultures. The DNA-SIP data can help evaluate capability of different microbial groups in labile organic matter decomposition and discover microbial taxa with previously unknown biogeochemical functions. Secondly, the microcosm study can provide clues to studying the potential specific microbial roles in labile organic matter (small peptide as a model here) decomposition, especially in some microenvironments in the ocean. Some microenvironments in natural seawater like marine snow are enriched with labile organic matter such as proteins. Marine snow that aggregate detritus, living organism and inorganic matter and transport much of the surface-derived matter to ocean floor are typically enriched with microbial communities and serve as "hot-spot" loci for microbial metabolic functions related to organic matter decomposition (Alldredge and Silver, 1988; Fenchel, 2002). With as many as four hundred per liter in surface seawater, marine snow supports two to five orders of magnitude higher bacterial production than the surrounding water and are associated with elevated level of hydrolytic enzyme activities (Alldredge and Silver, 1988). The identification of various microbes in peptide decomposition in microcosm studies may be extrapolated to labile organic matter decomposition processes in these microenvironments that are important for carbon and nitrogen cycle in the ocean. Thirdly, understanding specific microbes participating in peptide decomposition among different

seawater environments can further determine the redistribution of nutrient and bioavailable carbon substrates since hydrolysis and uptake are the initial steps in organic matter remineralization cascade. For example, related to oxygen consumption during organic matter remineralization, our study is important for evaluating the oxygen condition in marine habitats to some extent as fast decomposition of organic matter provides a positive feedback to hypoxia. Lastly, investigating specific microbial types that decompose peptides is the first step for further studies to explain possibly different patterns of peptide decomposition observed in various environments and to understand the mechanism of microbial utilization of labile DOM in a broader perspective.

The role of phosphate in shaping bacterial community and determine peptide decomposition rates in coastal seawater was discussed in the Chapter 5 (Liu and Liu, 2016). N:P ratios of suspended and sinking particles (mean value of 22.3) are generally higher than the Redfield ratio of 16:1 (Karl et al., 2001), so external P is needed meet the P demand by fast-growing bacteria with N: P of ~13 (Makino et al., 2003). Thus, this phosphate effect on bacterial growth and peptide decomposition may be applicable to overall organic matter in natural seawater. But more studies are needed to determine if these results can be applied to oligotrophic seawater, which have different microbial community and water chemistry than coastal seawater.

With different bacterial groups showing different efficiency of peptide decomposition, their capabilities of peptide decomposition may be related to different peptide decomposition pathways (Chapter 5). For instance, fast-growing bacteria may take up peptide directly through peptide transporter instead of extracellular hydrolysis (Appendix II). This indicates that different bacteria may utilize peptide through different metabolic pathways. Whether this is related to their genome variation or specific gene expression is still largely unexplored. Analysis of functional genes related to peptide

decomposition pathways is needed to gain insights into mechanisms of peptide decomposition at the molecular level.

Overall, this dissertation offers insights into labile organic matter cycling, microbial ecology, and nutrient regeneration in seawater, and also opens more questions about the factors controlling the hydrolysis and decomposition patterns of labile organic matter, microbial behavior and functions in biogeochemical processes. Some future directions or questions related to our study may include:

1. We need to further develop analytical methods that have lower detection limit for peptides in seawater, especially focusing on measuring ambient plain peptides and proteins. For example, combining our LC-MS method with DOM concentrating techniques like solid phase extraction (Curtis-Jackson et al., 2009) may help to identify ambient peptides.
2. More studies across different marine environments are necessary for determining the factors controlling variation of hydrolysis/decomposition rates and pathways of peptides. For instance, mapping peptide hydrolysis and/or decomposition rates and pathways geographically at different regional scale is needed to estimate enzyme activities and carbon and nitrogen flux in the large and connected ocean environment. Large amounts of data are required to tease out co-varying environmental factors controlling peptide decomposition through some statistical analysis like multiple linear regressions. During this mapping process, we also need to consider using the same peptide substrate at the same concentration, which is important to derive a comparable pattern from different environments. Our preliminary data suggests that added peptide concentration may affect bacterial community structure during peptide incubation. Whether there is a

substrate concentration effect on microbial community development and therefore peptide decomposition pattern needs more investigation.

3. Linkage between bacterial communities and peptide decomposition through SIP or other techniques should be expanded to more seawater environments, such as coastal vs. open ocean and different ocean basins, in order to establish a global picture of microbial interactions with labile organic matter. This is also important to understand factors controlling the varied patterns of microbial utilization of peptides. For example, significant environmental variations are present between the coastal and open ocean and bacteria with different nutrition strategies are related to environments. While opportunitrophic bacteria are expected to be more abundant in coastal seawater supplied with episodic large DOM flux, oligotrophic bacteria may be dominant in open ocean environments with low-concentration DOM and nutrients. Whether the biogeographic distribution of these bacteria is coupled with their peptide decomposition functions can be tested.
4. Although the role of protists is implied strongly in our study, direct evidence is lacking. Techniques to tease apart the protists and particle-attached bacteria in the large-size fractions are needed to explore the relative individual roles of these microbes in peptide decomposition. One way to directly show the role of protists in peptide decomposition may be through DNA-SIP and protist 18S rRNA gene analysis to determine protists active in peptide metabolization.
5. In addition to microbial community structure analysis, it is necessary to focus on more metabolic pathways or functional genes involved in peptide decomposition to address future research needs. This goal may be achieved through the fast-developing metagenomics and metatranscriptomics. Metabolites formed during microbial utilization of peptides in incubation experiments may provide some

clues on their metabolic functions and refractory DOM formations as well. Target biomarker metabolites can be established using LC-tandem MS to indicate microbial biogeochemical functions.

Appendix I The mystery of rapid hydrolysis: discovering instantaneous hydrolysis of small peptides in seawater incubations

Instantaneous hydrolysis at the initial time point was observed in the peptide incubation, especially in the Sta. SC seawater (Chapter 4). Noticeable hydrolysis products, accounting for 0.01-2.2 μmol L^{-1}, were present at 0 h that should presumably be zero or at background levels (Figs. 4.1-4.5). This observation was not due to the contamination since no peptide fragments were detected in the AVFA standard or in the ambient seawater. We designed a short-term (2 h) peptide incubation experiment in Sept. 2014 to decipher the enzymes responsible for this instantaneous hydrolysis. Sta. SC seawater was subject to different treatments, including unfiltered seawater, 0.2 μm-filtered seawater, seawater amended with $HgCl_2$ to inhibit bacterial activities, autoclaved seawater and autoclaved 0.2 μm-filtered seawater.

While AVFA was hydrolyzed little in all treatments during 2 h (Fig. A1.1a), hydrolysis products such as VFA, FA, AV and A were much less in the autoclaved and autoclaved 0.2 μm-filtered seawater than in the other three treatments at the initial time point (Figs. A1.1b, c, d, e). This pattern suggests that autoclaving deactivated or denatured the enzymes that could contribute to the rapid hydrolysis within a couple of minutes. The similar fragments patterns between the unfiltered and 0.2 μm-filtered seawater indicate that the enzymes responsible for the instantaneous hydrolysis were present as free-dissolved (<0.2 μm) extracellular forms. The produced fragments in the $HgCl_2$ amended treatment indicates that these extracellular enzymes possibly contain no sulfhydryl groups as $HgCl_2$ could not inhibit enzymes without these functional groups. Low concentration of FA in the $HgCl_2$ treatment might be due to its oxidization by $HgCl_2$ (Liu et al., 2006) (Fig. A1.1c), but more investigation is needed. In contrast to A, production of V and F was highest in the unfiltered seawater due to more cell-associated

enzymes present in that treatment, but similar among all the other treatments (Figs. A1.1f, g), indicating that the instantaneous hydrolysis mostly occurred at the end terminus of peptides by exopeptidases.

Figure A1.1. Concentration of (a) AVFA and its hydrolyzed products (b) VFA, (c) FA, (d) AV, (e) A, (f) V, and (g) F with time during the 2-h incubation in the unfiltered (UNF) seawater, 0.2 μm filtered seawater, seawater amended with $HgCl_2$, autoclaved seawater and autoclaved 0.2 μm filtered seawater from the Sta. SC in Port Aransas, TX in Sept. 2014.

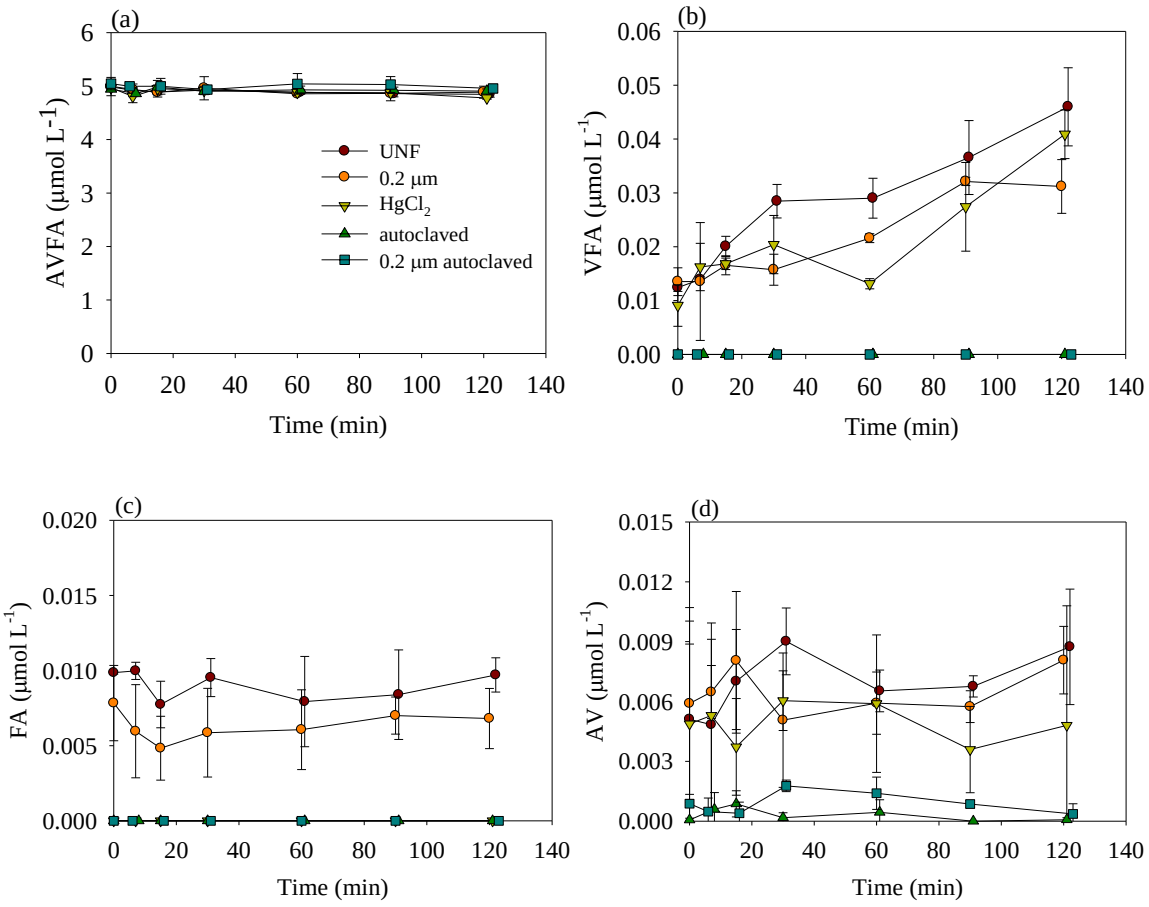

Figure A1.1 (continued)

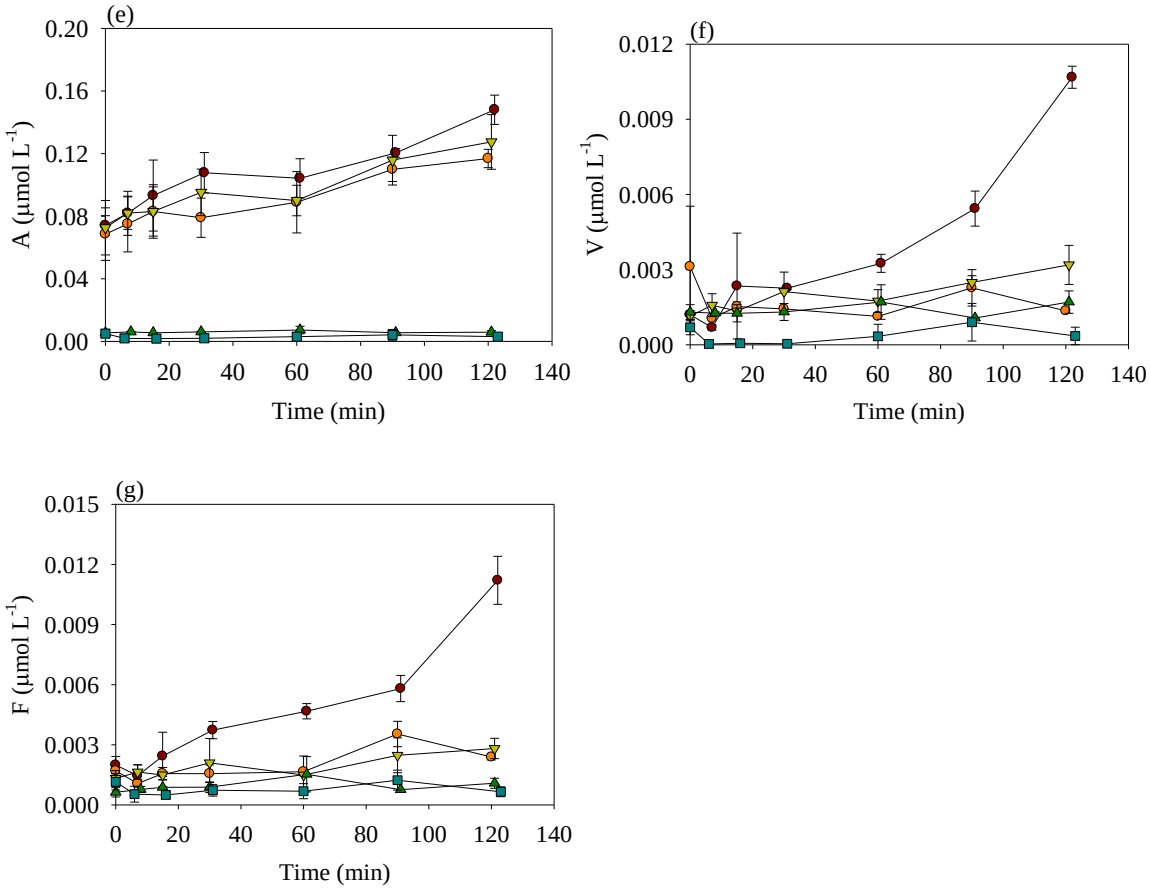

Appendix II PCR detection of oligopeptide transporter genes during peptide degradation in seawater

ABSTRACT

As peptides are commonly considered as effective in supplying multiple amino acids, direct peptide uptake with intracellular hydrolysis into amino acids, as opposed to extracellular hydrolysis of peptides into amino acids, may be more energy efficient to support bacterial growth. Oligopeptide transporters (oligopeptide permeases, Opp) play an important role in the uptake of tripeptides and larger peptides by bacteria, as demonstrated in studies using single bacterial species such as *E. coli*. However, whether this pathway holds in marine environments remains unclear. Here we developed a set of PCR primers to amplify Opp genes for several bacterial strains during peptide incubation in the bottom seawater in the northern Gulf of Mexico, and compared their relative abundances between the surface and bottom water incubations. We detected Opp genes of *Neptuniibacteria* and *Roseobacter* in the incubation samples. The amount of Opp genes in the bottom samples was at most five to 100 fold higher than that in the surface samples. This difference corresponded well with a higher percentage of certain bacteria, such as *Neptuniibacter* and *Roseobacter*, with incubation time in the bottom seawater than that in the surface seawater. This observation indicates that the existence of Opp genes might make these bacteria in the bottom seawater more competitive in peptide utilization than other bacteria and contribute to their rapid growth throughout the peptide incubation. Our study implies the dominance of peptide transporter genes, which are likely involved in the direct peptide uptake pathway during peptide decomposition, in the bottom seawater in northern Gulf of Mexico.

INTRODUCTION

Bacteria utilize peptides as a source of amino acids for building their biomass. There are two major pathways of this utilization in seawater. One is through extracellular hydrolysis of peptides into amino acids, either by enzymes dissolved in the water, attached to cell walls, or within the periplasmic space. The released amino acids are then taken up by bacteria via amino acid permeases. The other one is through transport of intact peptides directly by peptide permeases and further breakdown of peptides into amino acids by peptidases intracellularly (Sussman and Gilvarg, 1971; Chróst, 1991; Martinez and Azam, 1993; Arnosti, 2011). As peptides are commonly considered as more effective than mixture of amino acids in providing nutrition to bacteria and bacteria can sometimes grow more rapidly on peptides than free amino acids under similar concentrations (Law, 1978; Payne, 1980), the latter pathway can be more energy efficient.

Peptide transporters (peptide permeases) provide necessary nutrition to cells, and also are involved in signaling processes such as regulation of gene expression, sporulation, and chemotaxis to help bacteria better adjust to local environments (Detmers et al., 2001; Gardan et al., 2009). There are mainly three kinds of peptide transporters in bacteria: oligopeptide permease (Opp), dipeptide permease (Dpp) and tripeptide permease (Tpp). Two (Opp, Dpp) belong to the large ATP-binding cassette (ABC) transporter family and one (Tpp) belongs to the proton-dependent peptide transporter (PTR) family (Payne and Smith, 1994; Steiner et al., 1995; Daniel et al., 2006). While the Opp can transport peptides with five to six amino acids in *Salmonella typhimurium* and *Escherichia coli* or 6-18 amino acids in some Gram-positive bacteria, they have limited

capability of transporting some dipeptides. In contrast, the Dpp is complementary to the Opp and specifically transports dipeptides (Payne and Gilvarg, 1971; Jamieson and Higgins, 1984; Jenkinson et al., 1996; Lanfermeijer et al., 1999). The additional Tpp system has the ability to transport a large variety of tripeptides, especially with high affinity for peptides with hydrophobic amino acids, and it can also transport dipeptides although less effectively (Payne, 1983). With its wide range of accessibility to different-size peptide substrates and well-studied mechanism, the Opp transporter system is the focus of this study.

The Opp transporter system includes five subunits: an oligopeptide-binding protein (OppA) that is in the periplasmic space and captures substrates, two transmembrane proteins (OppB and OppC) forming the pore for peptide translocation, and two ATP-binding proteins (OppD and OppF) that link peptide translocation with energy through ATP hydrolysis (Payne and Smith, 1994). Previous studies have shown the important role of Opp transporter in peptide utilization. For instance, the OppA protein is larger than other periplasmic binding proteins with a molecular weight of 52,000 in *S. typhimurium* and also one of the most abundant periplasmic proteins in the Gram-negative bacteria *E. coli* and *S. typhimurium*, typically accounting for 5-8% of the total (Higgins and Hardie, 1983; Higgins et al., 1983; Guyer et al., 1985). OppD and OppF contain two regions of highly conserved sequences that form nucleotide-binding fold, providing strong evidence that peptide transport is energized by ATP hydrolysis (Walker et al., 1982; Higgins et al., 1985).

Peptide uptake through Opp transporter is well studied in single bacteria species, such as *E. coli*, *S. typhimurium*, *Pseudomonas aeruginosa*, and *Streptococcus faecalis* (Nisbet and Payne, 1982; Higgins and Hardie, 1983; Alves, 1984; Hulen and Legoffic, 1988). A few studies have investigated peptide transporter genes through metagenomics

and metatranscriptomics approach, and showed that widely distributed dipeptide and oligopeptide transporter sequences accounted for 11% of total dissolved organic carbon (DOC) transporter genes in coastal seawater (Poretsky et al., 2010). This indicates widespread of peptide transporters in marine environments.

In this study, we developed PCR primers to amplify Opp genes for certain rapidly-growing bacteria during the incubation of small oligopeptide alanine-valine-phenylalanine-alanine (AVFA), a fragment of ribulose-1,5-bisphosphate carboxylase/oxygenase (RuBisCO), in the surface (2 m) and bottom (17 m) seawater from one station in the northern Gulf of Mexico (nGOM). We detected Opp genes of *Neptuniibacteria* and *Roseobacter* in our samples, and the amount of Opp genes in the bottom samples was five to 100 fold higher than that in the surface samples. This difference corresponded well with faster peptide decomposition rate and an increasing percentage of certain bacteria, such as *Neptuniibacter* and *Roseobacter*, with incubation time in the bottom seawater than those in the surface seawater (Liu et al., 2013). This indicates that the existence of Opp genes might make these bacteria in the bottom seawater more competitive in peptide utilization than other bacteria and contribute to their rapid growth throughout the peptide incubation.

MATERIALS AND METHODS

Peptide incubation

The peptide AVFA was incubated in the dark for 76 h in the surface (2 m) and bottom (17 m) seawater collected from Sta. C6 (28° 51'N, 90° 22' W) in the nGOM onboard R/V *Pelican* during the May 2011 cruise. At each time point, a 12 mL aliquot was filtered through 0.2 μm Nylon filters (25 mm, Osmonics) and the filters were stored

at −20 °C for bacterial community analysis or Opp gene detection below. The detailed peptide incubation procedure was described in Liu et al. (2013).

Chemical and biological analysis

Peptide, amino acid, ammonium, bacterial abundance and bacterial community structure were analyzed in previous work as described in Liu et al. (2013) (Fig. A2.1). In brief, concentrations of AVFA and byproducts from its hydrolysis (VFA and FA) were measured by high performance liquid chromatography (HPLC, Shimadzu Prominence) equipped with a photodiode array detector. Amino acid concentrations were measured using HPLC with fluorescence detection after pre-column *o*-phthaldialdehyde (OPA) derivatization. Ammonium was analyzed in HPLC with post-column OPA derivatization. Bacteria were counted in an Accuri C6 flow cytometer after SYBR Green staining. Bacteria community structure was analyzed from DNA pyrosequencing of partial filter samples (three time points) sent to the Research and Testing Laboratory, Lubbock, TX. The rest of the filters (the other five time points) were preserved for the DNA extraction and Opp gene detection as described below.

Primer development

Primers for Opp genes were designed based on sequences obtained from the National Center for Biotechnology Information (NCBI) GenBank. Based upon the rapidly-growing bacterial genera in the bottom seawater incubation (Fig. A2.1f), which were most likely to have Opp genes as indicated previously (Liu et al., 2013), four genera (*Alteromonas*, *Roseobacter*, *Neptuniibacter*, *Vibrio*) were chosen to design primers because of the availability of Opp sequences in the NCBI GenBank. For each genus, one

to three major strains within that genus were found in the NCBI with their Opp protein sequences and corresponding protein coding DNA sequences (CDS) (Table A2.1). Different regions of Opp (OppA, OppBC and OppDF) were also selected for these strains for primer design if present in the NCBI GenBank. Using these CDS, primers were custom-designed through OligoPerfect™ Designer tool on the life technologies website (http://tools.lifetechnologies.com/content.cfm?pageid=9716&icid=fr-oligo-6) with optimal primer size set at 20 bp, annealing temperature (Tm) at 60 ºC, and G+C content at 50%. Primers designed for 200-300 bp DNA analysis sequences were selected for each strain and each Opp region (Table A2.1).

DNA extraction, PCR amplification and gel checking

DNA was extracted from filters that were not sent out for bacterial community structure analysis before (i.e., collected at time points of 10, 22, 33, 49, and 57 h during the incubation) using the MoBio PowerWater® DNA Isolation kit (MoBio Laboratories, Inc, Carlsbad, CA) following the manufacturer's protocol. Extracted DNA concentrations were quantified by a Nanodrop spectrophotometer (NanoVue Plus™, GE Healthcare).

Three sets of samples were amplified by PCR for different purposes: (1) to test working primers, extracted DNA of all available time points in the 17 m seawater incubation was mixed in equal-amounts and amplified by every designed primer for Opp genes; (2) to test the appropriate cycle number for PCR conditions before reaching the PCR plateau phase. DNA of the 17 m 57 h samples that had the moderate DNA concentrations among all samples (Table A2.2) was amplified by 25, 30, 35, and 40 PCR cycles using a 16S rRNA gene primer and one working Opp primer *Neptuniibacter caesariensis* OppDF, respectively; (3) after working primers for Opp genes in (1) (Table

A2.3) were determined, all extracted DNA samples from the 2 m and 17 m seawater incubations were amplified by two working primers, *Neptuniibacter caesariensis* OppDF and *Roseobacter sp.*1 OppDF.

Bacterial Opp genes were amplified by PCR using the primers designed here. For every 25 μL reaction, 5 μL DNA template (final concentration <250 ng), 0.6 μL Opp forward primer (20 $\mu mol \cdot L^{-1}$), 0.6 μL Opp reverse primer (20 $\mu mol \cdot L^{-1}$), 12.5 μL GoTaq® Green Master Mix, 2X (Promega, Madison, WI) that contains GoTaq® DNA polymerase, deoxynucleoside triphosphate (dNTP) (400 $\mu mol \cdot L^{-1}$ each), and 3 $mmol \cdot L^{-1}$ $MgCl_2$ in 2X Green GoTaq® reaction buffer (pH 8.5), and 6.3 μL nuclease-free water were mixed on ice. Negative controls were included with same components as above except for replacing the DNA template with the nuclease-free water. PCR amplification followed the program: a first denaturation step at 94ºC for 4 min, followed by 35 cycles of 30 s denaturation at 94ºC, 30 s annealing at 55ºC and 1 min elongation at 72ºC, and a final elongation at 72ºC for 10 min, in a thermal cycler (Eppendorf Mastercycler gradient). In addition, bacterial 16S rRNA genes of each sample were amplified by PCR to serve as positive controls. The 25 μL reaction mix for 16S rRNA gene amplification contains 1 μL DNA template, 1 μL 16S forward primer 27F 5'-AGAGTTTGATCMTGGCTCAG-3' (10 $\mu mol \cdot L^{-1}$), 1 μL 16S reverse primer 1492R 5'-CGGTTACCTTGTTACGACTT-3' (10 $\mu mol \cdot L^{-1}$), 12.5 μL GoTaq® Green Master Mix, 2X and 9.5 μL nuclease-free water. The PCR amplification for 16S rRNA genes followed the same program as described above.

PCR products were checked on the 1% agarose gel staining with ethidium bromide. Gels were visualized under UV and the band intensity was quantified by the peak area integrations using ImageJ.

Sanger Sequencing

A few PCR products were sent to the DNA Sequencing Facility in the Institute for Cellular and Molecular Biology in the University of Texas at Austin for Sanger sequencing. PCR products were purified by the Agencourt CleanSEQ system (Beckman Coulter) and then sequenced in a capillary-based AB 3730 DNA Analyzer. Chromatograms were processed through BioEdit v7.2.5 to assemble the forward and reverse sequences. Obtained DNA sequences were compared with the reference DNA and protein sequences from the NCBI using the blast and blastx tools.

RESULTS

Peptide decomposition and bacterial growth

As described in Liu et al. (2013), AVFA decomposition was faster in the 17 m seawater than in the 2 m seawater, with nearly one order of magnitude higher decomposition rate in the 17 m seawater than that in the 2 m seawater during 27-49 h (Fig. A2.1a). However, more than twice amounts of peptide fragments, VFA and FA, were released in the 2 m seawater than in the 17 m seawater during the entire incubation, accounting for 17% of decreased AVFA in the 2 m seawater at 76 h (Fig. A2.1b). Consistently, the production of amino acids was also higher in the 2 m seawater than in the 17 m seawater, reaching 1-2 orders of magnitude difference at certain time points (Fig. A2.1c). A major fraction of decomposed AVFA (42-60%) were released as ammonium in the 17 m seawater, almost twice as high as that in the 2 m seawater (Fig. A2.1d). Production of peptide fragments and amino acids was less in the 17 m seawater incubation than in the 2 m seawater, suggesting direct uptake of intact peptide by bacteria

as the peptide decomposition pathway in the 17 m seawater in contrast to the extracellular hydrolysis pathway in the 2 m seawater (more discussion in Liu et al. (2013)). The direct uptake could involve Opp genes in the 17 m seawater.

Decomposed AVFA supported a six-fold increase in bacterial abundance within 22 h in the 2 m seawater incubation, but no consistent pattern was seen in the 17 m seawater incubation (Fig. A2.1e). However, certain bacteria types grew rapidly in the 17 m seawater incubation, outcompeting other bacteria in the 2 m seawater incubation (Fig. A2.1f). These bacteria genera included *Neptuniibacter*, *Roseobacter*, *Marinobacterium*, *Vibrio*, *Amphritea*, *Thalassomonas*, *Pseudoalteromonas*, and *Ruegeria*, which increased from 0-2% of the overall bacterial community at 2 h to 4-22% at 27 h or 41 h and were potential candidates for possessing Opp genes and playing a role in peptide transport process.

Design of PCR primers for Opp genes

Based on the rapidly-growing bacteria genera in the 17 m seawater incubation, 2-5 protein sequences and their corresponding CDS for each bacteria genus were selected for designing primers based on the availability of these sequences in NCBI (Table A2.1). Since these sequences might come from different regions in the Opp genes and complete Opp gene sequence for every bacteria strain is not available, no conserved regions were found for Opp genes among these bacteria using the ClustalW program. Thus, primers were designed for individual bacteria strain and Opp protein fragments respectively. For *Neptuniibacter*, two protein fragments, peptide-binding protein OppA and ATP-binding protein OppDF, from the species strain *Neptuniibacter caesariensis* MED92 (EAR60493.1) were chosen; for *Roseobacter*, OppA from two *Roseobacter sp.* strains

GAI101 (EEB83649.1) and CCS2 (EBA10778.1), and OppDF from *Roseobacter sp.* GAI101 (EEB83452.1) and MED193 (EAQ46635.1) were chosen; for *Vibrio*, OppA from *Vibrio sp.* AND4 (EDP60307.1) and OppDF from *Vibrio sp.* EJY3 (AEX20542.1) were chosen; for *Alteromonas*, membrane protein (OppBC, AEF04126.1) and three OppDF fragments (AEF04129.1, AEF02084.1, YP_004469387.1) from *Alteromonas sp.* SN2 were chosen.

PCR amplification of Opp genes in peptide incubation samples

Concentrations of extracted DNA from incubation samples ranged from 2.3 to 48.0 ng μL^{-1} (Table A2.2). Out of all twelve primers tested on the mixture of 17 m time-points incubation samples, three yielded positive amplification results with PCR products of the expected size (Table A2.3). These three primers were for OppDF of *Roseobacter sp.* GAI101, OppA of *Neptuniibacter caesariensis* MED92 and OppDF of *Neptuniibacter caesariensis* MED92. In addition to the PCR products of expected size for the Opp genes, some other weaker PCR products of unexpected size were observed in the amplification with the primer for OppDF of *Roseobacter sp.* GAI101. However, this did not affect our study since we focused on detecting Opp genes rather than accurate quantification.

The PCR cycle number test showed that for the *Neptuniibacter* OppDF gene, PCR products were not detectable within 30 cycles, whereas the quantity of PCR amplification products with expected 241 bp size increased exponentially from 30 to 40 cycles without reaching plateau (Fig. A2.2). For the positive control with 16S primers, the amplification of PCR products with 1465 bp size exponentially increased with cycle number from 25 to 40 cycles and did not reach a plateau. Thus, moderate number of 35 cycles was chosen for the PCR amplification.

Using two working OppDF primers for two different bacteria genera, *Neptuniibacter* and *Roseobacter*, PCR products with expected Opp gene size were shown for both 2 m and 17 m incubation samples (Figs. A2.3a and A2.3b). PCR amplifications of negative controls without DNA template showed no products of expected size (data not shown), indicating Opp gene amplification with the sample DNA. At a few time-point samples, other weaker PCR products with larger unexpected and nonspecific size were shown, such as in the *Neptuniibacter* OppDF gene amplification of the 17 m 10 h, 22 h, and 57 h samples (Fig. A2.3a). However, this result did not affect our further qualitative analysis as stated above. To eliminate the DNA concentration difference among extracted samples (Table A2.2), PCR amplification of all incubation samples using 16S primers were also conducted and peak areas of PCR products were integrated. These positive controls showed that amplifications of all samples with 16S primers were successful (data not shown).

Comparing Opp genes (corrected for differences in 16S amplification among the samples) between the 2 m and 17 m incubation samples, the abundance of Opp genes for both *Neptuniibacteria* and *Roseobacter* in the 17 m seawater were more than in the 2 m seawater during incubation (Figs A2.3c and A2.3d), especially with two orders of magnitude difference for *Neptuniibacter* and five times difference for *Roseobacter* at 33 h when peptide was decomposed rapidly in the 17 m seawater (Fig. A2.1a). With incubation time, amounts of Opp genes for both *Neptuniibacter* and *Roseobacter* first increased from 10 h to 33-49 h and then decreased afterwards in the 2 m and 17 m seawater. The Opp gene trends corresponded well with changes in bacterial communities, such as the percentage increase of *Neptuniibacter* and *Roseobacter* at 41h in the 2 m seawater and their even larger increase at 27 h and 41 h in the 17 m seawater (Fig. A2.1f).

To assess whether the increase of Opp gene amount was only due to the increase of all bacteria with time (Fig. A2.1e), Opp gene integrated peak area was normalized to bacterial abundance through time (Figs. A2.3e and A2.3f). Normalized Opp gene amount of *Neptuniibacter* and *Roseobacter* in the 17 m seawater was five to 100 fold higher than that in the 2 m seawater, indicating the increase of Opp gene amounts was closely related to the change of certain bacteria types, such as *Neptuniibacter* and *Roseobacter*, rather than all bacteria.

Similarity of assembled sequences with NCBI reference sequences

To test the specificity of amplified PCR products, selected samples were sequenced by Sanger sequencing. Assembled OppA or OppDF gene sequences of *Neptuniibacter* in incubation samples showed great similarities (92-97%) to the reference DNA and protein sequences from NCBI using the blast and blastx tools (Table A2.4). However, assembled DNA sequences of OppDF genes of *Roseobacter* were not significantly similar to their NCBI reference DNA sequences, and only 34-62% similar to their reference protein sequences, probably due to the interference from other non-specific PCR products.

DISCUSSION

Based on the previous chemical analysis, only 0.1-13% of AVFA was hydrolyzed to peptide fragments and amino acids in the 17 m seawater while 28-100% of decomposed AVFA was converted to peptide fragments and amino acids in the 2 m seawater throughout the incubation time (Figs. A2.1a, A2.1b, and A2.1c). This pattern suggested that peptide decomposition pathway of direct peptide uptake was more

dominant in the 17 m than in the 2 m seawater. From this study, we further showed the potential and importance of direct peptide uptake pathway in the 17 m seawater through the Opp gene detection. If equally distributed among each bacteria type, Opp genes would be expected to change little with time in the 17 m seawater as bacterial abundance only changed slightly in throughout incubation (Fig. A2.1e). Meanwhile, more Opp genes would also be expected in the 2 m than in the 17 m seawater before 33 h and not much difference between these two waters afterwards. However, more Opp genes were present in the 17 m than in the 2 m incubation and the increase of Opp genes with incubation time before 41 h corresponded well with the pattern of rapid growth of certain bacteria types, such as *Neptuniibacter* and *Roseobacter*, in the 17 m incubation (Figs. A2.3 and A2.1f). This result indicates that more Opp genes were associated with these rapidly-growing bacteria, and that the existence of Opp genes might contribute to their rapid growth of these bacteria throughout the peptide incubation and fast peptide decomposition rate in the bottom seawater.

Consistent with our result, previous studies found oligopeptide transport capability can differ among bacteria. Peptide uptake rates varied several orders of magnitude among different strains of *Lactococcus lactis* and *E. coli*, and their relative growth rate also differed from 0% to 100% (Payne and Bell, 1979; Charbonnel et al., 2003). Opp gene numbers can differ among different bacteria as well. While the Opp system of most *L. lactis* strains contain only one OppA gene, *Streptococcus thermophiles* possess three homologous genes encoding oligopeptide-binding proteins that may help to broaden substrate specificity and enhance peptide transport efficiency (Garault et al., 2002; Lamarque et al., 2004). Oligopeptides with different amino acid compositions tend to compete with each other for the transport in *E. coli*, indicating of only one Opp transport system with low substrate specificity present in *E. coli* (Payne 1968; Payne,

1971; Sussman and Gilvarg, 1971). However, another oligopeptide transporter system other than Opp was discovered in *L. lactis* and *Bacillus subtilis* (Lamarque et al., 2004; Wright et al., 2004), which may be associated with dual functions, including both peptide uptake and environmental sensing (Lamarque et al., 2011). All these pieces of evidence indicate that some bacteria may be better or more potent at peptide transport and contribute more to labile organic matter decomposition than others.

As peptide transport systems are independent of amino acid transport system (Payne and Gilvarg, 1971), direct peptide uptake via peptide transporter can be more efficient for peptide utilization than extracellular hydrolysis into amino acids with subsequent uptake of amino acids. On one hand, extracellular hydrolysis is often the rate-limiting step in organic matter remineralization (Hoppe, 1991; Davey et al., 2001; Arnosti, 2011), which slows down the overall bacterial growth on organic matter substrates. On the other hand, peptides can be superior to mixtures of amino acids for bacterial growth when many types of amino acids are needed. There is also competition among the uptake or catabolism of required amino acids by enzymes targeting them (Payne, 1980). For example, a strain of *Streptococci* grows more efficiently on peptide containing arginine than free arginine due to the protection of peptide-bound arginine from degradation by arginine dihydrolase (Gale, 1945). The efficiency of peptide utilization through Opp system is reflected in our results as higher Opp gene abundance and faster peptide decomposition were present in the bottom water than in the surface water.

Regulation of Opp may be complicated, as previous studies led to different conclusions. At the transcription level, transcription of the Opp gene in *S. typhimurium* was unaffected by the changes of carbon and nitrogen sources, such as peptides and amino acids (Jamieson and Higgins, 1984). In coastal seawater, transcripts of transporter

genes can also constitutively express regardless of substrates, leading to mismatch between transporter expression and substrate flux (Poretsky et al., 2010). However, Opp gene transcription in *E. coli* increased with the presence of leucine and alanine in the medium (Andrews and Short, 1986). At the protein level, oligopeptide transport in *E.coli* appeared to be constitutive and expressed at high levels based on the observation that various nutrient limitations did not affect bacterial uptake mediated by Opp (Higgins and Hardie, 1983; Payne and Smith, 1994). But whether this holds true in other bacteria needs more investigation. More transcription studies about Opp gene expression and activity are needed to provide more information about how the Opp system functions in environmental incubation samples when combined with our current study of detecting Opp gene existence.

This study broadens our understanding of the Opp gene in the complex environmental incubation samples from previous studies with single bacteria strains and revealed differences in Opp gene abundance among different bacteria types among bacterial communities in the seawater. Using low-cost and quick PCR amplification with customized PCR primers, we detected Opp genes of certain bacterial types, such as *Neptuniibacter* and *Roseobacter*, in the peptide incubation samples. This simple method may be applied to other environmental samples to obtain a quick look at the Opp gene existence. With further optimization of this PCR method, such as finding universal primers for Opp genes from different bacteria when more Opp gene sequences are available and eliminating non-specific amplifications for quantitative analysis, we can expand our knowledge of Opp gene more in marine environments. In addition, the combination of detecting the Opp genes with measuring the Opp gene transcription using mRNA or protein expression using metaproteomics are also needed in future studies.

Table A2.1. Sequences and protein coding DNA sequence (CDS) positions of designed primers for the amplification of oligopeptide transporter (Opp) genes from different bacteria species.

Primer name[a]	Species strain	NCBI protein accession No.	CDS position	Sequence (5'-3')
Alteromonas sp. OppBC F	SN2	AEF04126.1	220-239	CTACAAGGCGATTGGGGTTA
Alteromonas sp. OppBC R	SN2	AEF04126.1	477-496	ACAAAGGCGCAATATCAAGG
Alteromonas sp. OppDF1 F	SN2	AEF04129.1	232-251	TTGGCGAAATACAACCAACA
Alteromonas sp. OppDF1 R	SN2	AEF04129.1	459-478	GTTGGCCATCAGACAGCATA
Alteromonas sp. OppDF2 F	SN2	AEF02084.1	180-199	CAGTGCAAGTGAAGGGGAAT
Alteromonas sp. OppDF2 R	SN2	AEF02084.1	439-458	TGTTGCTGACCACCTGAAAG
Alteromonas sp. OppDF3 F	SN2	YP_004469387.1	485-504	GAAAATGGCTTGCCCAGTAA
Alteromonas sp. OppDF3 R	SN2	YP_004469387.1	669-688	TGCTATTGCGCTTAATGACG
*Roseobacter sp.*1 OppA F	GAI101	EEB83649.1	289-308	CAGAATGAAAACCCGCTGTT
*Roseobacter sp.*1 OppA R	GAI101	EEB83649.1	471-490	CAGAATGAAAACCCGCTGTT
*Roseobacter sp.*2 OppA F	CCS2	EBA10778.1	394-413	CTGTTTCCACATCTGGCTGA
*Roseobacter sp.*2 OppA R	CCS2	EBA10778.1	639-658	CGTCGACCGTGATGTTATTG
*Roseobacter sp.*1 OppDF F	GAI101	EEB83452.1	338-357	ACAGTGGCCTGTACCGAAAC
*Roseobacter sp.*1 OppDF R	GAI101	EEB83452.1	618-637	CATGCAGATGGTGTTCCAAG
*Roseobacter sp.*3 OppDF F	MED193	EAQ46635.1	1409-1428	GCAGCGATGTCAGTGTGACT
*Roseobacter sp.*3 OppDF R	MED193	EAQ46635.1	1671-1690	ACAGTTCACCCGGTGCTATC
Neptuniibacter caesariensis OppA F	MED92	EAR60496.1	691-710	GGCTTCAGTGGGTAGCTCTG
Neptuniibacter caesariensis OppA R	MED92	EAR60496.1	966-985	TGACTTTCGCCAGGAGAACT
Neptuniibacter caesariensis OppDF F	MED92	EAR60493.1	1013-1032	ATCTGCTCCTGGATGGTCAC
Neptuniibacter caesariensis OppDF R	MED92	EAR60493.1	1234-1253	TTGGTGAAACGCTACTGCTG
*Vibrio sp.*1 OppA F	AND4	EDP60307.1	868-887	ACACCCGCAAATAACGTCTC
*Vibrio sp.*1 OppA R	AND4	EDP60307.1	1080-1099	GCATAAGCGCAAGTGCATAA
*Vibrio sp.*2 OppDF F	EJY3	AEX20542.1	663-682	TGACCGTGTGGCAGTTATGT
*Vibrio sp.*2 OppDF F	EJY3	AEX20542.1	892-911	TCCAACAACGGACCAGTGTA

Table A2.1 (continued)

a, Primer name includes the bacteria name (different strains of the same species are indicated by different numbers), oligopeptide transporter protein (OppA for peptide-binding protein, OppBC for membrane protein and OppDF for ATP-binding protein, different fragments of the same protein are indicated by different numbers), and primer strand (F for forward primer and R for reverse primer).

Table A2.2. Extracted DNA concentrations of the AVFA incubation samples.

Sample name	DNA concentration (ng μL^{-1})	Sample name	DNA concentration (ng μL^{-1})
2m 10h	11.9	17m 10h	2.3
2m 22h	29.0	17m 22h	48.0
2m 33h	41.0	17m 33h	2.8
2m 49h	13.8	17m 49h	2.8
2m 57h	8.5	17m 57h	7.1

Table A2.3. PCR amplification results of designed Opp primer test on the AVFA 17 m incubation samples (all time points mixture).

Target[a]	PCR products[b]
Alteromonas sp. OppBC	-
Alteromonas sp. OppDF1	-
Alteromonas sp. OppDF2	-[c]
Alteromonas sp. OppDF3	-
*Roseobacter sp.*1 OppA	-
*Roseobacter sp.*2 OppA	-
*Roseobacter sp.*1 OppDF	+[d]
*Roseobacter sp.*3 OppDF	-
Neptuniibacter caesariensis OppA	+
Neptuniibacter caesariensis OppDF	+
*Vibrio sp.*1 OppA	-
*Vibrio sp.*2 OppDF	-

a, same as names from Table 1.
b, + as PCR products of expected size and – as no PCR products of expected size.
c, no PCR products of expected size; only PCR products of unexpected and nonspecific size.
d, PCR products of expected size along with other weaker PCR products of unexpected and nonspecific size.

Table A2.4. Comparison of Opp DNA and amino acid sequences similarities between selected sample genes and reference genes from NCBI.

Sample	Primer[a]	DNA Similarity (%)	Amino acid similarity (%)
2m 33h+49h[b]	*Roseobacter sp.*1 OppDF	NS	34
17m 33h	*Roseobacter sp.*1 OppDF	NS	62
17m 33h+49h[b]	*Roseobacter sp.*1 OppDF	NS	44
17m 49h	*Neptuniibacter caesariensis* OppA	94	95
2m 22h	*Neptuniibacter caesariensis* OppDF	95	97
2m 49h	*Neptuniibacter caesariensis* OppDF	96	96
17m 33h	*Neptuniibacter caesariensis* OppDF	95	92
17m 49h	*Neptuniibacter caesariensis* OppDF	96	94

a, same as names from Table 1.
b, two samples were combined for sequencing.
NS, no significant similarity.

Figure A2.1. (a) AVFA decomposition, (b) peptide fragments produced from AVFA decomposition, (c) amino acids production from AVFA decomposition, (d) ammonium production from AVFA decomposition, (e) bacterial abundance changes and (f) percentage of 17 m rapid-growing bacterial genera in the C6 station 2 m and 17 m seawater. All the data in this figure was replotted from Liu et al. (2013).

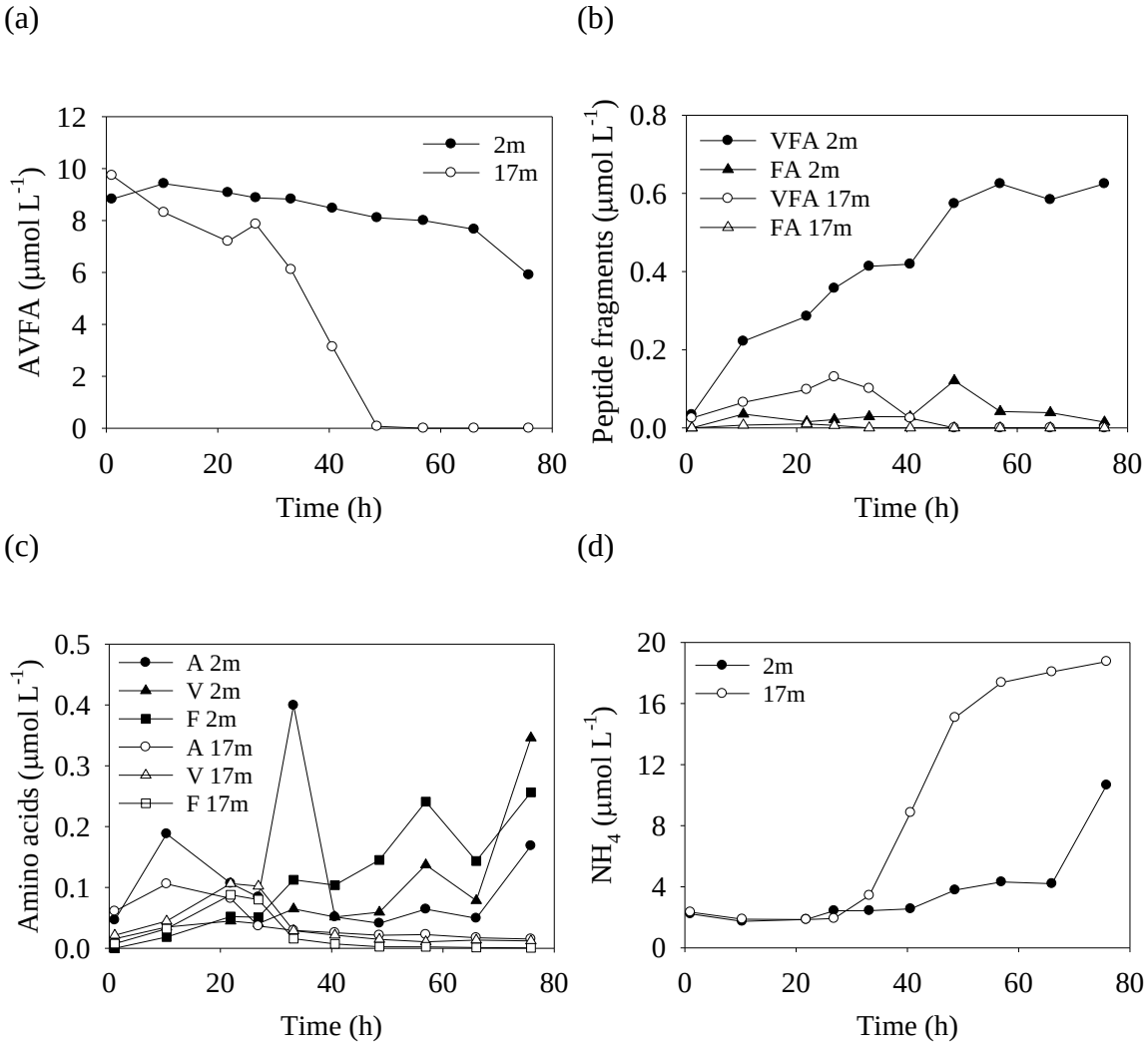

Figure A2.1 (continued)

(e)

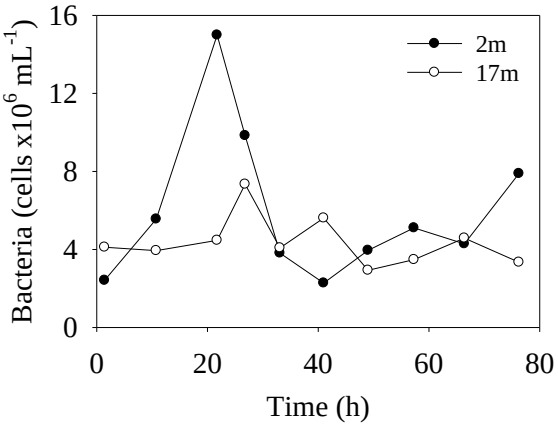

(f)

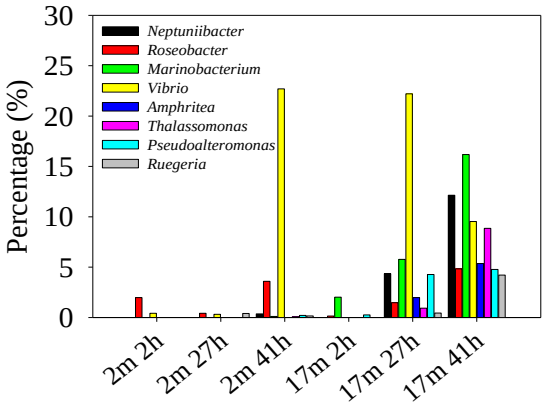

Figure A2.2. PCR cycle number test. (a) Agarose gel of 17m 57h DNA PCR products with different cycle numbers using *Neptuniibacter caesariensis* OppDF (Nep OppDF) primer (241 bp PCR product) and 16S primer (~1465 bp PCR product). Lanes: 1, 1Kb Plus DNA ladder (Invitrogen); 2, Nep OppDF primer with 25 PCR cycles; 3, Nep OppDF primer with 30 PCR cycles; 4, Nep OppDF primer with 35 PCR cycles; 5, Nep OppDF primer with 40 PCR cycles; 6, 1Kb Plus DNA ladder (Invitrogen); 7, 16S primer with 25 PCR cycles; 8, 16S primer with 30 PCR cycles; 9, 16S primer with 35 PCR cycles; 10, 16S primer with 40 PCR cycles; (b) plot of the peak area of gel bands shown in (a) integrated using ImageJ vs. PCR cycles numbers. Exponential regression was shown for all 16S primer amplification samples and Nep OppDF primer amplification samples with 30, 35, 40 PCR cycle numbers.

(a)

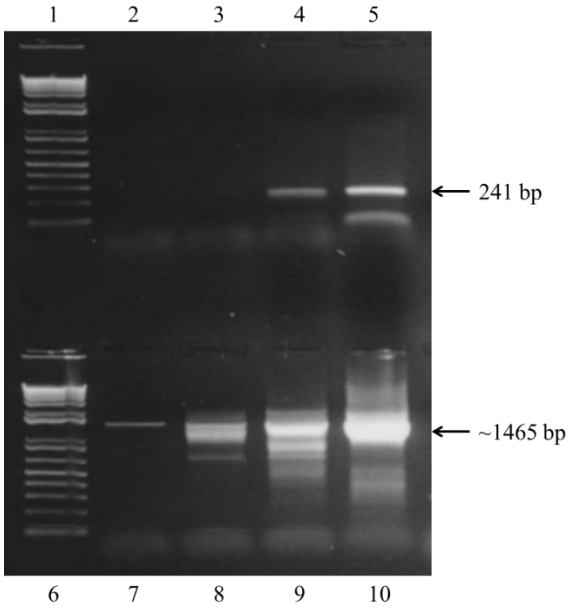

(b)

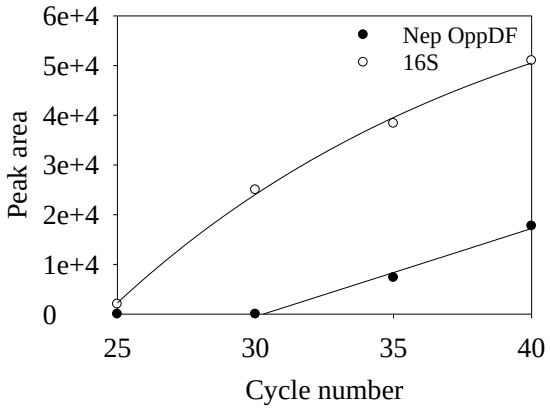

Figure A2.3. (a) Agarose gel of 2 m and 17 m AVFA incubation DNA PCR products using *Neptuniibacter caesariensis* OppDF (Nep OppDF) primer (241 bp PCR product). Lanes: 1, 1Kb Plus DNA ladder (Invitrogen); 2, 2m 10h sample; 3, 2m 22h sample; 4, 2m 33h sample; 5, 2m 49h sample; 6, 2m 57h sample; 7, 1Kb Plus DNA ladder (Invitrogen); 8, 17m 10h sample; 9, 17m 22h sample; 10, 17m 33h sample; 11, 17m 49h sample; 12, 17m 57h sample; (b) Agarose gel of 2m and 17m AVFA incubation DNA PCR products using *Roseobacter sp.1* OppDF (Ros OppDF, see name in Table 1) primer (300 bp PCR product). Lanes are same as (a); (c) plot of the peak area ratio between gel bands 2-6, 8-12 shown in (a) and their corresponding gel bands of DNA PCR products using 16S primer versus AVFA incubation time; (d) plot of the peak area ratio between gel bands 2-6, 8-12 shown in (b) and their corresponding gel bands of DNA PCR products using 16S primer versus AVFA incubation time; (e) plot of the peak area ratio in (c) normalized to bacterial abundance versus AVFA incubation time; (f) plot of the peak area ratio in (d) normalized to bacterial abundance versus AVFA incubation time.

(a) (b)

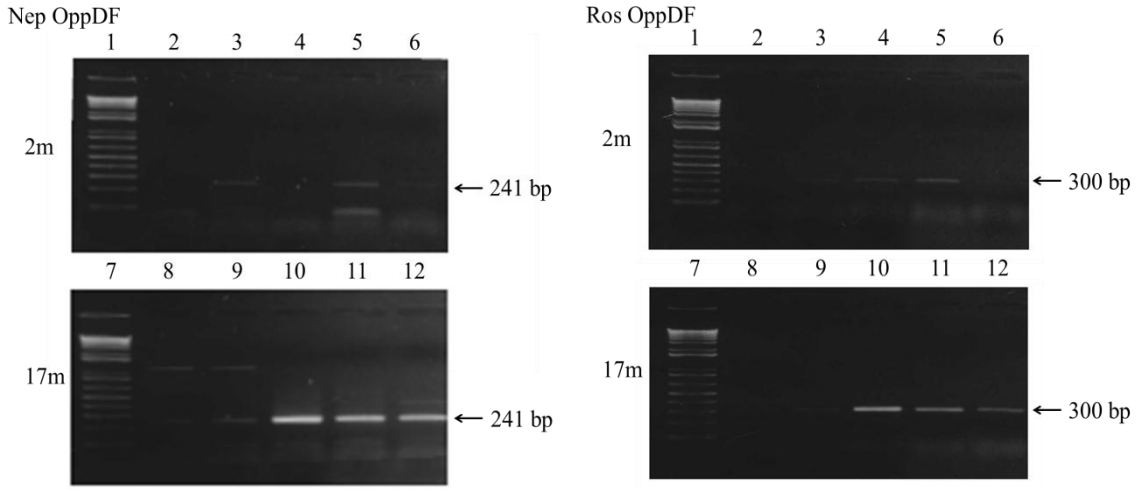

Figure A2.3 (continued)

(c)

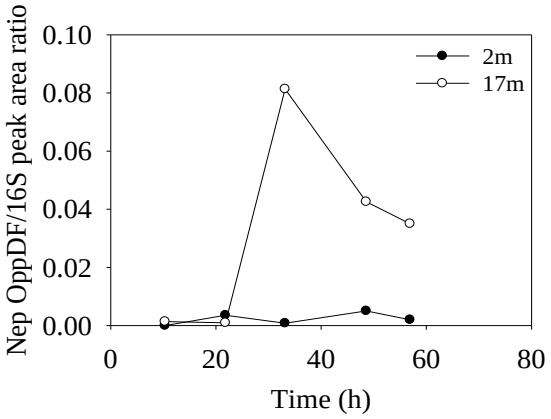

(d)

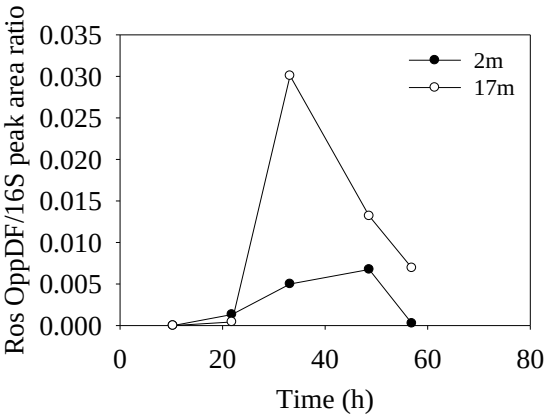

(e)

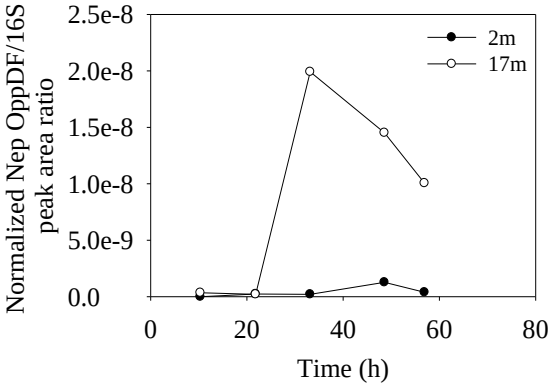

(f)

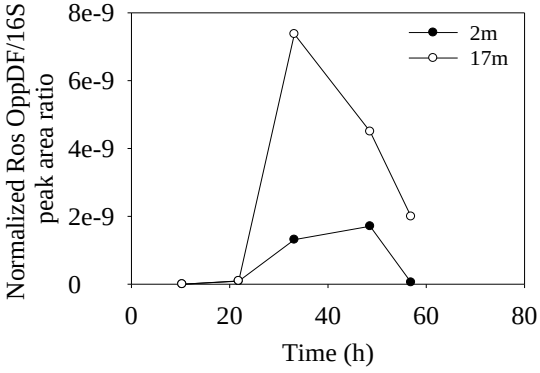

References

Ahn, J.J., Akram, K., Lee, J., Kim, K.S., Kwon, J.H., 2012. Identification of a gamma-irradiated ingredient (garlic powder) in Korean barbeque sauce by thermoluminescence analysis. J. Food Sci. 77(4): C476-C480.

Alldredge, A.L., Silver, M.W., 1988. Characteristics, dynamics and significance of marine snow. Prog. Oceanog. 20: 41-82.

Aluwihare, L.I., Repeta, D.J., 1999. A comparison of the chemical characteristics of oceanic DOM and extracellular DOM produced by marine algae. Mar. Ecol. Prog. Ser. 186: 105-117.

Aluwihare, L.I., Repeta, D.J., Pantoja, S., Johnson, C.G., 2005. Two chemically distinct pools of organic nitrogen accumulate in the ocean. Science 308: 1007-1010.

Alves, R.A., 1984. The influence of membrane components on the uptake of peptides by gram-negative bacteria. Ph.D. Thesis, Durham University.

Andren, P.E., Emmett, M.R., Caprioli, R.M., 1994. Micro-electrospray-zeptomole-attomole per microliter sensitivity for peptides. J. Am. Soc. Mass Spectr. 5(9): 867-869.

Andrews, J.C., Short, S.A., 1986. Opp-lac operon fusions and transcriptional regulation of the *Escherichia-Coli* Trp-linked oligopeptide permease. J. Bacteriol. 165(2): 434-442.

Antia, N.J., Harrison, P.J., Oliveira, L., 1991. The role of dissolved organic nitrogen in phytoplankton nutrition, cell biology and ecology. Phycologia 30: 1-89.

Appel, W., 1986. Chymotrypsin - molecular and catalytic properties. Clin. Biochem. 19: 317-322.

Arnosti, C., 2003. Microbial extracellular enzymes and their role in dissolved organic matter cycling, in: Findlay, S.E.G., Sinsabaugh, R.L. (Eds.) Aquatic Ecosystems Interactivity of Dissolved Organic Matter. Academic Press, Burlington, MA, pp. 315-342.

Arnosti, C., 2004. Speed bumps and barricades in the carbon cycle: substrate structural effects on carbon cycling. Mar. Chem. 92: 263-273.

Arnosti, C., 2011. Microbial extracellular enzymes and the marine carbon cycle. Annu. Rev. Mar. Sci. 3: 401-425.

Arnosti, C., Durkin, S., Jeffrey, W.H., 2005. Patterns of extracellular enzyme activities among pelagic marine microbial communities: implications for cycling of dissolved organic carbon. Aquat. Microb. Ecol. 38: 135-145.

Arora, G., Lee, B.H., 1992. Purification and characterization of aminopeptidase from *Lactobacillus-Casei Ssp Casei* LLG. J. Dairy Sci. 75: 700-710.

Arrieta, J.M., Herndl, G.I., 2002. Changes in bacterial β-glucosidase diversity during a coastal phytoplankton bloom. Limnol. Oceanogr. 47: 594-599.

Auer, B., Arndt, H., 2001. Taxonomic composition and biomass of heterotrophic flagellates in relation to lake trophy and season. Freshwater Biol. 46: 959-972.

Azam, F., 1998. Microbial control of oceanic carbon flux: The plot thickens. Science 280: 694-696.

Beardsley, C., Pernthaler, J., Wosniok, W., Amann, R., 2003. Are readily culturable bacteria in coastal North Sea waters suppressed by selective grazing mortality? Appl. Environ. Microb. 69: 2624-2630.

Bell, T.H., Yergeau, E., Martineau, C., Juck, D., Whyte, L.G., Greer, C.W., 2011. Identification of nitrogen-incorporating bacteria in petroleum-contaminated Arctic soils by using [^{15}N]DNA-based stable isotope probing and pyrosequencing. Appl. Environ. Microb. 77: 4163-4171.

Benz, R., 1988. Structure and function of porins from gram-negative bacteria. Annu. Rev. Microbiol. 42: 359-393.

Berg, G.M., Repeta, D.J., Laroche, J., 2002. Dissolved organic nitrogen hydrolysis rates in axenic cultures of *Aureococcus anophagefferens* (Pelagophyceae): Comparison with heterotrophic bacteria. Appl. Environ. Microb. 68: 401-404.

Berg, C., Beckmann, S., Jost, G., Labrenz, M., Jurgens, K., 2013. Acetate-utilizing bacteria at an oxic-anoxic interface in the Baltic Sea. FEMS Microbiol. Ecol. 85: 251-261.

Bidle, K.D., Fletcher, M., 1995. Comparison of free-living and particle-associated bacterial communities in the Chesapeake Bay by stable low-molecular-weight RNA analysis. Appl. Environ. Microb. 61: 944-952.

Billen, G., 1991. Protein degradation in aquatic environments. in: Chróst, R.J. (Eds.) Microbial Enzymes in Aquatic Environments. Brock/Springer, New York, NY, pp. 123-143.

Bolleter, W.T., Bushman, C.J., Tidwell, P.W., 1961. Spectrophotometric determination of ammonia as indophenol. Anal. Chem. 33(4): 592-594.

Bongiorni, L., Pusceddu, A., Danovaro, R., 2005. Enzymatic activities of epiphytic and benthic thraustochytrids involved in organic matter degradation. Aquat. Microb. Ecol. 41: 299-305.

Bradley, P.B., Sanderson, M.P., Nejstgaard, J.C., Sazhin, A.F., Frischer, M.E., Killberg-Thoreson, L.M., Verity, P.G., Campbell, L., Bronk, D.A., 2010. Nitrogen uptake

by phytoplankton and bacteria during an induced Phaeocystis pouchetii bloom, measured using size fractionation and flow cytometric sorting. Aquat. Microb. Ecol. 61: 89-104.

Breed G.A., Jackson G.A., Richardson T.L., 2004. Sedimentation, carbon export and food web structure in the Mississippi River plume described by inverse analysis. Mar. Ecol. Prog. Ser. 278: 35-51.

Brock, T.D., 1971. Microbial growth rate in nature. Bacteriol. Rev. 35: 39-58.

Bronk, D.A., 2002. Dynamics of DON, in: Hansell, D.A., Carlson, C.A. (Eds.), Biogeochemistry of Marine Dissolved Organic Matter. Academic Press, San Diego, CA, pp. 153-247.

Brüssow, H., 2007. Bacteria between protists and phages: From antipredation strategies to the evolution of pathogenicity. Mol. Microbiol. 65: 583-589.

Buckley, D.H., Huangyutitham, V., Hsu, S.F., Nelson, T.A., 2007. Stable isotope probing with ^{15}N achieved by disentangling the effects of genome G+C content and isotope enrichment on DNA density. Appl. Environ. Microb. 73: 3189-3195.

Delange, R.J., Smith, E.L., 1971. Leucine aminopeptidase and other N-terminal exopeptidases, in: Boyer, P.D. (Eds.), The Enzymes. Vol 3. Academic Press, London, pp. 82-102.

Detmers, F. J. M., Lanfermeijer, F.C., Poolman, B., 2001. Peptides and ATP binding cassette peptide transporters. Res. Microbiol. 152(3-4): 245-258.

Campbell B.J., Kirchman D.L., 2013. Bacterial diversity, community structure and potential growth rates along an estuarine salinity gradient. ISME J. 7: 210-220.

Caporaso, J.G., Bittinger, K., Bushman, F.D., DeSantis, T.Z., Andersen, G.L., Knight, R., 2010a. PyNAST: a flexible tool for aligning sequences to a template alignment. Bioinformatics 26: 266-267.

Caporaso, J.G., Kuczynski, J., Stombaugh, J., Bittinger, K., Bushman, F.D., Costello, E.K., Fierer, N., Pena, A.G., Goodrich, J.K., Gordon, J.I., Huttley, G.A., Kelley, S.T., Knights, D., Koenig, J.E., Ley, R.E., Lozupone, C.A., McDonald, D., Muegge, B.D., Pirrung, M., Reeder, J., Sevinsky, J.R., Tumbaugh, P.J., Walters, W.A., Widmann, J., Yatsunenko, T., Zaneveld, J., Knight, R., 2010b. QIIME allows analysis of high-throughput community sequencing data. Nat. Methods 7: 335-336.

Carlson, C.A., 2002. Production and removal processes, in: Hansell, D.A., Carlson, C.A. (Eds), Biogeochemistry of Marine Dissolved Organic Matter. Academic Press, San Diego, CA, pp. 91-151.

Carlsson, P., Graneli, E., 1998. Utilization of dissolved organic matter (DOM) by phytoplankton, including harmful species, in: Anderson, D.M., Cembella, A.D.,

Hallegraeff, G.M. (Eds.), Physiological Ecology of Harmful Algal Blooms. Springer, New York, NY, pp. 509-524.

Carney, R.L., Mitrovic, S.M., Jeffries, T., Westhorpe, D., Curlevski, N., Seymour, J.R., 2015. River bacterioplankton community responses to a high inflow event. Aquat. Microb. Ecol. 75: 187-205.

Charbonnel, P., Lamarque, M., Piard, J., Gilbert, C., Juillard, V., Atlan, D., 2003. Diversity of oligopeptide transport specificity in *Lactococcus lactis* species - A tool to unravel the role of OppA in uptake specificity. J. Biol. Chem. 278(17): 14832-14840.

Chen, Y.Q., Ntai, I., Kelleher, N.L., 2012. A proteomic survey of nonribosomal peptide and polyketide biosynthesis in Actinobacteria. J. Proteome. Res. 11: 85-94.

Christianson D.W., Lipscomb W.N., 1989. Carboxypeptidase A. Acc. Chem. Res. 22: 62-69.

Christie-Oleza, J.A., Fernandez, B., Nogales, B., Bosch, R., Armengaud, J., 2012. Proteomic insights into the lifestyle of an environmentally relevant marine bacterium. ISME J. 6: 124-135.

Chróst R.J., 1990. Microbial ectoenzymes in aquatic environments, in: Overbeck, J., Chróst, R.J. (Eds.) Aquatic Microbial Ecology: Biochemical and Molecular Approaches. Springer-Verlag, New York, NY, pp. 47-78.

Chróst R.J., 1991. Environmental control of the synthesis and activity of aquatic microbial ectoenzymes, in: Chróst, R.J. (Eds.) Microbial Enzymes in Aquatic Environments. Springer-Verlag, New York, NY, pp. 29-59.

Connelly, T.L., Baer, S.E., Cooper, J.T., Bronk, D.A., Wawrik, B., 2014. Urea uptake and carbon fixation by marine pelagic bacteria and archaea during the Arctic summer and winter seasons. Appl. Environ. Microb. 80: 6013-6022.

Cottrell M.T., Kirchman D.L., 2000. Natural assemblages of marine proteobacteria and members of the *Cytophaga-Flavobacter* cluster consuming low- and high-molecular-weight dissolved organic matter. Appl. Environ. Microb. 66: 1692-1697.

Cunha, A., Almeida, A., Coelho, F.J.R.C, Gomes, N.C.M, Oliveria, V., Santos, A.L., 2010. Bacterial extracellular enzymatic activity in globally changing aquatic ecosystems, in: Méndez-Vilas, A. (Eds.) Current research, Technology and Education Topics in Applied Microbiology and Microbial Biotechnology. Formatex, Badajoz, Spain, pp. 124-135.

Curtis-Jackson, P.K., Masse, G., Gledhill, M., Fitzsimons, M. F., 2009. Characterization of low molecular weight dissolved organic nitrogen by liquid chromatography-electrospray ionization-mass spectrometry. Limnol. Oceanogr.-Meth. 7: 52-63.

Dai, Y.Q., Li, L., Roser, D.C., Long, S.R., 1999. Detection and identification of low-mass peptides and proteins from solvent suspensions of *Escherichia coli* by high performance liquid chromatography fractionation and matrix-assisted laser desorption/ionization mass spectrometry. Rapid Commun. Mass. Spectr. 13(1): 73-78.

Damen, C.W.N., Rosing, H., Schellens, J.H.M., Beijnen, J.H., 2008. Quantitative aspects of the analysis of the monoclonal antibody trastuzumab using high-performance liquid chromatography coupled with electrospray mass spectrometry. J. Pharmaceut. Biomed. 46(3): 449-455.

Daniel, H., Spanier, B., Kottra, G., Weitz, D., 2006. From bacteria to man: Archaic proton-dependent peptide transporters at work. Physiology 21: 93-102.

Dauwe, B., Middelburg, J.J., Herman, P.M.J., Heip, C.H.R., 1999. Linking diagenetic alteration of amino acids and bulk organic matter reactivity. Limnol. Oceanogr. 44: 1809-1814.

Davey, K.E., Kirby, R.R., Turley, C.M., Weightman, A.J., Fry, J.C., 2001. Depth variation of bacterial extracellular enzyme activity and population diversity in the northeastern North Atlantic Ocean. Deep-Sea Res. Pt. II 48: 1003-1017.

Delinsky, D.C., Hill, K.T., White, C.A., Bartlett, M.G., 2004. Quantitation of the large polypeptide glucagon by protein precipitation and LC/MS. Biomed. Chromatogr. 18(9): 700-705.

Delong, E.F., Franks, D.G., Alldredge, A.L., 1993. Phylogenetic diversity of aggregate-attached vs free-living marine bacterial assemblages. Limnol. Oceanogr. 38: 924-934.

Dong, H.P., Hong, Y.G., Lu, S.H., Xie, L.Y., 2014. Metaproteomics reveals the major microbial players and their biogeochemical functions in a productive coastal system in the northern South China Sea. Env. Microbiol. Rep. 6: 683-695.

Dowd, S.E., Callaway, T.R., Wolcott, R.D., Sun, Y., McKeehan, T., Hagevoort, R.G., Edrington, T.S., 2008. Evaluation of the bacterial diversity in the feces of cattle using 16S rDNA bacterial tag-encoded FLX amplicon pyrosequencing (bTEFAP). BMC Microbiol. 8: 125, doi:10.1186/1471-2180-8-125.

Dupuy, C., Ryckaert, M., Le Gall, S., Hartmann, H.J., 2007. Seasonal variations in planktonic community structure and production in an atlantic coastal pond: The importance of nanoflagellates. Microb. Ecol. 53: 537-548.

Eilers, H., Pernthaler, J., Amann, R., 2000. Succession of pelagic marine bacteria during enrichment: a close look at cultivation-induced shifts. Appl. Environ. Microb. 66: 4634-4640.

Eglinton, T.I., Repeta, D.J., 2004. Organic matter in the contemporary ocean, in: Elderfield, H. (Eds.) The Oceans and Marine Geochemistry. Elsevier-Pergamon, Oxford, 6, pp. 145-180.

Elser, J.J., Sterner, R.W., Gorokhova, E., Fagan, W.F., Markow, T.A., Cotner, J.B., Harrison, J.F., Hobbie, S.E., Odell, G.M., Weider, L.J., 2000. Biological stoichiometry from genes to ecosystems. Ecol. Lett. 3: 540-550.

Emerson, S., Hedges, J., 2008. Chemical Oceanography and the Marine Carbon Cycle, 1st ed. Cambridge.

Emmett, M.R., Caprioli, R.M., 1994. Micro-electrospray mass-spectrometry - ultra-high-sensitivity analysis of peptides and proteins. J. Am. Soc. Mass. Spectr. 5(7): 605-613.

Fenchel, T., 2002. Microbial behavior in a heterogeneous world. Science 296(5570): 1068-1071.

Ferguson, E.L., Buckley, E.N., Palumbo, A.V., 1984. Response of marine bacterioplankton to differential filtration and confinement. Appl. Environ. Microbiol. 47: 49-55.

Fierer, N., Bradford, M.A., Jackson, R.B., 2007. Toward an ecological classification of soil bacteria. Ecology 88: 1354-1364.

Findlay, S., Sinsabaugh, R.L., 2003. Aquatic Ecosystems: Interactivity of Dissolved Organic Matter. Academic Press, San Diego, CA.

Fodelianakis, S., Papageorgiou, N., Pitta, P., Kasapidis, P., Karakassis, I., Ladoukakis, E.D., 2014. The pattern of change in the abundances of specific bacterioplankton groups is consistent across different nutrient-enriched habitats in Crete. Appl. Environ. Microb. 80: 3784-3792.

Foreman, C.M., Franchini, P., Sinsabaugh, R.L., 1998. The trophic dynamics of riverine bacterioplankton: Relationships among substrate availability, ectoenzyme kinetics, and growth. Limnol. Oceanogr. 43(6): 1344-1352.

Fortunato, C.S., Herfort, L., Zuber, P., Baptista, A.M., Crump, B.C., 2012. Spatial variability overwhelms seasonal patterns in bacterioplankton communities across a river to ocean gradient. ISME J. 6: 554-563.

Fuhrman, J.A., 1987. Close coupling between release and uptake of dissolved free amino-acids in seawater studied by an isotope-dilution approach. Mar. Ecol. Prog. Ser. 37: 45-52.

Fuhrman, J.A., Hagstrom, A., 2008. Bacterial and archaeal community structure and its patterns, in: Kirchman, D.L. (Eds) Microbial Ecology of the Oceans. Wiley-Blackwell, Hoboken, NJ, pp. 45-90.

Galand, P.E., Potvin, M., Casamayor, E.O., Lovejoy, C., 2010. Hydrography shapes bacterial biogeography of the deep Arctic Ocean. ISME J. 4(4): 564-576.

Gale, E.F., 1945. The arginine, ornithine and carbon dioxide requirements of streptococci (Lancefield group D) and their relation to arginine dihydrolase activity. Brit. J. Exp. Pathol. 26: 225-233.

Garault, P., Le Bars, D., Besset, C., Monnet, V., 2002. Three oligopeptide-binding proteins are involved in the oligopeptide transport of *Streptococcus* thermophilus. J. Biol. Chem. 277(1): 32-39.

Garcia, M.C., 2005. The effect of the mobile phase additives on sensitivity in the analysis of peptides and proteins by high-performance liquid chromatography-electrospray mass spectrometry. J. Chromatogr. B 825(2): 111-123.

Gardan, R., Besset, C., Guillot, A., Gitton, C., Monnet, V., 2009. The oligopeptide transport system is essential for the development of natural competence in *Streptococcus* thermophilus strain LMD-9. J. Bacteriol. 191(14): 4647-4655.

Gardner, W.S., St. John, P.A., 1991. High-performance liquid chromatographic method to determine ammonium ion and primary amines in seawater. Anal. Chem. 63: 537-540.

Gharahdaghi, F., Weinberg, C.R., Meagher, D.A., Imai, B.S., Mische, S.M., 1999. Mass spectrometric identification of proteins from silver-stained polyacrylamide gel: A method for the removal of silver ions to enhance sensitivity. Electrophoresis 20(3): 601-605.

Gihring, T.M., Humphrys, M., Mills, H.J., Huettel, M., Kostka, J.E., 2009. Identification of phytodetritus-degrading microbial communities in sublittoral Gulf of Mexico sands. Limnol. Oceanogr. 54(4): 1073-1083.

Gilar, M., Belenky, A., Wang, B.H., 2001. High-throughput biopolymer desalting by solid-phase extraction prior to mass spectrometric analysis. J. Chromatogr. A 921(1): 3-13.

Glibert, P.M., Legrand, C., 2006. The diverse nutrient strategies of harmful algae: Focus on osmotrophy, in: Granéli, E., Turner, J.T. (Eds) Ecology of Harmful Algae. Springer, New York, NY, pp. 163-175.

Gonzales, T., RobertBaudouy, J., 1996. Bacterial aminopeptidases: Properties and functions. FEMS Microbiol. Rev. 18: 319-344.

Görtz, H., Maier, G., 1991. A bacterial infection in a ciliate from sewage sludge. Endocytobiosis & Cell Res. 8: 45-52.

Griffith, P., Shiah, F., Gloersen, K., Ducklow, H.W., Fletcher, M., 1994. Activity and distribution of attached bacteria in Chesapeake Bay. Mar. Ecol. Prog. Ser. 108: 1-10.

Guyer, C.A., Morgan, D.G, Osheroff, N., Staros, J.V., 1985. Purification and characterization of a periplasmic oligopeptide binding-protein from *Escherichia-Coli*. J. Biol. Chem. 260(19): 812-818.

Harvey, H.R., Dyda, R.Y., Kirchman, D.L., 2006. Impact of DOM composition on bacterial lipids and community structure in estuaries. Aquat. Microb. Ecol. 42(2): 105-117.

Hashimoto, S., Fujiwara, K., Fuwa, K., Saino, T., 1985. Distribution and characteristics of carboxypeptidase activity in pond, river, and seawaters in the vicinity of Tokyo. Limnol. Oceanogr. 30: 631-645.

He, F., Emmett, M.R., Hakansson, K., Hendrickson, C.L., Marshall, A.G., 2004. Theoretical and experimental prospects for protein identification based solely on accurate mass measurement. J. Proteome. Res. 3(1): 61-67.

Hedges, J.I., Eglinton, G., Hatcher, P.G., Kirchman, D.L., Arnosti, C., Derenne, S., Evershed, R.P., Kogel-Knabner, I., de Leeuw, J.W., Littke, R., Michaelis, W., Rullkotter, J., 2000. The molecularly-uncharacterized component of nonliving organic matter in natural environments. Org. Geochem. 31: 945-958.

Herlemann, D.P.R., Labrenz, M., Jurgens, K., Bertilsson, S., Waniek, J.J., Andersson, A.F., 2011. Transitions in bacterial communities along the 2000 km salinity gradient of the Baltic Sea. ISME J. 5: 1571-1579.

Hertkorn, N., Benner, R., Frommberger, M., Schmitt-Kopplin, P., Witt, M., Kaiser, K., Kettrup, A., Hedges, J.I., 2006. Characterization of a major refractory component of marine dissolved organic matter. Geochim. Cosmochim. Ac. 70(12): 2990-3010.

Higgins, C.F., Hardie, M.M., 1983. Periplasmic protein associated with the oligopeptide permeases of *Salmonella-Typhimurium* and *Escherichia-Coli*. J. Bacteriol. 155(3): 1434-1438.

Higgins, C.F., Hardie, M.M., Jamieson, D., Powell, L.M., 1983. Genetic-map of the Opp (oligopeptide permease) locus of *Salmonella-Typhimurium*. J. Bacteriol. 153(2): 830-836.

Higgins, C.F., Hiles, I.D., Whalley, K., Jamieson, D.J., 1985. Nucleotide binding by membrane-components of bacterial periplasmic binding protein-dependent transport-systems. Embo. J. 4(4): 1033-1039.

Hitchcock, G.L., Wiseman, W.J., Boicourt, W.C., Mariano, A.J., Walker, N., Nelsen, T.A., Ryan, E., 1997. Property fields in an effluent plume of the Mississippi river. J. Mar. Syst. 12: 109-126.

Holben, W.E., 2011. GC fractionation allows comparative total microbial community analysis, enhances diversity assessment, and facilitates detection of minority

populations of bacteria, in: de Bruijn, F.J. (Eds.), Handbook of Molecular Micorbial Ecology, Volume I: Metagenomics and Complementary Approaches. Wiley-Blackwell, Hoboken, NJ, pp. 183-196.

Hollibaugh, J.T., Azam, F., 1983. Microbial degradation of dissolved proteins in seawater. Limnol. Oceanogr. 28: 1104-1116.

Hoppe, H.G., 1983. Significance of exoenzymatic activities in the ecology of brackish water - measurements by means of methylumbelliferyl-substrates. Mar. Ecol. Prog. Ser. 11: 299-308.

Hoppe, H.G., Kim, S.J., Gocke, K., 1988a. Microbial decomposition in aquatic environments: combined process of extracellular enzyme activity and substrate uptake. Appl. Environ. Microb. 54: 784-790.

Hoppe, H.G., Schramm, W., Bacolod, P., 1988b. Spatial and temporal distribution of pelagic microorganisms and their proteolytic activity over a partly destroyed coral reef. Mar. Ecol. Prog. Ser. 44: 95-102.

Hoppe, H.G., 1991. Microbial extracellular enzyme activity: A new key parameter in aquatic ecology, in: Chróst, R.J. (Eds.) Microbial Enzymes in Aquatic Environments. Springer, New York, NY, pp. 60-83.

Hulen, C., Legoffic, F., 1988. Peptidase-N and alanyl-peptide transport in *Pseudomonas-Aeruginosa*. FEMS Microbiol. Lett. 49(2): 167-172.

ICH Q2(R1), 2005. Validation of analytical procedures: Text and methodology. International Conference on Harmonisation of Technical Requirements for Registration of Pharmaceuticals for Human Use.

Inoue, K., Ikemura, A., Tsuruta, Y., Tsutsumiuchi, K., Hino, T., Oka, H., 2012. On-line solid-phase extraction LC-MS/MS for the determination of Ac-SDKP peptide in human plasma from hemodialysis patients. Biomed. Chromatogr. 26(2): 137-141.

Iwaki, H., Nishimura, A., Hasegawa, Y., 2012. Isolation and characterization of marine bacteria capable of utilizing phthalate. World J. Microb. Biot. 28: 1321-1325.

Jamieson, D.J., Higgins, C.F., 1984. Anaerobic and leucine-dependent expression of a peptide-transport gene in *Salmonella-Typhimurium*. J. Bacteriol. 160(1): 131-136.

Jenkinson, H.F., Baker, R.A., Tannock, G.W., 1996. A binding-lipoprotein-dependent oligopeptide transport system in *Streptococcus gordonii* essential for uptake of hexa- and heptapeptides. J. Bacteriol. 178(1): 68-77.

Jones, M.N., 1984. Nitrate reduction by shaking with cadmium - alternative to cadmium columns. Water Res. 18: 643-646.

Karl, D.M., 2014. Microbially mediated transformations of phosphorus in the sea: new views of an old cycle. Ann. Rev. Mar. Sci. 6: 279-337.

Karl, D.M., Bjorkman, K.M., Dore, J.E., Fujieki, L., Hebel, D.V., Houlihan, T., Letelier, R.M., Tupas, L.M., 2001. Ecological nitrogen-to-phosphorus stoichiometry at station ALOHA. Deep Sea Res., Part II 48(8−9): 1529−1566.

Karner, M., Ferrierpages, C., Rassoulzadegan, F., 1994. Phagotrophic nanoflagellates contribute to occurrence of α-glucosidase and aminopeptidase in marine environments. Mar. Ecol. Prog. Ser. 114: 237-244.

Karner, M., Rassoulzadegan, F., 1995. Extracellular enzyme activity: Indications for high short-term variability in a coastal marine ecosystem. Microb. Ecol. 30: 143-156.

Kendall, M.G., 1990. Rank correlation methods, 5th ed. Oxford University Press, New York.

Kirchman, D.L., 2002. The ecology of *Cytophaga-Flavobacteria* in aquatic environments. FEMS Microbiol. Ecol. 39: 91-100.

Kirchman, D.L., 2008. Microbial ecology of the oceans, 2nd ed. Wiley-Blackwell, Hoboken, NJ.

Kirchman, D.L., Hodson, R., 1984. Inhibition by peptides of amino acid uptake by bacterial populations in natural waters: implications for the regulation of amino acid transport and incorporation. Appl. Environ. Microb. 47: 624-631.

Kirchman, D.L., Mitchell, R., 1982. Contribution of particle-bound bacteria to total microheterotrophic activity in five ponds and two marshes. Appl. Environ. Microbiol. 43: 200-209.

Kirchman, D.L., Dittel, A.I., Malmstrom, R.R., Cottrell, M.T., 2005. Biogeography of major bacterial groups in the Delaware Estuary. Limnol. Oceanogr. 50: 1697-1706.

Kisand, V., Zingel, P., 2000. Dominance of ciliate grazing on bacteria during spring in a shallow eutrophic lake. Aquat. Microb. Ecol. 22: 135-142.

Kleindienst, S., Herbst, F.A., Stagars, M., von Netzer, F., von Bergen, M., Seifert, J., Peplies, J., Amann, R., Musat, F., Lueders, T., Knittel, K., 2014. Diverse sulfate-reducing bacteria of the *Desulfosarcina*/*Desulfococcus* clade are the key alkane degraders at marine seeps. ISME J. 8: 2029-2044.

Klindworth, A., Pruesse, E., Schweer, T., Peplies, J., Quast, C., Horn, M., Glockner, F.O., 2013. Evaluation of general 16S ribosomal RNA gene PCR primers for classical and next-generation sequencing-based diversity studies. Nucleic Acids Res. doi: 10.1093/nar/gks808.

Klut, M.E., Bisalputra, T., Antia, N.J., 1987. Some observations on the structure and function of the dinoflagellate pusule. Can. J. Bot. 65: 736-744.

Kostiainen, R., Bruins, A.P., 1996. Effect of solvent on dynamic range and sensitivity in pneumatically-assisted electrospray (ion spray) mass spectrometry. Rapid Commun. Mass Spectr. 10(11): 1393-1399.

Kuznetsova, M., Lee, C., 2002. Dissolved free and combined amino acids in nearshore seawater, sea surface microlayers and foams: influence of extracellular hydrolysis. Aquat. Sci. 64: 252-268.

Kyte, J., Doolittle, R.F., 1982. A simple method for displaying the hydropathic character of a protein. J. Mol. Biol. 157: 105-132.

Lamarque, M., Aubel, D., Piard, J., Gilbert, C., Juillard, V., Atlan, D., 2011. The peptide transport system Opt is involved in both nutrition and environmental sensing during growth of *Lactococcus lactis* in milk. Microbiol. 157: 1612-1619.

Lamarque, M., Charbonnel, P., Aubel, D., Piard, J., Atlan, D., Juillard, V., 2004. A multifunction ABC transporter (Opt) contributes to diversity of peptide uptake specificity within the genus *Lactococcus*. J. Bacteriol. 186(19): 6492-6500.

Lampert, W., 1978. Release of dissolved organic carbon by grazing phytoplankton. Limnol. Oceanogr. 23: 831-834.

Lanfermeijer, F.C., Picon, A., Konings, W.N., Poolman, B., 1999. Kinetics and consequences of binding of nona- and dodecapeptides to the oligopeptide binding protein (OppA) of *Lactococcus lactis*. Biochemistry 38(44): 14440-14450.

Larsson, U., Hagstrom, A., 1979. Phytoplankton exudate release as an energy-source for the growth of pelagic bacteria. Mar. Biol. 52(3): 199-206.

Law, B.A., 1978. Peptide utilization by group-N *Streptococci*. J. Gen. Microbiol. 105(Mar): 113-118.

Lazdunski, C., Busuttil, J., Lazdunski, A., 1975. Purification and properties of a periplasmic aminoendopeptidase from *Escherichia-Coli*. Eur. J. Biochem. 60: 363-369.

Lee, C., 1992. Controls on organic-carbon preservation - the use of stratified water bodies to compare intrinsic rates of decomposition in oxic and anoxic systems. Geochim. Cosmochim. Ac. 56(8): 3323-3335.

Lee, C., Hedges, J.I., Wakeham, S.G., Zhu, N., 1992. Effectiveness of various treatments in retarding microbial activity in sediment trap material and their effects on the collection of swimmers. Limnol. Oceanogr. 37: 117-130.

Lee, C., Wakeham, S.G., Hedges, J.I., 2000. Composition and flux of particulate amino acids and chloropigments in equatorial Pacific seawater and sediments. Deep-Sea Res. Pt. I 47: 1535-1568.

Lee, S., Fuhrman, J.A., 1987. Relationships between biovolume and biomass of naturally derived marine bacterioplankton. Appl. Environ. Microb. 53: 1298-1303.

Legrand, C., Carlsson, P., 1998. Uptake of high molecular weight dextran by the dinoflagellate *Alexandrium catenella*. Aquat. Microb. Ecol. 16: 81-86.

Lewis, E.J., 1973. Protein, peptide and free amino-acid composition in species of Champia from Saurashtra coast, India. Bot. Mar. 16(3): 145-147.

Lin, X.J., McKinley, J., Resch, C.T., Kaluzny, R., Lauber, C.L., Fredrickson, J., Knight, R., Konopka, A., 2012. Spatial and temporal dynamics of the microbial community in the Hanford unconfined aquifer. ISME. J. 6: 1665-1676.

Lindroth, P., Mopper, K., 1979. High performance liquid chromatographic determination of subpicomole amounts of amino acids by precolumn fluorescence derivatization with *o*-phthaldialdehyde. Anal. Chem. 51: 1667-1674.

Liu, H.H., Lam, L., Dasgupta, P.K., 2011a. Expanding the linear dynamic range for multiple reaction monitoring in quantitative liquid chromatography-tandem mass spectrometry utilizing natural isotopologue transitions. Talanta 87: 307-310.

Liu, S., Liu Z., 2014. A new method to measure small peptides amended in seawater using high performance liquid chromatography coupled with mass spectrometry. Mar. Chem. 164: 16-24.

Liu, S., Liu, Z., 2015. Comparing extracellular enzymatic hydrolysis between plain peptides and their corresponding analogs in the northern Gulf of Mexico Mississippi River plume. Mar. Chem. 177: 398-407.

Liu, S., Riesen, A., Liu, Z., 2015. Differentiating the role of different-sized microorganisms in peptide decomposition during incubations using size-fractioned coastal seawater. J. Exp. Mar. Biol. Ecol. 472: 97-106.

Liu, Z., Lee, C., 2006. Drying effects on sorption capacity of coastal sediment: The importance of architecture and polarity of organic matter. Geochim. Cosmochim. Ac. 70: 3313-3324.

Liu, Z., Lee, C., Wakeham, S.G., 2006. Effects of mercuric chloride and protease inhibitors on degradation of particulate organic matter from the diatom *Thalassiosira pseudonana*. Org. Geochem. 37: 1003-1018.

Liu, Z., Mao, J., Peterson, M.L., Lee, C., Wakeham, S.G., Hatcher, P., 2009. Characterization of sinking particles from the northwest Mediterranean Sea using advanced solid-state NMR. Geochim. Cosmochim. Ac. 73(4): 1014-1026.

Liu, Z., Kobiela, M.E., McKee, G.A., Tang, T.T., Lee, C., Mulholland, M.R., Hatcher, P.G., 2010. The effect of chemical structure on the hydrolysis of tetrapeptides along a river-to-ocean transect: AVFA and SWGA. Mar. Chem. 119: 108-120.

Liu, Z., Sleighter, R.H., Zhong, J., Hatcher, P.G., 2011b. The chemical changes of DOM from black waters to coastal marine waters by HPLC combined with ultrahigh resolution mass spectrometry. Estuar. Coast. Sci. 92: 205-216.

Liu, Z., Liu, S., Liu, J., Gardner, W.S., 2013. Differences in peptide decomposition rates and pathways in hypoxic and oxic coastal environments. Mar. Chem. 157: 67-77.

Liu, Z., Liu, J., Gardner, W.S., Shank, G.C., Ostrom, N.E., 2014. The impact of *Deepwater Horizon* oil spill on petroleum hydrocarbons in surface waters of the northern Gulf of Mexico. Deep-Sea Res. Pt. II, http://dx.doi.org/10.1016/j.dsr1012.2014.1001.1013i.

Liu, Z., Liu, S., 2016. High phosphate concentrations accelerate bacterial peptide degradation in hypoxic bottom waters of the northern Gulf of Mexico. Environ. Sci. Technol. 50: 676-684.

Lopez, C.V.G., Garcia, M.D.C., Fernandez, F.G.A., Bustos, C.S., Chisti, Y., Sevilla, J.M.F., 2010. Protein measurements of microalgal and cyanobacterial biomass. Bioresource Technol. 101(19): 7587-7591.

Luo, C.L., Xie, S.G., Sun, W.M., Li, X.D., Cupples, A.M., 2009. Identification of a novel toluene-degrading bacterium from the candidate phylum TM7, as determined by DNA stable isotope probing. Appl. Environ. Microb. 75: 4644-4647.

Makino, W., Cotner, J.B., Sterner, R.W., Elser, J.J., 2003. Are bacteria more like plants or animals? Growth rate and resource dependence of bacterial C : N : P stoichiometry. Funct. Ecol. 17: 121-130.

Marie, D., Partensky, F., Jacquet, S., Vaulot, D., 1997. Enumeration and cell cycle analysis of natural populations of marine picoplankton by flow cytometry using the nucleic acid stain SYBR Green I. Appl. Environ. Microb. 63: 186-193.

Marshall, A.G., Hendrickson, C.L., 2008. High-resolution mass spectrometers. Annu. Rev. Anal. Chem. 1: 579-599.

Martinez, J., Azam, F., 1993. Periplasmic aminopeptidase and alkaline phosphatase activities in a marine bacterium: implications for substrate processing in the sea. Mar. Ecol. Prog. Ser. 92: 89-97.

Martinez, J., Smith, D.C., Steward, G.F., Azam, F., 1996. Variability in ectohydrolytic enzyme activities of pelagic marine bacteria and its significance for substrate processing in the sea. Aquat. Microb. Ecol. 10: 223-230.

Mayali, X., Weber, P.K., Brodie, E.L., Mabery, S., Hoeprich, P.D., Pett-Ridge, J., 2012. High-throughput isotopic analysis of RNA microarrays to quantify microbial resource use. ISME. J. 6: 1210-1221.

Mayali, X., Stewart, B., Mabery, S., Weber, P.K., 2015. Temporal succession in carbon incorporation from macromolecules by particle-attached bacteria in marine microcosms. Environ. Microbiol. Rep. doi: 10.1111/1758-2229.12352.

McBride, M.J., Xie, G., Martens, E.C., Lapidus, A., Henrissat, B., Rhodes, R.G., Goltsman, E., Wang, W., Xu, J., Hunnicutt, D.W., Staroscik, A.M., Hoover, T.R., Cheng, Y.Q., Stein, J.L., 2009. Novel features of the polysaccharide-digesting gliding bacterium *Flavobacterium johnsoniae* as revealed by genome sequence analysis. Appl. Environ. Microb. 75: 6864-6875.

Mccaman, M.T., Villarejo, M.R., 1982. Structural and catalytic properties of peptidase-N from *Escherichia-Coli* K-12. Arch. Biochem. Biophys. 213: 384-394.

McCarren, J., Becker, J.W., Repeta, D.J., Shi, Y., Young, C.R., Malmstrom, R.R., Chisholm, S.W., DeLong, E.F., 2010. Microbial community transcriptomes reveal microbes and metabolic pathways associated with dissolved organic matter turnover in the sea. Proc. Natl. Acad. Sci. 107: 16420-16427.

McCarthy, M.J., Carini, S.A., Liu, Z.F., Ostrom, N.E., Gardner, W.S., 2013. Oxygen consumption in the water column and sediments of the northern Gulf of Mexico hypoxic zone. Estuar. Coast. Shelf Sci. 123: 46-53.

McDonald, S.M., Plant, J.N., Worden, A.Z., 2010. The mixed lineage nature of nitrogen transport and assimilation in marine eukaryotic phytoplankton: A case study of *Micromonas*. Mol. Biol. Evol. 27: 2268-2283.

Meador, T.B., Aluwihare, L.I., Mahaffey, C., 2007. Isotopic heterogeneity and cycling of organic nitrogen in the oligotrophic ocean. Limnol. Oceanogr. 52(3): 934-947.

Meyer-Reil, L.A., Koster, M., 1992. Microbial life in pelagic sediments - the impact of environmental parameters on enzymatic degradation of organic material. Mar. Ecol. Prog. Ser. 81: 65-72.

Mohapatra, B.R., Fukami, K., 2004. Production of aminopeptidase by marine heterotrophic nanoflagellates. Aquat. Microb. Ecol. 34: 129-137.

Moran, M.A., Belas, R., Schell, M.A., Gonzalez, J.M., Sun, F., Sun, S., Binder, B.J., Edmonds, J., Ye, W., Orcutt, B., Howard, E.C., Meile, C., Palefsky, W., Goesmann, A., Ren, Q., Paulsen, I., Ulrich, L.E., Thompson, L.S., Saunders, E., Buchan, A., 2007. Ecological genomics of marine roseobacters. Appl. Environ. Microb. 73: 4559-4569.

Morozov, L., 1979. Mirror symmetry breaking in biochemical evolution. Origins Life Evol. B 9: 187-217.

Mou, X., Sun, S., Edwards, R.A., Hodson, R.E., Moran, M.A., 2008. Bacterial carbon processing by generalist species in the coastal ocean. Nature 451: 708-712.

Mouriño-Pérez, R.R., Worden, A.Z., Azam, F., 2003. Growth of *Vibrio cholerae* O1 in Red Tide Waters off California. Appl. Environ. Microbiol. 69: 6923-6931.

Mow-Robinson, J.M., Rheinheimer, G., 1985. Comparison of bacterial populations from the Kiel Fjord in relation to the presence or absence of benthic vegetation. Bot. Mar. 28: 29-39.

Mulholland, M.R., Gobler, C.J., Lee, C., 2002. Peptide hydrolysis, amino acid oxidation, and nitrogen uptake in communities seasonally dominated by *Aureococcus anophagefferens*. Limnol. Oceanogr. 47: 1094-1108.

Mulholland, M.R., Lee, C., 2009. Peptide hydrolysis and the uptake of dipeptides by phytoplankton. Limnol. Oceanogr. 54: 856-868.

Mulholland, M.R., Lee, C., Glibert, P.M., 2003. Extracellular enzyme activity and uptake of carbon and nitrogen along an estuarine salinity and nutrient gradient. Mar. Ecol. Prog. Ser. 258: 3-17.

Münster, U., Einio, P., Nurminen, J., 1989. Evaluation of the measurements of extracellular enzyme activities in a polyhumic lake by means of studies with 4-methylumbelliferyl-substrates. Arch. Hydrobiol. 115: 321-337.

Murphy, J., Riley, J.P., 1962. A modified single solution method for determination of phosphate in natural waters. Anal. Chim. Acta 26(1): 31-36.

Murray, A.E., Arnosti, C., De La Rocha, C.L., Grossart, H.P., Passow, U., 2007. Microbial dynamics in autotrophic and heterotrophic seawater mesocosms. II. Bacterioplankton community structure and hydrolytic enzyme activities. Aquat. Microb. Ecol. 49: 123-141.

Nagata, T., 2008. Organic matter-bacteria interactions in seawater, in: Kirchman, D.L. (Eds.) Microbial Ecology of the Oceans. Wiley-Blackwell, Hoboken, NJ, pp. 207-242.

Nelson, C.E., Carlson, C.A., 2012. Tracking differential incorporation of dissolved organic carbon types among diverse lineages of Sargasso Sea bacterioplankton. Environ. Microbiol. 14: 1500-1516.

Neufeld, J.D., Dumont, M.G., Vohra, J., Murrell, J.C., 2007a. Methodological considerations for the use of stable isotope probing in microbial ecology. Microb. Ecol. 53: 435-442.

Neufeld, J.D., Schafer, H., Cox, M.J., Boden, R., McDonald, I.R., Murrell, J.C., 2007b. Stable-isotope probing implicates Methylophaga spp and novel Gammaproteobacteria in marine methanol and methylamine metabolism. ISME J. 1: 480-491.

Neufeld, J.D., Wagner, M., Murrell, J.C., 2007c. Who eats what, where and when? Isotope-labelling experiments are coming of age. ISME J. 1: 103-110.

Niessen, W.M.A., 2006. LC-MS analysis of peptides enabling technoligies, in Niessen, W.M.A. (Eds.) Liquid Chromatography-Mass Spectrometry, Taylor, pp. 463-492.

Nisbet, T.M., Payne, J.W., 1982. The characteristics of peptide uptake in *Streptococcus-Faecalis* - studies on the transport of natural peptides and antibacterial phosphonopeptides. J. Gen. Microbiol. 128(Jun): 1357-1364.

Nunn, B.L., Norbeck, A., Keil, R.G., 2003. Hydrolysis patterns and production of peptide intermediates during protein degradation in marine systems. Mar. Chem. 83: 59-73.

Obayashi, Y., Suzuki, S., 2005. Proteolytic enzymes in coastal surface seawater: significant activity of endopeptidases and exopeptidases. Limnol. Oceanogr. 50: 722-726.

Obayashi, Y., Suzuki, S., 2008. Occurrence of exo- and endopeptidases in dissolved and particulate fractions of coastal seawater. Aquat. Microb. Ecol. 50: 231-237.

Ogawa, H., Amagai, Y., Koike, I., Kaiser, K., Benner, R., 2001. Production of refractory dissolved organic matter by bacteria. Science 292(5518): 917-920.

Oksanen, J., Blanchet, F.G., Kindt, R., Legendre, P., Minchin, P.R., O'Hara, R.B., Simpson, G.L., Solymos, P., Stevens, M.H., Wagner, H., 2016. Package 'Vegan'. http://cran.r-project.org.

Ong, S.E., Mann, M., 2005. Mass spectrometry-based proteomics turns quantitative. Nat. Chem. Biol. 1(5): 252-262.

Orsi, W.D., Smith, J.M., Liu, S., Liu, Z., Sakamoto, C.M., Wilken, S., Poirier, C., Richards, T.A., Keeling, P.J., Worden, A.Z., Santoro, A.E., 2016. Diverse, uncultivated bacteria and archaea underlying the cycling of dissolved protein in the ocean. ISME J. (accepted).

Ouverney, C.C., Fuhrman, J.A., 1999. Combined Microautoradiography-16S rRNA probe technique for determination of radioisotope uptake by specific microbial cell types in situ. Appl. Environ. Microbiol. 65(7): 3264-3264.

Pantoja, S., Lee, C., 1999. Peptide decomposition by extracellular hydrolysis in coastal seawater and salt marsh sediment. Mar. Chem. 63: 273-291.

Pantoja, S., Lee, C., Marecek, J.F., Palenik, B.P., 1993. Synthesis and use of fluorescent molecular probes for measuring cell-surface enzymatic oxidation of amino acids and amines in seawater. Anal. Biochem. 211: 210-218.

Pantoja, S., Lee, C., Marecek, J.F., 1997. Hydrolysis of peptides in seawater and sediment. Mar. Chem. 57: 25-40.

Pantoja, S., Rossel, P., Castro, R., Cuevas, L.A., Daneri, G., Cordova, C., 2009. Microbial degradation rates of small peptides and amino acids in the oxygen minimum zone of Chilean coastal waters. Deep-Sea Res. Pt. II 56: 1019-1026.

Payne, J.W., 1968. Oligopeptide transport in *Escherichia Coli* - specificity with respect to side chain and distinction from dipeptide transport. J. Biol. Chem. 243(12): 3395-3402.

Payne, J.W., 1971. Requirement for protonated alpha-amino group for transport of peptides in *Escherichia-Coli*. Biochem. J. 123(2): 245-253.

Payne, J.W., 1980. Transport and utilization of peptides by bacteria, in: Payne, J.W. (Eds.) Microorganisms and Nitrogen Sources. John Wiley and Sons, New York, pp. 211-256.

Payne, J. W. 1983. Peptide transport in bacteria - methods, mutants and energy coupling. Biochem. Soc. Trans. 11(6): 794-798.

Payne, J.W., Gilvarg, C., 1971. Peptide transport, in: Meister, A. (Eds.) Adv. Enzymol. Relat. Areas Mol. Biol. 35, Wiley-Blackwell, Hoboken, NJ, pp. 187-244.

Payne, J.W., Bell, G., 1979. Direct determination of the properties of peptide transport systems in *Escherichia-Coli*, using a fluorescent-labeling procedure. J. Bacteriol. 137(1): 447-455.

Payne, J.W., Smith, M.W., 1994. Peptide transport by micro-organisms, in: Rose, A.H., Tempest, D.W. (Eds.) Advances in Microbial Physiology 36, Wiley-Blackwell, Hoboken, NJ, pp. 1-80.

Pernthaler, J., 2005. Predation on prokaryotes in the water column and its ecological implications. Nat. Rev. Microbiol. 3: 537-546.

Petritis, K., Brussaux, S., Guenu, S., Elfakir, C., Dreux, M., 2002. Ion-pair reversed-phase liquid chromatography-electrospray mass spectrometry for the analysis of underivatized small peptides. J. Chromatogr. A 957(2): 173-185.

Polz, M.F., Hunt, D.E., Preheim, S.P., Weinreich, D.M., 2006. Patterns and mechanisms of genetic and phenotypic differentiation in marine microbes. Philos. Trans. Roy. Soc. B 361(1475): 2009-2021.

Pomeroy, L.R., Sheldon, J.E., Sheldon, W.M., 1994. Changes in Bacterial Numbers and Leucine Assimilation during Estimations of Microbial Respiratory Rates in Seawater by the Precision Winkler Method. Appl. Environ. Microbiol. 60(1): 328-332.

Poretsky, R.S., Sun, S.L., Mou, X.Z., Moran, M.A., 2010. Transporter genes expressed by coastal bacterioplankton in response to dissolved organic carbon. Environ. Microbiol. 12: 616-627.

Powell, M.J., Sutton, J.N., Del Castillo, C.E., Timperman, A.I., 2005. Marine proteomics: generation of sequence tags for dissolved proteins in seawater using tandem mass spectrometry. Mar. Chem. 95: 183-198.

Rabalais, N.N., Turner, R.E., Wiseman, W.J., 2001. Hypoxia in the Gulf of Mexico. J. Environ. Qual. 30: 320-329.

Radajewski, S., Ineson, P., Parekh, N.R., Murrell, J.C., 2000. Stable-isotope probing as a tool in microbial ecology. Nature 403: 646-649.

Radajewski, S., McDonald, I.R., Murrell, J.C., 2003. Stable-isotope probing of nucleic acids: a window to the function of uncultured microorganisms. Curr. Opin. Biotech. 14: 296-302.

Rappé, M.S., Connon, S.A., Vergin, K.L., Giovannoni, S.J., 2002. Cultivation of the ubiquitous SAR11 marine bacterioplankton clade. Nature 418: 630-633.

Redmond, M.C., Valentine, D.L., Sessions, A.L., 2010. Identification of novel methane-, ethane-, and propane-oxidizing bacteria at marine hydrocarbon seeps by stable isotope probing. Appl. Environ. Microbiol. 76: 6412-6422.

Rego, J.V., Billen, G., Fontigny, A., Somville, M., 1985. Free and attached proteolytic activity in water environments. Mar. Ecol. Prog. Ser. 21: 245-249.

Rheinheimer, G., Gocke, K., Hoppe, H.G., 1989. Vertical distribution of microbiological and hydrographic-chemical parameters in different areas of the Baltic Sea. Mar. Ecol. Prog. Ser. 52: 55-70.

Roboz, J., Yu, Q.T., Meng, A.K., Vansoest, R., 1994. On-line buffer removal and fraction selection in gradient capillary high-performance liquid-chromatography prior to electrospray mass-spectrometry of peptides and proteins. Rapid Commun. Mass Spectr. 8(8): 621-626.

Roth, L.C., Harvey, H.R., 2006. Intact protein modification and degradation in estuarine environments. Mar. Chem. 102: 33-45.

Saier, M.H., 2000. Families of transmembrane transporters selective for amino acids and their derivatives. Microbiology 146: 1775-1795.

Salerno, M., Stoecker, D.K., 2009. Ectocellular glucosidase and peptidase activity of the mixotrophic dinoflagellate *Prorocentrum Minimum* (Dinophyceae). J. Phycol. 45: 34-45.

Schechter, I., 1970. On active sites of proteases - cleavage of peptide bonds involving dialanine residues by carboxypeptidase A. Eur. J. Biochem. 14: 516-520.

Schmidt, A., Karas, M., Dulcks, T., 2003. Effect of different solution flow rates on analyte ion signals in nano-ESI MS, or: When does ESI turn into nano-ESI? J. Am. Soc. Mass Spectr. 14(5): 492-500.

Schut, F., Prins, R.A., Gottschal, J.C., 1997. Oligotrophy and pelagic marine bacteria: Facts and fiction. Aquat. Microb. Ecol. 12: 177-202.

Sellner, K.G., Doucette, G.J., Doucette, G.J., Kirkpatrick, G.J., 2003. Harmful algal blooms: causes, impacts and detection. J. Ind. Microbiol. Biotechnol. 30: 383-406.

Sherr, E.B., Caron, D.A., Sherr, B.F., 1993. Staining of heterotrophic protists for visualization via epifluorescence microscopy, in: Kemp, P.F., Sherr, B.F., Sherr, E.B., Cole, J.J. (Eds.) Handbook of Methods in Aquatic Microbial Ecology. Lewis, Boca Raton, FL, pp. 213-227.

Sherr, E.B., Sherr, B.F., 1993. Preservation and storage of samples for enumeration of heterotrophic protists, in: Kemp, P.F., Sherr, B.F., Sherr, E.B., Cole, J.J. (Eds.) Handbook of Methods in Aquatic Microbial Ecology. Lewis, Boca Raton, FL, pp. 207-212.

Simon, M., Billerbeck, S., Kessler, D., Selje, N., Schlingloff, A., 2012. Bacterioplankton communities in the Southern Ocean: composition and growth response to various substrate regimes. Aquat. Microb. Ecol. 68: 13-28.

Sinsabaugh, R.L., 1994. Enzymatic Analysis of Microbial Pattern and Process. Biol. Fert. Soils 17(1): 69-74.

Šimek, K., Kojecka, P., Nedoma, J., Hartman, P., Vrba, J., Dolan, J.R., 1999. Shifts in bacterial community composition associated with different microzooplankton size fractions in a eutrophic reservoir. Limnol. Oceanogr. 44: 1634-1644.

Smith, D.M., Snow, D.E., Rees, E., Zischkau, A.M., Hanson, J.D., Wolcott, R.D., Sun, Y., White, J., Kumar, S., Dowd, S.E., 2010. Evaluation of the bacterial diversity of Pressure ulcers using bTEFAP pyrosequencing. BMC Med. Genomics 3: 41, doi:10.1186/1755-8794-3-41.

Smith, E.L., 1948. Action of carboxypeptidase on peptide derivatives of L-tryptophan. J. Biol. Chem. 175: 39-47.

Smith, E.L., Spackman, D.H., 1955. Leucine aminopeptidase. V. Activation, specificity, and mechanism of action. J. Biol. Chem. 212: 271-299.

Snyder, L.R., Kirkland, J.J., Glajch, J.L., 1997. Practical HPLC Method Development, 2nd ed. Wiley.

Somville, M., Billen, G., 1983. A method for determining exoproteolytic activity in natural waters. Limnol. Oceanogr. 28: 190-193.

Steen, A.D., Arnosti, C., 2013. Extracellular peptidase and carbohydrate hydrolase activities in an Arctic fjord (Smeerenburgfjord, Svalbard). Aquat. Microb. Ecol. 69: 93-99.

Steen, A.D., Vazin, J.P., Hagen, S.M., Mulligan, K.H., Wilhelm, S.W., 2015. Substrate specificity of aquatic extracellular peptidases assessed by competitive inhibition assays using synthetic substrates. Aquat. Microb. Ecol. 75: 271-281.

Stein, R.L., 2011. Kinetics of Enzyme Action. John Wiley & Sons, Hoboken, NY.

Steiner, H.Y., Naider, F., Becker, J.M., 1995. The PTR family - a new group of peptide transporters. Mol. Microbiol. 16(5): 825-834.

Sterner, R.W., Elser, J.J., 2002. Ecological Stoichiometry: The Biology of Elements from Molecules to the Biosphere. Princeton University Press, Princeton, NJ.

Sterner, R.W., Andersen, T., Elser, J.J., Hessen, D.O., Hood, J.M., McCauley, E., Urabe, J., 2008. Scale-dependent carbon : nitrogen : phosphorus seston stoichiometry in marine and freshwaters. Limnol. Oceanogr. 53: 1169-1180.

Stevenson, F.J., 1994. Humus Chemistry: Genesis, Composition, Reactions, 2nd ed. Wiley, New York.

Stoecker, D.K., 1999. Mixotrophy among dinoflagellates. J. Eukaryot. Microbiol. 46: 397-401.

Stoecker, D.K., Gustafson, D.E., 2003. Cell-surface proteolytic activity of photosynthetic dinoflagellates. Aquat. Microb. Ecol. 30: 175-183.

Strickland, J.D.H., Parsons, T.R., 1968. A Practical Handbook of Seawater Analysis. Queen's Printer, Ottawa.

Sussman, A.J., Gilvarg, C., 1971. Peptide Transport and Metabolism in Bacteria. Annu. Rev. Biochem. 40: 397-408.

Tabor, P.S., Neihof, R.A., 1982. Improved micro-auto-radiographic method to determine individual microorganisms active in substrate uptake in natural-waters. Appl. Environ. Microb. 44: 945-953.

Talbot, V., Bianchi, M., 1997. Bacterial proteolytic activity in sediments of the Subantarctic Indian Ocean sector. Deep-Sea Res. Pt. II 44(5): 1069-1084.

Tang, K.Q., Page, J.S., Smith, R.D., 2004. Charge competition and the linear dynamic range of detection in electrospray ionization mass spectrometry. J. Am. Soc. Mass Spectr. 15(10): 1416-1423.

Tanoue, E., 1995. Detection of dissolved protein molecules in oceanic waters. Mar. Chem. 51(3): 239-252.

Tanoue, E., 1996. Characterization of the particulate protein in Pacific surface waters. J. Mar. Res. 54(5): 967-990.

Taylor, A., 1993. Aminopeptidases - structure and function. FASEB J. 7: 290-298.

Teeling, H., Fuchs, B.M., Becher, D., Klockow, C., Gardebrecht, A., Bennke, C.M., Kassabgy, M., Huang, S.X., Mann, A.J., Waldmann, J., Weber, M., Klindworth, A., Otto, A., Lange, J., Bernhardt, J., Reinsch, C., Hecker, M., Peplies, J., Bockelmann, F.D., Callies, U., Gerdts, G., Wichels, A., Wiltshire, K.H., Glockner, F.O., Schweder, T., Amann, R., 2012. Substrate-controlled succession of marine bacterioplankton populations induced by a phytoplankton bloom. Science 336: 608-611.

Teske, A., Durbin, A., Ziervogel, K., Cox, C., Arnosti, C., 2011. Microbial community composition and function in permanently cold seawater and sediments from an Arctic fjord of Svalbard. Appl. Environ. Microbiol. 77(6): 2008-2018.

Thao, N.V., Obayashi, Y., Yokokawa, T., Suzuki, S., 2014. Coexisting protist-bacterial community accelerates protein transformation in microcosm experiments. Front. Mar. Sci. 1: doi: 10.3389/fmars.2014.00069.

Uhlik, O., Jecna, K., Leigh, M.B., Mackova, M., Macek, T., 2009. DNA-based stable isotope probing: a link between community structure and function. Sci. Total Environ. 407: 3611-3619.

Unanue, M., Ayo, B., Azua, I., Barcina, I., Iriberri, J., 1992. Temporal variability of attached and free-living bacteria in coastal waters. Microb. Ecol. 23: 27-39.

Velji, M.I., Albright, L.J., 1993. Improved sample preparation for enumeration of aggregated aquatic substrate bacteria, in: Kemp, P.F., Sherr, B.F., Sherr, B.E., Cole, J.J. (Eds.) Handbook of Methods in Aquatic Microbial Ecology. Lewis, Boca Raton, FL, pp. 139-142.

Ventura, M., Canchaya, C., Tauch, A., Chandra, G., Fitzgerald, G.F., Chater, K.F., van Sinderen, D., 2007. Genomics of Actinobacteria: Tracing the evolutionary history of an ancient phylura. Microbiol. Mol. Biol. Res. 71: 495-548.

Vollenweider, R.A., Marchetti, R., Viviani, R., 1992. Marine Coastal Eutrophication, Elsevier Science Publishers B.V., Netherlands.

Voget, S., Wemheuer, B., Brinkhoff, T., Vollmers, J., Dietrich, S., Giebel, H., Beardsley, C., Sardemann, C., Bakenhus, I., Billerbeck, S., Daniel, R., Simon, M., 2015. Adaptation of an abundant Roseobacter RCA organism to pelagic systems revealed by genomic and transcriptomic analyses. Appl. Environ. Microbiol. 9: 371-384.

Wade, L.G., 1995. Organic Chemistry. Prenctice Hall, Englewood Cliffs, NJ.

Walker, J.E., Saraste, M., Runswick, M.J., Gay, N.J., 1982. Distantly related sequences in the α-subunits and β-subunits of ATP synthase, myosin, kinases and other ATP-

requiring enzymes and a common nucleotide binding fold. EMBO J. 1(8): 945-951.

Wang, X., Sharp, C.E., Jones, G.M., Grasby, S.E., Brady, A.L., Dunfield, P.F., 2015. Stable-isotope probing identifies uncultured *Planctomycetes* as primary degraders of a complex heteropolysaccharide in soil. Appl. Environ. Microbiol. 81: 4607-4615.

Wawrik, B., Boling, W.B., Van Nostrand, J.D., Xie, J.P., Zhou, J.Z., Bronk, D.A., 2012a. Assimilatory nitrate utilization by bacteria on the West Florida Shelf as determined by stable isotope probing and functional microarray analysis. FEMS Microbiol. Ecol. 79: 400-411.

Wawrik, B., Callaghan, A.V., Bronk, D.A., 2009. Use of inorganic and organic nitrogen by *Synechococcus* spp. and diatoms on the West Florida Shelf as measured using stable isotope probing. Appl. Environ. Microb. 75: 6662-6670.

Wawrik, B., Mendivelso, M., Parisi, V.A., Suflita, J.M., Davidova, I.A., Marks, C.R., Van Nostrand, J.D., Liang, Y.T., Zhou, J.Z., Huizinga, B.J., Strapoc, D., Callaghan, A.V., 2012b. Field and laboratory studies on the bioconversion of coal to methane in the San Juan Basin. FEMS Microbiol. Ecol. 81: 26-42.

Weber, F., del Campo, J., Wylezich, C., Massana, R., Jurgens, K., 2012. Unveiling trophic functions of uncultured protist taxa by incubation experiments in the brackish Baltic Sea. PLoS. ONE 7(7): e41970. doi:10.1371/journal.pone.0041970.

Weiss, M.S., Abele, U., Weckesser, J., Welte, W., Schiltz, E., Schulz, G.E., 1991. Molecular architecture and electrostatic properties of a bacterial porin. Science 254(5038): 1627-1630.

Wilkes, S.H., Bayliss, M.E., Prescott, J.M., 1973. Specificity of *Aeromonas* aminopeptidase toward oligopeptides and polypeptides. Eur. J. Biochem. 34: 459-466.

Wright, L., Blagova, E., Levdikov, V.M., Brannigan, J.A., Pattenden, R.J., Chambers, J., Wilkinson, A.J., 2004. Crystallization of the oligopeptide-binding protein AppA from *Bacillus subtilis*. Acta Crystallogr. D 60: 175-177.

Xue, J.H., Lee, C., Wakeham, S.G., Armstrong, R.A., 2011. Using principal components analysis (PCA) with cluster analysis to study the organic geochemistry of sinking particles in the ocean. Org. Geochem. 42: 356-367.

Yau, S., Lauro, F.M., Williams, T.J., DeMaere, M.Z., Brown, M.V., Rich, J., Gibson, J.A.E., Cavicchioli, R., 2013. Metagenomic insights into strategies of carbon conservation and unusual sulfur biogeochemistry in a hypersaline Antarctic lake. ISME J. 7: 1944-1961.

Yolanda, S., 2007. Aminopeptidases, in: Polaina, J., MacCabe, A.P. (Eds.) Industrial Enzymes: Structure, Function and Applications. Springer, Netherlands, pp. 243-262.

Zang, X., Nguyen, R.T., Harvey, H.R., Knicker, H., Hatcher, P.G., 2001. Preservation of proteinaceous material during the degradation of the green alga *Botryococcus braunii*: A solid-state 2D ^{15}N ^{13}C NMR spectroscopy study. Geochim. Cosmochim. Ac. 65(19): 3299-3305.

Zemb, O., Lee, M., Gutierrez-Zamora, M.L., Hamelin, J., Coupland, K., Hazrin-Chong, N.H., Taleb, I., Manefield, M., 2012. Improvement of RNA-SIP by pyrosequencing to identify putative 4-*n*-nonylphenol degraders in activated sludge. Water Res. 46: 601-610.

Ziervogel, K., Karlsson, E., Arnosti, C., 2007. Surface associations of enzymes and of organic matter: Consequences for hydrolytic activity and organic matter remineralization in marine systems. Mar. Chem. 104: 241-252.

Vita

Shuting Liu was born and grew up in Nanjing, China. She graduated from Nanjing University and received her Bachelor of Science degree in Environmental Science in May, 2010. She was enrolled in the Ph.D. program in the Marine Science Institute, The University of Texas at Austin in Aug., 2010.

Permanent email: shutingliu@utexas.edu

This dissertation was typed by Shuting Liu.